U.S. DEPARTMENT OF THE INTERIOR
BUREAU OF RECLAMATION

WATEREUSE RESEARCH

Ozone Pretreatment of a Non-Nitrified Secondary Effluent Before Microfiltration

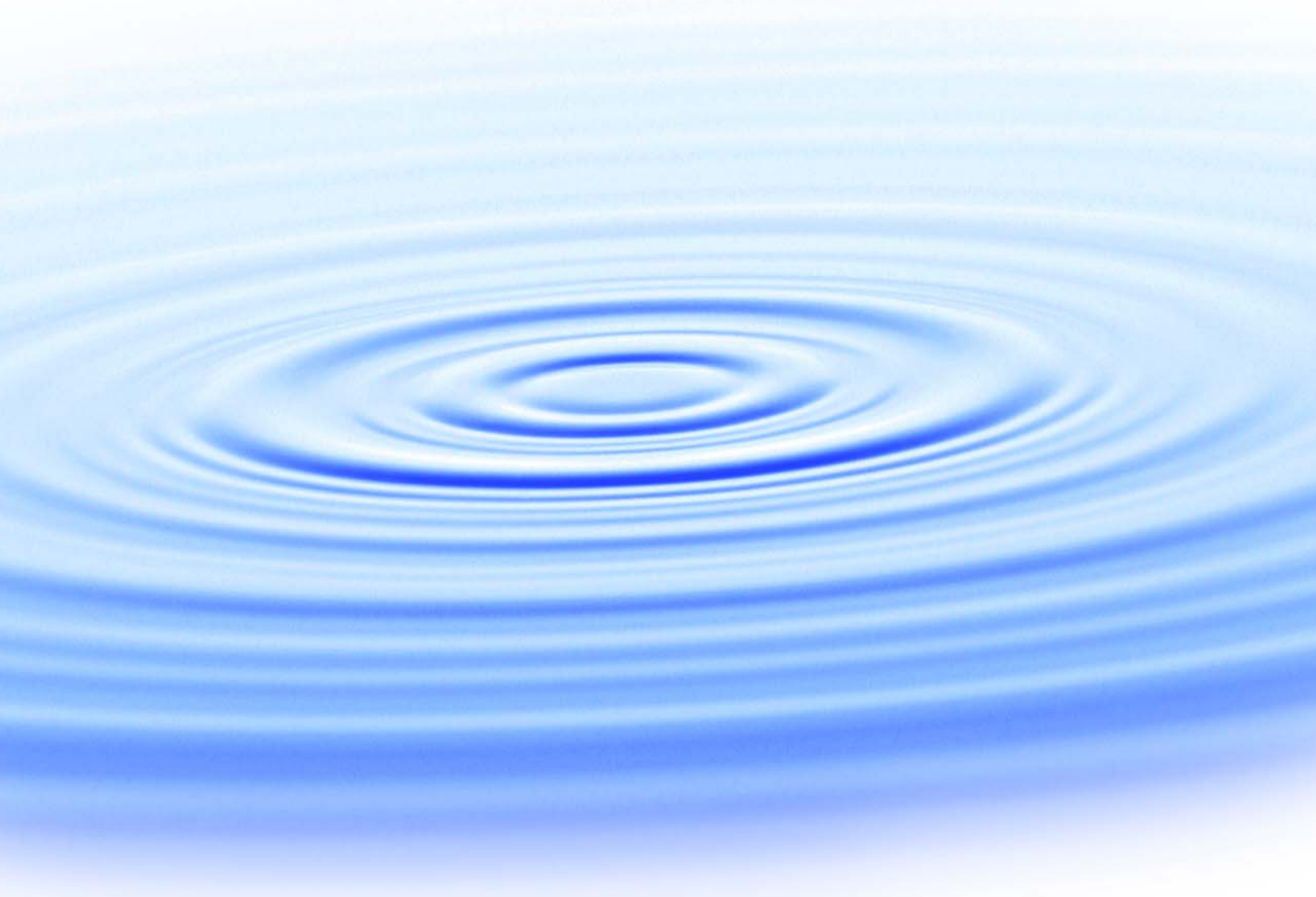

WateReuse Research Foundation

Ozone Pretreatment of a Non-Nitrified Secondary Effluent Before Microfiltration

About the WateReuse Research Foundation

The mission of the WateReuse Research Foundation is to conduct and promote applied research on the reclamation, recycling, reuse, and desalination of water. The Foundation's research advances the science of water reuse and supports communities across the United States and abroad in their efforts to create new sources of high quality water for various uses through reclamation, recycling, reuse, and desalination while protecting public health and the environment.

The Foundation sponsors research on all aspects of water reuse, including emerging chemical contaminants, microbiological agents, treatment technologies, reduction of energy requirements, concentrate management and desalination, public perception and acceptance, economics, and marketing. The Foundation's research informs the public of the safety of reclaimed water and provides water professionals with the tools and knowledge to meet their commitment of providing a reliable, safe product for its intended use.

The Foundation's funding partners include the supporters of the California Direct Potable Reuse Initiative, Water Services Association of Australia, Pentair Foundation, and Bureau of Reclamation. Funding is also provided by the Foundation's Subscribers, water and wastewater agencies, and other interested organizations.

Ozone Pretreatment of a Non-Nitrified Secondary Effluent Before Microfiltration

Marc Serna
West Basin Municipal Water District

R. Shane Trussell
Trussell Technologies

Fredrick W. Gerringer
Trussell Technologies

Cosponsors

Bureau of Reclamation
West Basin Municipal Water District

WateReuse Research Foundation
Alexandria, VA

Disclaimer

This report was sponsored by the WateReuse Research Foundation and cosponsored by Bureau of Reclamation and West Basin Municipal Water District. The Foundation, it's Board Members, and the project cosponsors assume no responsibility for the content of this publication or for the opinions or statements of facts expressed in the report. The mention of trade names of commercial products does not represent or imply the approval or endorsement of the WateReuse Research Foundation, its Board Members, or the cosponsors. This report is published solely for informational purposes.

For more information, contact:

WateReuse Research Foundation
1199 North Fairfax Street, Suite 410
Alexandria, VA 22314
703-548-0880
703-548-5085 (fax)
www.WateReuse.org/Foundation

WateReuse Research Foundation Project Number: WRRF-10-11
WateReuse Research Foundation Product Number: 10-11-1

ISBN: 978-1-941242-09-4
Library of Congress Control Number: 2014938961

Printed in the United States of America

Printed on Recycled Paper

Contents

Figures

Tables

Acronyms

AFM	atomic force microscopy
AOP	advanced oxidation process
AWTF	Leo J. Vander Lans Advanced Water Treatment Facility
CDPH	California Department of Public Health
CEC	contaminant of emerging concern
CI	chemical ionization
CIP	clean-in-place
CT	concentration-time
DBP	disinfection byproduct
DCM	dichloromethane
DDI	distilled deionized
DI	deionized
DMA	dimethylamine
DMS	dimethyl sulfide
DOC	dissolved organic carbon
ECLWRF	Edward C. Little Water Recycling Facility
EDC	endocrine disrupting compound
EDS	energy dispersive spectroscopy
EEM	excitation-emission matrix
EFM	enhanced flux maintenance
EfOM	effluent organic matter
Fe	iron
$FeCl_3$	ferric chloride
FRI	fluorescence regional integration
FTIR	Fourier transform infrared
GC	gas chromatograph
gfd	gal/ft^2/day
GWRS	Groundwater Replenishment System
H_2O_2	hydrogen peroxide
HCl	hydrochloric acid
HMI	human-machine interface
$HO_2^{\bullet}$	hyperoxide radical
HOBr	hypobromous acid
HOCl	hypochlorous acid
HRT	hydraulic retention time
HTP	Hyperion Treatment Plant
IOD	initial ozone dose
IPR	indirect potable reuse

k’	first order ozone decay rate constant
LC	liquid chromatography
LOX	liquid oxygen
MF	microfiltration
Mn	manganese
MnO_2	manganese dioxide
MRM	multiple reaction monitoring
MS	mass spectrometer
MW	molecular weight
N/M	not measured
N_2O_4	dinitrogen tetroxide
$Na_2S_2O_4$	sodium hydrosulfite
$Na_2S_2O_5$	sodium metabisulfite
ND	not detected
NDMA	N-nitrosodimethylamine
NDPA	N-nitrosodi-n-propylamine-d14
NO^+	nitrosyl cation
NO_2^-	nitrite
NOM	natural organic matter
O/S	oxygen-to-sulfur
O&M	operation and maintenance
$O_2^{-\bullet}$	superoxide radical
O_3	ozone
O_3:DOC	ozone-to-dissolved organic carbon
O_3:TOC	ozone-to-total organic carbon
OBr^-	hypobromite
OCWD	Orange County Water District
$OH^\bullet$	hydroxyl radical
OH^-	hydroxyl ion
ORP	oxidation-reduction potential
PAH	polyaromatic hydrocarbon
PBDE	polybrominated disphenyl ether
PPCP	pharmaceuticals and personal care product
PVDF	polyvinylidene fluoride
RO	reverse osmosis
$S_2O_4^{2-}$	hydrosulfite
$S_2O_5^{2-}$	metabisulfite
SEC	size-exclusion chromatography
SEM	scanning electron microscopy
SM	Standard Method

SPE	solid phase extraction
SRT	solids retention time
SUVA	specific ultraviolet absorbance
TDS	total dissolved solids
TMP	transmembrane pressure
TOC	total organic carbon
UDMH	1,1-dimethylhydrazine
UF	ultrafiltration
USBR	United States Bureau of Reclamation
USEPA	United States Environmental Protection Agency
UV	ultraviolet
UVA	ultraviolet absorbance
UVT	ultraviolet transmittance
WRD	Water Replenishment District
WWTP	wastewater treatment plant

Foreword

The WateReuse Research Foundation, a nonprofit corporation, sponsors research that advances the science of water reclamation, recycling, reuse, and desalination. The Foundation funds projects that meet the water reuse and desalination research needs of water and wastewater agencies and the public. The goal of the Foundation's research is to ensure that water reuse and desalination projects provide sustainable sources of high-quality water, protect public health, and improve the environment.

An Operating Plan guides the Foundation's research program. Under the plan, a research agenda of high-priority topics is maintained. The agenda is developed in cooperation with the water reuse and desalination communities including water professionals, academics, and Foundation subscribers. The Foundation's research focuses on a broad range of water reuse and desalination research topics including:

- Defining and addressing emerging contaminants, including chemicals and pathogens
- Determining effective and efficient treatment technologies to create 'fit for purpose' water
- Understanding public perceptions and increasing acceptance of water reuse
- Enhancing management practices related to direct and indirect potable reuse
- Managing concentrate resulting from desalination and potable reuse operations
- Demonstrating the feasibility and safety of direct potable reuse

The Operating Plan outlines the role of the Foundation's Research Advisory Committee (RAC), Project Advisory Committees (PACs), and Foundation staff. The RAC sets priorities, recommends projects for funding, and provides advice and recommendations on the Foundation's research agenda and other related efforts. PACs are convened for each project to provide technical review and oversight. The Foundation's RAC and PACs consist of experts in their fields and provide the Foundation with an independent review, which ensures the credibility of the Foundation's research results. The Foundation's Project Managers facilitate the efforts of the RAC and PACs and provide overall management of projects.

Secondary wastewater effluent water quality can have a negative impact on microfiltration (MF) membranes used for indirect potable reuse (IPR) treatment. Previous research indicated pretreating secondary wastewater effluent with ozone before polypropylene MF membranes improved MF performance. Similar research was needed for polyvinylidene fluoride (PVDF) MF membrane. The objective of this research was to optimize the operation of PVDF MF membranes after ozonation of wastewater effluent and evaluate the impacts of ozonation on other aspects of IPR treatments and the performance of reverse osmosis (RO) membranes that treat MF filtrate.

Richard Nagel
Chair
WateReuse Research Foundation

Melissa Meeker
Executive Director
WateReuse Research Foundation

Acknowledgments

This project was funded by the WateReuse Research Foundation in cooperation with the Bureau of Reclamation and West Basin Municipal Water District.

The project team thanks the following individuals for their contributions: Deana Bollaci (WateReuse Research Foundation), the Project Advisory Committee of Eric Wert (Southern Nevada Water Authority), Ben Stanford (Hazen and Sawyer) and Frank Leitz (US Bureau of Reclamation); Ralph Valencia, Seho Chang and Gregg Oelker (United Water); Scott Toomey, Charles Liu, Scott Caothien and Lou Matera (Pall Corp.); Tarn Victor (JBI Water and Wastewater); John Overby (Ozone Water Systems); Greg Stanczak (Trussell Technologies); Kerwin Rakness (Process Applications); Shane Snyder, Darryl Jones and Selene Ruiz Hernandez (University of Arizona); Dan Gerrity (University of Nevada, Las Vegas); Gerry Filteau (Separation Processes, Inc.); Mehul Patel (Orange County Water District); Paul Fu (Water Replenishment District of Southern California). The project team also thanks Orange County Water District and Water Replenishment District of Southern California for providing water samples from Groundwater Replenishment System and Leo J. Vander Lans Advanced Water Treatment Facility, respectively.

Principal Investigators
Marc Serna, *West Basin Municipal Water District*
R. Shane Trussell, *Trussell Technologies, Inc.*
Fredrick W. Gerringer, *Trussell Technologies, Inc.*

Project Team
Rajen Budhia, *West Basin Municipal Water District*

Teresa Venezia, *Trussell Technologies, Inc.*

Project Advisory Committee
Eric Wert, *Southern Nevada Water Authority*
Ben Stanford, *Hazen and Sawyer*
Frank Leitz, *US Bureau of Reclamation*

Executive Summary

In the indirect potable reuse (IPR) treatment train at West Basin Municipal Water District's (West Basin's) Edward C. Little Water Recycling Facility (ECLWRF), polypropylene microfiltration (MF) membranes provide pretreatment for reverse osmosis (RO) membranes followed by an advanced oxidation process (AOP) using ultraviolet light and hydrogen peroxide (UV/H_2O_2). Wastewater effluent organic matter (EfOM) is the primary factor limiting MF performance when treating secondary wastewater effluent at water reuse plants such as ECLWRF. Fouling by EfOM can lower membrane flux, increase the frequency of chemical cleaning and contribute to irreversible fouling that reduces membrane longevity and overall treatment efficiency. Over the past 15 years, the quality of the non-nitrified secondary effluent feeding ECLWRF has been worsening. This change in water quality has increased MF fouling by EfOM at ECLWRF and contributed to reducing MF fluxes by 12 to 52% below design. Simultaneously, the frequency of chemical cleanings has increased from the original design of once every 3 weeks to approximately once per week.

Studies have shown high molecular weight (MW) organics are associated with more fouling. Oxidation of EfOM, whether biologically or chemically, can lower MW of EfOM and reduce organic fouling. An earlier pilot study at ECLWRF demonstrated this principle by showing preozonation significantly improved the performance of polypropylene MF membranes. West Basin responded by including preozonation in a project to increase MF capacity at ECLWRF. However, the increased capacity included polyvinylidene fluoride (PVDF) MF membranes that were not included in the original pilot study. West Basin commissioned the pilot study described in this report to evaluate ozonation before PVDF MF membranes and to investigate other aspects of using ozone in an IPR treatment train. Goals of this project are listed here:

- Characterize EfOM in the plant influent, MF filtrate, and MF backwash at water recycling plants with different wastewater effluent sources to determine the effect of different levels of wastewater treatment on organic fouling potential.
- Evaluate ultraviolet transmittance at 254 nm (UVT) and oxidation-reduction potential for automated ozone dose control.
- Optimize the performance and operating conditions of PVDF MF membranes with preozonation.
- Compare RO performance between the treatment trains with and without ozone.
- Compare the concentrations of N-nitrosodimethylamine (NDMA), contaminants of emerging concern (CECs) and bromate between the treatment trains with and without ozone.

Pilot testing included parallel operation of two of the following three treatment trains at different times during the project:

- Ferric chloride ($FeCl_3$), MF, and RO ($FeCl_3$-MF-RO)
- Ozone, MF and RO (O_3-MF-RO)
- Ozone, $FeCl_3$, MF, and RO (O_3-$FeCl_3$-MF-RO)

Test results demonstrated ozonation generally had a beneficial effect on the performance of PVDF MF membranes. Automated ozone dose control based on UVT was proven to be an effective approach for adjusting the ozone dose based on water quality. Ozonation improved MF feed and backwash water quality, reduced or eliminated the need for $FeCl_3$ addition in the MF feed, reduced the frequency of daily chlorine/caustic cleanings that remove organic foulants, increased MF flux and backwash intervals when applied before $FeCl_3$, removed CECs, and showed no evidence of higher biological or organic fouling on the RO membranes. The effects on the MF process were caused by the chemical oxidation of EfOM by ozone and would likely slow irreversible fouling, extend membrane replacement intervals, reduce usage of chemicals, such as $FeCl_3$ and chlorine, and improve the performance of MF backwash water recovery processes by reducing coagulant demand. CEC removal potentially could decrease the environmental impact of these pollutants caused by RO concentrate disposal. As shown by the previous pilot study of preozonation for polypropylene MF membranes, there is the potential to increase MF capacity of existing membrane facilities. The magnitude of these benefits would be project specific, depending on factors such as wastewater effluent quality, organic fouling potential in the MF feed, baseline MF process without ozonation, use of coagulants, and handling of MF backwash water.

The effect of ozonation on RO performance potentially was beneficial but ultimately inconclusive. For more than half of pilot testing with RO, the feed pressure and specific flux of the RO unit in the ozone train were 20% better than they were for the RO unit in the control train. These data were consistent with other research showing ozone pretreatment improved RO performance (Pisarenko et al., 2011; Stanford et al., 2011; Stanford et al., 2013). RO elements were moved, along with the corresponding feed water, from one RO unit to the other one. This switch was performed to determine if drifting permeate and concentrate flows of the RO unit in the O_3-MF train was caused by a mechanical problem. Afterward, membrane performance was similar, because the feed pressure of the RO elements in the O_3-MF train increased while the feed pressure of the RO elements in the $FeCl_3$-MF train did not change. Further research of ozonation before MF-RO is required to determine if the difference between RO feed pressure and specific flux during the first several months was a real benefit that could decrease energy usage or increase water production.

This project also uncovered some challenges with ozonating wastewater effluent and as pretreatment to PVDF MF membranes. Pilot testing showed the potential for manganese fouling of PVDF MF membranes caused by overdosing ozone. Mitigation measures, such as automated ozone dose control and $FeCl_3$ addition, were able to prevent this fouling. It is important to note there was no evidence of manganese fouling during the previous study with polypropylene MF membranes, suggesting that the problem could be linked to the material properties of PVDF membranes. High NDMA formation by ozonation was likely caused by a significant amount of precursors in the poorly oxidized non-nitrified secondary effluent feeding the pilot plant. Higher NDMA concentrations in the RO feed of the ozone train caused RO permeate concentrations in the ozone train to exceed those of the treatment train without ozone. Potential mitigation measures for high NDMA formation could include a combination of lower ozone doses, precursor identification and source control, and a larger capacity AOP to treat RO permeate. Bromate, a known disinfection byproduct of ozone, was detected after ozonation, but high rejection by RO reduced bromate concentrations below the detection limit in the RO permeate. Therefore, bromate formation during ozonation was not a concern, because it did not affect RO permeate water quality.

The results of this study presented opportunities for future research. One possibility is the optimization of the ozone dose to establish an appropriate balance between MF performance and NDMA formation. Other areas for process optimization would be maximizing water flux, backwash intervals, and chemical cleaning intervals with and without $FeCl_3$ addition. Jar tests comparing backwash water of MF with and without preozonation could delineate the benefits of ozonation on MF backwash water recovery processes. Additional testing of RO after MF with and without preozonation could determine whether the lower RO feed pressure and higher RO specific flux in the ozone train during the first few months of testing could be sustainable at full scale.

One final advantage of adding preozonation to a water reuse treatment train was related to the draft recycled water regulations by the California Department of Public Health released in November 2011. Those regulations proposed removal criteria for enteric viruses, Giardia cysts, and Cryptosporidium oocysts that might not be achieved by IPR treatment with MF-RO and UV/H_2O_2 that do not have enough removal credits by surface spreading or subsurface treatment. MF-RO-UV/H_2O_2 also would be inadequate for satisfying pathogen removal requirements for direct potable reuse. In both of these situations, adding a properly designed and operated preozonation system to a MF-RO-UV/H_2O_2 train could improve MF performance, CEC destruction, and other aspects of treatment while also satisfying disinfection requirements for indirect and direct potable reuse.

Chapter 1

Introduction

1.1 Background

Microfiltration (MF) is one of the most important unit processes for treating wastewater for indirect potable water reuse. MF provides pretreatment for reverse osmosis (RO) membranes by removing the particulates, bacteria and colloidal organics that cause fouling. However, MF is vulnerable to fouling by the constituents it removes. Biological and particulate fouling can adversely affect MF membranes, but controls such as disinfection, backwashing, and chemical cleaning can limit their contribution to membrane fouling (Huang et al., 2009). Therefore, organic fouling from wastewater effluent organic matter (EfOM) is frequently the main factor limiting MF performance in water recycling plants treating secondary wastewater effluent. Organic fouling can lower membrane flux and increase the chemical cleaning frequency while gradually contributing to irreversible fouling that reduces membrane longevity and overall treatment efficiency.

An example of the effect of organic fouling of MF membranes treating non-nitrified secondary effluent is available at West Basin Municipal Water District's Edward C. Little Water Recycling Facility (ECLWRF). The Hyperion Treatment Plant treats domestic and industrial sewage and provides ECLWRF with the non-nitrified secondary effluent it treats for various reuse applications. Influent water quality at ECLWRF as indicated by turbidity had been degrading from 1997 through 2009 (Figure 1.1). The consequence of the worsening water quality was organic fouling that reduced operating fluxes of the polypropylene MF membranes by 12 to 52% below design, depending on the age of the membranes and current water quality. These MF membranes were designed for chemical cleanings every three weeks, but the cleanings are performed much more frequently (Figure 1.2) to address organic fouling that still occurs even when operating significantly below the design flux.

Before identifying an effective control strategy for organic fouling, the nature of organic constituents that cause fouling must be better understood. Research using size-exclusion chromatography (SEC) has indicated that high molecular weight (MW) polysaccharides are the most significant organic foulant for MF and UF membranes (Lozier et al., 2008). Other research has used ultrafiltration fractionation in combination with protein and carbohydrate measurements to confirm the importance of MW to organic fouling of membrane bioreactors (Trussell et al., 2009). Therefore, treatment processes that reduce MW of organic foulants should improve MF performance.

Options for reducing organic fouling at plants such as ECLWRF include improved biological treatment, chemical coagulation, or chemical oxidation. Improved biological oxidation can reduce organic fouling (Trussell et al., 2009), but infrastructural, operational and economic constraints can make this approach infeasible. Chemical coagulation with metal salts can coagulate organic colloids to form floc that is more easily removed by MF membranes (Huang et al., 2009). However, metal salts can cause rapid fouling if the dose is too high, emphasizing the importance of balancing organic fouling control with the avoidance of inorganic fouling. Mitigation measures could include strategies such as more frequent chemical cleaning with citric acid or similar chemicals that can remove inorganic foulants.

Another risk is the impact on the performance of downstream RO membranes, which can be fouled by coagulant carryover from upstream processes (Gabelich et al., 2006a).

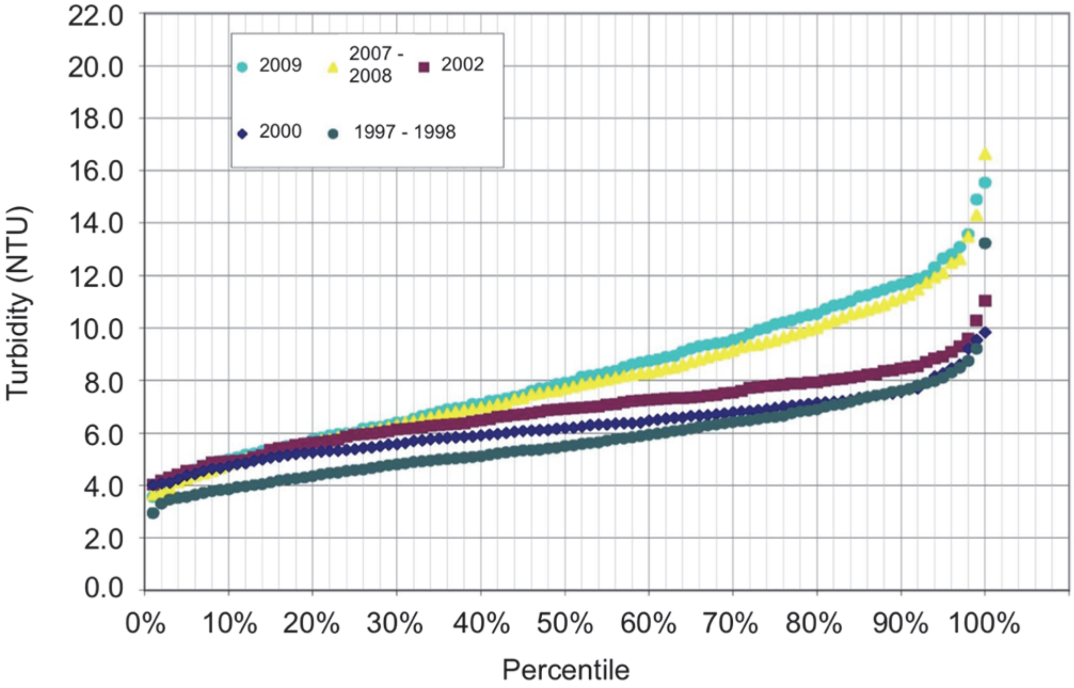

Figure 1.1. Influent turbidity at ECLWRF from 1997 through 2009.

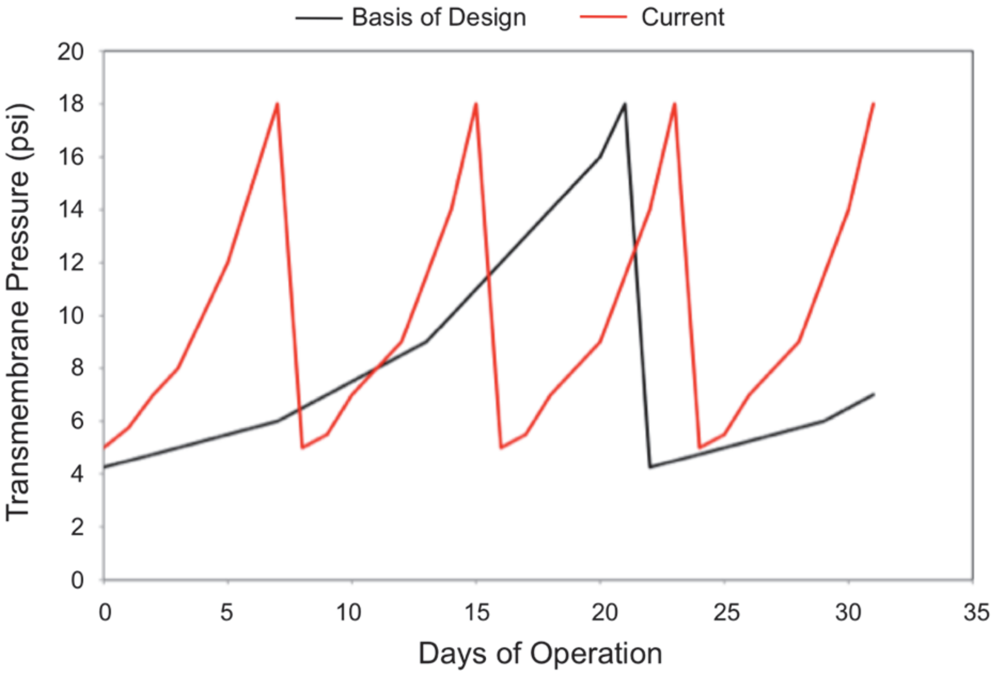

Figure 1.2. Example of current MF cleaning intervals (red) versus the design MF cleaning interval (black).

Chemical oxidation is an alternative approach to achieving the desired oxidation of organic compounds without improving biological treatment. Free chlorine could be a possibility with nitrified wastewater treatment effluents, but the kinetics and stoichiometry of breakpoint chlorine chemistry makes free chlorine impractical with non-nitrified wastewater treatment effluents. Even if breakpoint chlorination were performed, chlorinated disinfection byproducts could be a significant concern at the high chlorine doses that would be required. Polypropylene MF membranes, which are intolerant of strong oxidants, such as free chlorine, are used at recycling facilities such as ECLWRF. Protecting polypropylene MF membranes from free chlorine oxidation and biological fouling would require ammonia addition to form chloramines after breakpoint chlorination had been performed.

Ozonation is another approach to chemical oxidation that does not have the same limitations as chlorine oxidation. Ozone demand is an important factor affecting the required ozone dose, but it does not pose the practical challenges of breakpoint chlorination. Dissolved ozone decays quickly in water compared to free chlorine, and the rate of decay should be higher than normal in a non-nitrified secondary effluent compared to other applications such as drinking water disinfection. Therefore, a properly designed control system has the potential to balance chemical oxidation of EfOM for improving MF performance while ensuring dissolved ozone dissipation before polypropylene MF membranes. These factors suggest MF pretreatment with ozone could be a viable approach to reducing organic fouling when biological oxidation, chemical coagulation, or chlorine oxidation are impractical or uneconomical by comparison.

Previous pilot testing of MF pretreatment with ozone using non-nitrified secondary effluent and polypropylene MF membranes at ECLWRF demonstrated that the concept of organic fouling control by ozonation was feasible (Gerringer et al., 2011). However, there are still many aspects of this treatment process requiring further investigation. For example, researching the use of ozone as pretreatment for polyvinylidene (PVDF) MF membranes would be more applicable to newer treatment plants, because PVDF typically is used in new installations or retrofits of existing MF processes. Other studies have shown ozonation of wastewater effluents can form N-nitrosodimethylamine (NDMA) (Andrzejewski and Nawrocki, 2007; von Gunten et al., 2010; Zimmermann et al., 2010). The purpose of this study was to investigate the implications of using preozonation in an IPR treatment train with PVDF MF and RO.

1.2 Important Considerations for the Use of Ozone in an Indirect Potable Reuse Treatment Train

Although the primary purpose of MF pretreatment with ozone would be to reduce organic fouling, there are other operational and water quality considerations that are pertinent to the implementation of ozone.

1.2.1 Ozone Dose Control

Ozone dose control is an important operational parameter for MF pretreatment with ozone. Because this process is not intended for disinfection, maintaining an ozone residual is unnecessary. In addition, residual ozone could signify an inefficient process that is increasing costs and posing a potential oxidation hazard for the downstream polymeric membranes. An optimized ozone dose control strategy would be capable of adjusting the dose in response to real-time water quality changes, thereby producing a relatively stable MF feed water quality with regard to organic fouling potential.

Selecting an appropriate control parameter is a critical component for the implementation of this treatment strategy. Common water quality parameters with the potential to control the ozone dose include ultraviolet transmittance at 254 nm (UVT) and oxidation-reduction potential (ORP). ORP is strongly affected by low dissolved ozone residuals (OzoneLab^{TM} Ozone Exposure Services, 2011) and could be used as a control parameter under those conditions. UVT measures the concentration of high molecular weight chromophores that may be present in wastewater treatment effluent, indicating how much "reactive" organic material is present. Ultraviolet absorbance at 254 nm, which is directly related to UVT, decreases with specific ozone consumption and can be analyzed easily and continuously (Bahr et al, 2007). Therefore, UVT is potentially a more sensitive indicator of how much ozone should be delivered and also has the advantage of permanently changing after ozonation. This factor compares favorably to ORP, which can decrease significantly once the ozone residual dissipates.

1.2.2 Effect on Downstream RO Performance

Another consideration is how MF pretreatment with ozone affects downstream processes and the ultimate product water quality. If reduced organic fouling for the MF membrane translates into better performance by the RO membranes, then implementation of this process would be viewed even more favorably. However, smaller organic molecules produced by ozone could pass through the MF membrane and potentially contribute to organic or biological fouling of downstream RO membranes. If organic fouling simply is shifted from the MF membranes to the RO process, this strategy might not be cost effective. Therefore, the effect of ozone pretreatment on RO performance and product water quality must be evaluated.

1.2.3 Ozonation Byproducts

The two ozonation byproducts of interest for this project were bromate and NDMA. Bromate is a potential human carcinogen with a U.S. Environmental Protection Agency (USEPA) maximum contaminant level of 10 µg/L based on an annual average in drinking water (USEPA, 2011). It can form during ozonation of bromide-containing waters through a series of reactions involving ozone and secondary oxidants such as hydroxyl and carbonate radicals (von Gunten, 2003a). Although RO membranes easily reject bromate (Marhaba and Medlar, 1994; USBR, 2009a; Sarp et al., 2011), documenting bromate formation and removal is important for understanding the effect of ozonation on the water quality of an IPR treatment train.

NDMA is a known animal carcinogen and designated as a probable human carcinogen by USEPA with a lifetime risk of contracting cancer of 10^{-6} at 0.7 ng/L (USEPA, 2009). For California drinking water, the Office of Environmental Health Hazard Assessment has established a public health goal of 3 ng/L, and the California Department of Public Health (CDPH) has established a notification limit of 10 ng/L (CDPH, 2012). NDMA can be created in municipal wastewater treatment effluents by direct introduction of NDMA into the sewer system from industrial discharges and the formation of NDMA during chlorination of NDMA precursors (Najm and Trussell, 2001). However, recent research indicates ozonation of wastewater treatment effluents can form NDMA (Andrzejewski and Nawrocki, 2007; von Gunten et al., 2010; Zimmermann et al., 2010). Significant NDMA formation from ozonation could have important implications on the sizing and design of advanced oxidation processes, which are included in all indirect potable reuse (IPR) treatment plants. Research is required to quantify the potential effect of MF pretreatment with ozone on NDMA formation in wastewater treatment effluent.

1.2.4 Contaminants of Emerging Concern

Another potential effect of MF pretreatment with ozone is the removal of contaminants of emerging concern (CECs). These compounds are not completely removed during wastewater treatment and are typically unregulated by federal and state agencies. Molecular ozone and hydroxyl radicals play a role in CEC oxidation, and many compounds have published kinetic rate constants that can be used to predict oxidation efficiency. Research has shown oxidation processes such as ozone can remove many CECs from wastewater effluents (Snyder et al., 2007) without adding hydrogen peroxide because EfOM serves as a promoter for free radical reactions. Snyder et al. (2007) found compounds with phenolic structures were removed below their detection limits. Similar results were recorded for compounds such as carbamazepine, gemfibrozil, hydrocodone, diclofenac, erythromycin, naproxen, oxybenzone, sulfamethoxazole, and trimethoprim. The potential beneficial effect of ozone on CECs could improve the value of implementing MF pretreatment with ozone in an IPR treatment train.

1.3 Research Objectives

This project investigated MF pretreatment with ozone for the treatment of a non-nitrified secondary effluent in a water reuse treatment train. Research used bench- and pilot-scale experiments design for improved scientific understanding of the benefits and limitations of this strategy for organic fouling control. This investigation also studied process optimization and ozone dose control to improve implementation at full-scale water recycling plants.

Specific objectives of this project are listed here:

1. Characterize organics in the plant influent, MF filtrate, and MF backwash at water recycling plants with different wastewater effluent sources to determine the effect of different levels of wastewater treatment on organic fouling potential.
2. Evaluate the efficacy of using UVT or ORP as the input parameter for automated ozone dose control.
3. Optimize the performance and operating conditions of PVDF MF membranes with preozonation.
4. Compare RO performance in the treatment trains with and without ozone.
5. Compare NDMA and CEC concentrations in the treatment trains with and without ozone.

The format of this report generally follows the objectives as listed. Chapter 2 provides a literature review summarizing research relevant to the objectives of this project. Chapter 3 compares EfOM characteristics at different water recycling plants and the ozone pilot plant used in this study. Chapter 4 presents ozone demand and decay data for the source water (non-nitrified secondary effluent) and evaluates ozone dose control by UVT and ORP. Chapter 5 describes MF performance, fouling, and water quality data during 8 months of pilot testing. Chapter 6 compares RO performance in treatment trains with and without MF pretreatment with ozone. Chapter 7 investigates the effect of ozone on the fate of CECs and

NDMA through the treatment train. Chapter 8 provides a comprehensive discussion of the test results, overall conclusions from the project, and recommendations for future research.

Chapter 2

Literature Review

2.1 Introduction

The scarcity of fresh water resources has created a great demand for innovative wastewater reuse technologies. Much of the water consumed in most cities eventually flows into wastewater treatment plants, becoming a potential source for water reuse applications. Wastewater is the only potential water source that will increase with the demand for fresh water that accompanies a growing population. Therefore, it is important to explore treatment technologies that will allow society to utilize this water source safely and efficiently.

Reuse of municipal wastewater requires treatment that meets quality standards specific for a particular application. The main issues associated with reuse of municipal wastewater are related to pathogens and micropollutants that can pass through conventional wastewater treatment plants and threaten public health. The level of treatment needed for water reuse varies based on the application. For example, landscape irrigation might only require tertiary treatment (filtration) and disinfection, but industrial applications, such as boiler water feed, typically requires advanced treatment such as microfiltration (MF) and reverse osmosis (RO). Indirect potable reuse (IPR) commonly includes MF and RO (Drewes et al., 2002) followed by an advanced oxidation process (AOP) for the removal of contaminants of emerging concern (CECs). CECs include chemicals such as pharmaceuticals and personal care products (PPCPs), endocrine disrupting compounds (EDCs), pesticides, and other unregulated micropollutants. When reused water is discharged to an aquatic environment, CECs can have an adverse effect on the environment (Asano et al., 2007).

During treatment for IPR applications, MF provides pretreatment for RO by removing particulates and colloidal organics that contribute to RO fouling. However, MF fouling is the major impediment to maintaining stable performance, because it lowers membrane flux, increases the frequency of chemical cleaning, and contributes to irreversible fouling that reduces treatment efficiency and membrane longevity. Several studies (Jarusutthirak et al., 2002; Croué et al., 2003; Her et al., 2003; Nguyen et al., 2009) have shown that organic matter is one of the main causes of membrane fouling, and the cake layer on membrane surface is mostly produced by high molecular weight (MW) organics. Pretreatment strategies that remove large MW organics could reduce organic fouling of MF membranes.

Free chlorine could be used to control organic fouling for polyvinylidene fluoride (PVDF) MF membranes treating nitrified secondary effluent. However, breakpoint chlorination chemistry can make it impractical to use free chlorine for non-nitrified secondary effluent. West Basin Municipal Water District's Edward C. Little Water Recycling Facility (ECLWRF) treats non-nitrified secondary effluent with polypropylene MF membranes that cannot tolerate free chlorine. A potential alternative to free chlorine oxidation for the control of organic fouling is ozonation, which has been shown to reduce the size of high MW organics (Camel and Bermond, 1998; Świetlik et al., 2004) and effectively reduce organic fouling (Hashino et al., 2001). Ozone also can be used for AOP in advanced wastewater treatment to oxidize CECs and reduce estrogenic activity. Recent research shows that a typical disinfection dose removes a large variety of EDCs and PPCPs below detection limits

(Snyder et al., 2007a, 2007b), suggesting MF pretreatment with ozone could provide the benefit of CEC removal.

However, ozonation also has been shown to produce byproducts that may pose risks to public health. For example, ozone can react with bromide ion to form bromate (Glaze et al., 1993), a suspected human carcinogen (U.S. Bureau of Reclamation [USBR], 2009a). In addition, recent studies have shown ozonation of wastewater treatment plant effluents can form N-nitrosodimethylamine (NDMA) (Andrzejewski and Nawrocki, 2007; von Gunten et al., 2010; Zimmermann et al., 2010). These findings demonstrate the need for additional research to investigate the byproducts of ozonation of non-nitrified secondary effluent.

This literature review has been developed to summarize previous research that is relevant to the use of ozone to pretreat non-nitrified secondary effluent. This document will discuss ozone chemistry, the effect of ozone on NDMA and CEC, and MF and RO fouling. The cited literature does not always involve the same type of water (non-nitrified secondary effluent), because some areas had limited research available on this type of water. In research that used other water sources, it is possible the water quality could have had a significant effect on the reported results.

2.2 MF Fouling

MF is an important unit process for treating wastewater for indirect potable water reuse. Its application has grown dramatically in the past decades, thanks to its efficacy in producing high-quality water at a relatively low cost (Furukawa, 2008). MF membranes are porous or non-porous water permeable polymeric films or ceramic matrices that can remove a wide range of aquatic substances through size exclusion (Huang et al., 2009). MF provides pretreatment for RO membranes, because it removes particulates, bacteria, and colloidal organics that cause fouling. However, MF is also vulnerable to fouling by the materials it removes. Fouling lowers membrane flux and increases the frequency of chemical cleaning while gradually contributing to irreversible fouling that reduces treatment efficiency and membrane longevity.

2.2.1 Fouling Mechanisms

MF fouling occurs when particulates, colloidal organics, microorganisms, or inorganic salts causes pore blockage, pore constriction, and cake formation. Pore blocking and constriction are mainly caused by small colloids that adsorb inside the pores, increasing membrane resistance. Cake formation is caused by larger colloids and particulates that create a layer of resistance to filtrate flow (Hilal et al., 2005) and lower membrane permeability (Huang et al., 2009; Farahbakhsh et al., 2004). Biofouling is caused mostly by biofilm growth on the membrane surface that reduces system performance (Al-Ahmad et al., 2000) and causes irreversible membrane damage (Lim and Bai, 2003).

Fouling can be characterized as reversible or irreversible. Reversible fouling is typically associated with cake formation (Ahmad et al., 2004), minimally influenced by membrane surface chemistry (Taniguchi et al., 2003), and can be removed through physical processes such as backwashing. This contrasts organic fouling, which is caused by high MW colloidal organics (MWH, 2005) that cause power blockage and constriction. Most organic fouling is reversible and can be removed by chemical cleaning. However, there is a portion of this fouling that is irreversible, meaning it causes a permanent loss of membrane performance.

Unlike reversible particulate fouling, irreversible fouling is strongly dependent on membrane surface chemistry (Taniguchi et al., 2003). Commercially available membranes are made mainly from hydrophobic polymers (e.g., polysulfone, polyethersulfone, polypropylene, polyethylene, and PVDF) for their outstanding chemical resistance and mechanical/thermal properties (Reddy et al., 2003; Wang et al., 1999). Research has demonstrated membrane materials play an important role in membrane fouling by influencing solute adsorption (Wakeman and Williams, 2002). An example of this dependence is a study showing irreversible fouling from a wastewater effluent was higher for a MF membrane made from PVDF compared to a MF membrane made from polyacrylonitrile (Kimura et al., 2006). The variability in irreversible fouling was likely caused by interactions between the colloidal organics and the membrane materials, which have different chemical properties.

Organic colloids are aquatic organic particles in the size range of 1 nm to 1 µm, including organic macromolecules such as polysaccharide, peptidoglycans, proteins, humic aggregates, and their clusters (Amy, 2008). The most severe type of fouling—pore blockage—can be caused by colloids, such as non-humic macromolecules (10 to 50 kDa), with a size similar to membrane pores (Lee et al., 2004). Research using size-exclusion chromatography (SEC) demonstrated high MW polysaccharides are likely to be the most significant organic foulants (Lozier et al., 2008). Kimura et al. (2004) found polysaccharide-like organic matter caused irreversible fouling. Other studies have suggested proteins also play a significant role in fouling. Nguyen et al. (2009) found proteins and polysaccharide-like compounds were significant foulants on MF and ultrafiltration (UF) membranes treating activated sludge-lagoon effluent. Research of MF membrane bioreactors also suggested high MW proteins and polysaccharides were important sources of fouling (Trussell et al., 2009). Chon et al. (2010) used SEC, fluorescence and infrared spectroscopy, and XAD 8/4 resins to show the hydrophilic fractions of organic matter—including protein-like substances and polysaccharides—were responsible for severe membrane fouling.

A potential reason for the effect of high MW organics on membrane performance is diffusivity. Larger organic macromolecules have lower diffusion coefficients, which were shown to increase concentrations and reduce solubility at the surface of UF membranes (Schäfer et al., 2004). As they accumulate, these colloidal organics can cause pore blockage and create a cake layer that increases flux resistance (Jarusutthirak et al., 2002).

2.2.2 Pretreatment Strategies

The identification of organic colloids as major foulants has been an important advance for the use of MF membrane (Huang et al., 2007; Laabs et al., 2004; Lee et al., 2004), because it can lead to effective pretreatment or control strategies that improve performance and reliability while reducing operating costs. Depending on the pretreatment strategy implemented, some combination of the physical, chemical and biological properties of the MF feed water will be modified. Huang et al. (2009) describes the mechanisms, effects, and applications of several pretreatment strategies for minimizing fouling of low-pressure membranes. These strategies include coagulation, adsorption, preoxidation, and prefiltration and can also compensate for poor removal of CECs and disinfection byproducts (DBPs) by MF (Huang et al., 2009).

Pretreatment strategies must be tailored to address the source of the fouling in a particular situation. Organics are the primary source of MF fouling in the non-nitrified secondary effluent feeding ECLWRF. Preliminary testing showed the source water contains a high percentage of high MW colloidal organics that are associated with MF fouling. Therefore, pretreatment processes targeting these foulants have the best chance of improving MF performance.

Possible pretreatment strategies at ECLWRF include coagulation, adsorption, biological oxidation and preoxidation. Coagulation can limit membrane fouling by aggregation of the colloidal fraction, thereby reducing pore blockage and constriction (Al-Malack and Anderson, 1996). However, this approach could require additional steps to clean the MF membranes (e.g., citric acid for iron removal) and coagulant residuals could affect downstream RO performance. Adsorption involves removing organic foulants using materials, such as powdered activated carbon, that are much larger than the pores of the membrane. However, these materials can increase fouling of MF membranes and can be difficult to remove from the treatment train (Huang et al., 2009). Preoxidation relies on an oxidant, such as ozone, to alter the physical and chemical properties of the organic material (Song et al., 2010). Prefiltration is unlikely to provide sufficient pretreatment, because the physical process used to separate particulates from the MF feed water would have poor removal of high MW colloidal organics. Considering the advantages and disadvantages of each pretreatment strategy, as well as the limited space available at ECLWRF, ozonation was selected for further study. Consequently, this literature review focuses on issues related to the use of ozone to pretreat non-nitrified secondary effluent in a water reuse treatment train including MF and RO.

2.3 Ozonation of Secondary Effluent

2.3.1 Effect of Ozonation on Organic Matter

The ozonation of organic pollutants involves two types of oxidation reactions, either direct reaction by molecular ozone (ozonolysis) or indirect reaction through radical species formed by the decomposition of ozone in water. Direct reaction with molecular ozone is favored at acidic pH. The Criegee mechanism, which cleaves molecules at carbon double bonds, is the reaction expected when molecular ozone reacts with organics (Langlais et al., 1991). It is also known that aromatic compounds are decomposed selectively through ozonolysis. These reactions create carbonyl functional groups, such as ketones and aldehydes, on the resulting organic molecules, which are smaller than the parent molecule.

Conversely, at high pH (> 8) when hydroxyl ion (OH^-) concentration is higher, the indirect reactions with radical species become more favorable. Equation 1.1 shows the ozone decomposition reaction with hydroxyl ion to produce hyperoxide ($HO_2^{\bullet}$) and superoxide radicals ($O_2^{-\bullet}$). Subsequent decomposition reactions produce hydroxyl radicals ($OH^{\bullet}$) that react with organics, although the intermediate radical species also could be involved with oxidation reactions. Other initiators of free radical reactions include hydrogen peroxide, humic substances, and ultraviolet light. Free radical reactions are nonselective and very powerful chain reactions, which can lead organic compounds to the ultimate mineralization (Rakness, 2005).

$$O_3 + OH^- \xrightarrow{k_1} HO_2^{\bullet} + O_2^{\bullet -} \qquad (1.1)$$

Research has shown ozonation reduces the size of high MW organics (Camel and Bermond, 1998; Świetlik et al., 2004) and effectively reduce organic fouling (Hashino et al., 2001). MW is reduced, because molecular ozone and/or hydroxyl radicals cleave the chemical bonds of organic molecules. This transformation creates smaller molecules with higher polarity than the original compounds. Polarity increases, because larger MW organics tend to be more hydrophobic than smaller MW organics and polar oxygen functional groups are added during oxidation. MW plays an important role in reactions with ozone, because higher MW organics tend to be more reactive with ozone than lower MW organics. Higher MW organics also can act both as a radical promoter and a hydroxyl radical scavenger (Westerhoff et al., 1999). In addition, the reduction of dissolved organic carbon,including mineralization of small organic molecules and the breaking of large MW molecules, are the main criteria for fouling reduction (Zhu et al., 2010). Ozonation also has been shown to improve the biodegradability of secondary effluent from a wastewater treatment plant (Wang et al., 2007).

2.3.2 CEC Removal by Ozonation

CECs refer to trace chemicals and other substances with typically low concentrations that are in the environment and may pose public health or ecological risks. These chemicals are found in drinking water sources impacted by wastewater effluents (Guo and Krasner, 2009) and can be added to the environment through the use of reclaimed water to irrigate crops (Calderón-Preciado, 2011). Their prevalence and persistence have led some researchers to suggest using them as markers for sewage contamination of ground, surface, and coastal waters (Nakada et al., 2008). Review articles are available that summarize the occurrence, fate, and effects of CECs on freshwater sources (Pal et al., 2010). However, CECs are not included in routine monitoring for drinking water nationwide but might be candidates for future regulation. The state of California does include CEC monitoring as part of the permit requirements for IPR, indicating regulations could depend on the source water being used and the intended purpose of the treated water. This section of the literature review will introduce different types of CECs before discussing ozone oxidation of these compounds.

CECs fit into different categories based on their sources and potential effects on humans or the environment. Common types of CECs are EDCs, pesticides, polyaromatic hydrocarbons (PAHs), polybrominated disphenyl ethers (PBDEs), and PPCPs. Table 2.1 lists specific chemicals within each classification, their sources, and the risks posed to the environment or public health. Additional discussion of the different types of CECs is included following the table and the paragraphs after it.

It has been shown that some CECs are persistent, and their complete removal cannot be achieved during conventional wastewater treatment process (Lishman et al., 2006; Ikehata et al., 2003). Removal of CECs via an AOP, such as ultraviolet light and hydrogen peroxide (UV/H_2O_2), typically is required for IPR. Ozone also can react directly with many CEC compounds (Wert et al., 2009), resulting in significant reduction at typical concentration used for water disinfection (Snyder et al., 2007a; Esplugas et al., 2007). Table 2.2 lists the removal of selected contaminants from treated secondary and tertiary effluent during ozone disinfection. A discussion of specific types of CECs and their removal by ozonation follow the table.

Table 2.1. Names, Sources, and Potential Environmental or Public Health Risks of Specific Chemicals within Each Listed Classification of CECs

Class	Name	Source	Potential Risks
EDC	17-α-ethinylestradiol	Oral contraceptive	Endocrine disruptor that can affect reproduction and sexual differentiation of wild fish (Scholz and Gutzeit, 2000).
EDC	Cholesterol	Plant and animal steroid	Endocrine disruptor (USBR, 2009b)
EDC	Estrone, 17β-estradiol, 17α-estradiol; estriol	Naturally occurring estrogen	Endocrine disruptor that can cause feminization of male fish (Lange and Dietrich, 2002; Thorpe et al., 2001).
EDC	Trenbolone	Steroid	Endocrine disruptor (Hotchkiss and Nelson, 2007)
Other	5-methyl-1H-benzotriazole	Aircraft deicing and anti-icing fluid	It bioaccumulates in fish fat and has adverse effects on aquatic life (Cancilla et al., 2003).
Other	Bisphenol A	Plasticizer	Some studies of laboratory animals exposed to bisphenol A found subtle effects on fetal development and newborns (National Toxicology Program, 2010).
Other	Tributyl phosphate (TBP)	Extractant and plasticizer	Endocrine disruptor
PAH	2,6-dimethyl-naphthalene		Several studies demonstrate the endocrine disrupting harm of the PAH group as a whole (Chakravarti et al., 2008; Kummer et al., 2008; Perera et al., 2009).
PBDE	DecaBDE	Flame retardants	Of all PBDEs, only DecaBDE has been tested for carcinogenicity (Janssen, 2007) and is considered by United States Environmental Protection Agency (USEPA) a possible human carcinogen (USEPA, 2005).
Pesticides	1,2,3-trichloropropan	Pesticide	Suspect carcinogen (Minnesota Department of Health, 2010)
Pesticides	Atrazine	Herbicide	Endocrine disruptor that has been found to disrupt sexual development of frogs at concentrations 30 times lower than levels allowed by USEPA (3 ppb) (Hayes et al., 2002).

Class	Name	Source	Potential Risks
Pesticides	DDT, DDE, DDD, DEET	Pesticide	Genotoxicity and endocrine disruption, diabetes, suspect carcinogen on humans. Toxic for crayfish, daphnids, sea shrimp, and many species of fish. They bioaccumulate and biomagnify up the food chain (McGlynn et al., 2008).
Pesticides	Diazinon	Insecticide	Endocrine disruptor that is toxic to birds, mammals, beneficial insects, and freshwater, estuarine and marine animals (National Pesticide Information Center, 2009, Cox, 2000).
PPCP	Benzophenone	Household and industrial chemical	Considered toxic and has had reproductive effects on organisms (Schlecht et al., 2004; Schlompf et al., 2001).
PPCP	Caffeine	Stimulant	Little research available; may be toxic for aquatic life because leads to an increase in growth of certain bacteria and a dramatic increase in ammonia concentrations (Gibson et al., 2009).
PPCP	Carbamazepine	Anticonvulsant	Carbamazepine exposure may result in growth retardation after in utero exposure and may also induce hypothyroidism (Mettayil et al., 2009; Horacek et al., 2007).
PPCP	Carbaryl	Household and industrial chemical	Highly toxic to fish (Xu, 2000)
PPCP	Cotinine	Antidepressant, tobacco, nicotine metabolite	Cotinine is a metabolite of nicotine in the body. It results from exposure to nicotine. It has been shown to have adverse effects on sperm parameters (Jorsarei et al., 2008).
PPCP	Gemfibrozil	Drug used to lower lipid levels	According to the results of Zurita et al. (2007), gemfibrozil should be classified as harmful to aquatic organisms.
PPCP	Ibuprofen	Anti-inflammatory	May affect the way fish spawn (Pomati et al., 2004).
PPCP	Indomethacin	Anti-inflammatory	Unknown
PPCP	Isophorone	Household and industrial chemical	Classified by USEPA as a Group C, possible human carcinogen (USEPA, 1999).

Class	Name	Source	Potential Risks
PPCP	Sulfamethoxazole, sulfathiazole, penicillin, enrofloxacin, carbadox, roxithromycin, azithromycin, clarithromycin, sulfadiazine, sulfathiazole, sulfapyridine.	Antibiotics	Antibiotic drugs discharged into municipal sewage may affect the biological process in sewage treatment plants, persist in aquatic environments, and contribute to the increasing resistance of pathogenic bacteria (Al-Ahmad et al., 1999). They may also affect aquatic organisms (Yamashita et al., 2006).
PPCP	Triclosan	Antibacterial agent	Potential endocrine disrupting properties on humans; toxic to aquatic bacteria at levels found in the environment (Veldhoen et al., 2006; Fair et al., 2009).

Table 2.2. Removal of Selected CEC Compounds in Full-Scale Treatment Systems that Include Ozone Disinfection

Analyte	Class	% Removal of CEC by Ozonation			# of Systems Used to Calculate Removal
		Minimum	Average	Maximum	
Bisphenol A	Other	76	86	100	3
Caffeine	PPCP	95	95	95	1
Carbamazepine	PPCP	> 71	88	100	6
DEET	Pesticide	48	67	100	5
Diclofenac	PPCP	100	100	100	1
Estradiol	EDC	> 93	95	97	2
Estrone	EDC	> 29	76	100	3
Galaxolide	PPCP	55	55	55	1
Gemfibrozil	PPCP	> 50	76	> 99	3
Ibuprofen	PPCP	> 41	73	100	4
Iopromide	PPCP	25	38	50	2
Naproxen	PPCP	> 92	97	100	4
Sulfamethoxazole	PPCP	> 90	93	99	4
Triclosan	PPCP	> 69	89	100	4

Source: USEPA, 2010

2.3.2.1 EDCs

This class of chemicals includes both naturally and synthetically occurring compounds and is frequently considered as a subset of PPCP, because many originate from pharmaceuticals. Estrogenic hormones are potent endocrine disruptors, discharged in the environment through wastewater effluent and agricultural runoff. Concentrations of hormones above 1 ng/L have been observed both in municipal wastewater effluent and effluent-dominated receiving waters (Desbrow et al., 1998; Kolodziej et al., 2003). Research has shown EDC concentrations of 1 ng/L can be enough to cause feminization of male fish (Lange and Dietrich, 2002).

Huber et al. (2004, 2005) showed the removal of several estrogenic hormones (e.g., 17β-estradiol and estrone) and the reduction of the estrogenic activity of 17α-ethinylestradiol from secondary treated wastewater at an ozone dose of 2 mg/L. Baig et al. (2008) also documented the removal of selected EDCs and oestrogenic compounds from secondary municipal wastewater at an ozone dose of 12 mg/L.

2.3.2.2 PPCPs

PPCPs include a large group of human-prescribed drugs (e.g., antidepressants, blood pressure), over-the-counter medications (e.g., ibuprofen), bactericides (e.g., triclosan), sunscreens, synthetic musks; veterinary medicines such as antimicrobials, antibiotics, anti-fungals, growth promoters, and hormones. Some chemicals, such as 17-α-ethinylestradiol, could be classified as both a PPCP and EDC. PPCPs enter domestic wastewater from toilets, bathtubs, laundry machines, and sinks. Several PPCPs were reported in wastewater effluent, surface water, and groundwater in Europe as early as 1990 (Buser et al., 1999, 1998a,b; Heberer and Stan, 1997). Triclosan, which is an antibacterial agent used in many soaps, is one of the most commonly detected PPCP (Buxton, 2000). It can react with free chlorine in tap water to form chloroform gas, which is classified as a probable human carcinogen by USEPA.

Several researches show the removal of PPCPs by ozone. Complete depletion of triclosan has been achieved with 4-mg/L ozone dose applied to effluent samples from conventional wastewater treatment plants (Suarez et al., 2007).

Akmehmet and Otker (2003) demonstrated the effectiveness of ozone treatment in degrading enrofloxacin and synthetic penicillin in synthetic wastewater at an applied ozone dose of 2.96 g/L. Ternes et al. (2003) showed the complete removal or conversion of 0.62 mg/L of sulfamethoxazole, indomethacin, and naproxen with 5 mg/L applied ozone dose in a biologically treated wastewater sample. Removal of carbadox and trimethoprim in the same research exceeded 95%. Huber et al (2005) found that an ozone dosage of 2 mg/L applied to secondary treated municipal wastewater at pH 7 can remove 90 to 99% of macrolides (i.e., roxithromycin, azithromycin, erythromycin-H_2O and clarithromycin) and sulfonamides (i.e., sulfadiazine, sulfathiazole, sulfapyridine and sulfamathoxazole).

Sui et al. (2010) tested the removal of 13 pharmaceuticals, including antibiotic, antilipidemic, anti-inflammatory, anti-hypertensive, anticonvulsant, stimulant, and antipsychotic and caffeine present in the secondary effluent of Beijing wastewater treatment plants. Ozonation MF/RO processes were reported to be very effective, lowering all target compounds except caffeine below their detection limits. The ozone dosage and contact time in the reaction tank was 5 mg/L and 15 min, respectively, and the pH was 6.5 to 8.0.

2.3.2.3 Pesticides

Pesticides represent a large number of unrelated chemicals that are used to prevent, destroy and repel a living organism that occurs where it is not wanted. Many pesticides are persistent organic pollutants introduced into the environment through agricultural runoff (Burkhardt-Holm, 2011).

Even though they are mostly removed via biodegradation and adsorption during wastewater treatment process, some pesticides with more hydrophilic characteristics require additional treatments to be removed. Nanofiltration, RO, and AOP are very effective in removing remaining pesticides. Ozone was generally effective at removing pesticides, herbicides, and insecticides, although it was ineffective on herbicides, such as atrazine, and pesticides, such as DDT and DEET (USBR, 2009b). Ozone followed by RO has been found effective in removing DEET (Sui et al., 2010).

2.3.2.4 PAHs, PBDEs and Other CECs

PBDEs are components of commercial formulations used in flame retardants, plastics of television cabinets and computers, consumer electronics, and small appliances. PAHs (also known as poly-aromatic hydrocarbons or polynuclear aromatic hydrocarbons) are potent atmospheric pollutants that are released during incomplete combustion of coal, oil, gas, or other organic substances. Other CECs include chemicals such as plasticizers (e.g., Bisphenol A) and nanomaterials (e.g., carbon nanotubes or nano-scale particulate titanium dioxide) (USBR, 2009b).

Diverse physical-chemical properties of these compounds make the removal very difficult through single treatments. Removal of bisphenol A from wastewater treatment plant secondary effluent by ozone has been documented by Bertanza et al. (2010).

2.4 Ozonation Byproducts

Several byproducts can be formed from the reactions of ozone and hydroxyl radicals with the organics and inorganics in water. The oxidation of natural organic matter (NOM) by ozone can lead to byproduct formation of nitrosamines, aldehydes, organic acids, and ketones (Glaze, 1986, 1987). Halogenated disinfection byproducts (DBPs) can be formed if bromide is present in the water (von Gunten, 2003a,b). An efficient ozone-dose control system can minimize ozone byproduct formation significantly (Bahr et al., 2007).

2.4.1 Bromate

Bromate is a potential human carcinogen with a maximum contaminant level of 10 µg/L based on an annual average in drinking water (USEPA, 2011). It can form during ozonation of bromide-containing waters through a series of reactions involving ozone and secondary oxidants such as hydroxyl and carbonate radicals (von Gunten, 2003a). Von Gunten and Pinkrnell (2000) provide a detailed accounting of the reaction pathways for bromate formation from bromide.

Many water quality parameters may influence bromate formation, but pH is one of the more important ones. At low pH (<7), either less $OH^{\bullet}$ formation will reduce the oxidation rate of hypobromous acid (HOBr) or a shift of HOBr and hypobromite (OBr^-) equilibrium to HOBr may prevent oxidation of OBr^- by ozone (MWH, 2005). While water temperature is a relatively minor factor, lower temperatures are associated with lower bromate formation caused by the temperature dependence of the dissociation coefficient (Croué et al., 1996). Ammonia addition can inhibit bromate formation by reacting with HOBr to form bromamine (MWH, 2005). As HOBr is consumed, the equilibrium reaction between OBr^- and HOBr continuously forms more HOBr, thus reducing the concentration of OBr^- available to react with ozone to form bromate.

Research has shown bromate concentrations increase with ozone dose (Zimmermann et al., 2010). Another recent study investigated bromate formation in wastewater applications. Wert et al. (2007) found bromate formation occurred in a tertiary wastewater effluent when the ozone dose exceeded the instantaneous ozone demand of the water being treated. Bromate formation exceeded 10 µg/L when the ozone dose was 4.5 mg/L or higher (ozone to total organic carbon [O_3:TOC] ratio of 0.6 or higher).

Studies have demonstrated RO membranes can remove bromate effectively from water (Marhaba and Medlar, 1994; USBR, 2009a; Sarp et al., 2011). Bromate concentrations in RO permeate are usually below the detection limit (Tam et al., 2003). Gyparakis and Diamadopoulos (2007) found RO membranes rejected 96.1% of bromate when treating ozonated seawater affected by groundwater. A similar removal efficiency also was found by van der Hoek et al. (1998). These findings are less important for drinking water applications, because removing bromate with RO membranes probably would be prohibitively expensive. However, high bromate rejection by RO membranes would mitigate the use of ozonation to improve low-pressure membrane performance during treatment for IPR, because RO membranes already are included in these treatment trains.

2.4.2 NDMA

NDMA is a known animal carcinogen and designated as a probable human carcinogen by the USEPA with a lifetime risk of contracting cancer of 10^{-6} at 0.7 ng/L (USEPA, 2009). For California drinking water, the Office of Environmental Health Hazard Assessment has established a public health goal of 3 ng/L and the California Department of Public Health (CDPH) has established a notification limit of 10 ng/L (CDPH, 2012). NDMA can be created in municipal wastewater effluents in two ways: (1) by the direct introduction of NDMA into the sewer system from industrial discharges and (2) during Title 22 chlorination of NDMA precursors (Najm and Trussell, 2001). Mitch and Sedlak (2002a) used model compounds to indicate dimethylamine (DMA), tertiary amines with DMA functional groups, and dimethylamides act as NDMA precursors during chloramination. DMA and tertiary amines containing DMA functional groups are both industrial chemicals and natural products of the metabolism of plants, mammals, and microorganisms. NDMA formation from these tertiary amines proceeds in two steps: nitrosation of DMA to NDMA and dealkylation of tertiary amine to DMA by reaction with chloramines or hypochlorite (Li et al., 2010).

Nitrosation during chlorine addition forms nitrosyl cation (NO^+) or other nitrogen-containing species during acidification of nitrite (NO_2^-). The nitrosyl reacts with DMA to form NDMA in a reaction that is very fast at pH 3.4 but slow at neutral pH. Reaction kinetics is enhanced by the presence of hypochlorous acid (HOCl), which rapidly oxidizes nitrite and eventually leads to the formation of a highly reactive intermediate, dinitrogen tetroxide (N_2O_4). This compound reacts with DMA to form NDMA. Equations 2-1 to 2-5 show the relevant chemical reactions (Li et al., 2010):

$$HOCl + NO_2^- \Rightarrow NO_2Cl + OH^- \qquad (2\text{-}1)$$

$$NO_2Cl + NO_2^- \Rightarrow N_2O_4 + Cl^- \qquad (2\text{-}2)$$

$$NO_2Cl + OH^- \Rightarrow NO_3^- + H^+ + Cl^- \qquad (2\text{-}3)$$

$$H^+ + NH_2Cl + NO_2^- \Rightarrow NH_3^- + H^+ + NO_2Cl \qquad (2\text{-}4)$$

$$DMA + N_2O_4 \Rightarrow NDMA \qquad (2\text{-}5)$$

During chloramination NDMA formation occurs by the reaction with organic nitrogen precursors via 1,1-dimethylhydrazine (UDMH) intermediate. UDMH formation increases with pH. In the presence of bromide NDMA formation is much more pH sensitive (Choi and Valentine, 2002; Mitch and Sedlak, 2002b).

$$NH_2Cl + \left(CH_3\right)_2 \Rightarrow \left(CH_3\right)_2 NNH + H^+ + Cl^- \qquad (2\text{-}6)$$

$$NH_2Cl + \left(CH_3\right)_2 NNH \ + H_2O \Rightarrow \left(CH_3\right)_2 NNO + 2NH_3 + 2H^+ + 2Cl^- \qquad (2\text{-}7)$$

Another NDMA formation pathway has been proposed during chlorination, in which dichloramine reacts with DMA precursor to form Cl-UDMH, and NDMA via oxidation by dissolved oxygen (Schreiber and Mitch, 2006).

$$NHCl_2 + (CH_3)_2 NH \Rightarrow (CH_3)_2 NNHCl + H^+ + Cl^- \qquad (2\text{-}8)$$

$$(CH_3)_2 NNHCl + O_2 \Rightarrow (CH_3)_2 NNO + HOCl \qquad (2\text{-}9)$$

A pathway involving hydroxylamine, which can be formed during ozonation and react with DMA to form UDMH, has been used to explain NDMA formation during ozonation at neutral and alkaline pH (Yang et al., 2009). Andrzejewski and Nawrocki (2007) also showed NDMA formation as result of strong oxidants, like ozone, reacting with DMA at higher pH (~10).

In a recent study by von Gunten et al. (2010), NDMA was formed during ozonation of waters containing dimethyl sulfide (DMS) when bromide was also present. During ozonation, bromide is oxidized to HOBr that reacts with primary amine of DMS to form Br-DMS. Br-DMS is then transformed in NDMA by ozone. NDMA will also form during ozonation of DMS in the presence of HOBr. Choi and Valentine (2003) showed bromide catalyze NDMA formation via HOCl-nitrite.

NDMA formation potential is strongly dependent on O_3:DMA ratio (Andrzejewski and Nawrocki, 2007). Higher O_3:DMA ratios were found to increase the NDMA/DMA conversion rate with increasing contact time. However, O_3:DMA ratios of 3.4 and higher were associated with peak NDMA/DMA conversion rates at 45 min of contact time and declining conversion rates beyond that. This result shows that increasing ozone dose and contact time initially increase NDMA formation until reaching a point where additional ozone begins to remove NDMA or reduce the rate of its formation.

2.5 Ozone Dose Control

Ozone dosage is an important operational parameter and should be optimized to harness the maximum process benefit at the lowest cost. Using too little ozone will save operational costs associated with the ozone system but will not achieve treatment goals. Excessive ozone doses consume more power and liquid oxygen than is beneficial and could increase negative side effects such as higher DBP formation (Liberti et al., 2000). The dose control method should employ automated adjustment of ozone production based on changing water quality to optimize operation and reduce operator attention.

Ozone is used as a disinfectant in drinking water treatment, which requires residual ozone to achieve the required level of disinfection using Ct (disinfectant concentration x contact time) calculations (Liberti et al, 2000). Determining the ozone residual is accomplished by measuring the liquid-phase ozone residual. However, ozone residual measurements are less reliable at low concentrations, making control by other water quality parameters more desirable under certain circumstances. Ultraviolet transmittance (UVT) and oxidation-reduction potential (ORP) are two possibilities for ozone dose control. UVT is related to ultraviolet absorbance at 254 nm (UVA), which is a common parameter used to measure aromatic organic compounds. UVA decreases with specific ozone consumption and can be analyzed easily and continuously (Bahr et al, 2007). Therefore, online UVT/UVA measurements are another tool that can be used to optimize the ozone dose to meet treatment objectives (Wert et al., 2009).

ORP is strongly affected by low ozone residuals (OzoneLab Ozone Exposure Services, 2011) and could be used in applications that do not require persistent residuals for any length of time. MF pretreatment is an example of such an application, because an ozone residual is unnecessary to achieve the required level of oxidation and could harm downstream membranes. Ozone decomposition forms oxygen and free radicals, the potential of the water to oxidize chemical species increases, thereby increasing ORP (Rakness, 2005). Developing a control system that targets a specified range of ORP immediately after ozonation could provide the desired level of control. ORP measurements for ozone-dose control have worked well in clean water systems but are more difficult in complex water systems (Suslow, 2004).

2.6 Effect of Ozonated Water on Membrane Processes

2.6.1 Low-Pressure Membranes

Several studies have shown the effectiveness of preozonation in reducing fouling of low-pressure membranes. In Lee et al. (2005c), influent wastewater from a municipal wastewater treatment plant was pretreated with ozone before MF filtration by PVDF membranes. Lower MW of organic compounds after ozonation reduced the thickness of the fouling layer and decreased permanent flux decline. Nguyen and Roddick (2010) showed a reduction in UF fouling by adding 10 mg/L of ozone to a highly colored activated sludge effluent. Genz et al. (2011) found preozonation with increasing ozone doses from 2 to 10 mg/L decreased the rate of flux decline during filtration of secondary effluent by a polymeric UF membrane. However, an increase in irreversible fouling, possibly caused by the formation of colloidal iron, also was observed after multiple filtration cycles. Zhu et al. (2008) investigated the effect of secondary effluent preozonation on MF membrane fouling in terms of membrane resistance. Results of that bench-scale study showed a dosage of 4.9 mg O_3/mg suspended solids reduced particle size and filtration resistance. Park et al. (2010) found a 5-mg/L ozone dose reduced flux decline by 38% in a bench-scale filtration system using a PVDF MF membrane.

Other research investigated the effect of maintaining an ozone residual through the membrane filter on organic fouling. These studies used PVDF and ceramic membranes, because those materials are tolerant of strong oxidants such as ozone. Schlichter et al. (2003) showed oxidizing a model humic acid solution (19 mg/L) with ozone (O_3:TOC ratio of 2.6) significantly reduced organic fouling of ceramic MF and UF membranes. The same study indicated ozone had no effect on fouling caused by inorganic suspended solids. Lehman and Liu (2009) demonstrated that ozone degraded colloidal NOM was responsible for fouling ceramic MF membranes. You et al. (2007) tested PVDF UF membranes that were treating tertiary effluent from an industrial park wastewater treatment plant. After 2 h of filtration, ozone pretreatment with a 4.0 mg/L residual in the MF filtrate limited flux loss to 10% compared to 45% without ozonation. Maintaining an ozone residual through the membrane also was shown to restore flux loss caused by organic fouling during filtration without ozonation.

2.6.2 High-Pressure Membranes

RO fouling affects membrane performance by lowering membrane flux, increasing operating pressure, and decreasing permeate water quality (Brown et al., 2008). There are several types of fouling that can occur in RO membrane systems: inorganic fouling or scaling (Shih et al., 2005; Lee and Lee, 2000), particulate and colloidal fouling (Gabelich et al., 2006a; Hoek and Elimelech, 2003), organic fouling (Hong and Elimelech, 1997; Lee et al., 2005b), biological fouling or biofouling (Schneider et al., 2005), and oxidative fouling (Gabelich et al., 2005).

After ozonation, there could be changes to the biological, organic, and oxidative fouling potential of the water. Ozonation is known to increase measures of the bioavailability of organic carbon such as assimilable organic carbon (Ramseier et al., 2011) and biodegradable dissolve organic carbon (Siddiqui et al., 1997). This effect can increase the risk of biofouling and is the reason ozonation typically is followed with biofiltration in water treatment applications. Research has shown ozonation changes organic matter characteristics such as polarity and size distribution (Gerringer et al., 2009). It is possible these changes could alter the organic fouling potential of the water, although it is unclear if the effect would be beneficial or detrimental. Polyamide RO membranes are also known to be very sensitive to ozone exposure (Glater et al., 1983). Therefore, the RO membranes must not be exposed to ozone residuals or else the membranes will be irreversibly damaged. Changes to scaling and particulate/colloidal fouling should be unchanged, because ozonation is unlikely to affect the solubility of scalants, such as calcium phosphate, and MF/UF pretreatment will continue to remove particulates and colloidal materials.

It is unclear what the net results on RO performance would be in a treatment train of ozonation, MF, and RO that was treating non-nitrified secondary wastewater effluent. There has been bench-scale research showing ozone pretreatment improved RO performance by providing better solids and organic removal (Brown et al., 2008). However, that study was performed using a simulated surface water rather than wastewater effluent and, therefore, might not be relevant. Wang et al. (2010) showed ozone pretreatment reduced RO fouling by transforming reactive functional groups of protein- and fulvic-like compounds into less sorbable organics. This improvement was at the cost of reduced rejection of small organic compounds and higher salt passage. Other studies (Pisarenko et al., 2011; Stanford et al., 2011, 2013) also have showed ozone pretreatment benefitted RO performance.

Chapter 3

Comparison of EfOM Characteristics at Three Water Recycling Plants

3.1 Introduction

Organic matter characteristics and concentration have been shown to affect organic fouling of microfiltration (MF) membranes (Chon et al., 2010; Nguyen et al., 2009; Lee et al., 2004). When MF is used in a water reuse treatment train, the effluent organic matter (EfOM) remaining after wastewater treatment that will have significant effects on organic fouling. Municipal water treatment plants that supply wastewater effluent to water recycling plants provide different levels of treatment based on the use and operation of the available unit processes. Because treatment affects the concentration and characteristics of EfOM, water recycling plants with the same MF membranes and operating set points could experience significantly different fouling rates. Therefore, comparing influent EfOM characteristics at water recycling plants with different levels of upstream wastewater treatment should indicate which wastewater effluent has more organic fouling potential and the relative importance of each unit process.

Common components of wastewater include primary treatment (sedimentation), secondary treatment (biological process and sedimentation), and tertiary treatment (beyond secondary). Primary treatment relies on physical separation of solids from sewage by gravity. Secondary treatment follows primary treatment by a biological process to reduce biological oxygen demand and, if design and operated properly, to remove nutrients such as nitrogen and phosphorus. After biological treatment, sedimentation removes suspended solids from the treated wastewater. Tertiary treatment refers to the addition of one or more processes that go beyond secondary treatment. Filtration, disinfection, and nutrient removal (if not achieved during secondary treatment) are examples of processes that could be classified as tertiary treatment. According to the U. S. Environmental Protection Agency (USEPA), centralized wastewater treatment system serve more than 75% of the country’s population (USEPA, 2004). The Clean Water Act requires all wastewater treatment plants (WWTPs) to provide secondary treatment, and it is estimated that more than 30% of those plants go beyond secondary treatment (USEPA, 2004). Therefore, a comparison of EfOM characteristics of WWTPs providing secondary and tertiary treatment would be relevant to most areas in the United States, especially if advanced wastewater treatment processes involving MF are being considered.

The degree of treatment, particularly biological oxidation, was expected to affect the fouling potential of EfOM. A study comparing the fouling rates of membranes in a membrane bioreactor found a longer solids retention time (SRT) lowered organic fouling because the additional biological oxidation reduced the molecular weight of the organics in the mixed liquor (Trussell et al., 2009). Other research has demonstrated organic fouling is associated with high molecular weight (MW) organics (Lozier et al., 2008). These studies demonstrated the importance of MW, which is influenced by the degree of biological oxidation on organic fouling of MF membranes.

3.2. Methods and Materials

3.2.1 Water Recycling Plants

One set of grab samples from three water recycling plants (Table 3.1) were collected for analysis on June 6, 2011. These facilities use MF to filter different types of municipal wastewater effluent as pretreatment for reverse osmosis desalination and advanced oxidation with ultraviolet light and hydrogen peroxide. West Basin Municipal Water District's (West Basin's) Edward C. Little Water Recycling Plant (ECLWRF) treats non-nitrified secondary effluent from the Hyperion Treatment Plant, Orange County Water District's (OCWD's) Groundwater Replenishment System (GWRS) treats nitrified secondary effluent from Orange County Sanitation District's wastewater treatment plants in Fountain Valley and Huntington Beach, and Water Replenishment District (WRD) of Southern California's Leo J. Vander Lans Advanced Water Treatment Facility (AWTF) treats nitrified and disinfected tertiary effluent from the Long Beach Water Reclamation Plant. Plant influent and MF filtrate were collected from all of these facilities. MF backwash was collected only at ECLWRF and GWRS because the layout or the MF backwash piping at AWTF did not permit the collection of MF backwash.

Table 3.1. Information Regarding the Water Recycling Plants Where Samples Were Collected for Comparing Plant Influent, MF Filtrate, and MF Backwash EfOM

Water District	Water Recycling Facility	Source Water	WWTP SRT (days)
West Basin	ECLWRF	Non-nitrified secondary effluent	1.5
OCWD	GWRS	Nitrified secondary effluent	5.5
WRD	AWTF	Nitrified tertiary effluent	8

3.2.2 Experimental Methods

EfOM samples were characterized by total organic carbon (TOC), MW fractionation, and excitation-emission matrix (EEM) fluorescence spectroscopy. These parameters were used as indicators of the relative organic fouling potential of the wastewater effluents being tested. The methods used to analyze for MW distribution and EEM fluorescence spectroscopy are described in more detail in the following.

3.2.2.1 MW Fractionation Experiments

One method for EfOM characterization was to measure the MW distribution of TOC, UVA, proteins, and carbohydrates. MW distribution was measured using 10 kDa ultrafiltration (UF) membranes (PLGC06210, Millipore, Billerica, MA) in a 200 mL stirred cell (Model 8200, Millipore, Billerica, MA). The stirred cell had a magnetic stirrer that mixed the sample to reduce cake formation and concentration polarization at the membrane surface. An argon gas cylinder pressurized the stirred cell to 30 psig to filter the water samples. Before filtration, the UF membranes were soaked in a deionized (DI) water bath (Barnstead Nanopure Ultrapure Water System, Thermo Scientific, Dubuque, IA) with water changes every 15 min for 1 h. After soaking, the UF membrane was placed in the stirred cell and filtered 100 mL of DI water. The filtered DI water was discarded and 160 mL of sample was added to the stirred cell. Only 80 mL of sample were filtered to minimize the increase in organic colloid concentration that occurred during filtration.

Fractionated and unfractionated samples were analyzed for TOC, UVA, proteins, and carbohydrates. Proteins and carbohydrates were measured using the methods described by Lowry et al. (1951) and Dubois et al. (1956), respectively. TOC and UVA were analyzed following Standard Methods 5310C and 5910B, respectively. The filtered sample contained colloidal and dissolved constituents that passed through the 10 kDa filter (MW < 10 kDa). The organic characteristics measured in the filtered sample were subtracted from the same characteristics of the unfiltered sample to calculate the values for the > 10 kDa fraction.

3.2.2.2 EEM Fluorescence Spectroscopy

The transformation of EfOM can be evaluated with highly sensitive EEMs, which qualitatively and quantitatively describe changes in fluorescence intensity. To develop an EEM, the organic matter in a water sample is excited by light of various wavelengths (e.g., 240−470 nm), and the corresponding fluorescent emissions are recorded over a similar range of wavelengths (e.g., 280−580 nm). These wavelength ranges are selected because of their applicability to environmental matrices in addition to instrument limitations. After collecting the excitation-emission intensities, the raw data set is then processed with mathematical software to account for blank response, correct for instrument- and matrix-specific effects, and to plot the final image. In addition to developing EEM images, this process also provides underlying fluorescence spectra (i.e., EEM cross sections at a particular excitation wavelength) that can be correlated to contaminant oxidation and disinfection.

Samples were collected in amber bottles, shipped in coolers with ice packs to the University of Arizona, and stored at 4 °C covered in aluminum foil to avoid degradation from ambient light. Samples were filtered with 0.7 µm muffled Whatman GF/F glass filters (GE Healthcare Life Sciences, Piscataway, NJ). Excitation-emission matrices were collected in a 3 mL square quartz cuvette cell (light path 10 mm × 10 mm, using a Cary 50 Eclipse fluorescence spectrophotometer (Agilent Technologies, Santa Clara, CA) and plotted with MATLAB (MathWorksTM, Natick, MA).

The spectra were collected at 5 nm increments for excitation (240−470 nm) and 1 nm increments for emission (280−580 nm). The slits were set up at 5 and 2.5 nm, respectively, with a scan average time of 0.1 s. Note there were exceptions for the first and sixth samples collected at the pilot plant. For the first sample, the excitation wavelengths measured were 240 to 450 nm. The raw EEM data were corrected for inner filtering effects (MacDonald, et al., 1997) and were used for regional integration.

Figure 3.1 is an EEM characteristic of secondary wastewater effluent because it includes intense fluorescence in all three regions, particularly in the regions associated with soluble microbial products and fulvic acids. As shown in Figure 3.1, EEMs include an upper boundary resulting from “bleeding” when the excitation and emission wavelengths are approximately equal to each other. Molecules cannot emit light at energy levels greater than the excitation source so emissions at wavelengths less than the excitation wavelength are ignored. Therefore, the region above the upper boundary is always blank. EEMs sometimes include a lower boundary characteristic of second-order light scattering, which occurs at emission wavelengths that are approximately twice the excitation wavelength. In contrast to the upper boundary, fluorescence data can be collected below the second-order scattering boundary. Figure 3.1 also provides delineations for the three organic regions described in Stanford et al. (2011), which were adapted from the five organic regions introduced by Chen et al. (2003). The regions were modified to account for the limitations (e.g., effective excitation range) of the spectrofluorometer used in this study. The regions also account for 15-nm safety factors near the “bleeding” and second-order scatter boundaries. Fluorescence in each region indicated the presence of specific organic fractions (Table 3.2).

The fluorescence intensities can be integrated within each zone using the three-region fluorescence regional integration (FRI) method proposed by Stanford et al. (2011), which was adapted from the five-region FRI method developed by Chen et al. (2003). It is important to note that the FRI method provides normalized total fluorescence intensities to correct for the different projected areas associated with each region. Changes in the total fluorescence intensities in each region can then be observed after treatment to assess the rate of change for each organic fraction. This indicates which fractions a particular treatment process preferentially targets. Example FRI data for the EEM in Figure 3.1 are provided in Table 3.3.

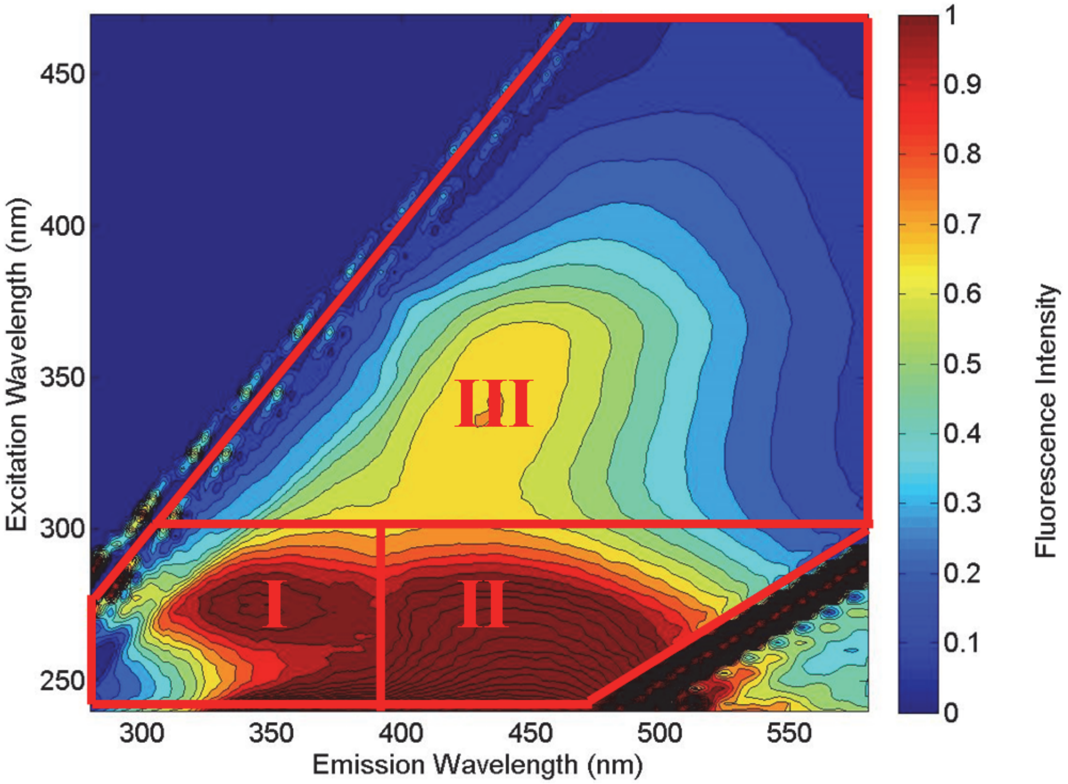

Figure 3.1. Excitation emission matrix for secondary effluent.

Table 3.2. EEM Fluorescence Regions

Region	Organic Fraction	Wavelength Range Excitation (nm)	Wavelength Range Emission (nm)
1	Aromatic proteins and soluble microbial products (SMPs)	240 – 300	280 – 380
2	Fulvic-like substances	240 – 300	380 – 580
3	Humic-like substances	300 – 480	300 – 580

Table 3.3. Example FRI Data for Secondary Effluent EEM

Region	Fluorescence	% Contribution
1	14,697	38
2	18,401	47
3	5777	15
Total	38,875	100

Note: Total fluorescence and relative contribution values are normalized to the projected regional areas.

3.3. Results and Discussion

There are two primary differences between the water recycling plants used in this study. First, the Long Beach Water Reclamation Plant feeding AWTF includes tertiary filtration and disinfection. These processes are not included before GWRS and ECLWRF. The second difference between the municipal wastewater treatment plants upstream of these water recycling facilities is SRT (Table 3.1). A longer SRT improves biological oxidation and is associated with reduced organic fouling during membrane filtration (Trussell et al., 2009).

The information in Table 3.1 indicates AWTF treated a nitrified wastewater effluent with the longest SRT and tertiary filtration. GWRS influent also was nitrified but had a lower SRT than AWTF and was not filtered. The low SRT of the activated sludge process upstream of ECLWRF produced a non-nitrified secondary effluent that also was unfiltered. Longer SRTs provide better biological oxidation and tertiary filtration provides additional benefits for solids removal. On the basis of this information, the quality of the wastewater effluents supplying the water recycling plants is expected to follow this trend: ECLWRF < GWRS < AWTF. This water quality trend should carry through to the MF filtrate and MF backwash samples. The following discusses how experimental results compared with expectations.

3.3.1 TOC and MW Distribution

TOC data for the plant influent, MF filtrate and MF backwash samples from the water recycling facilities are shown in Figure 3.2. These data indicate influent TOC concentrations are inversely proportional to the SRT of the upstream biological treatment process. The difference between SRT of 1.5 and 5.5 days was significant (19.7 versus 10.8 mg/L, respectively), whereas the difference between 5.5 and 8 days was much smaller (10.8 versus

9.0, respectively). The likely caused of higher TOC in ECLWRF influent was poor biological oxidation during secondary treatment. The lower influent TOC at AWTF relative to GWRS could be caused by a longer SRT, removal of particulate organics by filtration, or both.

Because MF removes particulate organics, MF filtrate data can be used to approximate the relative differences in the concentrations of colloidal and dissolved organics. As with the plant influent data, the TOC concentration in MF filtrate was highest at ECLWRF, indicating there was more colloidal and dissolved organics entering that water recycling facility. Although GWRS influent had a 20% higher TOC concentration than AWTF influent, the concentration was similar in their MF filtrates (7.2 and 7.6 mg/L, respectively). These data suggest the difference in water quality between GWRS influent and AWTF influent was attributed to the removal of particulates by tertiary filtration before AWTF.

The trend of the MF backwash data in Figure 3.2 follows a similar trend as the influent and MF filtrate data for ECLWRF and GWRS. No backwash data are available for AWTF, because the MF backwash piping did not permit a sample to be collected. However, lower TOC removal by MF at AWTF compared to GWRS suggested the TOC concentration in MF backwash at AWTF would have been lower than it was at GWRS. Water reuse plants, such as ECLWRF. recover water from MF backwash by adding coagulants before a clarifier that thickens the solids. Because there is a stoichiometric relationship between TOC concentration and coagulant dose (O'Melia et al., 1999), solids handling costs associated with coagulant addition should be lower at water reuse plants treating wastewater effluent with better biological oxidation.

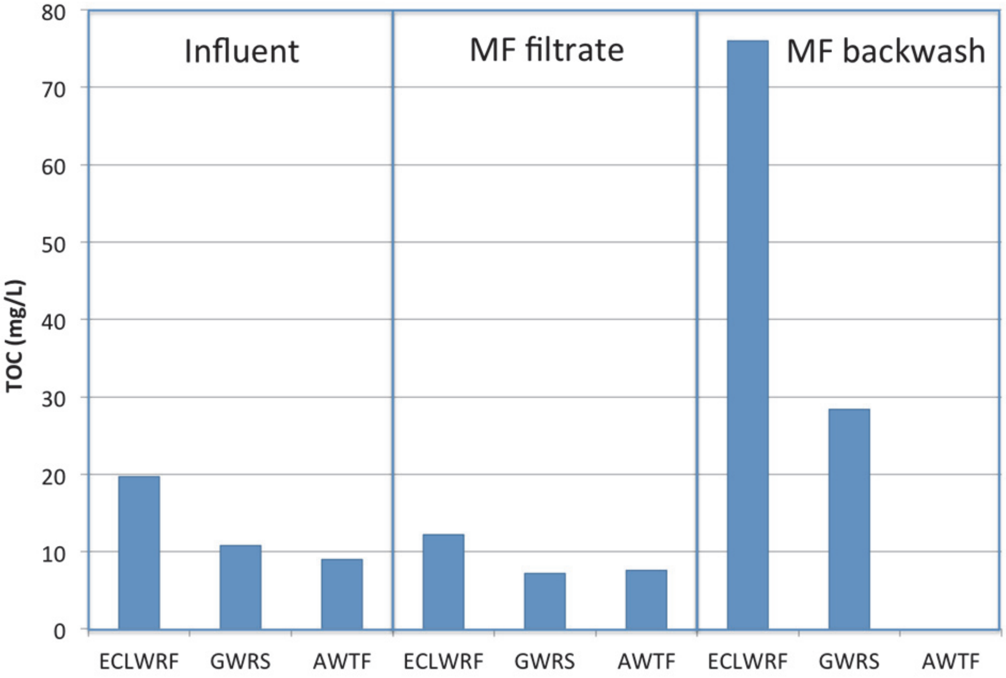

Figure 3.2. TOC concentrations for water samples collected from ECLWRF, GWRS, and AWTF.

Note: No MF backwash sample was collected from AWTF.

MW distribution data for UVA, carbohydrates, and proteins are displayed in Figures 3.3 to 3.5, respectively. Although the TOC samples were not fractionated for size, the MW distribution of TOC probably would have followed the trends in the Figures 3.3 to 3.5. As expected, the trends for these data were similar to each other and the trend of the unfractionated TOC samples. ECLWRF influent samples have the highest total concentrations and absorbance, followed by GWRS influent and then AWTF influent. This trend was found for both MW fractions: > 10 kDa and < 10 kDa. This finding is significant for the larger fraction because these are the organics most associated with organic fouling of low-pressure membranes (Lozier et al., 2008). Therefore, these data suggest organic fouling of MF membranes would be highest for ECLWRF lower for GWRS, and lowest for AWTF.

The same general trends for influent samples are seen for the MF filtrate samples. AWTF samples were the least changed by filtration, indicating a low amount of organics were removed during MF and available to cause fouling. MF filtrate from GWRS had similar UVA, and carbohydrate and protein concentrations as MF filtrate from AWTF. Except for protein concentration, ECLWRF had the largest reductions in concentrations and absorbance, suggesting the MF membranes at that plant removed the most organics. This removal also would be expected to result in the most organic fouling because the larger size fractions for UVA and carbohydrates were preferentially removed.

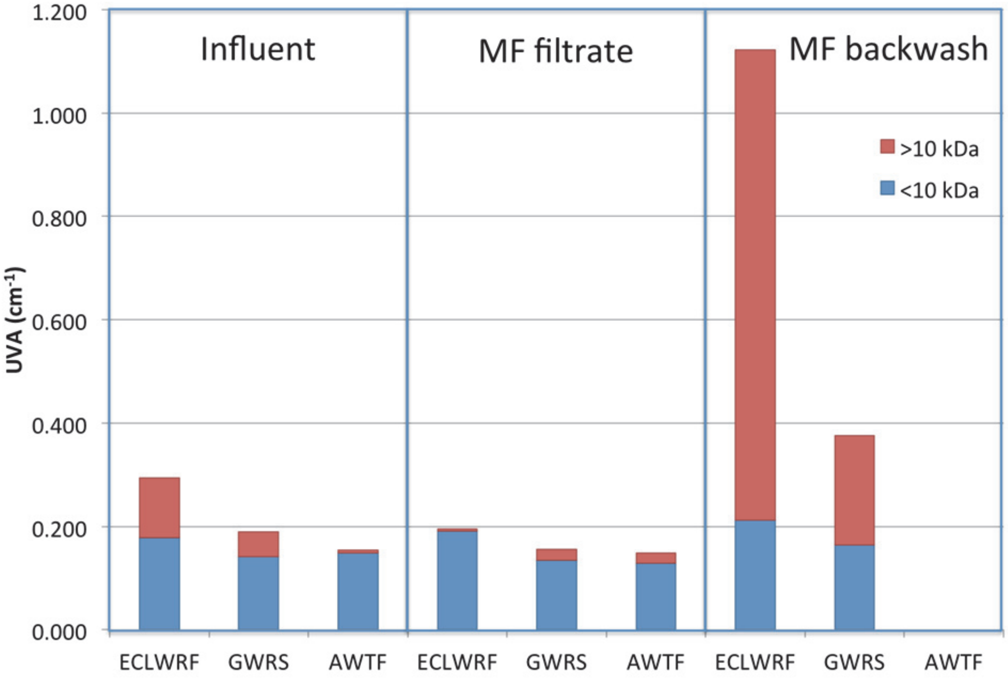

Figure 3.3. MW distribution of UVA for water samples collected from ECLWRF, GWRS, and AWTF.

Note: No MF backwash sample was collected from AWTF.

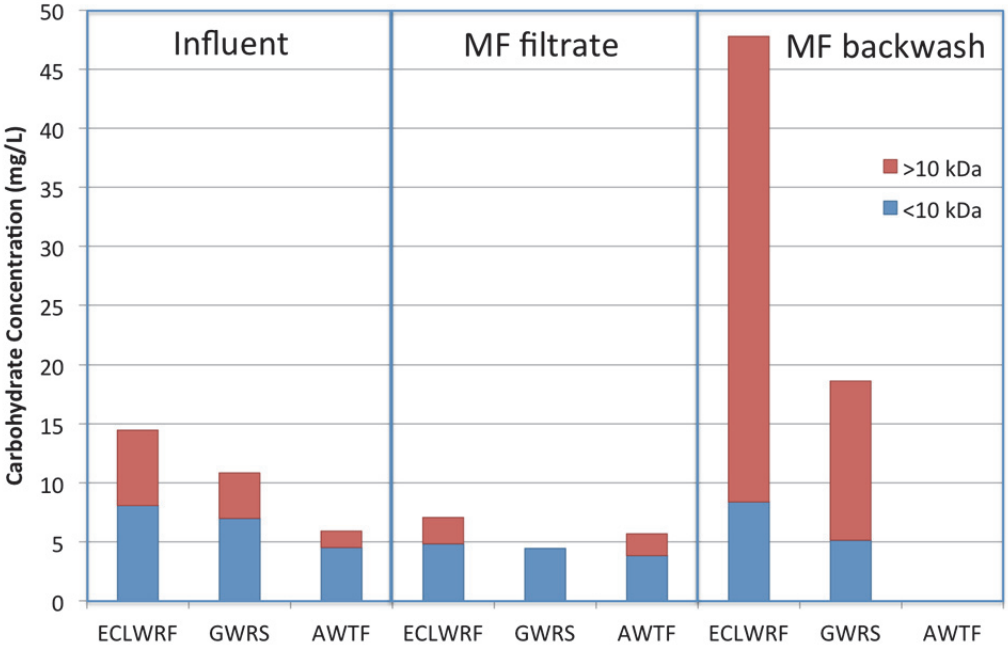

Figure 3.4. MW distribution of carbohydrates for water samples collected from ECLWRF, GWRS, and AWTF.

Note: No MF backwash sample was collected from AWTF.

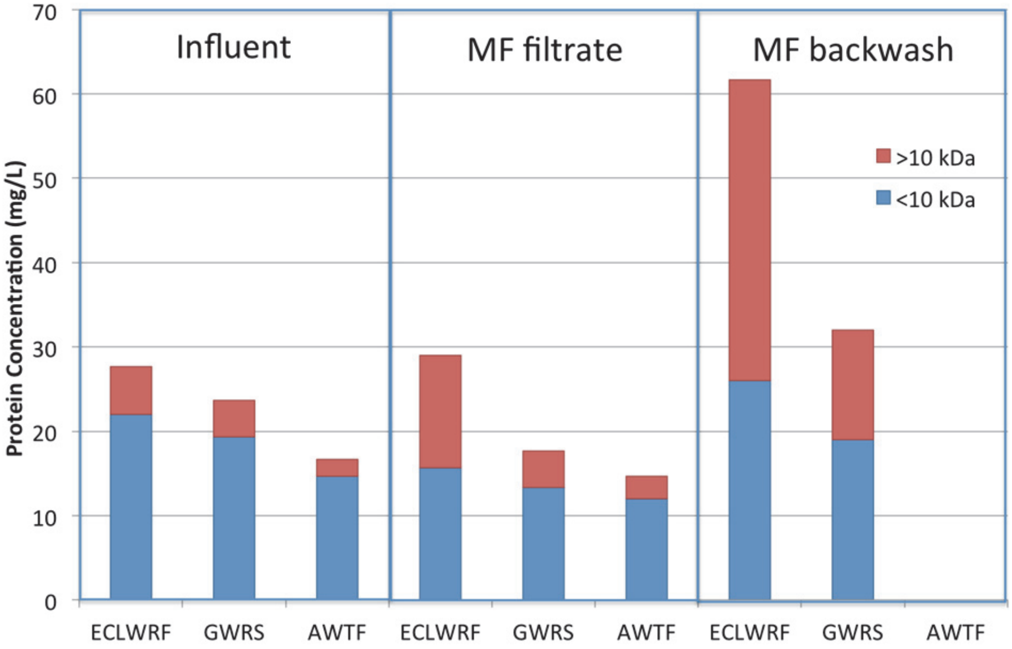

Figure 3.5. MW distribution of proteins for water samples collected from ECLWRF, GWRS, and AWTF.

Note: No MF backwash sample was collected from AWTF.

MF backwash was only available at ECLWRF and GWRS because there was no place to sample MF backwash from AWTF. If MF backwash samples could have been collected at AWTF, the expectation was the results would have been the same or better than it was at GWRS. A comparison of ECLWRF and GWRS data showed UVA, carbohydrates, and proteins were two to three times higher in MF backwash at ECLWRF. In addition, the larger MW fraction constituted a larger proportion of the organics in the MF backwash for ECLWRF than GWRS. The higher organic content of the MF backwash at ECLWRF indicates the MF membranes at this plant were removing more organics from the water than GWRS. The retention of high MW organics on the MF membranes at ECLWRF would likely cause higher rates of organic fouling (Trussell et al., 2009; Lozier et al., 2008) and could increase the membrane replacement frequency owing to irreversible fouling.

3.4. EEM Fluorescence Spectroscopy

Images from EEM fluorescence spectroscopy of samples collected from the influent, MF filtrate, and MF backwash of ECLWRF, GWRS, and AWTF are shown in Figure 3.6. A color scale from blue (minimum) to red (maximum) displays the fluorescence intensity of the EEM images. Table 3.4 shows the regional and total fluorescence intensity for each sample normalized to the ECLWRF influent sample.

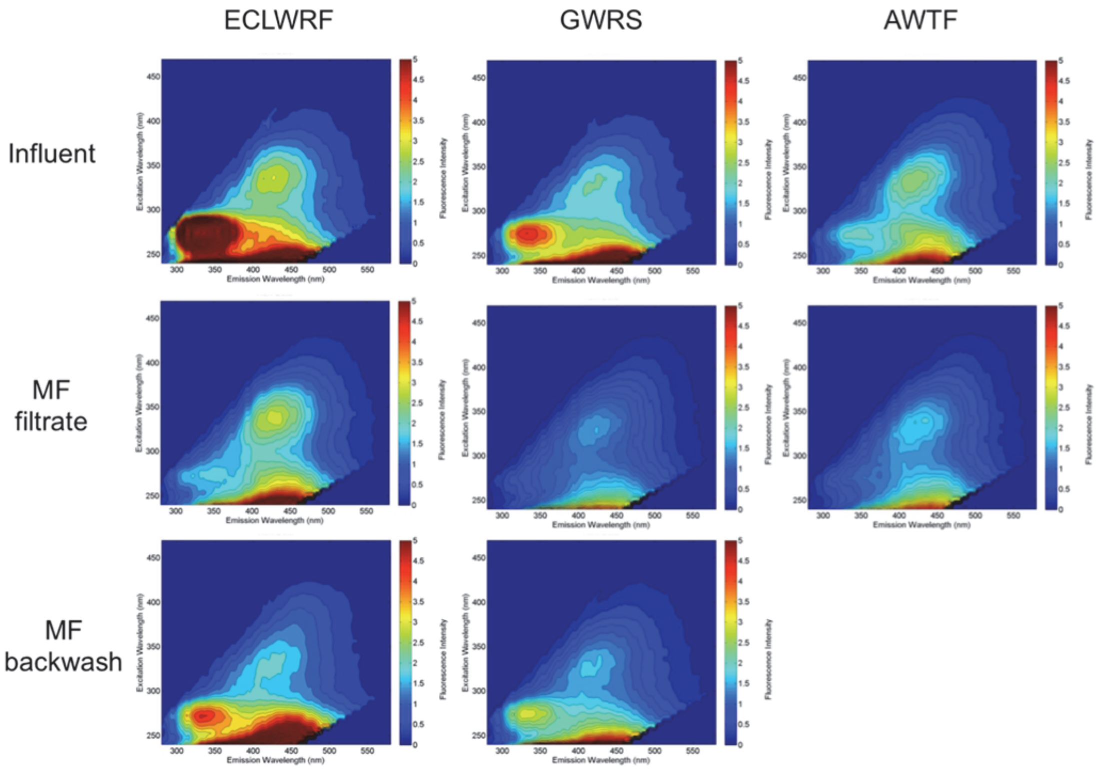

Figure 3.6. EEM spectra of plant influent, MF filtrate, and MF backwash samples from ECLWRF, GWRS, and AWTF.

Notes: No MF backwash sample was available from AWTF. For each image, the x-axis corresponds with the emission wavelength and the y-axis corresponds with the excitation wavelength. The fluorescence intensity scale is to the right of each image.

Table 3.4. Integrated Regional and Total Fluorescence for Each Sample

	Normalized Fluorescence Intensity							
	ECLWRF			GWRS			AWTF	
Region	Influent	MF Filtrate	MF Backwash	Influent	MF Filtrate	MF Backwash	Influent	MF Filtrate
I	1.00	0.29	0.52	0.52	0.16	0.36	0.28	0.17
II	1.00	0.75	1.03	0.88	0.45	0.62	0.70	0.52
III	1.00	0.92	0.78	0.78	0.52	0.59	0.79	0.62
Total	1.00	0.50	0.71	0.66	0.28	0.46	0.46	0.33

Notes: Samples were normalized to the ECLWRF influent sample. MF backwash data were not available for AWTF.

Comparing EEM images of the influent samples at the water reuse plant shows the fluorescence was the most intense for ECLWRF. This result followed the TOC, UVA, protein, and carbohydrate data. Because other research associated those data with a higher fouling potential than the influent to the other water reuse plants, the difference between these images also would be indicative of a higher fouling potential for ECLWRF influent. The largest difference between the images is in Region I, which is associated with aromatic proteins and SMPs. This difference is demonstrated more clearly by comparing the summation of the Region I fluorescence for ECLWRF influent (1.00) to GWRS influent (0.52) and AWTF (0.28). Fluorescence in Region I is associated with wastewater effluents (Baker et al., 2001), indicating wastewater treatment upstream of GWRS and AWTF have reduced the wastewater character of those effluents more than wastewater treatment upstream of ECLWRF.

Linear regressions (Microsoft® Excel® for Mac 2011, Microsoft Corp., Bellevue, WA) of plots of the SRT of the upstream WWTPs versus the corresponding normalized fluorescence data for Regions I to III of the influent samples showed a strong negative correlation between SRT and fluorescence intensity (Figure 3.7). Although there were only three data points available for each linear regression, this figure suggested a higher SRT decreased fluorescence intensity from ECLWRF (SRT = 1.5 days) to GWRS (SRT = 5.5 days) to AWTF (SRT = 8.0 days). The larger decrease in Region I fluorescence compared with Regions II and III (Figure 3.7) indicated aromatic proteins and SMPs could be more sensitive to the biological oxidation provided by a longer SRT.

The trend in the EEM data between ECLWRF and the other plants holds for the MF filtrate samples. The intensity of the fluorescence peaks (Figure 3.6), and the regional and total fluorescence (Table 3.4) are higher in the MF filtrate for ECLWRF. Reductions in fluorescence intensity after MF had the following trend among the regions: I > II > III. This result indicated more organics from Region I were retained on the MF membranes. Research into MBR fouling has demonstrated aromatic proteins (Meng et al., 2011) and SMPs (Rosenberger et al., 2006), both of which are located in Region I, are important contributors to organic fouling. Therefore, it is likely organics in Region I would cause fouling on MF membranes at the water reuse plants included in this study. Considering the influent Region I fluorescence and removal by MF at these plants, membranes at ECLWRF would be expected to experience the highest rate of organic fouling, followed by GWRS and then AWTF.

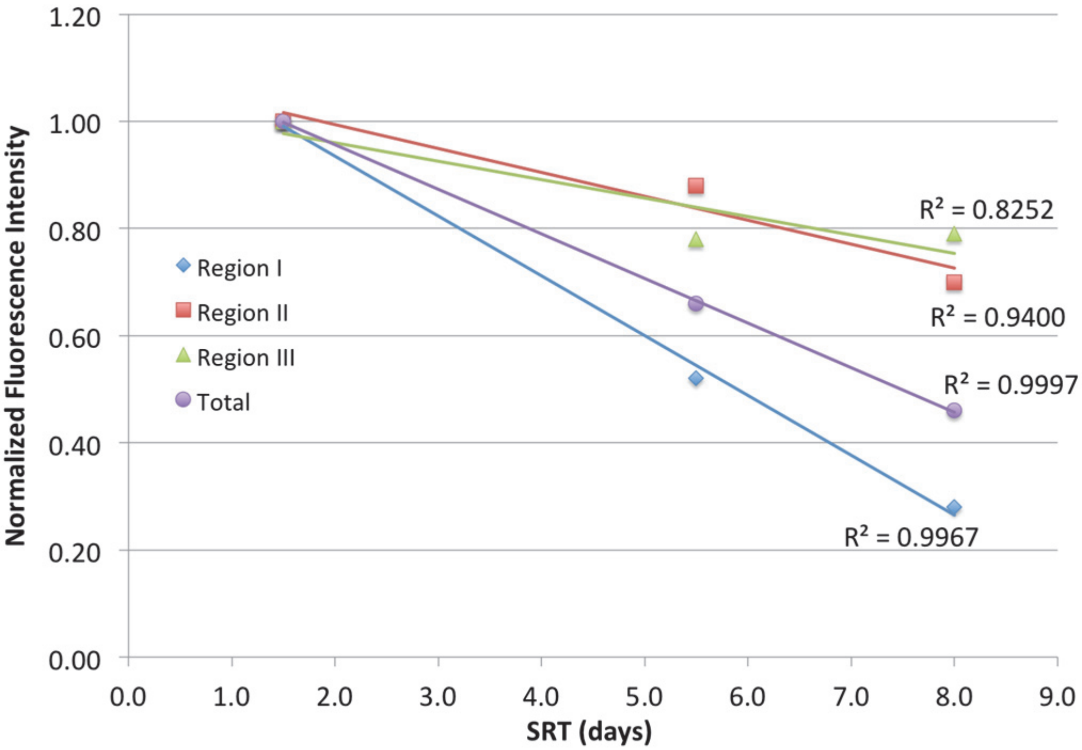

Figure 3.7. SRT of the WWTPs that supply the water reuse plants with wastewater effluent.

Note: This is versus plotted versus the regional and total fluorescence for the corresponding water reuse plant influent.

MF backwash data in Figure 3.6 and Table 3.4 indicated fluorescence intensity was higher for ECLWRF than GWRS (no MF backwash could be collected at AWTF). This finding was consistent with the differences among TOC, UVA, carbohydrate, and protein concentrations in MF backwash at the two water reuse plants. Note regional and total fluorescence values were generally lower in the MF backwash compared to the influent. This result contrasts with TOC, UVA, carbohydrate and protein data (Figures 3.2 to 3.5, respectively), which were significantly higher in the MF backwash. The likely cause of this difference is the filtration step of the EEM procedure, which was not duplicated in the measurement of the other water quality parameters. The cake layer removed by backwashing has been shown to contain high MW organics (Lee et al., 2005a) that should be more easily removed by that filtration step than lower MW organics.

3.5. Conclusions

Organic characterization of the wastewater effluents entering ECLWRF, GWRS, and AWTF demonstrated water quality was better from WWTPs that had higher SRTs. ECLWRF influent had higher concentrations of TOC, carbohydrates, and protein, and more UVA than the influents to the other treatment plants. In addition, more of the organics in ECLWRF influent were in the larger MW fraction (>10 kDa) associated with MF fouling (Trussell et al., 2009; Lozier et al., 2008). Organic characterization also found less of the large MW organics in MF filtrate, particularly at ECLWRF. These data indicated MF membranes at ECLWRF, which treated non-nitrified secondary effluent, were likely to experience more organic fouling than MF membranes at GWRS and AWTF, which treated nitrified secondary effluent and nitrified tertiary effluent, respectively. The difference between influent water quality at GWRS and AWTF was less pronounced but still noticeable, suggesting organic fouling of MF membranes could be higher at GWRS.

These findings have great significance when evaluating wastewater effluents for water reuse treatment trains using MF membranes. Low SRT WWTPs with high levels of organic foulants would require different pretreatment and design criteria than high SRT plants with lower levels of organic foulants. Higher SRTs provide better biological oxidation, suggesting improvements in upstream secondary treatment process as one method to reducing organic fouling. Another possible approach would be to substitute biological oxidation with chemical oxidation, which has been shown to reduce organic fouling of MF membranes treating wastewater effluents (Genz et al., 2011; Zhu et al., 2008; Lee et al., 2005c). Providing chemical oxidation that transforms influent water quality of a plant like ECLWRF to the water quality plants like GWRS and AWTF would have the potential to reduce MF fouling significantly. The effect of ozone oxidation of ECLWRF influent on water quality and MF performance is discussed in Chapters 4 and 5, respectively.

Chapter 4

Ozone Demand/Decay and Automated Ozone Dose Control

4.1 Introduction

Various approaches were taken to better understand the fate of ozone in the non-nitrified secondary effluent treated by the pilot plant. Bench-scale ozone demand and decay tests provided a basis of comparison with other waters and an understanding of the transferred ozone doses required to maintain an ozone residual. The persistence of an ozone residual was a concern because ozone exposure could damage microfiltration (MF) membranes, MF module components, or reverse osmosis (RO) membranes. Experiments with the pilot-scale ozone system investigated the effect of incremental increases in the transferred ozone dose on ultraviolet absorbance at 254 nm (UVA), ultraviolet transmittance at 254 nm (UVT) and oxidation-reduction potential (ORP).

Additional testing was performed to evaluate water quality parameters for ozone dose control. UVA was a good candidate, because it decreases with specific ozone consumption and can be easily and continuously analyzed (Bahr et al., 2007). UVA, which is directly related to UVT, has been used to optimize ozone dose to meet treatment objectives (Wert et al., 2009), suggesting it could be a useful parameter for this study. ORP was another parameter considered for controlling ozone dose because it can be significantly increased by ozonation (Lucas et al., 2009), has been used to control oxidant addition in other research (Yang et al., 2001), and has been shown to be promising for controlling ozonation (Yu and Yu, 2000). ORP has been shown to work well in clean water systems but is more challenging to implement in complex water systems (Suslow, 2004), which includes the non-nitrified secondary effluent used during pilot testing. Considering these earlier research efforts, UVT and ORP were selected as the water quality parameters to be tested for controlling automated adjustments to the ozone dose. The goal of this control strategy was to minimize the ozone dose while still providing enough oxidation of the effluent organic matter (EfOM).

4.2 Bench-Scale Ozone Demand and Decay Testing

These tests were intended to evaluate the ozone demand and rate of residual decay of the pilot plant influent at West Basin Municipal Water District's Edward C. Little Water Recycling Plant (ECLWRF). These data would help develop an understanding of the amount of ozone required to achieve the project goal controlling organic fouling of MF membranes. In addition, these experiments permitted comparisons with the ozone demand of other wastewater effluents.

4.2.1 Methods and Materials

4.2.1.1 Bench-Scale Ozonation of Pilot Plant Influent Samples

The approach described here was adapted from the method for measuring ozone demand described by Rakness (2005). A stock ozone solution was prepared by bubbling gas from an ozone generator (ATALS 30, Absolute Ozone, Edmonton, Canada) through deionized (DI) water. To minimize ozone decay, the DI water was cooled to −0.4 ºC with dry ice and its pH was lowered to 3.5 by adding 0.1 mL of 2.5 N hydrochloric acid per L of DI water. The ozone concentration of the stock was calculated using the gravimetric indigo standard method (Bader and Hoigne, 1982). The stock solution was collected in a 125 mL Erlenmeyer flask containing 10 mL of indigo trisulfonate reagent. The sample volume was gravimetrically determined by comparing the total weight of the indigo-sample mixture and the empty flask with the initial weight of the indigo and flask. The initial weight of indigo was the weight of the blank that is prepared adding 10 mL of indigo trisulfonate reagent and 90 mL of DI water in a 125 mL Erlenmeyer flask. Ozone decolorized the indigo trisulfonate reagent, allowing the concentration to be determined by measuring the change in absorbance at 600 nm using the following equation 4.1:

$$\frac{mg}{L}O_3 = \frac{(A_B \times 100) - (A_S \times V_T)}{f \times V_S \times b} \tag{4.1}$$

A_B and A_S = absorbance of blank and sample, respectively, at 600 nm;

V_S = volume of reacted sample in mL [(final weight – tare weight) g x 1.0 mL/g] – 10 mL;

V_T = total volume of reacted sample in mL [(final weight – tare weight) g x 1.0 mL/g];

b = path length of light in the spectrophotometer (1 cm);

f = sensitivity coefficient (0.42/mg/cm).

Absorbance at 600 nm was measured by a spectrophotometer (DR 5000, Hach Co., Loveland, CO), and ozone concentration was calculated using equation 1. Once the stock solution of ozone was created and its concentration measured, a known volume of this stock solution was added to a known volume of pilot plant influent and stirred for 10 s. During the first minute, samples were withdrawn every 20 s and added to flasks containing 2 mL of indigo solution to measure the ozone residual. The ozone demand was defined as the ozone consumed during the first minute of the experiment. After the first minute, the sampling frequency was reduced to once per minute until the ozone residual was less than 0.1 mg/L. This decay profile was used to determine the ozone demand and rate of decay of the water sample.

4.2.1.2 Sample Collection and Analysis

Two pilot plant influent samples were collected on different days in April 2011 and another pilot plant influent sample was collected in January 2012. All samples were measured for UVA, turbidity, and total organic carbon (TOC) and then ozonated following the method described in Section 4.2.1.1. Water quality data and test conditions are shown in Table 4.1. The first April sample was dosed with 15.9 and 12.0 mg/L ozone (Tests 1 and 2, respectively) and the second April sample (Test 3) was dosed with 15.9 mg/L ozone. During Tests 1 and 2, ozone residual measurements were made every 20 s for the first minute after ozone addition and every minute thereafter until the residual dissipated. After observing the high ozone demand and rapid residual decay after those tests, ozone residual measurements for Test 3 were performed every 15 s for the first 3 min after dosing and then every minute until the residual was gone.

Table 4.1. Water Quality and Test Conditions for Bench-Scale Ozone Demand and Decay Experiments Using Pilot Plant Influent Water

Test	Ozone Dose (mg/L)	TOC (mg/L)	O_3:TOC Ratio	Temp (°C)	UVA (cm^{-1})	UVT (%)	SUVA (L/mg•m)	Turbidity (NTU)
1	12.0	12.7	0.9	20.3	0.404	39.4	3.2	9.2
2	15.9	12.7	1.3	20.3	0.404	39.4	3.2	9.2
3	15.9	13.0	1.2	23.5	0.440	36.3	3.4	10.1
4	4.6	10.6	0.4	19.7	0.271	53.6	2.6	5.4
5	5.5	10.6	0.5	20.3	0.271	53.6	2.6	5.4
6	10.6	10.6	1.0	20.3	0.271	53.6	2.6	5.4
7	16.0	10.6	1.5	19.7	0.271	53.6	2.6	5.4

Note: Sample pH was not measured but would have been approximately 7.0 for all experiments.

The sample from January 2012 was dosed with 4.6, 5.5, 10.6 and 16.0 mg/L. The lowest dose was the minimum dose that could be delivered by the pilot plant ozone system as it was configured during sampling. The dose of 5.5 mg/L was the dose set by the automated dose control system based on a dead band of 58 to 60% for the ozone effluent UVT at the time of sample collection. More details regarding the automated ozone dose control system are provided in Section 4.3. The dose of 10.6 mg/L matched the TOC concentration, so this test condition had an ozone to TOC (O_3:TOC) ratio of 1.0. The highest dose matched the maximum design dose for the full-scale ozone system that was being installed at ECLWRF. Ozone residual measurements were performed every 20 s for the first minute, every minute until 10 min, every 2 min until 20 min, and every 6 min thereafter.

Factors such as ozone dose, natural organic matter characteristics and concentration, pH, and temperature affect ozone demand (Rakness, 2005). For all measured parameters, the water quality of the April 2011 samples was 20 to 80% worse than the water quality of the January 2012 sample (Table 4.1). These differences highlight the temporal variability in the non-nitrified secondary effluent feeding the pilot plant. The EfOM concentrations as measured by TOC and aromaticity in the secondary effluent for Tests 1 to 3 should result in high ozone demand and more rapid ozone decay compared with the later tests with better quality secondary effluent. Although the pH of the water samples was not measured before testing, the pH of daily grab samples at the pilot plant where the samples were collected averaged 7.0 with a standard deviation of 0.1. Therefore, it is likely the pH before adding the stock ozone solution was approximately 7.0. The temperature was approximately 20 °C for all tests except Test 3, when it was 23.5 °C.

4.2.1.3 Instantaneous Ozone Demand Calculation

There is no consensus in the literature regarding the definition of instantaneous ozone demand (IOD), which includes the initial demand and rapid decay after ozonation. Common definitions include the ozone consumption during the first 20 s (Hasegawa et al., 2008), 30 s (Wert et al., 2009), and 1 minute (Rakness, 2005) after ozonation. This report uses the definition in Hasegawa et al. (2008), which is expressed mathematically as the transferred ozone dose minus the ozone residual 20 s after ozonation. Because ozone residual was measured every 15 s during the first minute of Test 3, IOD for that test was calculated using the residual measured 15 s after ozonation, as this was the measurement closest to 20 s. The ozone concentration was integrated over the contact time to determine the ozone concentration-time (CT) following Rakness et al. (2005).

4.2.2 Results and Discussion

Ozone demand and decay curves from Tests 1 to 7 are shown in Figure 4.1. Figure 4.2 focuses on the first 7 min of data from Figure 4.1 to provide more detail for the tests with residuals that dissipated quickly. The ozone demand and decay curves follow the general pattern that would be expected based on the water quality data shown in Table 4.1. Ozone decay was high during Tests 1 to 3, as shown by the rapid decline in ozone residual during those tests. Even with a transferred ozone dose of 15.9 mg/L during Tests 2 and 3, the ozone residual dissipated in less than 6 min. At a similar dose during Test 7, the ozone residual was persistent for more than 30 min. Because temperature and pH were similar during Tests 2 and 7, EfOM characteristics and concentration were the likely cause of the difference between their ozone demand and decay curves. Research has shown a positive correlation between specific UVA (SUVA) and reactivity with oxidants such as ozone (Westerhoff et al., 1999), suggesting the higher SUVA values during Tests 2 and 3 contributed to higher ozone demand and faster ozone decay.

Figure 4.3 shows the first-order reaction rate kinetics of the ozone residual for Tests 1, 2, 3, 6, and 7. The slopes of those lines provide the first-order ozone decay rate constants (k′) for the corresponding test. Table 4.2 displays the ozone dose, O_3:TOC ratio, IOD, k′ and ozone CT for all of the tests. These data show IOD and k′ were highest for the experiments using the poor quality secondary effluent (Tests 1 to 3) compared to the tests using better quality secondary effluent (Tests 6 and 7). CT was higher during Tests 6 and 7 than Tests 1 to 3, but even the relatively low CTs when using poor quality secondary effluent indicated there should have been significant disinfection during the time an ozone residual was present. These data demonstrate disinfection is a potentially beneficial side effect of using ozone for MF pretreatment in a water reuse treatment train.

Comparisons with other published data can be performed be selecting O_3:TOC ratios that are the same or similar to those used in this research. Bench-scale testing of three tertiary wastewater effluents by Wert et al. (2009) measured k′ ranging from 0.36 to 0.59 min^{-1} when the O_3:TOC ratio was 1.0. Comparable O_3:TOC ratios during Test 1 (0.9) and Test 6 (1.0) produced k′ values of 3.07 and 0.1 min^{-1}, respectively. The secondary effluent used for Test 1 exhibited a much faster ozone decay rate than the tertiary effluents used in Wert et al. (2009). Conversely, the ozone residual was much more stable in the secondary effluent tested during Test 6 than it was in the tertiary effluents from Wert et al. (2009). These data highlight the significant variability in the rate of ozone decay in the secondary effluent that was treated used during pilot testing.

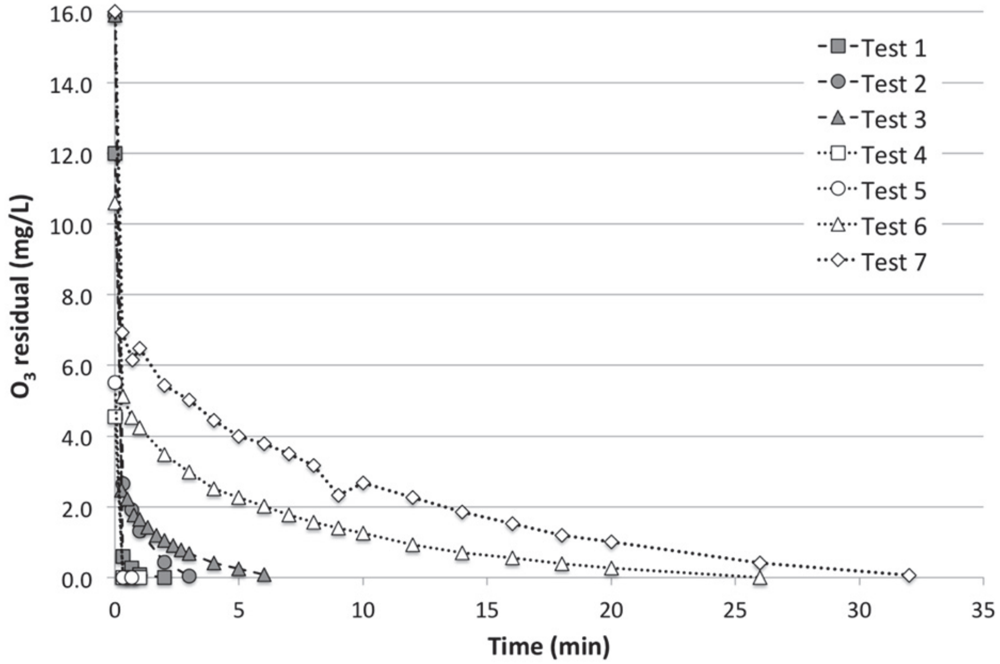

Figure 4.1. Results of ozone demand and decay tests.

Note: The initial ozone dose was reported at 0 min with subsequent data representing the measured ozone residual.

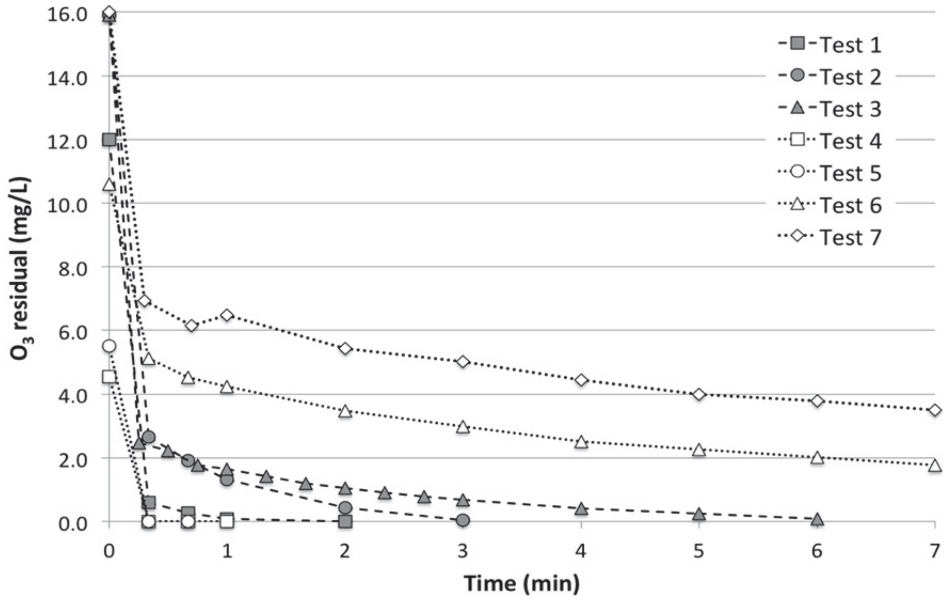

Figure 4.2. Results of the first 7 min of the ozone demand and decay tests.

Note: The initial ozone dose was reported at 0 min with subsequent data representing the measured ozone residual.

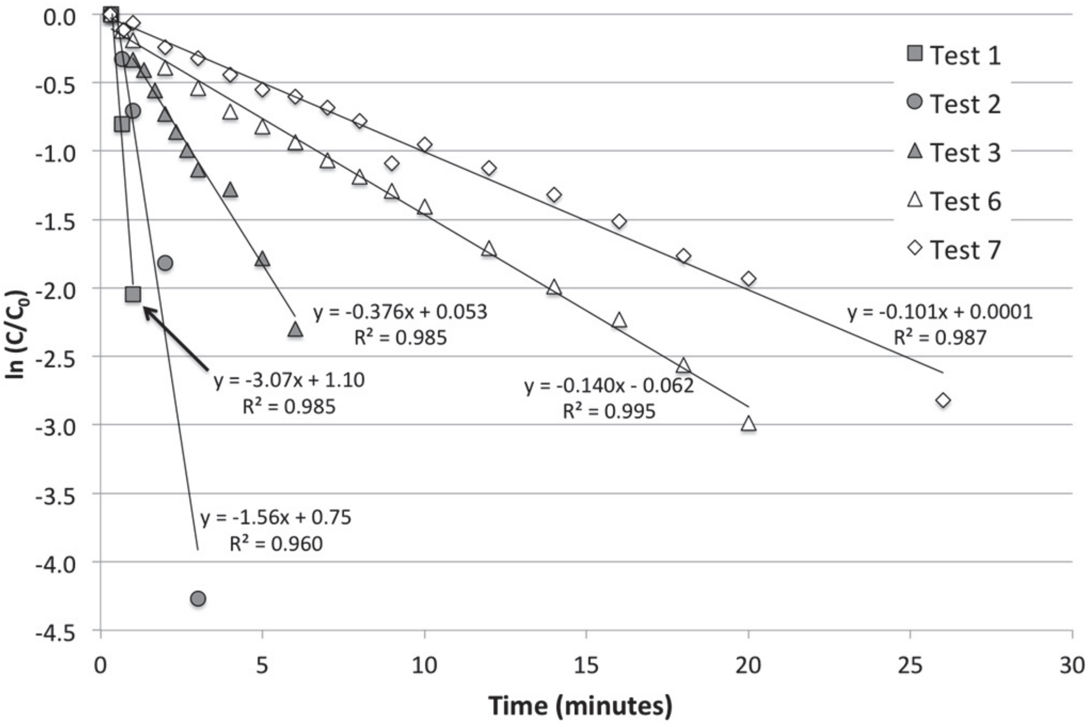

Figure 4.3. First-order reaction rate kinetics after satisfying IOD.

Note: Tests 4 and 5 were omitted from this figure because an ozone residual was never detected.

Table 4.2. Data from Ozone Demand and Decay Testing

Test	Ozone Dose (mg/L)	O_3:TOC Ratio	IOD (mg/L)	k′ (min^{-1})	CT (mg-min/L)
1	12.0	0.9	11.4	3.07	0.5
2	15.9	1.3	13.2	1.56	2.8
3	15.9	1.2	13.4	0.38	6.4
4	4.6	0.4	> 4.6	NA	NA
5	5.5	0.5	> 5.5	NA	NA
6	10.6	1.0	5.5	0.14	37.4
7	16.0	1.5	9.1	0.10	67.9

Note: NA = not applicable

Results from these tests indicate maintaining an ozone residual in the source water could be difficult when TOC and UVA were high (approximately 13 mg/L and 0.40 cm^{-1}, respectively). Therefore, controlling ozone dose based on ORP could be challenging because ORP will not remain elevated without the presence of an ozone residual. UVT, which is mathematically related to UVA, could be an easier parameter for control because it detects a permanent change caused by reactions of hydroxyl radicals or molecular ozone with organic matter. Once the ozone residual dissipates, those changes are still measureable. However, it might be more challenging to control based on UVT if an ozone residual is present at the point of measurement, because UVT will continue to change after the control point. Proper selection of a sampling location for the UVT analyzer could solve this problem.

Another implication of these data is automated ozone dose control should be able to protect the MF system from ozone residuals. Automated control based on ozone effluent UVT set the ozone dose at 5.5 mg/L (O_3:TOC = 0.5), which was low enough that no ozone residual was detected by the first measurement after ozonation (T = 20 s). In a full-scale plant, the hydraulic retention time (HRT) between ozone addition and the MF system could be designed to reduce the likelihood of a residual reaching the MF membranes.

4.3 Investigation of UVT and ORP for Automated Ozone Dose Control

These experiments studied the efficacy of using UVT and ORP for automated ozone dose control at the pilot plant. The goal was to evaluate these parameters to determine which one was the preferred option to use with the dose control system.

4.3.1 Methods and Materials

4.3.1.1 Pilot-Scale Ozone System

Liquid oxygen was fed to an ozone generator (OZAT CFS-1, Ozonia North America, Leonia, NJ). To increase operational flexibility, this generator was replaced with a larger one (OZAT CFS-3, Ozonia North America, Leonia, NJ) between Runs 1 and 2. A portion of the gas stream leaving the ozone generator was diverted to a gas phase ozone analyzer (Model 465H, Teledyne API, San Diego, CA) to measure the percentage of ozone by weight. The ozone gas was added to the non-nitrified secondary effluent by a venturi injector (Model 1583-A, Mazzei Injector Co., Bakersfield, CA). A static mixer (Model #1.25-40-4-4.2V-2, Koflo Corp., Cary, IL) located immediately after the injector provided additional mixing before the ozonated water was injected through two mixing nozzles (Model #2-N-14, Mazzei Injector Co., Bakersfield, CA) into the bottom of an 8 ft tall, 8 in. diameter degas column.

A process flow diagram for the degas and defoam columns is included in Figure 4.4. The ozonated water flowed up the 8-in. column, which had a HRT of approximately 1 minute at the target flow rate of 22 gpm. An 8-in. transfer pipe connected the degas column to the top of the 12-in. diameter defoam column. The ozonated water flowed out of the bottom of the defoam column, through a riser pipe, and then down into a 150-gallon equalization tank. The total HRT from the ozone injector to the outlet of the equalization tank was approximately 12 min at 22 gpm.

ORP was measured in the pilot plant influent, between the degas and defoam columns, and in the ozone effluent by ORP sensors (2717-WT, George Fischer Signet, El Monte, CA) in wet-tap assemblies (3719 Wet-Tap Assembly, George Fischer Signet, El Monte, CA). UVT in the pilot plant influent and ozone effluent was measured by Accuview Online UV% Transmission Analyzers (HF Scientific, Ft. Myers, FL). A dissolved ozone monitor (Model 499AOZ, Rosemount Analytical Liquid Division, Irvine, CA) measured the ozone residual leaving the equalization tank. Ozone dose could be set manually or controlled automatically by LabVIEW Professional (National Instruments Corp., Austin, TX) programmed and installed on a Microsoft computer. That program adjusted ozone dose up or down based on influent UVT, influent ORP, or ozone effluent UVT.

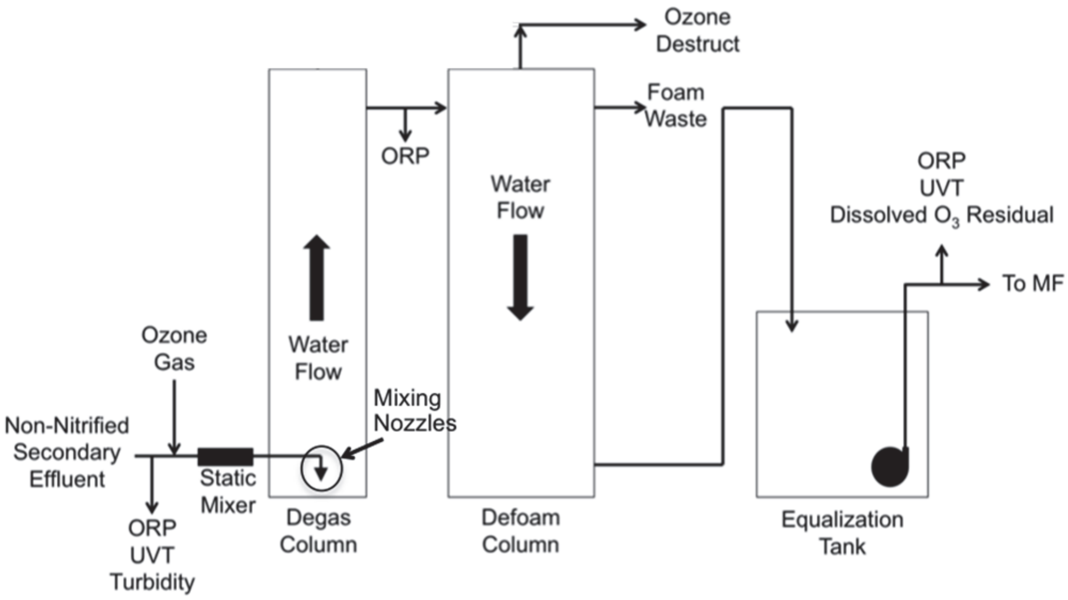

Figure 4.4. Process flow diagram for the pilot plant ozone system showing online instrumentation.

Foam was wasted from the top of the defoam column by an automated valve once every 32 min. A second gas phase ozone analyzer (Model 465H, Teledyne API, San Diego, CA) was used to measure ozone in the off-gas before it reached the destruct unit. A vacuum pump applied negative pressure to draw the off-gas through the gas phase ozone analyzer and destruct unit. Measuring the ozone concentration in the off-gas prior to the destruct unit indicated the ozone transfer efficiency was approximately 70%.

All data from the online instruments for the ozone system were recorded on a data logger (Ecograph T RSG30, Endress+Hauser, Greenwood, IN) and periodically downloaded to a laptop for storage and analysis.

4.3.1.2 Experimental Approach

Tests were conducted within a few hours on one day starting with the control (no ozone) condition, which added oxygen gas to the non-nitrified secondary effluent with the ozone generator power set at 0%. Data was not recorded until the measurement of the ORP probe between the columns stabilized (typically 5−10 min). After stabilization, instrument readings for influent OPR and UVT data were recorded, and a water sample was analyzed for UVA (DR 5000, Hach Co., Loveland, CO). ORP from the probe between the columns was recorded 1 minute after the influent readings were collected to match the HRT to that location. Simultaneously, a water sample was collected from that location and analyzed for ozone residual using Hach method 8311 (Ozone AccuVac® Ampules, Hach Co., Loveland, CO), which is based on the gravimetric method using indigo trisulfonate (Rakness, 2005). The UVT reading after the equalization tank was recorded 12 min after the influent data were recorded to equal the HRT of the ozone system. UVA samples were collected from the influent and ozone effluent when UVT data were recorded. After testing the control condition, the following transferred ozone doses were tested: 5.1, 8.8, 10.8, 11.9, and 12.3 mg/L. The same water quality data were recorded during each test. A dissolved ozone analyzer (Model 499AOZ, Rosemount Analytical Liquid Division, Irvine, CA) measured the ozone residual at the ozone effluent.

4.3.2 Results and Discussion

Data for influent UVT and ORP, after degas ORP, and ozone effluent UVT are shown in Figure 4.5. Influent UVT and ORP experienced minimal fluctuations during testing, indicating that water quality was relatively stable from the start to the finish of this test. When the ozone dose was 0 mg/L, the oxygen added to the secondary effluent still increased ORP by 275 mV. At doses up to 8.8 mg/L, ORP changes beyond what was achieved by oxygen alone were minimal, and no dissolved ozone residual was detected. However, increasing the ozone dose from 8.8 to 10.8 mg/L increased ORP from 346 to 549 mV, and an ozone residual of 0.08 mg/L was measured (Table 4.3). Subsequent increases in ozone dose to 11.9 and 12.3 mg/L yielded higher ORP readings (787 and 860 mV) and low ozone residuals (0.29 and 0.31 mg/L). The dissolved ozone residual in the ozone effluent stayed at 0 mg/L regardless of the transferred ozone dose.

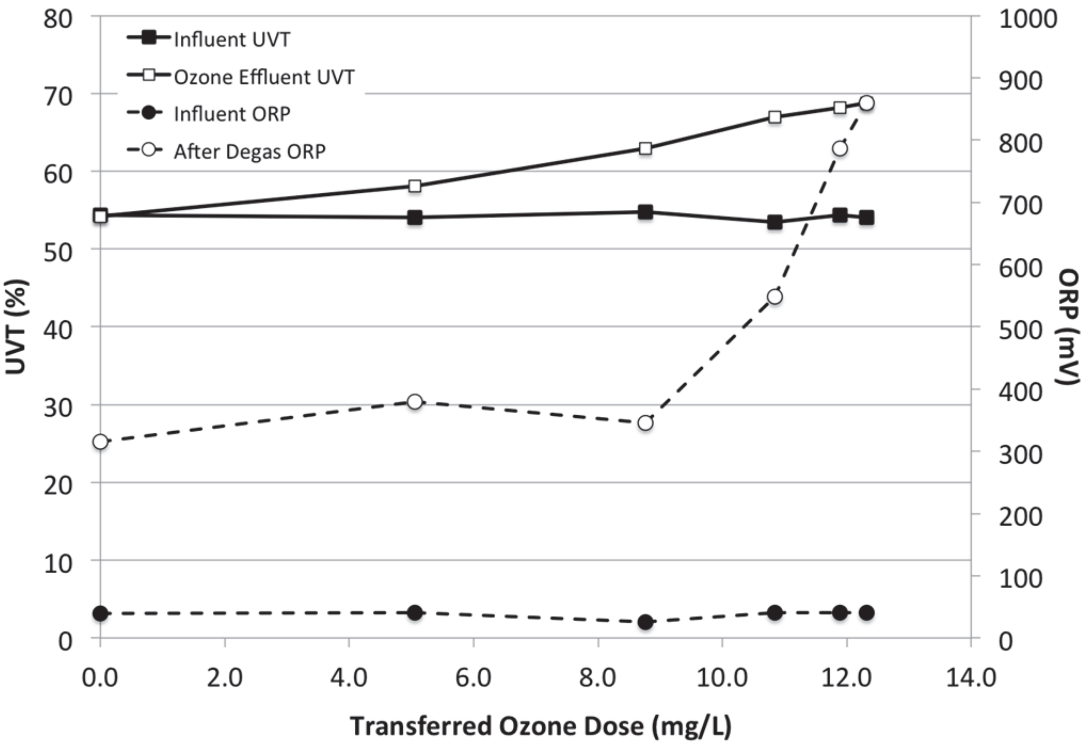

Figure 4.5. UVT and ORP response to increasing transferred ozone dose at the pilot plant.

Table 4.3. Data from Experiments Studying the Suitability of UVT and ORP for Automated Ozone Dose Control

			UVT		ORP	
Test Number	Transferred Ozone Dose (mg/L)	Ozone Residual After 1 Min (mg/L)	Ozone Influent (%)	Ozone Effluent (%)	Ozone Influent (mV)	Ozone Effluent (mV)
1	0.0	ND	54.4	54.2	40	315
2	5.1	ND	54.1	58.1	41	380
3	8.8	ND	54.8	62.9	26	346
4	10.8	0.08	53.4	67.0	41	549
5	11.9	0.29	54.4	68.2	40	787
6	12.3	0.31	54.1	68.8	40	860

Note: ND = not detected

Linear regressions of ozone dose versus ORP after the degas column and ozone dose versus ozone effluent UVT were plotted in Figure 4.6. Two linear regressions of the ORP data were performed. The first linear regression included ORP data when the ozone residual after 1 min was below detection and the second regression covered the data when an ozone residual was measured. When no ozone residual was detected, the correlation between ozone dose and ORP was weak and the slope of the regression line was small. This trend differed significantly from the liner regression of the ORP data when an ozone residual was detected (Table 4.3). That regression line had a steep slope, and the coefficient of determination (R^2-value indicated there was a strong correlation between ozone dose and ORP in the presence of an ozone residual.

These data showed ORP to be a poor candidate for automated ozone dose control when the ozone dose is too low to maintain a residual at the ORP sample location. However, if a residual is present, ORP appears to be a good option for controlling ozone dose. One approach to mitigate this limitation would be to locate the ORP probe at a location that is always expected to have an ozone residual. Ideally this would be somewhere after the off-gas has been separated from the water, because bubbles containing gaseous ozone could affect measurements by the probe. In the testing reported here, the ORP probe was located immediately after the off-gas column, and there still was no ozone residual measured with doses of 5.1 and 8.8 mg/L (Table 4.3). If those doses achieved the desire treatment goals, a probe located before gas separation might permit control by ORP if design features were included to prevent bubbles from affecting the probes measurements. This approach might require further study to demonstrate its feasibility.

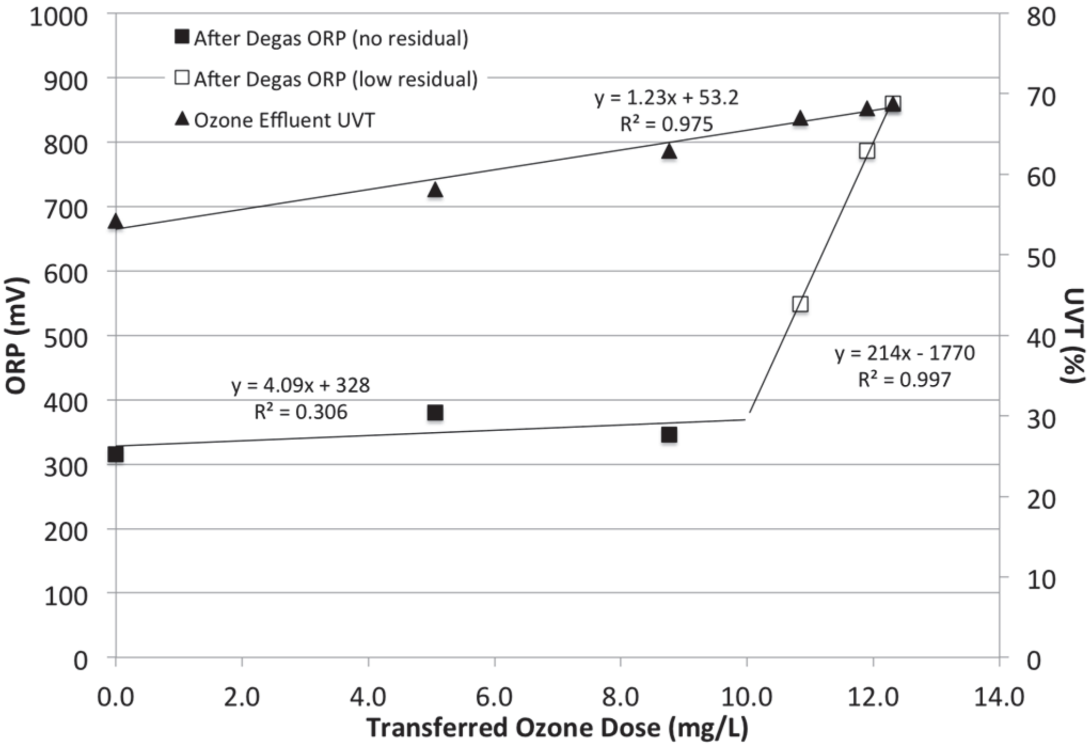

Figure 4.6. Plot of transferred ozone dose versus ORP and UVT with linear regression to evaluate the correlation between these parameters.

The response of UVT to an increasing ozone dose contrasted with the ORP data, because its change was gradual and consistent over the range of tested doses. The R^2-value showed the correlation between ozone dose and UVT was strong (Figure 4.6) whether or not an ozone residual was present at the location of the ORP probe. These data indicated controlling the dose based on the ozone effluent UVT was feasible and should allow tailoring the dose for a specific MF performance goal that is developed using MF feed UVT data. A dose control strategy using UVT would be more challenging if an ozone residual was present, because UVT could continue to change an unknown amount after the control point. Therefore, it would be best to locate the UVT analyzer at a location where an ozone residual is not expected under normal operation. Another approach would be to install a backup UVT analyzer a minimum HRT downstream of the primary UVT analyzer. If an ozone residual was detected at the primary analyzer, then the backup analyzer could be used instead. Proper design and implementation of the automated ozone dose control strategy would provide another layer of reliability to prevent overdosing that could create a residual at the primary UVT analyzer.

A comparison of UVT and ORP to be the control parameter for an automated ozone dosing strategy indicated UVT was the preferred option. UVT was shown to be effective at all transferred ozone doses that were tested, whereas ORP was only effective when the ozone dose was high enough for an ozone residual to be present. That limitation for ORP would constrain the range of ozone doses that could be used with a control strategy, which could lead to overdosing. If water quality goals changes, it would be harder to compensate for this change with a fixed ORP probe than a fixed UVT analyzer. Depending on the contactor design, moving a probe or analyzer to another location could be difficult. Both parameters have constraints regarding the location of the control point, but the primary constraint for an

UVT analyzer (no ozone residual present) would be easier to address than the primary constraint for an ORP probe (ozone residual must be present).

4.4 Automated Ozone Dose Control

Automated dose control was implemented during pilot testing as an approach to optimizing MF performance while minimizing the ozone dose. Instituting a successful dose control system that responds in real-time to water quality changes could reduce full-scale operations costs significantly while preserving the desired level of MF performance.

4.4.1 Methods and Materials

The ozone system used for this testing was described in Section 4.3.1.1. LabVIEW Professional (National Instruments Corp., Austin, TX) was programmed and installed on a Microsoft Windows-based desktop computer. A data logger (Ecograph T RSG30, Endress+Hauser, Greenwood, IN) sent 4-20 mA signals from the UVT and ORP instruments to the LabVIEW program. Those amperage signals were converted to voltage signals before the analog input module (NI 9205, National Instruments Corp., Austin, TX) connected to the computer. After the input signals were processed, a 4-20 mV signal was sent from an analog output module (NI 9265, National Instruments Corp., Austin, TX) to adjust the power on the ozone generator (OZAT CFS-3, Ozonia North America, Leonia, NJ).

The primary concept for the dose control strategy was based on feedback from ozone effluent UVT or ORP after the degas column. This approach required the selection of a dead band that encompassed an acceptable range for the specified water quality parameter. If the measurements of the controlling parameter were above (below) the limits of the dead band, the LabVIEW program would decrease (increase) the ozone generator power to lower (raise) the transferred ozone dose. This adjustment to the ozone dose would occur at intervals defined by the user to compensate for changing water quality. Some important user set points are listed here:

- Upper dead band limit (%UVT or mV)
- Lower dead band limit (%UVT or mV)
- Interval between adjustments to ozone generator power (minutes)
- Frequency of data input from the data logger (seconds)
- Number of data points to be averaged and compared to the dead band limits
- Gain up when generator power must be increased (%)
- Gain down when generator power must be decreased (%)
- Minimum ozone dose (mg/L)
- Maximum ozone dose (mg/L)

The details of these and other user set points will not be described in detail but provided an opportunity to fine-tune the program to achieve smooth and steady adjustments to ozone generator power and, therefore, ozone dose.

Two other ozone dose control concepts involving UVT also were tested. The first concept was using ozone influent UVT to set the ozone dose that was expected to be necessary to achieve the desired water quality. This option was also programmed into the LabVIEW program. Because the control point was located before ozone addition, there was no feedback mechanism for adjusting the ozone dose. Only the ozone influent UVT signal from the data logger was used to determine the ozone dose by adjusting the ozone generator power. A relationship between ozone influent UVT and ozone dose (Figure 4.7) was developed based on data from pilot testing that was part of an earlier project and from Runs 1 to 4 of this project. The text boxes on Figure 4.7 show the range of data for Phase 1 testing (Gerringer et al., 2011) and this research (Phase 2). The slope of the line was steeper when ozone influent UVT was lower because ozone demand was expected to increase under those conditions.

The last concept for ozone dose control was a hybrid of the approaches using ozone influent UVT and ozone effluent UVT. Under this scenario, the linear relationship between ozone influent UVT and transferred ozone dose from Figure 4.7 set the initial dose and adjusted it on a real-time basis. Feedback based ozone effluent UVT was used to trim this calculated ozone generator power setting if it was outside the dead band, which was determined by user input.

Automated ozone dose control was tested using ORP after the degas column, ozone influent UVT and ozone effluent UVT as the control parameters. However, testing with ORP was limited to preliminary testing to setup the control strategy and then collecting data on one day. More testing was not performed because control based on ORP limited the ozone doses that could be used during testing, because an ozone residual needed to be present for it to work. Table 4.4 shows the ozone dose control strategy and ozone effluent UVT target associated with each MF run. As indicated in Table 4.4, the dead band for the ozone effluent UVT target was adjusted down twice during Run 8.

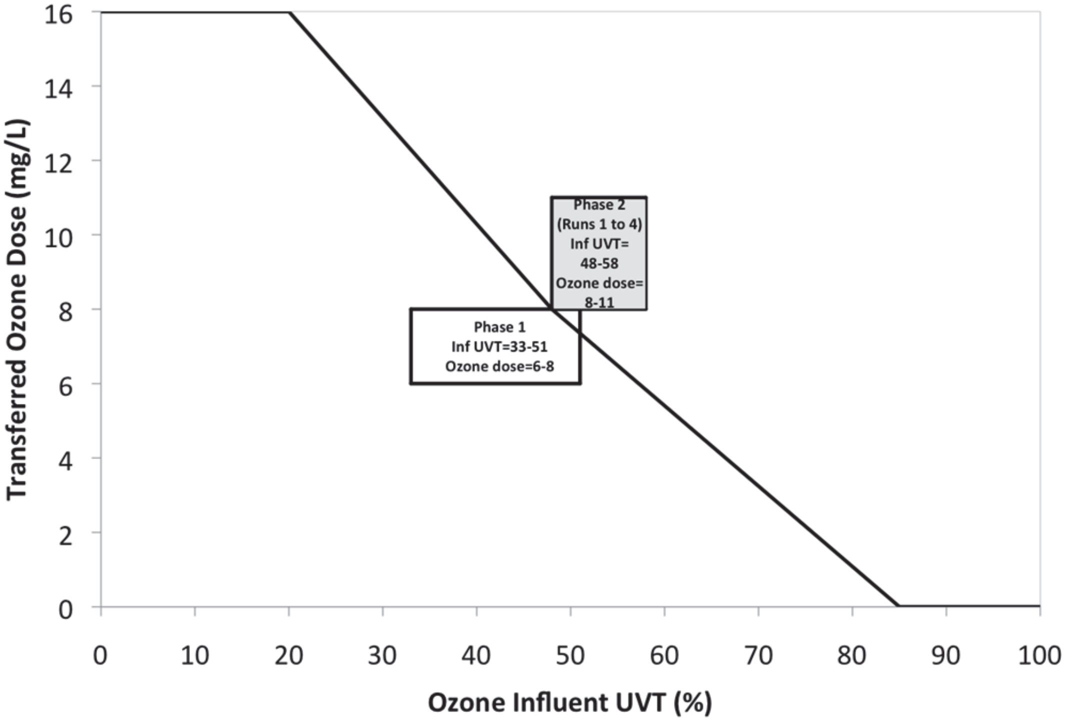

Figure 4.7. Curve based on previous (Phase 1) and current (Phase 2) ozone pilot data used to adjust ozone dose based on pilot plant influent UVT.

Table 4.4. UVT-based Ozone Dose Control Strategy and Ozone Effluent UVT Targets for Runs 5 to 8

Run	Basis of Automated Ozone Dose Control Strategy	Ozone Effluent UVT Target (%)
5	Ozone influent UVT	≥ 60.0[*]
6	Ozone influent UVT with trimming based on ozone effluent UVT	60.0 to 63.0
7	Ozone effluent UVT	59.0 to 61.0
8	Ozone effluent UVT	59.0 to 61.0[**] 58.0 to 60.0[***] 57.0 to 59.0[****]

Notes: [*] There was no maximum limit during Run 5.

[**] Min and max target from 12/1 to 12/15.

[***] Min and max target from 12/15 to 12/19.

[****] Min and max target from 12/19 to the end of Run 8.

4.4.2 Results and Discussion

4.4.2.1 Ozone Dose Control with ORP

Limited testing of ozone dose control using ORP after the degas column was performed with the ozone system. Figure 4.8 shows a screen shot with data from this experiment. The top graph shows ORP data and minimum and maximum values for the dead band (580 to 620 mV), and the bottom graph shows the automated adjustments made to keep the ozone effluent ORP within this range. This figure demonstrates the adjustments made to the power setting on the ozone generator over a period of 10 min to keep the ORP measurement inside the dead band. The ozone dose ranged from 11.8 to 12.1 mg/L during this test. Additional testing with other ranges for the dead band (585 to 615 mV and 590 to 610 mV) indicated the ozone dose control system could keep ORP within a dead band as narrow as 30 mV.

Data from this testing demonstrated ozone dose control based on ORP was feasible for this application. However, the limited flexibility to lower the transferred ozone dose because of the requirement for an ozone residual to be present resulted in the decision not to test ozone dose control based on ORP during a full MF run.

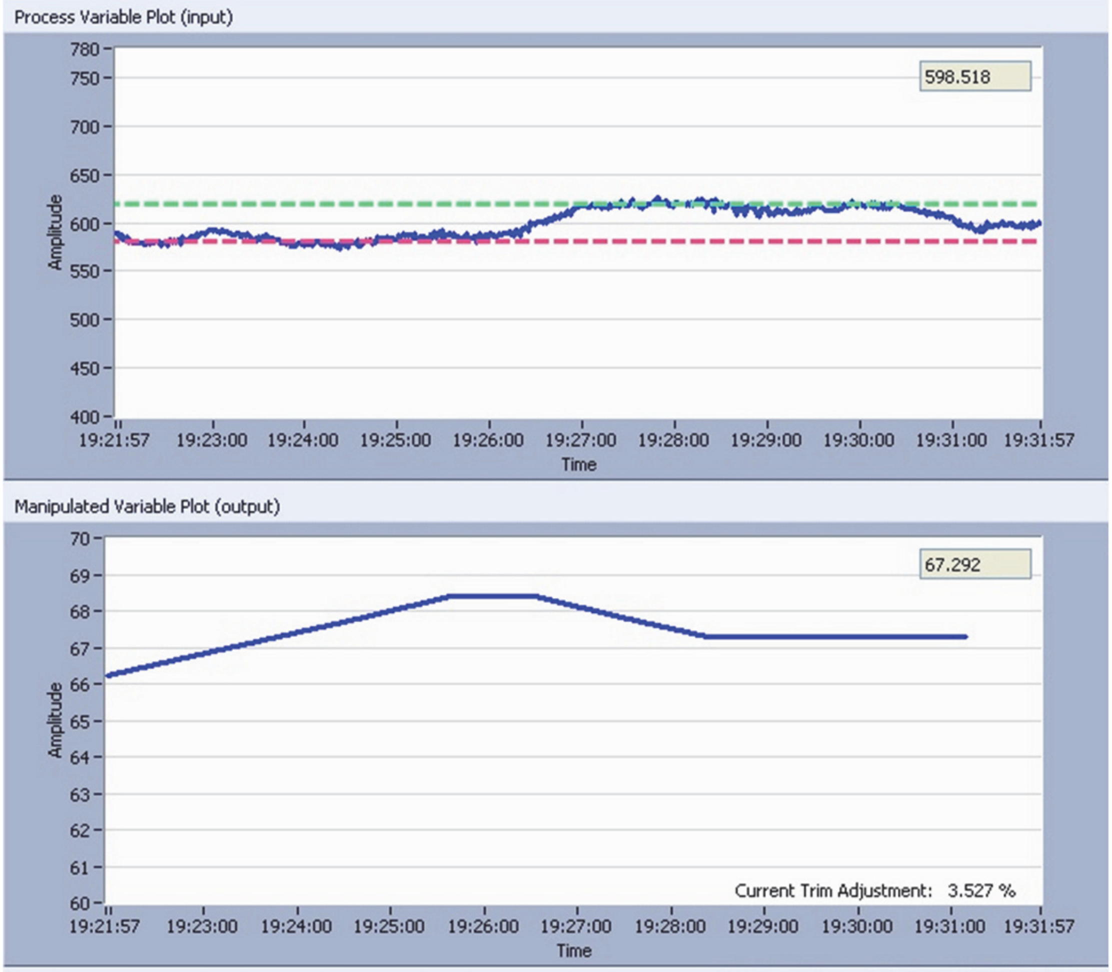

Figure 4.8. Screen shot showing data from ozone dose control based on ORP after the degas column.

Notes: The top graph shows ORP data and minimum (green) and maximum (red) values for the dead band (580 to 620 mV). The bottom graph shows the automated adjustments made to the power setting of the ozone generator to keep the ozone effluent ORP within the dead band.

Table 4.5. Average Water Quality Data During the Automated Ozone Dose Control Test with ORP as the Control Parameter

Water Quality Parameter	Sample Location		
	Ozone Influent	After Degas Column	Ozone Effluent
ORP (mV)	34	596	294
Turbidity (NTU)	6.8	---	4.1*
UVT (%)	51.4	---	65.5

* Measured at MF feed

Note: The transferred ozone dose ranged from 11.8 to 12.1 mg/L.

4.4.2.2 Ozone Dose Control with UVT

As shown in Table 4.4, different approaches to ozone dose control by UVT were used during Runs 5 to 8. Ozone influent UVT, ozone effluent UVT, and transferred ozone dose data from the online instruments for these runs are displayed in Table 4.6. Water quality was best during Run 5 and worst during Run 8. An upset at the wastewater treatment plant feeding ECLWRF caused the ozone influent UVT to drop to 10.7% for several hours during Run 8. UVT in this range typically is associated with primary effluent, not secondary effluent.

During Run 5, ozone dose was controlled by ozone influent UVT with a goal of a stable ozone effluent UVT of approximately 60%. Online data for ozone influent UVT, ozone effluent UVT, and transferred ozone dose are shown in Figure 4.9. UVT was generally above 60% during Run 5, but diurnal variability of approximately 5% UVT was not as stable as desired, and the absence of feedback control prevented automatic correction when values dipped below 60%. A signal error caused a stable transferred ozone dose between 10/2 and 10/5. A study with a longer duration could have time to develop a better relationship between influent UVT and ozone dose for achieving a minimum ozone effluent UVT of 60%. However, that effort would not necessarily achieve better results than ozone dose control incorporating ozone effluent UVT, which has the advantage of providing feedback for dose adjustment.

To address the challenges of satisfying the ozone effluent UVT goal of 60% based on ozone dose control by influent UVT, the hybrid approach to ozone dose control described in Section 4.4.1 was adopted for Run 6 (Figure 4.10). Combining ozone influent UVT control with trimming based on the ozone effluent UVT provided feedback control to help produce a more consistent ozone effluent water quality. The maximum ozone dose set point during this run was 13 mg/L. No ozone was generated between 10/29 and 11/3, because the liquid oxygen (LOX) tank was empty.

Comparing Run 5 data (Figure 4.9) to Run 6 data (Figure 4.10) showed the addition of ozone dose trimming based on ozone effluent UVT improved the stability of water quality in the ozone effluent. Including feedback control helped prevent ozone doses that were too high or too low. However, the dose trimming based on ozone effluent UVT was found to be the dominant factor determining ozone dose, because the doses set by the ozone influent UVT frequently would have resulted in the ozone effluent UVT being outside the dead band of 60 to 63%.

Table 4.6. Minimum, Average, and Maximum Ozone Influent and Effluent UVT and Transferred Ozone Dose for MF Runs 5 to 8

	Ozone Influent UVT (%)			Ozone Effluent UVT (%)			Transferred Ozone Dose (mg/L)		
MF Run	**min**	**avg**	**max**	**min**	**avg**	**max**	**min**	**avg**	**max***
5	37.1	59.6	68.6	50.7	63.9	83.0	3.7	5.5	13.2
6	35.9	51.3	63.4	42.1	61.7	74.7	5.3	11.3	13.2
7	40.4	52.3	59.5	50.6	60.0	69.0	4.9	9.7	13.2
8	10.7	49.4	58.8	12.0	58.3	70.0	4.6	10.0	17.3

Note: * Corresponds with maximum ozone dose set point for each MF run.

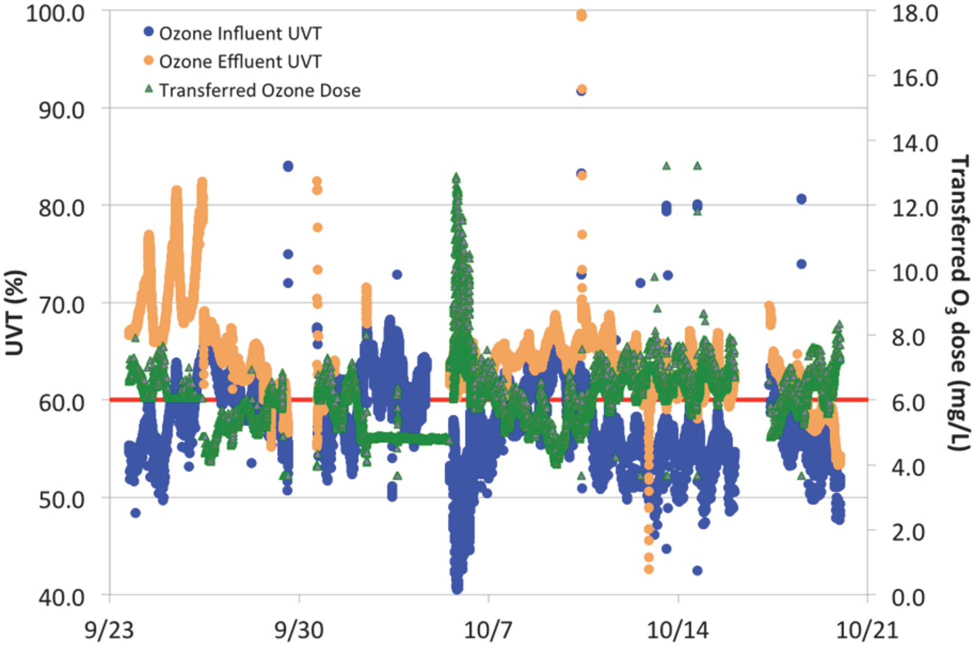

Figure 4.9. Ozone influent UVT, ozone effluent UVT and ozone dose during Run 5.

Note: Dose control used ozone influent UVT with an ozone effluent UVT target of 60% (horizontal red line). A signal error caused a constant ozone dose from 10/2 to 10/5.

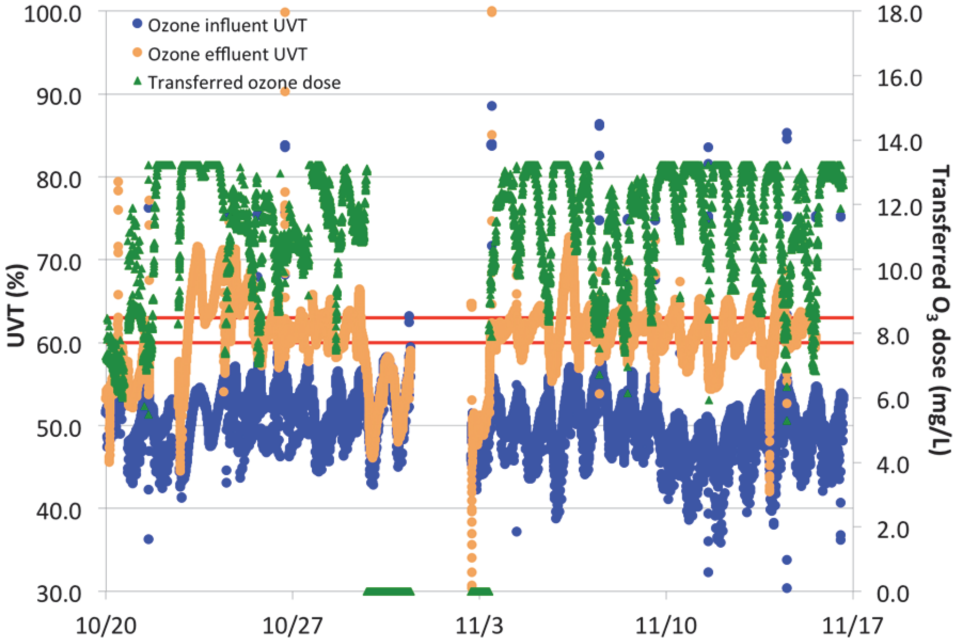

Figure 4.10. Ozone influent UVT, ozone effluent UVT, and ozone dose during Run 6.

Note: Dose control used ozone influent UVT trimmed by ozone effluent UVT with an ozone effluent UVT target of 60 to 63% (horizontal red lines). The highest ozone dose was limited to 13 mg/L. Empty LOX tanks prevented ozonation from 10/29 to 11/3.

It is important to note the ozone influent water quality was worse during Run 6 (UVT_{avg} = 51.3%) compared to Run 5 (UVT_{avg} = 59.6%). This difference required a higher average ozone dose (10.3 mg/L versus 5.5 mg/L, respectively) to achieve the water quality goals. These data indicate the effect of temporal changes in water quality on ozone dosing, which has significant implications regarding ozone capacity if a full-scale process is being designed.

Run 7 (Figure 4.11) was much shorter than the other runs, because it corresponded with high-flux testing. However, this run was the first with ozone dose control based solely on ozone effluent UVT. The dead band was 59 to 61% during Run 7 compared to 60 to 63% during Run 6. This change, along with a slightly better average ozone influent UVT (52.3%) reduced the average ozone dose to 9.7 mg/L.

As with Run 7, ozone dose control for Run 8 was based solely on ozone effluent UVT. The maximum ozone dose set point was increased to 17.3 mg/L but was lowered to 16.0 mg/L during the middle of the run. This adjustment was made so the maximum ozone dose at the pilot plant matched the maximum ozone design dose of the ozone system being installed at ECLWRF. The initial dead band was the same as Run 7 (59 to 61%) but was lowered to 58 to 60% after 14 days and to 57 to 59% after 4 more days. The dead band was lowered as the initial steps of ozone dose optimization with the goal of lowering ozone addition while maintaining acceptable MF performance. For a discussion of that topic, please see Chapter 5.

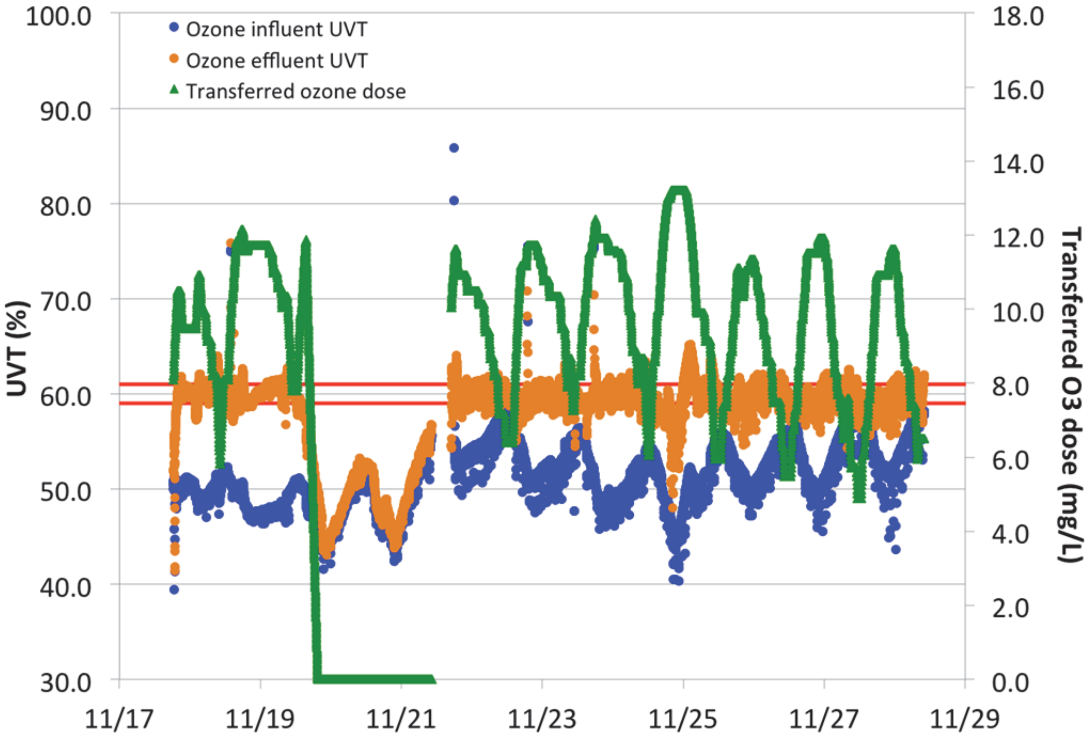

Figure 4.11. Ozone influent UVT, ozone effluent UVT, and transferred ozone dose during Run 7.

Note: Ozone dose control was based on ozone effluent UVT with a dead band (horizontal red lines) of 59 to 61%. No ozone was generated between the evenings of 11/19 and 11/21 because the LOX tank was empty.

During Run 8, average ozone influent UVT was 49.4% (Table 4.6), which was worse than the previous three runs. Online UVT and transferred ozone dose data are shown in Figure 4.12. There was an upset on 12/22 at the Hyperion Treatment Plant that supplied ECLWRF with non-nitrified secondary effluent. This upset caused the ozone influent UVT to change from 48 to 10% and finally return to 48% over 20 h. The poor water quality received during this time overwhelmed the ozone system, which only improved UVT to 18% when ozone influent UVT was the lowest. When the water quality was improving after the event, the UVT increase from a maximum ozone dose of 16.0 mg/L stabilized at approximately 14%. This UVT increase might represent the maximum level of improvement that can be expected when using an ozone dose of 16.0 mg/L under these conditions.

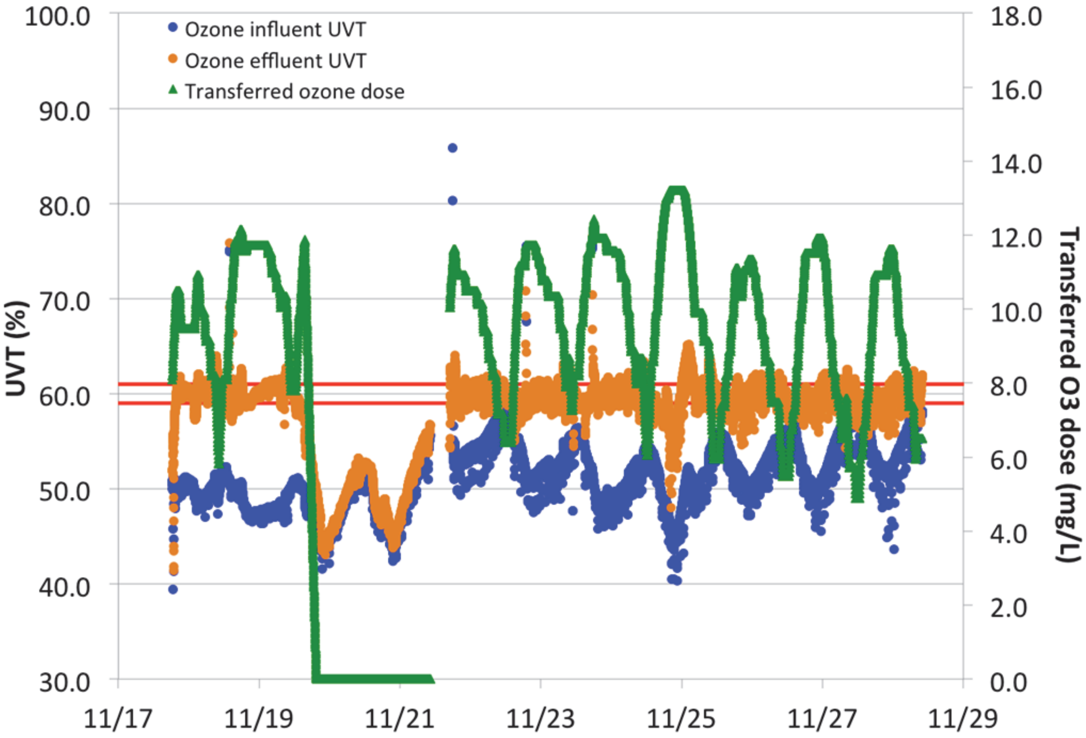

Figure 4.12. Ozone influent and effluent UVT data and transferred ozone dose data during Run 8.

Notes: Ozone dose control was based on ozone effluent UVT data. The horizontal black lines mark the dead band of 59 to 61% for the ozone effluent UVT from 12/1 to 12/15, 58 to 60% from 12/15 to 12/19, 57 to 59% from 12/19 till the end of Run 8. The minimum ozone influent UVT on 12/22 was 10%, which is below scale for the y-axis**.**

4.5 Conclusions

The research described in this chapter investigated ozone demand and decay in the non-nitrified secondary effluent feeding the pilot plant at ECLWRF, compared the feasibility of using UVT and ORP for ozone dose control, and tested automated ozone dose control based on ORP and UVT. Results from the ozone demand and decay tests demonstrated the secondary effluent has a high ozone demand and decay rate that depend on EfOM concentration and aromaticity. These characteristics of the secondary effluent treated at ECLWRF would be protective of downstream MF membranes, because it is difficult to create an ozone residual, and any residual created tends to decay quickly. The high ozone demand and rapid decay suggested ozone dose control based on ORP could be more challenging, because control using this parameter requires the presence of an ozone residual.

Ozone dose control based on UVT was shown to provide operational flexibility over a wide range of ozone doses, whereas control based on ORP limited the range of ozone dose that could be delivered. UVT changes with increasing ozone dose were gradual and did not depend on the presence of an ozone residual, because the oxidation reactions that change UVT are permanent until another process affects it. Gradual changes permit the fine-tuning of the ozone dose over a broad range of values. In addition, the permanent change in UVT would provide flexibility regarding the location of instrumentation. These factors contrast with ozone dose control using ORP, which is insensitive to increases in the transferred ozone dose until a residual is present. This limitation constrains the effective range of ozone doses that can be delivered using ORP as the control parameter, because the dose must reach a minimum threshold before a residual is present. An example of an application suitable under these constraints is disinfection, which requires the presence of an ozone residual to qualify for disinfection credits.

Pilot testing of automated ozone dose control was proven to be feasible using ORP and UVT. The more extensive testing with UVT was a consequence of its superior characteristics for controlling ozone dose. Ozone effluent UVT was shown to be the best approach for dose control, because it depends on feedback control instead of relying on a user-defined equation like control based on ozone influent UVT. Further testing to identify the optimal set points for the ozone dose control program could improve the ability of the system to keep the ozone effluent UVT within the specified dead band.

Chapter 5

MF Performance After Ozone Pretreatment

5.1 Introduction

Organic materials, particularly large molecular weight (MW) organics, are known to foul microfiltration (MF) membranes (Lozier et al., 2008; Trussell et al., 2009). Ozone, a strong oxidant that reduces MW of organic molecules (Camel and Bermond, 1998; Świetlik et al., 2004), has been shown to improve the performance of low-pressure membranes treating effluents from wastewater treatment processes (Lee et al., 2005a; Nguyen and Roddick, 2010; Zhu et al., 2008). A pilot study using polypropylene MF membranes at West Basin Municipal Water District's Edward C. Little Water Recycling Facility (ECLWRF) demonstrated the performance benefit of preozonation of non-nitrified secondary effluent (Gerringer et al., 2011).

The goal of the pilot-scale research described in this chapter was to optimize the use of ozone pretreatment before polyvinylidene fluoride (PVDF) MF membranes (O_3-MF) when treating the non-nitrified secondary effluent that is the source water for ECLWRF. This work expanded on Gerringer et al. (2011) by applying the concept of preozonation for effluent organic matter (EfOM) oxidation to PVDF MF membranes and by adjusting the operation of the ozone system and the MF unit to investigate options for maximizing MF performance. O_3-MF was tested in parallel with ferric chloride ($FeCl_3$) addition before PVDF MF ($FeCl_3$-MF), which had established a high benchmark for success during previous testing where it performed well on ECLWRF influent.

Ozone pretreatment presented unexpected challenges in the form of manganese (Mn) fouling that caused O_3-MF to shut down from high transmembrane pressure (TMP) before reaching the goal of 21 days between clean-in-places (CIPs). Investigation of potential mitigation measures focused on $FeCl_3$ addition in the MF feed to coagulate Mn, the inclusion of strong reductants (hydrosulfite [$S_2O_4^{2-}$] and metabisulfite [$S_2O_5^{2-}$]) in the citric acid enhanced flux maintenance (EFM) clean to reduce Mn that has fouled the membrane from insoluble Mn(IV) to soluble Mn(II), and automated ozone dose control to prevent overdosing that could oxidize soluble Mn(II) to insoluble Mn(IV). A comparison of $FeCl_3$-MF and MF with ozone pretreatment followed by $FeCl_3$ addition (O_3-$FeCl_3$-MF) demonstrated $FeCl_3$ addition could prevent Mn fouling in the absence of ozone dose control or strong reductants in the citric acid EFM. The last MF run, which did not include $FeCl_3$ addition or strong reductants in the citric acid EFM, exceeded the 21-day goal by using automated ozone dose control to prevent Mn fouling. Details of the MF pilot testing are presented in this chapter.

5.2 Methods and Materials

5.2.1 Pilot Plant

This pilot study was conducted at ECLWRF, a water recycling plant in El Segundo, CA, that treats non-nitrified secondary effluent from the Hyperion Treatment Plant (HTP), the largest municipal wastewater treatment plant owned and operated by the City of Los Angeles. HTP is a pure oxygen activated sludge secondary treatment plant with a solids retention time (SRT) of 1 to 2 days. This low SRT provides relatively poor oxidation of organics compared to wastewater treatment plants with longer SRTs.

The pilot plant consisted of two parallel treatment trains, one with ozone pretreatment and the other without ozone pretreatment. Each treatment train included a pilot-scale MF unit followed by a pilot-scale reverse osmosis (RO) unit. The treatment train with ozone included a custom-built ozone injection, dissolution, and foam removal system. Information regarding the pilot ozone system was provided in Chapter 4, Section 4.3.1.1. Two different configurations of the treatment trains were used during testing. The first configuration included the parallel operation of two MF-RO trains, one with ozone pretreatment and the other without it (Figure 5.1). For the second configuration, both MF pilot units treated ozonated water, and their filtrate flows were combined to feed one RO pilot unit (Figure 5.2). The second RO pilot unit was fed by filtrate from the full-scale MF units at ECLWRF. More details about the pilot equipment and treatment train configurations are provided in subsequent sections of this chapter.

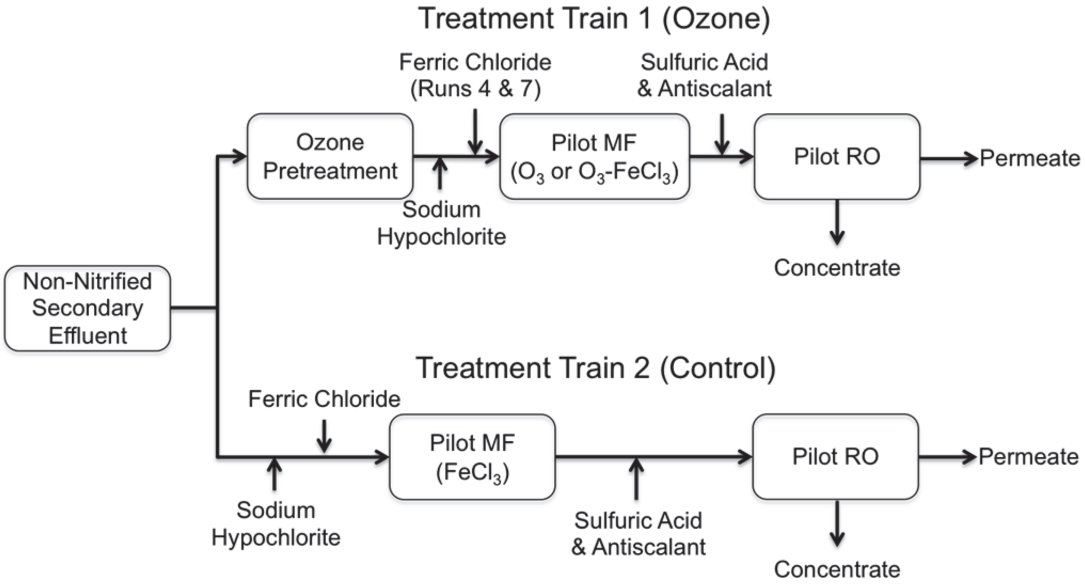

Figure 5.1. Process flow diagram for Runs 1 to 4 and 7.

Note: Pretreatment for each MF units is shown in parentheses. Neither RO unit operated during Run 7.

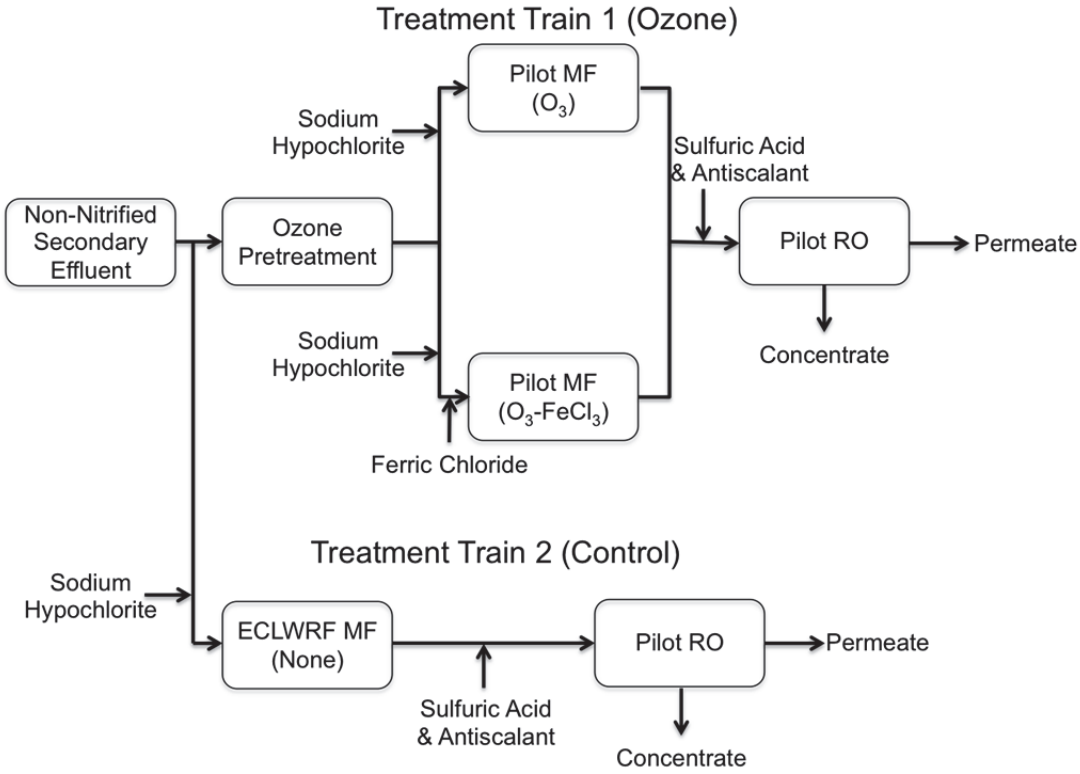

Figure 5.2. Process flow diagram for Runs 5, 6, and 8.

Note: Pretreatment for each MF units is shown in parentheses.

5.2.2 MF Units

Sodium hypochlorite (3 to 5 mg/L total chlorine residual) was added before the MF units to form chloramines and control biofouling on the downstream MF and RO membranes. The target dose for $FeCl_3$ in the MF feed varied between 0 and 14 mg/L depending on the treatment train and test run. Each MF unit (Aria®, Pall Corp., Port Washington, NY) had two pressurized PVDF membrane modules (Microza®, Pall Corp., Port Washington, NY) with nominal pore sizes of 0.1 µm. The target flux for both MF units was 27 gal/ft^2/day (gfd), although there were experiments that tested fluxes as high as 50 gfd. MF feed and filtrate turbidities were measured by 1720E Turbidimeter and FilterTrak 660 sc (Hach Co., Loveland, CO), respectively. The MF units continuously recorded turbidity, temperature, particle counts and operational data such as filtrate flow and TMP.

Both MF units had the capability of performing 30-min EFM cleans using chemicals such as chlorine to remove organic foulants and citric acid to remove inorganic foulants. EFMs circulated the cleaning solution past the feed-side, but not through, the membranes. After performing an EFM, the cleaning solution was flushed out and sent to the drain before filtration resumed or another EFM (e.g., chlorine EFM followed by citric acid EFM) began. Alternative EFMs using chemicals such as Iron Out (Summit Brands, Fort Wayne, IN) and hydrochloric acid were also performed and will be described in more detail in the chapter discussing MF performance. The CIP at the end of each run was performed with two solutions: (1) 3000 mg/L chlorine with 2.0% sodium hydroxide and (2) 2% citric acid. The standard CIP was a two hour wash at 90 to 95 °F with the chlorine/caustic solution followed by a two hour wash at 90 to 95 °F with the citric acid solution.

5.2.3 Water Quality Sampling Schedule and Methods

Table 5.1 shows the frequency of grab samples collected from the pilot plant influent to the MF filtrate for each treatment train. Total iron (Fe) and manganese (Mn) samples were not collected until Run 2 and were analyzed using Hach Methods 8365 and 8149, respectively (Hach Co., Loveland, CO). Turbidity was measured using Standard Method 2130B. Wastewater effluent organic matter (EfOM) characterization included MW fractionation and protein and carbohydrate concentrations measured as described in Chapter 3, Section 3.2.2.1. Excitation-emission matrix (EEM) fluorescence spectroscopy was performed as described in Chapter 3, Section 3.2.2.2.

5.2.4 Pilot Test Runs

Pilot testing included 8 separate MF runs with various adjustments made to the operating parameter for the two MF units: MF1 and MF2. These runs were conducted from May 2011 to January 2012, encompassing the transition of water temperatures and treatment from summer through autumn and into early winter. Ozone doses and test conditions for the MF units are shown in Table 5.2. While only two treatment trains were tested at once, there were three treatment trains tested during the 8 runs: $FeCl_3$-MF, O_3-MF, and MF with ozone pretreatment followed by $FeCl_3$ addition (O_3-$FeCl_3$-MF). Runs 1 to 4 and 7 included treatment trains of $FeCl_3$-MF and O_3-MF (Figure 5.1). Both MF pilot units treated ozonated water in Runs 5, 6 and 8, testing O_3-MF and O_3-$FeCl_3$-MF (Figure 5.2).

Table 5.1. Frequency of Grab Samples Collected from the Pilot Plant Influent Through the MF Filtrate for Each Treatment Train

	Sampling Frequency				
			MF Trains 1 and 2		
Water Quality Parameter	**Pilot Plant Influent**	**Ozone Effluent**	**Feed**	**Filtrate**	**Backwash**
EfOM Characteristics	Every 6 weeks	Every 6 weeks	---	Every 6 weeks	Every 6 weeks
Iron (total)	2 to 4 weekly	---	2 to 4 weekly	2 to 4 weekly	---
Mn (total)	1 to 2 weekly	---	1 to 2 weekly	1 to 2 weekly	---
TOC	Weekly	Weekly	---	Weekly	Weekly
Turbidity	Daily	Daily	---	Daily	Daily
UVA	Daily	Daily	---	Daily	Daily

Table 5.2. Ozone Doses and Operating Parameters of the MF Pilot Units for Runs 1 to 8

Run	MF Pilot Unit	Total Run Time (days)	MF Pretreatment	Avg. Ozone Dose (mg/L)	Target $FeCl_3$ Dose (mg/L)	MF Flux (gfd)	Backwash Interval (min)
1	1	21	$FeCl_3$	0	9.2	27	15
	2	20	O_3	8	0	27	15
2	1	24	$FeCl_3$	0	9.2	27	15
	2	25	O_3	8	0	27	15
3	1	22	$FeCl_3$	0	9.2	27	15
	2	14	O_3	9	0	27	15
4	1	29	$O_3 + FeCl_3$	9	10	27	15
	2	28	$FeCl_3$	0	10	27	15
5	1	26	O_3	6*	0	27	15
	2	35	$O_3 + FeCl_3$	6*	3**	27	30
6	1	21	O_3	10*	0	27	15
	2	22	$O_3 + FeCl_3$	10*	2	27	30
7	1	5	$FeCl_3$	0	10	35 to 45	15
	2	11	$O_3 + FeCl_3$	7*	10	40 to 50	15
8	1	33	O_3	8*	0	30	15
	2	24	$O_3 + FeCl_3$	8*	1	30	15

Notes: *Automated ozone dose control was based on influent or ozone effluent ultraviolet transmittance (UVT).
**Dose was 14 mg/L for the first week but 3 mg/L for the rest of testing.

EFM schedules and chemical concentrations for chlorine/caustic and citric acid EFMs are shown in Tables 5.3 and 5.4, respectively. Table 5.5 shows the basis of the automated ozone dose control strategy and ozone effluent UVT target for Runs 5 to 8. Additional information about the automated ozone dose control system can be found in Section 4.4 of this report. Pilot plant influent, ozone effluent, MF filtrate, and MF backwash samples were collected and analyzed for MW fractionation and EEM fluorescence spectroscopy during some runs as listed in Table 5.6.

Table 5.3. Chlorine/Caustic EFM Schedules and Concentrations During Runs 1 to 8

Run	Train	Scheduled Interval (days)	Chlorine Concentration (mg/L)	Caustic Concentration (mg/L)
1	1	1	640	0
	2	N/A	640	0
2	1	1	640	0
	2	2	640	0
3	1	1	640	0
	2	12	640	0
4	1	1	1700	700
	2	1	1700	700
5	1	3	1700	700
	2	3	1700	700
6	1	3	1700	700
	2	3	1700	700
7	1	2	1700	700
	2	1	1700	700
8	1	3	1700	700
	2	3	1700	700

Table 5.4. Citric Acid EFM Schedules and Concentrations During Runs 1 to 8

Run	Train	Scheduled Interval (days)	Citric Acid Concentration (mg/L)	Super Iron Out® Concentration (mg/L)
1	1	10	1900	0
	2	none	1900	0
2	1	10	1900	0
	2	10	1900	5000
3	1	10	1900	0
	2	6	20,000	0
4	1	10	2500	0
	2	10	2500	0
5	1	9	5000	5000
	2	9	5000	5000
6	1	9	5000	5000
	2	9	5000	0
7	1	none	N/A	N/A
	2	none	N/A	N/A
8	1	9	5000	0
	2	9	5000	0

Table 5.5. UVT-Based Ozone Dose Control Strategy and Ozone Effluent UVT Targets for Runs 5 to 8

Run	Basis of Automated Ozone Dose Control Strategy	Ozone Effluent UVT Target (%)
5	Ozone influent UVT	≥ 60.0*
6	Ozone influent UVT with trimming based on ozone effluent UVT	60.0 to 63.0
7	Ozone effluent UVT	59.0 to 61.0
8	Ozone effluent UVT	59.0 to 61.0** 58.0 to 60.0*** 57.0 to 59.0****

Notes: *There was no maximum limit during Run 5.

**Min and max target from 12/1 to 12/15.

***Min and max target from 12/15 to 12/19.

****Min and max target from 12/19 to the end of Run 8.

Table 5.6. MF Test Runs that Included Sample Collection for Analysis by MW Fractionation and EEM Spectroscopy

	Sample Collected for Analysis	
Run	MW Fractionation	EEM Spectroscopy
1	No	No
2	Yes	No
3	Yes	Yes
4	Yes	Yes
5	Yes*	Yes*
6	No	No
7	No	No
8	Yes	No

Note: *Two sets of samples were analyzed during Run 5.

It is important to note the diurnal cycle for water quality produced the best water quality in the morning (typically 9 a.m. to noon) and the worst water quality in the evening (typically 9 p.m. to midnight). Figure 5.3 provides an example of the diurnal variability of water quality in the pilot plant influent. Ultraviolet transmittance (UVT) changes of 10% (e.g., 55 to 45%) and turbidity changes of several NTU during a 24-hour period were common. Operational and logistical considerations led to grab samples being collected in the morning, when water quality was typically near its best for the day.

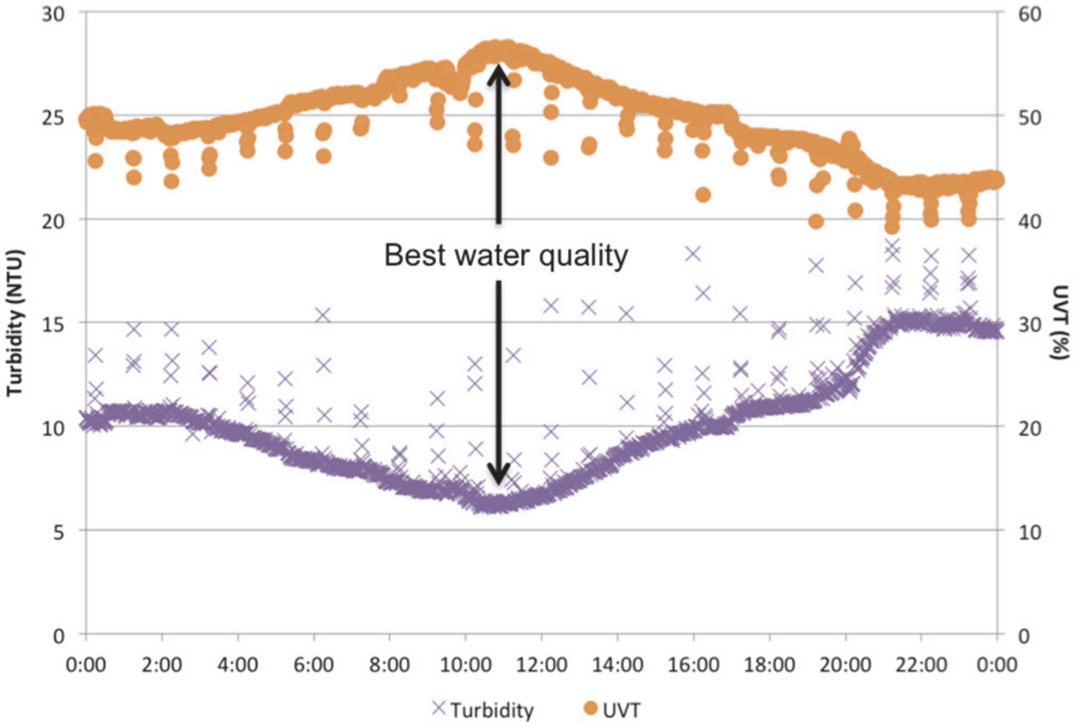

Figure 5.3. An example of diurnal variability at the pilot plant using online data of influent turbidity and UVT.

5.2.5 Foam Sample Collection and Analysis

Ozonation of the secondary effluent produced foam that was removed from the degas and defoam columns by surface wasting at intervals that varied from once to twice hourly. However, foam wasting diluted the foam with ozonated water and did not provide the best opportunity for characterizing the organics in the foam. A water trap connected to the ozone destruct tubing to minimize the moisture reaching the ozone destruct catalyst also captured foam that entered the tubing. That foam collapsed into a liquid that was drained by a valve at the bottom of the trap. One sample of collapsed foam was collected and analyzed for total organic carbon (TOC) and the MW distribution of ultraviolet absorbance at 254 nm (UVA), carbohydrates, and proteins following the procedure for EfOM characterization by MW fractionation (Chapter 3, Section 3.2.2.1).

5.3 Results and Discussion

5.3.1 Run 1 (5/11 to 6/8) – $FeCl_3$-MF versus O_3-MF

The first run compared O_3-MF with an average transferred ozone dose of 8 mg/L to $FeCl_3$-MF with a $FeCl_3$ dose of 9.2 mg/L. $FeCl_3$-MF had automatic daily 640-mg/L chlorine EFMs whereas no EFMs were scheduled for O_3-MF. Similarly, 1900-mg/L citric acid EFMs were scheduled every 10 days for $FeCl_3$-MF but none was scheduled for O_3-MF.

5.3.1.1 Water Quality

Water quality samples collected from the treatment trains were analyzed for TOC, turbidity and UVA (Table 5.7). Average data from these analyses showed ozonation increased TOC by 15% and reduced turbidity and UVA by 35% each. MF caused negligible changes in TOC, produced similar MF filtrate turbidity, and reduced UVA by approximately 35% for both treatment trains. Preozonation resulted in a lower UVA in O_3-MF filtrate compared to $FeCl_3$-MF filtrate. MF backwash data showed $FeCl_3$-MF produced backwash with higher TOC, turbidity, and UVA than O_3-MF.

5.3.1.2 MF Performance

TMP data for $FeCl_3$-MF and O_3-MF revealed the MF units performed differently during Run 1. The TMP of $FeCl_3$-MF (Figure 5.4) rose steadily until mechanical problems caused the MF unit to shut down after the first week of operation. Once that MF unit was returned to service, TMP stabilized and then declined until the end of Run 1, easily achieving the goal of 21 days of cumulative operation without a CIP. The MF unit was shut down because Run 1 was scheduled to end and not because a CIP was required to restore performance.

The TMP trend for O_3-MF was a gradual increase during the first 12 days of operation followed by a rapid rise in TMP on the 13th day (Figure 5.5). The MF unit automatically shut down once TMP exceeded 40 psi, because that was the maximum TMP set point. After a 640 mg/L chlorine EFM followed by a 1900 mg/L citric acid EFM, TMP dropped to approximately 5 psi and the MF unit resumed treating ozonated secondary effluent. After another few days of gradual increase, TMP began rising rapidly again, triggering an automatic shutdown on 6/1. It is important to note O_3-MF achieved 20 days of cumulative operation, only 1 day shy of the 21-day goal, with only one chlorine EFM and one caustic EFM. These data suggested including two appropriately scheduled chlorine EFMs, and citric acid EFMs could have been sufficient to achieve the 21-day goal without any automatic shutdowns caused by high TMP.

Table 5.7. Average TOC, Turbidity, and UVA Data During Run 1

Water Quality Parameter	Units	Pilot Plant Influent	Ozone Effluent	$FeCl_3$-MF		O_3-MF	
				Filtrate	Backwash	Filtrate	Backwash
TOC	mg/L	13 (1.0)	15 (0.6)	12 (0.6)	37*	15 (0.7)	24*
Turbidity	NTU	6.3 (1.6)	4.1 (2.3)	0.15 (0.04)	100 (56)	0.14 (0.03)	41 (16)
UVA	cm^{-1}	0.358 (0.064)	0.232 (0.060)	0.228 (0.043)	2.382 (1.126)	0.155 (0.042)	1.082 (0.318)

Notes: *Standard deviation was not calculated because only two samples were analyzed.
Standard deviations are presented in parentheses below the averages.

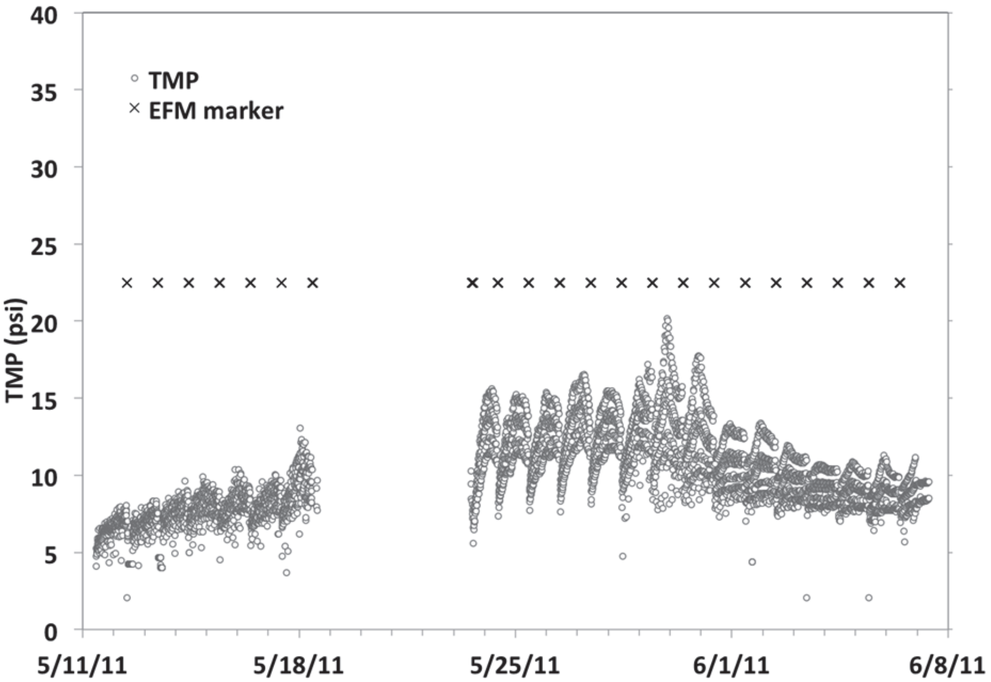

Figure 5.4. TMP data for Run 1 of $FeCl_3$-MF with X markers for chlorine EFMs.

Note: Mechanical problems with the MF unit caused the shutdown from 5/18 to 5/23.

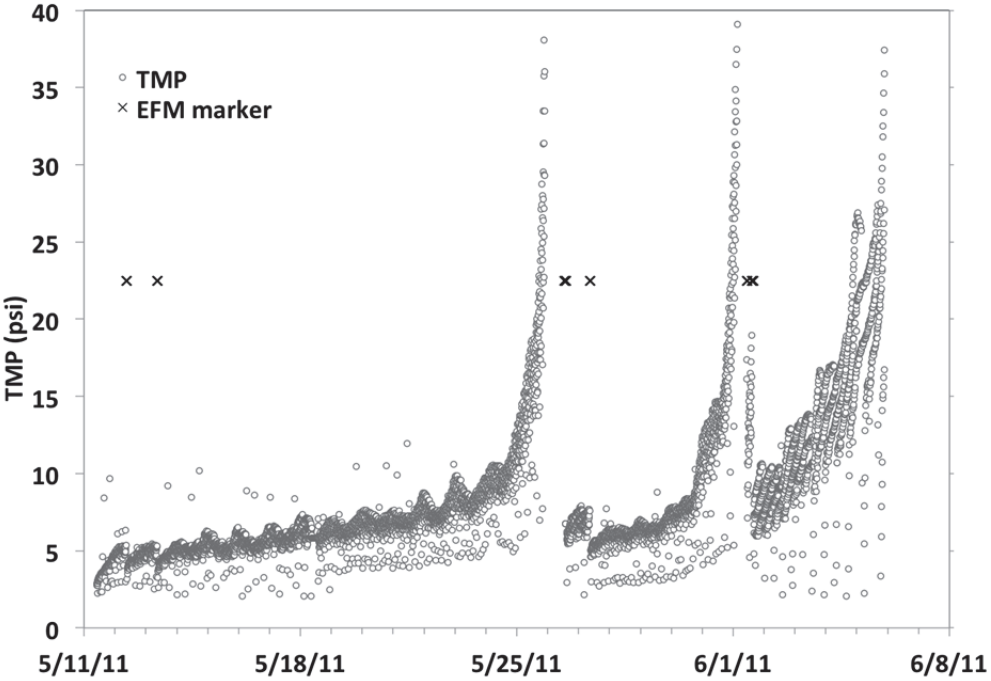

Figure 5.5. TMP data for Run 1 of O_3-MF with X markers for chlorine or citric acid EFMs.

Note: There was no ozone pretreatment from 6/1 until the final high TMP shutdown on 6/5.

A second set of chlorine and citric acid EFMs were performed before resuming filtration without ozone pretreatment. Comparing the TMP trend after the chlorine and citric acid

EFMs on 5/26 with the TMP trend after the EFMs on 6/1 suggested ozonation was improving daily performance compared to the same operating conditions without ozone. Considering the data for $FeCl_3$-MF, there were two likely explanations for the rapid rise in TMP that triggered the automatic shutdowns: (1) ozonation was not addressing a foulant that was removed by $FeCl_3$, or (2) ozonation was creating a foulant that was not completely removed by chlorine EFMs or citric acid EFMs. One possibility under the latter explanation was Mn, which was a known foulant of low-pressure membranes (Chae et al., 2008; Kimura et al., 2004; Takizawa et al., 2001) that was believed to be present the pilot plant influent. Ozone could oxidize Mn from soluble Mn(II) to insoluble Mn(IV). Iron (Fe) was another potential foulant, so regular sampling for these constituents was implemented after Run 1.

5.3.2 Run 2 (6/10 to 7/7) – $FeCl_3$-MF versus O_3-MF

After Run 1, chlorine/caustic and citric acid CIPs were performed in preparation for Run 2, which again compared $FeCl_3$-MF to O_3-MF. As a response to the shutdowns of O_3-MF owing to high TMP, an automatic 640-mg/L chlorine EFM every 48 h and a manually triggered 1900 mg/L citric acid EFM every 10 days were scheduled for that MF unit. EFM frequencies and concentrations for $FeCl_3$-MF were the same as Run 1. The transferred ozone dose and $FeCl_3$ dose were unchanged at 8 mg/L and 9.2 mg/L, respectively. Other MF operating conditions, such as backwash interval and flux, were unchanged.

5.3.2.1 Water Quality

Average TOC, turbidity, and UVA data for each treatment train (Table 5.8) showed ozonation increased TOC by 1 mg/L and reduced turbidity and UVA by 39 and 34%, respectively. As with Run 1, there was little to no change in average TOC by MF. MF filtrate turbidity was 23% higher for $FeCl_3$-MF compared to O_3-MF. UVA reduction by MF was similar in both treatment trains (approximately 40%) with ozonation resulting in a lower UVA in O_3-MF filtrate. Backwash TOC, turbidity, and UVA were 50 to 90% higher for $FeCl_3$-MF compared to O_3-MF. Data from Run 1 also indicated backwash water quality was worse for $FeCl_3$-MF.

Total Fe and total Mn data in Table 5.9 showed the pilot plant influent had average concentrations of 0.41 mg/L and 0.11 mg/L, respectively. Average total Fe concentrations were much higher in $FeCl_3$-MF feed, because $FeCl_3$ was being added. Because Mn is typically present in industrial $FeCl_3$ solutions, the elevated total Mn concentration in $FeCl_3$-MF feed also could have been caused by $FeCl_3$ addition. While the total Fe concentration was much lower in O_3-MF feed, the concentration in the filtrate of that MF unit was much higher compared to $FeCl_3$-MF. These data indicated $FeCl_3$ addition provided better removal of total Fe by $FeCl_3$-MF than was seen from O_3-MF. Total Mn concentrations in the filtrate of both MF units were similar.

Table 5.8. Average TOC, Turbidity, and UVA Data During Run 2

Water Quality Parameter	Units	Pilot Plant Influent	Ozone Effluent	$FeCl_3$-MF		O_3-MF	
				Filtrate	Backwash	Filtrate	Backwash
TOC	mg/L	13 (0.6)	14 (0.6)	12 (1.5)	60 (2.0)	13 (2.1)	32 (3.5)
Turbidity	NTU	7.0 (2.4)	4.3 (0.9)	0.16 (0.06)	132 (124)	0.13 (0.06)	77 (31)
UVA	cm^{-1}	0.354 (0.038)	0.235 (0.025)	0.208 (0.017)	2.187 (1.229)	0.145 (0.014)	1.488 (0.406)

Note: Standard deviations are presented in parentheses below the averages.

Table 5.9 Average Fe (Total) and Mn (Total) Data During Run 2

Water Quality Parameter	Units	Pilot Plant Influent	$FeCl_3$-MF		O_3-MF	
			Feed	Filtrate	Feed	Filtrate
Fe (total)	mg/L	0.41 (0.11)	6.3 (2.9)	0.06 (0.02)	0.73 (0.45)	0.17 (0.16)
Mn (total)	mg/L	0.11 (0.01)	0.14 (0.01)	0.09 (0.003)	0.11 (0.01)	0.09 (0.004)

Note: Standard deviations are presented in parentheses below the averages.

Run 2 included the analysis of one set of samples to determine the MW distribution of EfOM at different points within each treatment train. Samples were fractionated using UF membranes with a nominal MW cutoff of 10 kDa and analyzed for TOC, UVA, and protein concentration (Figure 5.6). Data showed ozonation increased the < 10 kDa fraction of TOC, similarly reduced both MW fractions of UVA, and preferentially reduced MW of proteins. In both treatment trains, MF primarily removed > 10 kDa organics and had little effect on the smaller MW fraction.

As with the water quality data in Table 5.8, the MF backwash data showed the biggest difference between the treatment trains. Both treatment trains showed the larger MW fraction was overrepresented in the backwash water compared to the smaller MW fraction. For example, the MW distribution of TOC was 56% > 10 kDa and 44% < 10 kDa in the influent sample but was approximately 90% > 10 kDa and 10% < 10 kDa in the backwash water of both treatment trains. While differences between TOC concentrations and MW distributions were small, protein concentration and UVA from $FeCl_3$-MF were noticeably higher. For those two parameters, the backwash water of $FeCl_3$-MF had higher concentrations of both MW fractions.

Combining the MW distribution data with the water quality data reported in Table 5.8 indicated $FeCl_3$-MF removed more large MW organics, such as proteins, than O_3-MF. Because these types of organics have been shown to cause organic fouling (Lozier et al., 2008; Trussell et al., 2009), the data provided indirect evidence of more organic foulants collecting on the membranes of $FeCl_3$-MF compared to O_3-MF.

Data from the analysis of collapsed foam collected from the pilot plant (Table 5.10) suggested the improvement in water quality was at least partially attributed to the physical separation of organics and other materials from the water in a process resembling dissolved air flotation. It is important to note foam production was dependent on ozonation, as demonstrated by negligible foaming when oxygen gas was added without ozone. The concentrations of TOC, carbohydrates, proteins, and UVA in the foam were >100 times higher than what was reported in Chapter 3 for ECLWRF influent, which was the same source of secondary effluent that supplied the pilot plant. The volume of foam produced by ozonation could not be quantified so the significance of foulant removal via flotation versus ozone oxidation was not defined.

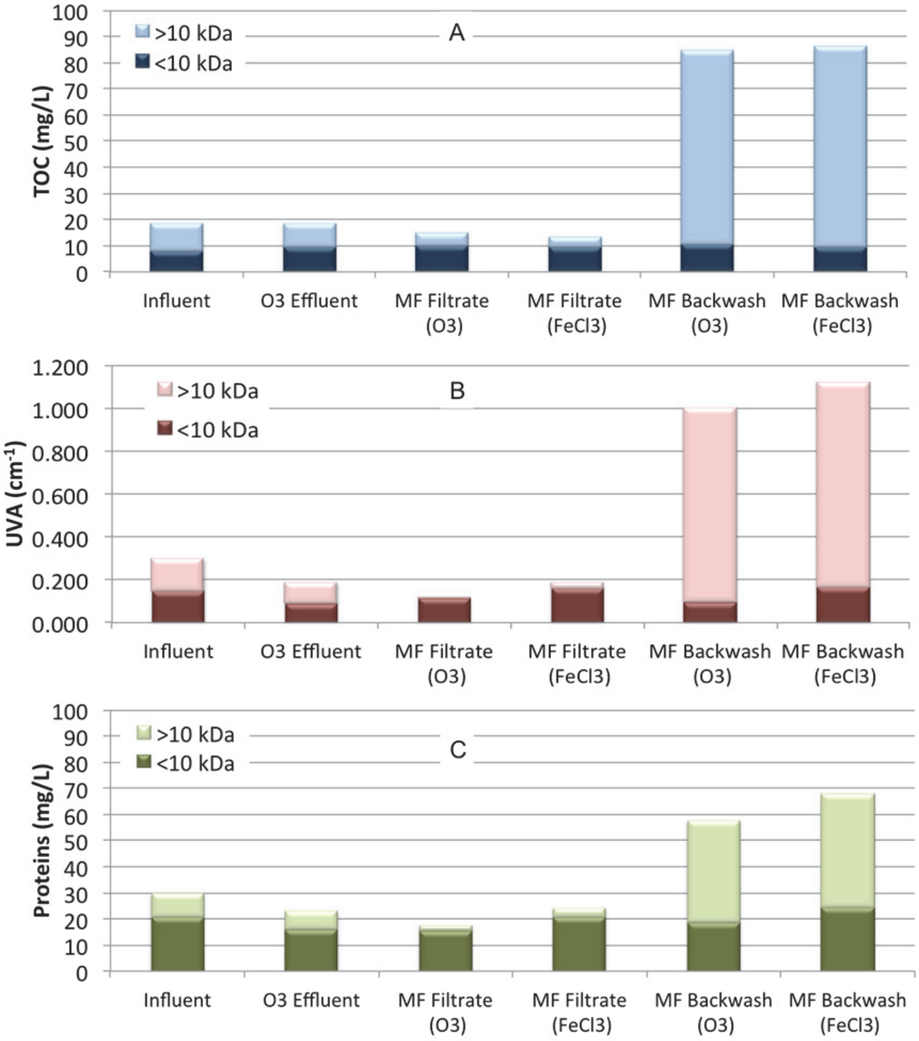

Figure 5.6. MW distribution of (A) TOC, (B) UVA, and (C) proteins of samples collected from the pilot plant during Run 2 on 6/13/11.

Note: This was with a transferred ozone dose of 8 mg/L.

Table 5.10. Water Quality Characteristics of Collapsed Foam Collected During Ozonation

Organic Fraction	TOC (mg/L)	Carbohydrates (mg/L)	Proteins (mg/L)	UVA (cm^{-1})
>10 kDa	N/M	1690	5440	63.9
<10 kDa	N/M	160	1400	10.9
Total	3,340	1850	6840	74.8

Note: N/M = not measured

5.3.2.2 MF Performance

Performance of $FeCl_3$-MF and O_3-MF during Run 2 are shown in Figures 5.7 and 5.8, respectively. $FeCl_3$-MF maintained a stable TMP between 6 and 8 psi during 25 days of cumulative operation. O_3-MF operated with a lower TMP than $FeCl_3$-MF until 6/25, the 16th day of operation. Beyond that day, the TMP of O_3-MF started rising beyond the stable TMP of $FeCl_3$-MF while recovering significantly after the chlorine EFM. On 6/29, the TMP of O_3-MF rose to 40 psi, causing it to shut down automatically. A 1900-mg/L citric acid EFM was performed after the shutdown and the unit was programmed to initiate a 640-mg/L chlorine EFM at a TMP set point of 21 psi in addition to its existing chlorine EFM trigger every 48 h. TMP data from 6/29 to 7/1 (Figure 5.7) indicated this approach was unsuccessful at restoring performance.

The generally good recovery after backwashing (data not shown) and the chlorine EFMs indicated the cake layer and organics were unlikely to be responsible for the poor performance and shutdowns during Run 2. Another possibility was inorganic fouling, which was targeted by the 5000 mg/L Super Iron Out® EFM performed on 7/1. Super Iron Out®, a commercial product commonly available at hardware stores, was used because it contains 15 to 40% sodium hydrosulfite ($Na_2S_2O_4$) and 15 to 40% sodium metabisulfite ($Na_2S_2O_5$) (Summit Brands, 2011), which are strong reductants that could help remove inorganic foulants such as Mn. Over the following 36 h, several chlorine EFMs were triggered by reaching the TMP set point of 21 psi, but none were triggered by high TMP over 4 ½ days after that. These results suggested the removal of some combination of inorganic foulants by the Super Iron Out® EFM and organics by the frequent chlorine EFMs successfully restored an acceptable level of performance to MF train 1 during the final days of Run 2.

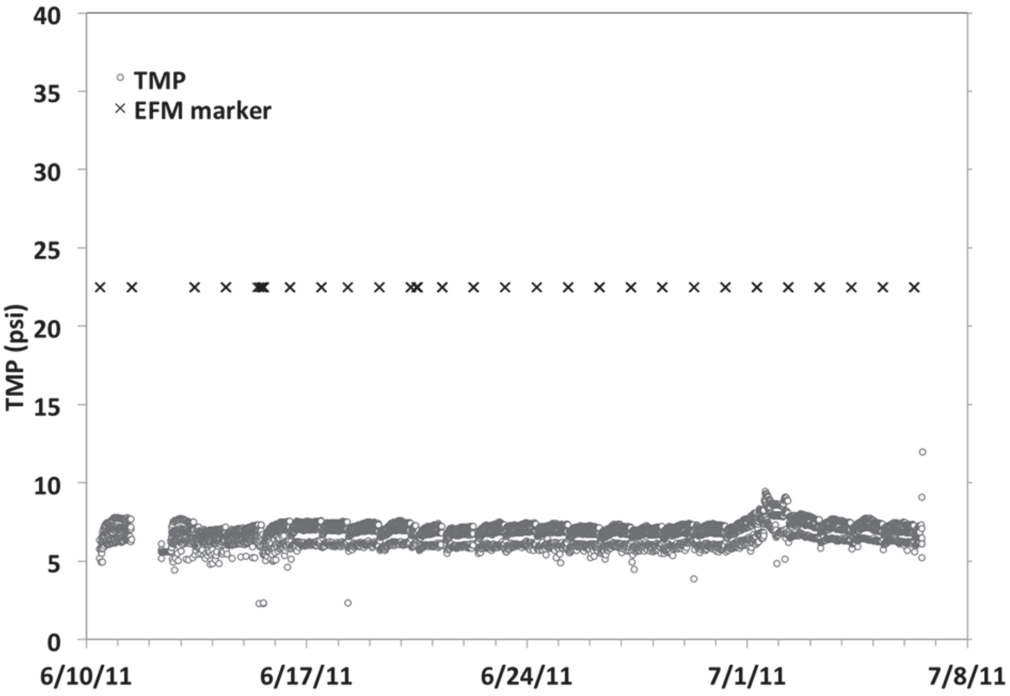

Figure 5.7. TMP data for Run 2 of $FeCl_3$-MF with X markers for daily chlorine EFMs.

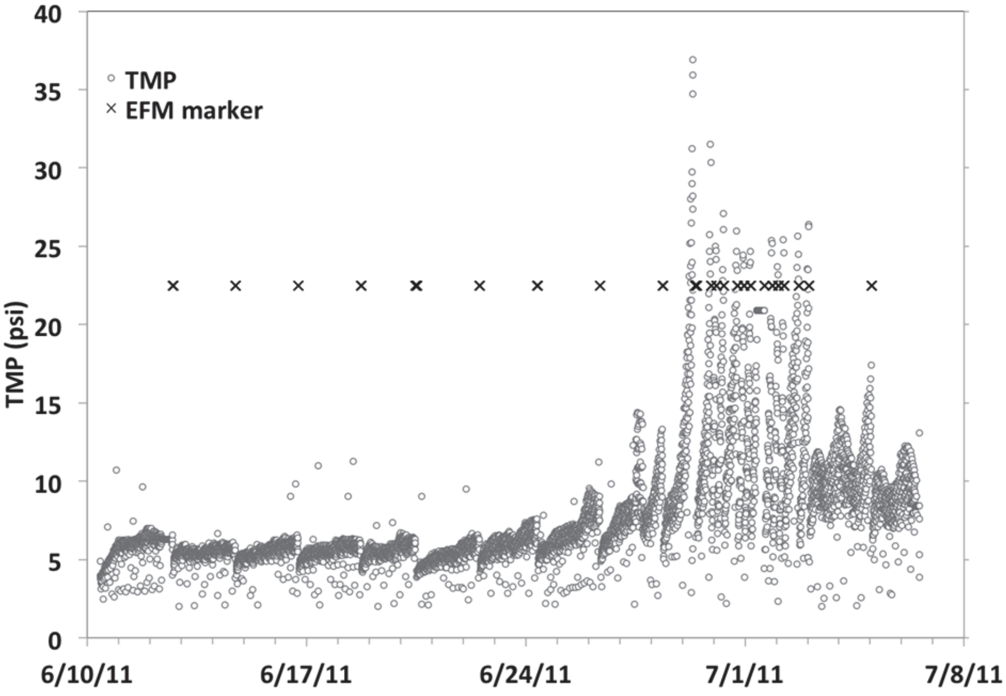

Figure 5.8. TMP data for Run 2 of O_3-MF with X markers for daily chlorine EFMs.

To test the theory that inorganic fouling was a significant contributor to fouling of O_3-MF during Run 2, both MF units were cleaned following a special CIP procedure. This procedure included an extended 2% citric acid CIP (4-hr wash followed by a 12-hr soak at 90 to 95 °F) followed by a 3000 mg/L chlorine plus 2% sodium hydroxide CIP (2-hr wash at 90 to 95 °F). Specific flux was calculated at different clean water flow rates before beginning the CIP, after the extended citric acid CIP, and after the chlorine/caustic CIP. $FeCl_3$-MF recovered most of its specific flux after the chlorine/caustic CIP (Figure 5.9) suggesting inorganic fouling of those membranes was minimal. However, O_3-MF recovered a significant amount of its specific flux after the extended citric acid CIP (Figure 5.10) indicating inorganic fouling had a greater effect on those membranes. The recovery after the chlorine/caustic CIP of O_3-MF also demonstrates organic fouling was significant.

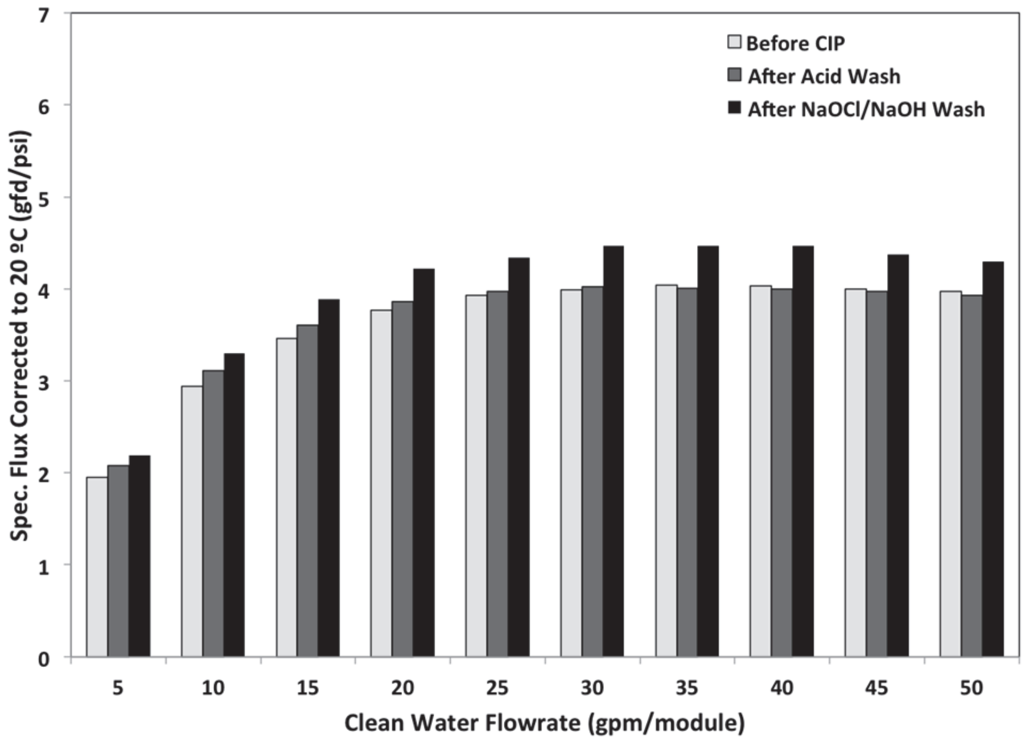

Figure 5.9. Specific fluxes of $FeCl_3$-MF at different clean water flow rates.

Note: This was before the CIP, after the extended citric acid CIP, and after the chlorine/caustic CIP at the end of Run 2.

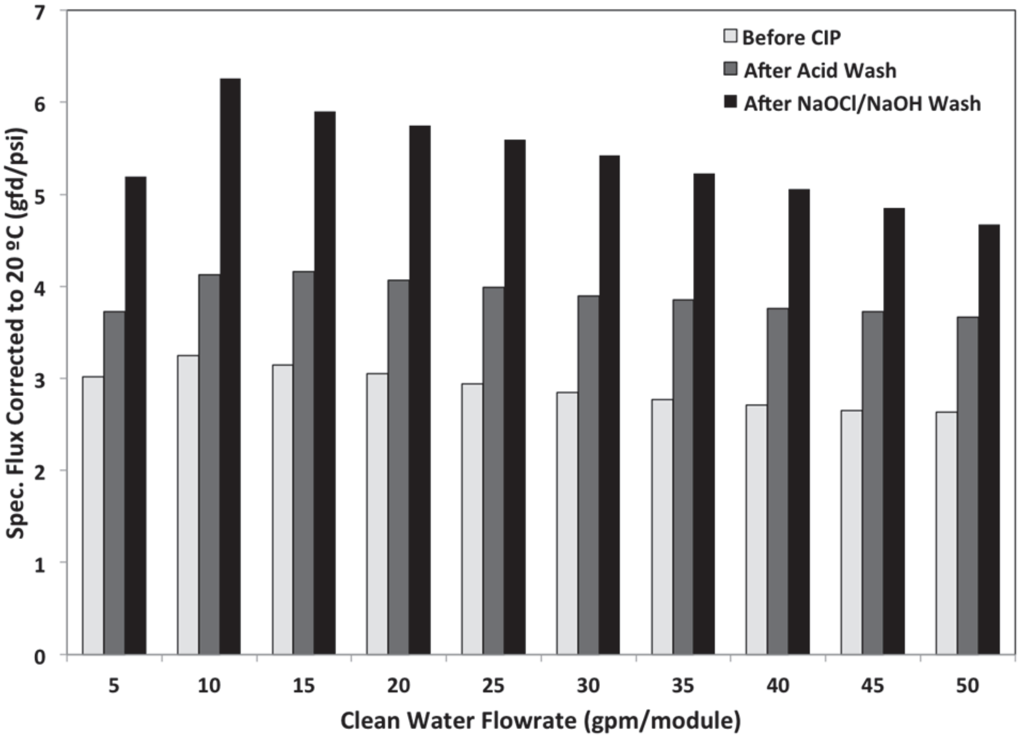

Figure 5.10. Specific fluxes of O_3-MF at different clean water flow rates.

Note: This was before the CIP, after the extended citric acid CIP, and after the chlorine/caustic CIP at the end of Run 2.

5.3.3 Run 3 (7/8 to 8/2) – $FeCl_3$-MF versus O_3-MF

In preparation for Run 3, additional modifications were made to the EFM schedule of O_3-MF. Automatic 2% citric acid EFMs were scheduled once every 6 days and manual chlorine EFMs were scheduled after every second citric acid EFM (once every 12 days). The more frequent and higher concentration citric acid EFM was intended to improve removal of inorganic foulants, likely to be Fe and/or Mn, that appeared to caused significant fouling of O_3-MF during Run 2. The transferred ozone dose was 8 mg/L at the start of testing before being increased to 12 mg/L to see if a higher ozone dose would improve MF performance. $FeCl_3$-MF continued with a dose of 10 mg/L of $FeCl_3$ in its feed and the same EFM schedule (chlorine EFM daily and citric acid EFM every 10 days).

5.3.3.1 Water Quality

Average water quality data from Run 3 are shown in Table 5.11 and followed the same general trends of the previous two experiments. Ozonation caused another small increase in TOC while decreasing turbidity and UVA by 33 and 34%, respectively. TOC removal averaged 2 mg/L for the $FeCl_3$-MF, whereas there was no difference between the O_3-MF feed and filtrate. MF filtrate turbidity was 30% higher for $FeCl_3$-MF compared to O_3-MF, continuing a trend from Runs 1 and 2. UVA reduction was 33% for O_3-MF and 35% for $FeCl_3$-MF with O_3-MF filtrate having the lower MF filtrate UVA owing to ozone pretreatment. Backwash TOC, turbidity, and UVA were 50 to 90% higher for $FeCl_3$-MF compared to O_3-MF. Lower TOC, turbidity, and UVA in O_3-MF backwash compared to $FeCl_3$-MF also continued the trend seen in the earlier runs.

There were a few notable differences between total Fe and total Mn data for Run 3 (Table 5.12) compared to Run 2 (Table 5.6). The total Fe concentration in the pilot plant influent was lower than it was in Run 2, but the total Mn concentrations were the same. $FeCl_3$-MF feed concentration of total Fe and total Mn were still high because of $FeCl_3$ addition before that MF unit. Because there was no $FeCl_3$ added to O_3-MF, concentrations of total Fe and total Mn in O_3-MF feed were similar to the influent. There was little difference between the total Fe and total Mn concentrations in MF filtrate of both treatment trains. These data indicated $FeCl_3$-MF was removing more Fe and Mn than O_3-MF. However, these data did not specify the form (e.g., $Fe(OH)_3$ and MnO_2) or oxidation state of Fe and Mn being removed.

As with Run 2, a set of water samples from the pilot plant was evaluated for MW distribution of TOC, UVA, proteins, and carbohydrates (Figure 5.11). The transferred ozone dose at the time of sample collection was 8 mg/L. The carbohydrate concentration of $FeCl_3$-MF Filtrate (Figure 5.11D) only displays the total concentration. MW distribution could not be determined because of a problem with the carbohydrate analysis of the sample after UF fractionation. Not enough of the original or fractionated sample remained to repeat the analysis.

Table 5.11. Average TOC, Turbidity, and UVA Data During Run 3

Water Quality Parameter	Units	Pilot Plant Influent	Ozone Effluent	$FeCl_3$-MF		O_3-MF	
				Filtrate	Backwash	Filtrate	Backwash
TOC	mg/L	13 (0.6)	14 (1.0)	11 (0.6)	30 (4.3)	13 (0.6)	22 (3.2)
Turbidity	NTU	5.4 (0.8)	3.6 (0.8)	0.13 (0.03)	98 (30)	0.10 (0.03)	35 (21)
UVA	cm^{-1}	0.308 (0.026)	0.204 (0.034)	0.199 (0.017)	2.914 (0.816)	0.136 (0.016)	0.844 (0.336)

Note: Standard deviations are presented in parentheses below the averages.

Table 5.12. Average Fe (Total) and Mn (Total) Data During Run 3

Water Quality Parameter	Units	Pilot Plant Influent	$FeCl_3$-MF		O_3-MF	
			Feed	Filtrate	Feed	Filtrate
Fe (total)	mg/L	0.26 (0.07)	7.9 (5.5)	0.07 (0.04)	0.31 (0.13)	0.06 (0.03)
Mn (total)	mg/L	0.11 (0.02)	0.18 (0.06)	0.10 (0.002)	0.12 (0.02)	0.10 (0.01)

Note: Standard deviations are presented in parentheses below the averages.

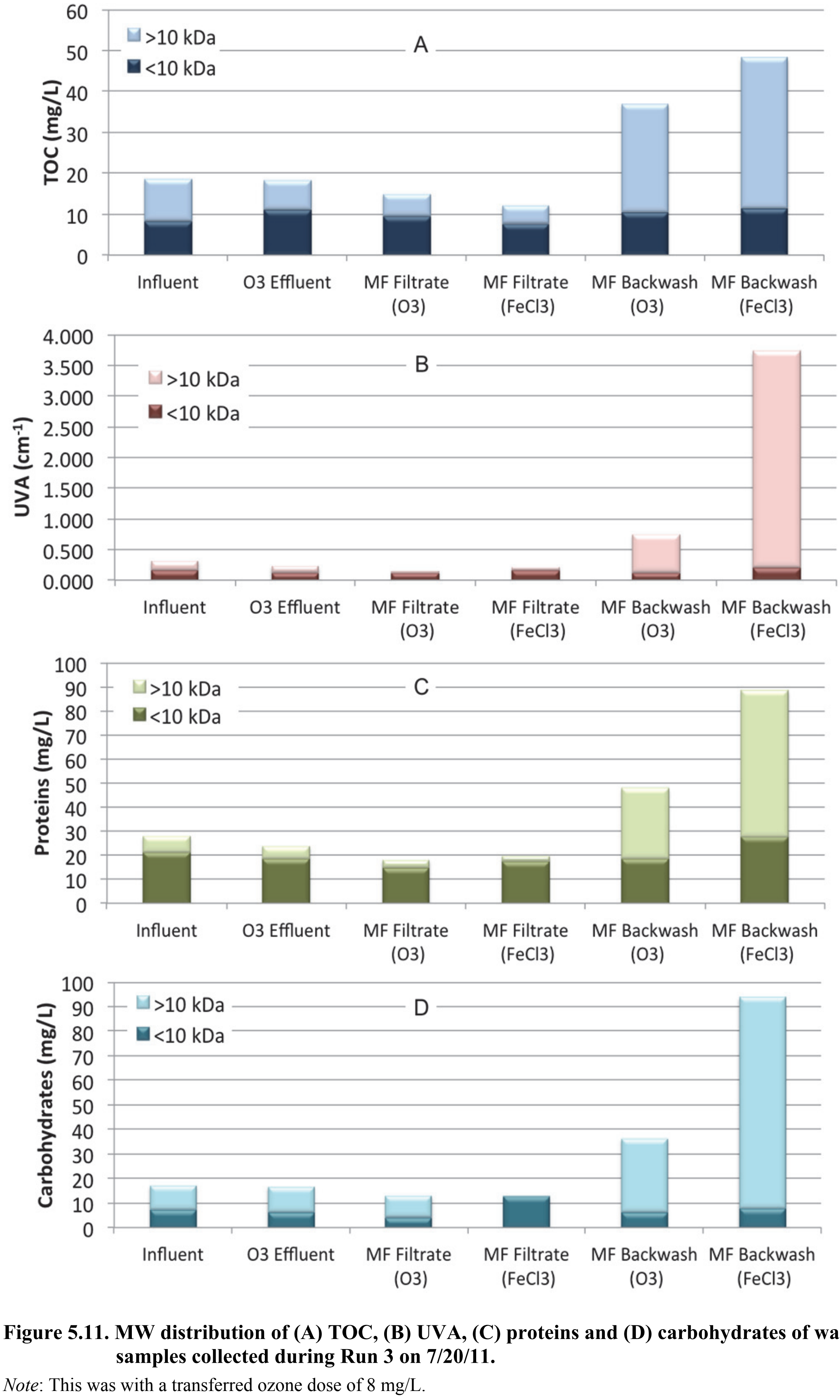

Figure 5.11. MW distribution of (A) TOC, (B) UVA, (C) proteins and (D) carbohydrates of water samples collected during Run 3 on 7/20/11.

Note: This was with a transferred ozone dose of 8 mg/L.

MW distribution trends of TOC, UVA, and proteins in the sample from Run 3 (Figure 5.11) generally followed the trends of the Run 2 sample (Figure 5.6). Ozonation preferentially reduced the > 10 kDa fraction of UVA and proteins while shifting TOC to the < 10 kDa fraction. In both treatment trains, MF preferentially removed organics with MW > 10 kDa. Measurements of TOC, UVA, proteins, and carbohydrates in MF backwash were significantly higher than they were in the influent, and measurements of $FeCl_3$-MF backwash exceeded those of O_3-MF backwash. In addition, a greater proportion of the organics in MF backwash were > 10 kDa. Carbohydrate analysis was not performed on Run 2 samples, but the trend of the carbohydrate data followed a similar pattern as the TOC, UVA, and protein data. One difference between carbohydrates and UVA and proteins was the total carbohydrate concentration and MW distribution was relatively unchanged by ozonation.

Samples collected for MW fractionation also were analyzed using fluorescence excitation-emission matrix (EEM) spectroscopy (Figure 5.12) to evaluate differences between the treatment trains. Regional and total fluorescence intensities of samples normalized to the pilot influent sample are shown in Table 5.10. A complete discussion of the regions and associated organic fractions EEM spectroscopy was included in Chapter 3, Section 3.2.2.2.

Figure 5.12 showed ozonation significantly reduced peak and regional intensity in all three regions of the EEM spectra (proteins and soluble microbial products, fulvic-like substances, and humic-like substances). The MF unit downstream of ozonation had little effect on the EEM spectra, because EfOM fluorescence already had been reduced significantly. The low intensity of the EEM spectra of O_3-MF backwash supported this conclusion. Because the membranes did not retain much of this material, fluorescent EfOM would be expected to cause minimal organic fouling.

The EEM spectra of $FeCl_3$-MF filtrate resembled O_3-MF filtrate, indicating these treatment trains had similar effects on the fluorescent character of EfOM. However, changes after ozonation primarily were caused by a combination of chemical oxidation and physical separation via flotation. Comparatively, $FeCl_3$-MF removed significant quantities of fluorescent EfOM by retaining them on the membrane. The regional and total intensities of the EEM spectra of $FeCl_3$-MF backwash exceeded the intensity of the EEM spectra of the influent and were four to six times higher than the intensity of O_3-MF backwash (Table 5.13). The high removal of fluorescent EfOM and high backwash fluorescence intensity indicated exposure of $FeCl_3$-MF to a relatively high concentration of organic foulants was likely.

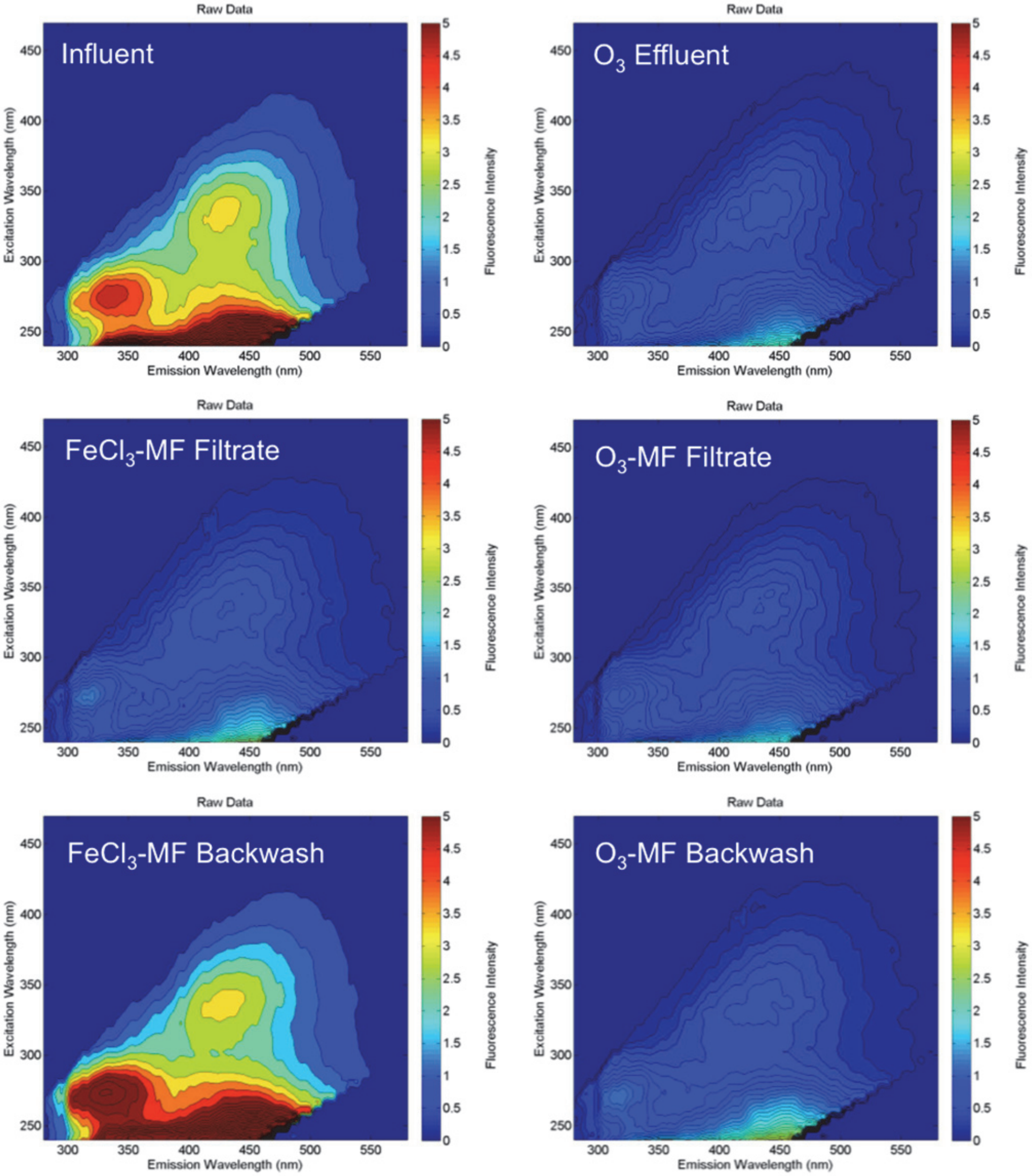

Figure 5.12. EEM images of samples collected during Run 3 on 7/20/11.

Notes: This is with a transferred ozone dose of 8 mg/L. The x-axis and y-axis correspond with the emission and excitation wavelengths, respectively. The fluorescence intensity scale is to the right of each image**.**

Table 5.13. Integrated Regional and Total Fluorescence for Each Sample Collected on 7/20/11

Region	Pilot Plant Influent	Ozone Effluent	$FeCl_3$-MF Filtrate	$FeCl_3$-MF Backwash	O_3-MF Filtrate	O_3-MF Backwash
1	1.00	0.16	0.21	1.27	0.17	0.22
2	1.00	0.20	0.24	1.20	0.18	0.26
3	1.00	0.23	0.26	1.08	0.20	0.25
Total	1.00	0.18	0.23	1.21	0.18	0.24

Note: This was normalized to the pilot influent sample. The transferred ozone dose at the time of the sampling was 8 mg/L.

5.3.3.2 MF Performance

As with the previous two runs, $FeCl_3$-MF performed well throughout the test (Figure 5.13). TMP did rise from 7/14 to 7/19, but this change was attributed to the failure of a chemical feed pump to add chlorine to the MF feed to form chloramines. Once chlorine addition resumed on 7/19, TMP gradually recovered. $FeCl_3$-MF surpassed the target CIP interval of 21 days and, judging by the final TMP, probably could have continued operating for several more days.

TMP data for O_3-MF during Run 3 are shown in Figure 5.14. This MF unit operated for 6 days before a mechanical problem required it to be shut down for repair. This shutdown occurred as O_3-MF was due for its first citric acid EFM, which was performed after the MF unit was returned to service on 7/18. After 2 more days, TMP began to rise again, so a manual 2% citric acid EFM followed by a 640-mg/L chlorine EFM were performed. O_3-MF recovered performance immediately after the EFMs, but a steady rise of TMP prompted the initiation of another set of manual EFMs. This time, the first EFM used a solution of 1% citric acid and 1% hydrochloric acid (HCl). Using this combination of citric acid and HCl lowered the solution pH to 1.2, which was lower than the pH 2.0 typically achieved with the 2% citric acid EFM. The normal 640-mg/L chlorine EFM was performed after the acid EFM.

As shown in Figure 5.14, TMP continued to rise after these EFMs were completed on 7/22, causing an automatic shutdown on high TMP in less than 12 h. After the unit was offline for a few days over a weekend, a 850 mg/L chlorine EFM was performed on 7/26. Initial recovery was favorable, although TMP rose a few psi over 24 h. On 7/27, an EFM of 1700 mg/L chlorine with 700 mg/L sodium hydroxide was followed by an EFM of 5% Super Iron Out®. The TMP of O_3-MF dropped below 5 psi and maintained an acceptable TMP for 4 days before another catastrophic rise in TMP caused an automatic shutdown.

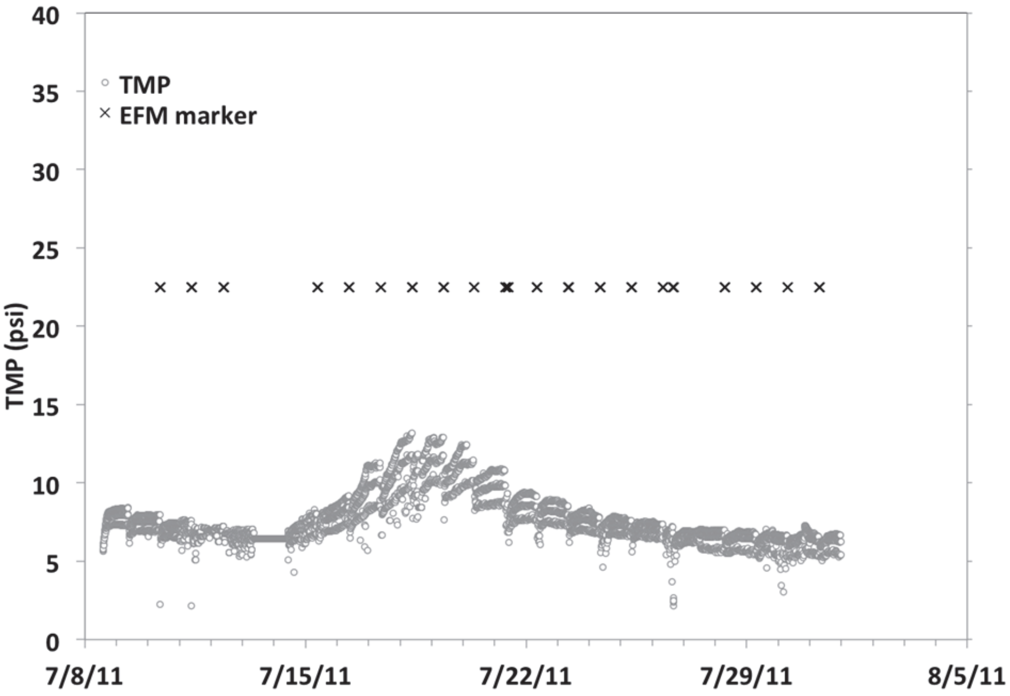

Figure 5.13. TMP data for Run 3 of $FeCl_3$-MF with X markers for daily chlorine EFMs.

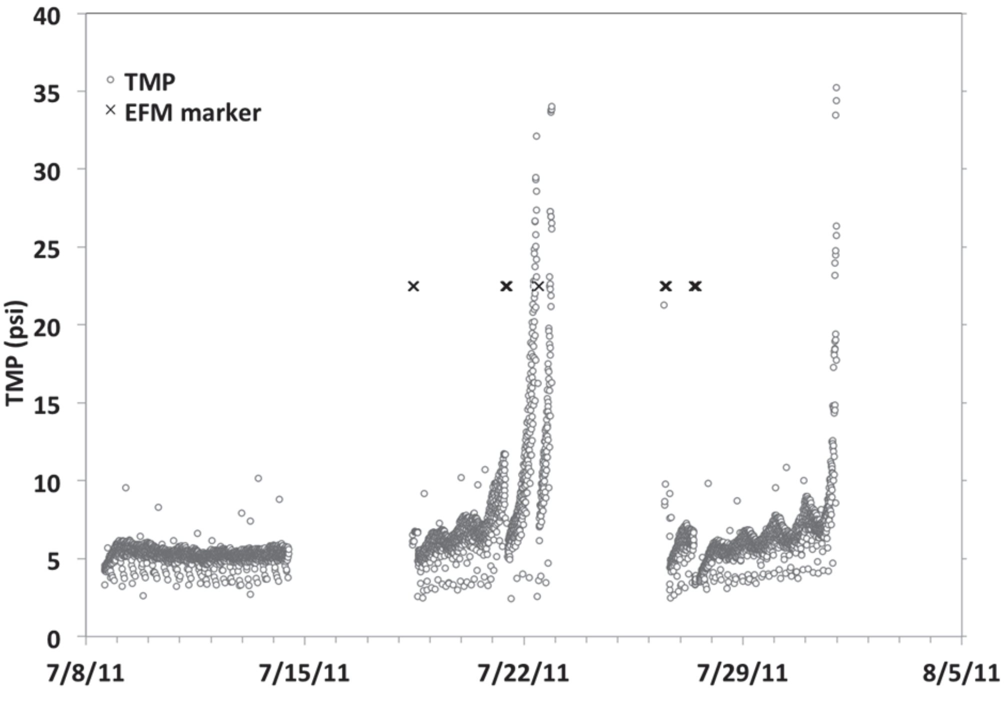

Figure 5.14. TMP data for Run 3 of O_3-MF.

Note: A mechanical problem and an operational delay caused the gaps from 7/14 to 7/18 and 7/22 to 7/26, respectively.

The combination of O_3-MF sitting idle for a few days after the shutdown on 7/23, the initial 850 mg/L chlorine EFM and the subsequent chlorine/caustic and Super Iron Out® EFMs recovered performance so the MF unit could operate for a few days at acceptable TMPs. During normal operation, ozone would have oxidized soluble Mn(II) into insoluble Mn(IV), most likely producing manganese dioxide (MnO_2). The flow of ozonated water through the MF modules would have continuously exposed them to MnO2 and would have maintained conditions favorable to Mn(IV). When O_3-MF was offline from 7/23 to 7/26, the conditions within the MF modules could have changed to promote the reduction of Mn(IV) to Mn(II), thereby dissolving some of the MnO_2 that fouling the membranes. This would be similar to a study of media filtration in water treatment that demonstrated the dissolution of MnO_2 when water chemistry changed from an oxidative environment (presence of free chlorine) to a reducing environment (absence of free chlorine) (Gabelich et al., 2006b).

Considering MF data from Runs 1 to 3, a theory explaining the high TMP in the MF unit after ozonation was developed. The exponential rises in TMP were not indicative of the development of a cake layer that gradually increased the applied pressure necessary to maintain the target operating flux. The TMP data were more indicative of fouling that caused pore blockage, possibly deep within the pore structure. When a pore was blocked, the surrounding pores needed to filter more water to maintain the same flux. The higher filtration rate of the surrounding pores to compensate for the blocked pore also increased the exposure of those pores to the source of fouling. Therefore, the fouling rate of the surrounding pores increased until another pore was blocked, which further increased the fouling of the remaining pores. The result was a pattern of accelerating pore blockages causing an exponential TMP increase and eventual shutdown of the MF unit. Backwashing and chlorine EFMs could prevent temporary relief by removing the cake layer and organic foulants but were ineffective at addressing the source of the problem: deep pore fouling by subcolloidal Mn. To ensure acceptable performance of O_3-MF, a strategy to minimize Mn fouling needed to be developed.

5.3.4 Run 4 (8/4 to 9/2) – $FeCl_3$-MF versus O_3-$FeCl_3$-MF

After three runs where O_3-MF was shutdown repeatedly by Mn fouling, $FeCl_3$ addition between ozonation and MF (O_3-$FeCl_3$-MF) was tested to determine if coagulation could improve MF performance. $FeCl_3$ was expected to coagulate Mn into larger particles that would be captured in the cake layer and removed by backwashing, thereby reducing deep pore fouling. Therefore, Run 4 compared MF performance of $FeCl_3$-MF and O_3-$FeCl_3$-MF. Test conditions included a manually set average transferred ozone dose of 11 mg/L that was reduced to 9 mg/L after one week. Both MF units received 10 mg/L $FeCl_3$, a daily EFM with a solution of 1,700 mg/L chlorine and 700 mg/L caustic, and a 2500 mg/L citric acid EFM every 10 days.

5.3.4.1 Water Quality

Average TOC, turbidity, and UVA data from Run 4 (Table 5.14) demonstrated pilot plant influent water quality was better than the previous three runs. Ozonation increased the average TOC by 1 mg/L and decreased the average turbidity and UVA by approximately 30% each. These changes were similar to what was observed during Runs 1 to 3. MF filtrate TOC and turbidity were the same for both treatment trains, but the lower UVA caused by ozonation persisted. Differences between MF backwash TOC, turbidity, and UVA were less than they were in the first three runs. These data indicated the addition of $FeCl_3$ improved TOC removal by the MF unit but also eliminated some of the water quality benefits of ozonation. The coagulation of organics that are captured by MF and then removed by backwashing could explain why O_3-$FeCl_3$-MF backwash more closely resembled $FeCl_3$-MF backwash than did O_3-MF backwash.

Total Fe and total Mn data for Run 4 (Table 5.15) indicated pilot plant influent concentrations were similar to those of Run 3. $FeCl_3$ addition in the MF feed increased total Fe and total Mn concentrations, although the Mn increase was much lower than the Fe increase. The higher Mn concentration in MF feed of O_3-$FeCl_3$-MF was probably related to the higher Fe concentration after $FeCl_3$ addition. More Mn in the MF feed explained the higher Mn concentration in O_3-$FeCl_3$-MF filtrate.

Data from water samples collected during Run 4 and analyzed for MW distribution are shown in Figure 5.15. Differences between the treatment trains largely followed those seen in the MW distribution data from Runs 2 and 3. Ozonation and MF continued to preferentially remove the > 10kDa fraction and backwash still had a higher proportion of > 10 kDa organics. One change compared to the earlier data was the MF backwash concentration of protein was higher in the ozone train. Otherwise, TOC, UVA, and carbohydrates were still lower in MF backwash from the treatment train with ozone pretreatment.

Table 5.14. Average TOC, Turbidity, and UVA Data During Run 4

Water Quality Parameter	Units	Pilot Plant Influent	Ozone Effluent	$FeCl_3$-MF		O_3-$FeCl_3$-MF	
				Filtrate	Backwash	Filtrate	Backwash
TOC	mg/L	12 (0.5)	13 (0.8)	11 (1.3)	28 (4.8)	11 (1.7)	30 (1.7)
Turbidity	NTU	4.8 (0.8)	3.4 (1.1)	0.14 (0.03)	78 (25)	0.14 (0.10)	66 (21)
UVA	cm^{-1}	0.280 (0.017)	0.189 (0.031)	0.196 (0.013)	2.668 (0.801)	0.131 (0.021)	2.194 (0.741)

Note: Standard deviations are presented in parentheses below the averages.

Table 5.15. Average Fe (Total) and Mn (Total) Data During Run 4

Water Quality Parameter	Units	Pilot Plant Influent	$FeCl_3$-MF		O_3-$FeCl_3$-MF	
			Feed	Filtrate	Feed	Filtrate
Fe (total)	mg/L	0.29 (0.12)	5.1 (2.1)	0.06 (0.03)	6.5 (2.9)	0.07 (0.02)
Mn (total)	mg/L	0.10 (0.02)	0.12 (0.03)	0.08 (0.02)	0.17 (0.03)	0.11 (0.03)

Note: Standard deviations are presented in parentheses below the averages.

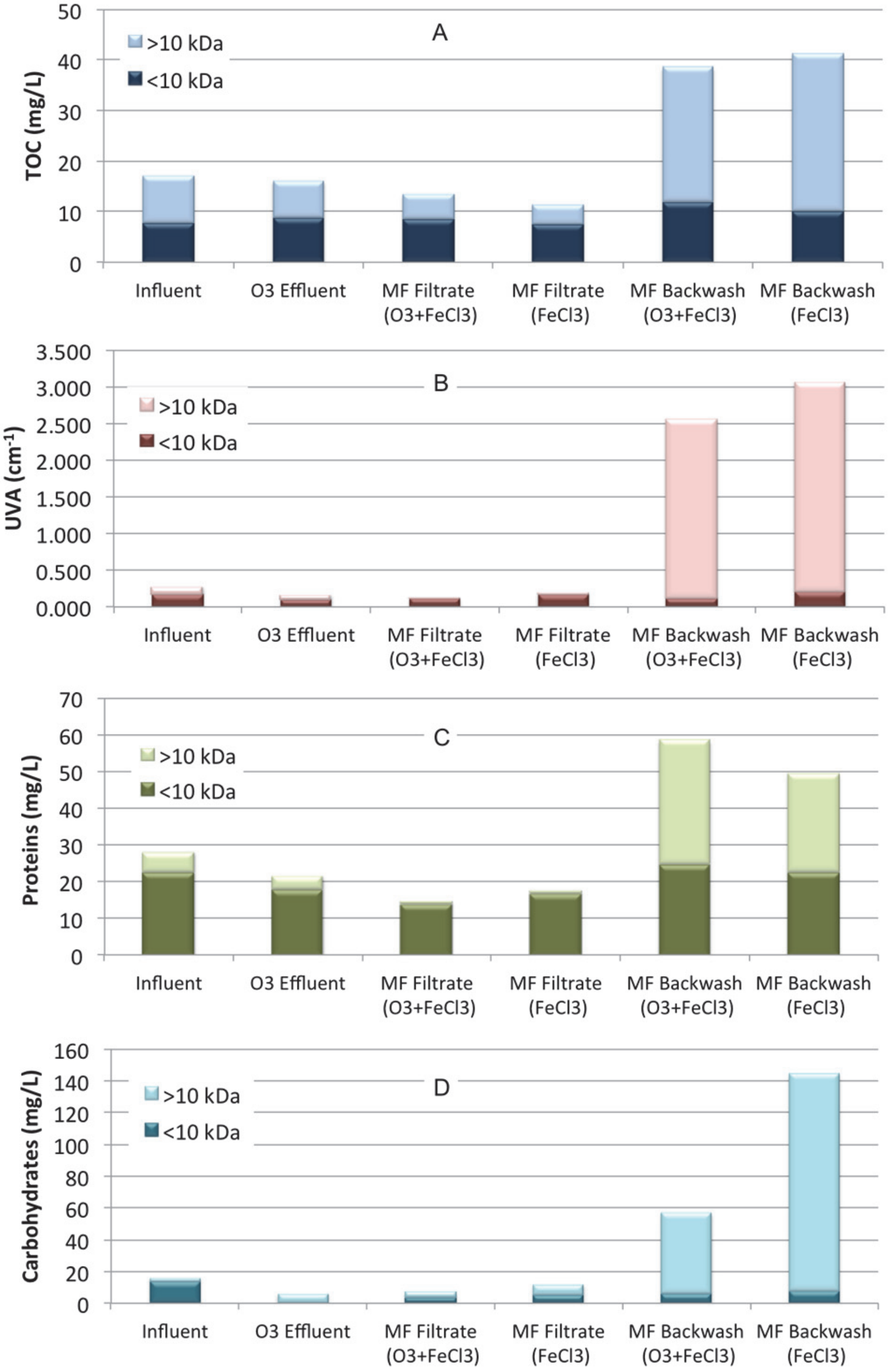

Figure 5.15. MW distribution of (A) TOC, (B) UVA, (C) proteins, and (D) carbohydrates of samples collected during Run 4 on 8/10/11.

Note: This had a transferred ozone dose of 11 mg/L.

Regional and total fluorescence intensities from EEM analysis of the Run 4 samples that were also analyzed for MW fractionation are shown in Table 5.16. The data was normalized to the pilot influent sample. Ozonation was shown to be sufficient to reduce fluorescence to levels similar to the Run 3 ozone effluent sample, although the transferred ozone dose was higher in Run 4 (11 mg/L) than Run 3 (8 mg/L). This higher dose probably accounted for the lower regional and total fluorescence in the ozone effluent (Table 5.16) compared to the previous run (Table 5.13). Comparing O_3-$FeCl_3$-MF filtrate to O_3-MF filtrate from Run 3 indicated the addition of $FeCl_3$ after ozonation improved fluorescence reduction by MF, particularly for the fulvic-like substances in Region II. This finding also held for O_3-$FeCl_3$-MF backwash in Run 4, although that also could be partially attributed to the higher ozone dose.

EEM images of the Run 4 samples analyzed for MW fractionation are shown in Figure 5.16. Compared to the EEM data from Run 3, the fluorescence of the pilot plant influent was higher during Run 4. With a $FeCl_3$ dose of 10 mg/L, $FeCl_3$-MF was not able to remove the same proportion of the regional and total fluorescence in the influent water as the MF unit did in Run 3. Because the influent fluorescence was higher, the relatively lower reduction of fluorescent organics caused $FeCl_3$-MF filtrate to have a higher intensity than the earlier filtrate sample for that treatment train. Although the EEM images of $FeCl_3$-MF backwash from Runs 3 and 4 were similar, the regional and total fluorescence of the backwash relative to the influent was higher during Run 4. These data suggested the Run 4 $FeCl_3$ dose was insufficient to reduce fluorescence the same percentage when the influent fluorescence was higher.

Table 5.16. Integrated Regional and Total Fluorescence for Samples Collected on 8/10/11

			$FeCl_3$-MF		O_3-$FeCl_3$-MF	
Region	**Pilot Influent**	**Ozone Effluent**	**Filtrate**	**Backwash**	**Filtrate**	**Backwash**
1	1.00	0.09	0.32	0.88	0.04	0.05
2	1.00	0.12	0.28	0.78	0.05	0.07
3	1.00	0.16	0.48	0.89	0.09	0.11
Total	1.00	0.11	0.31	0.83	0.05	0.07

Note: The sample was normalized to the pilot influent sample. The transferred ozone dose at the time of sampling was 11 mg/L.

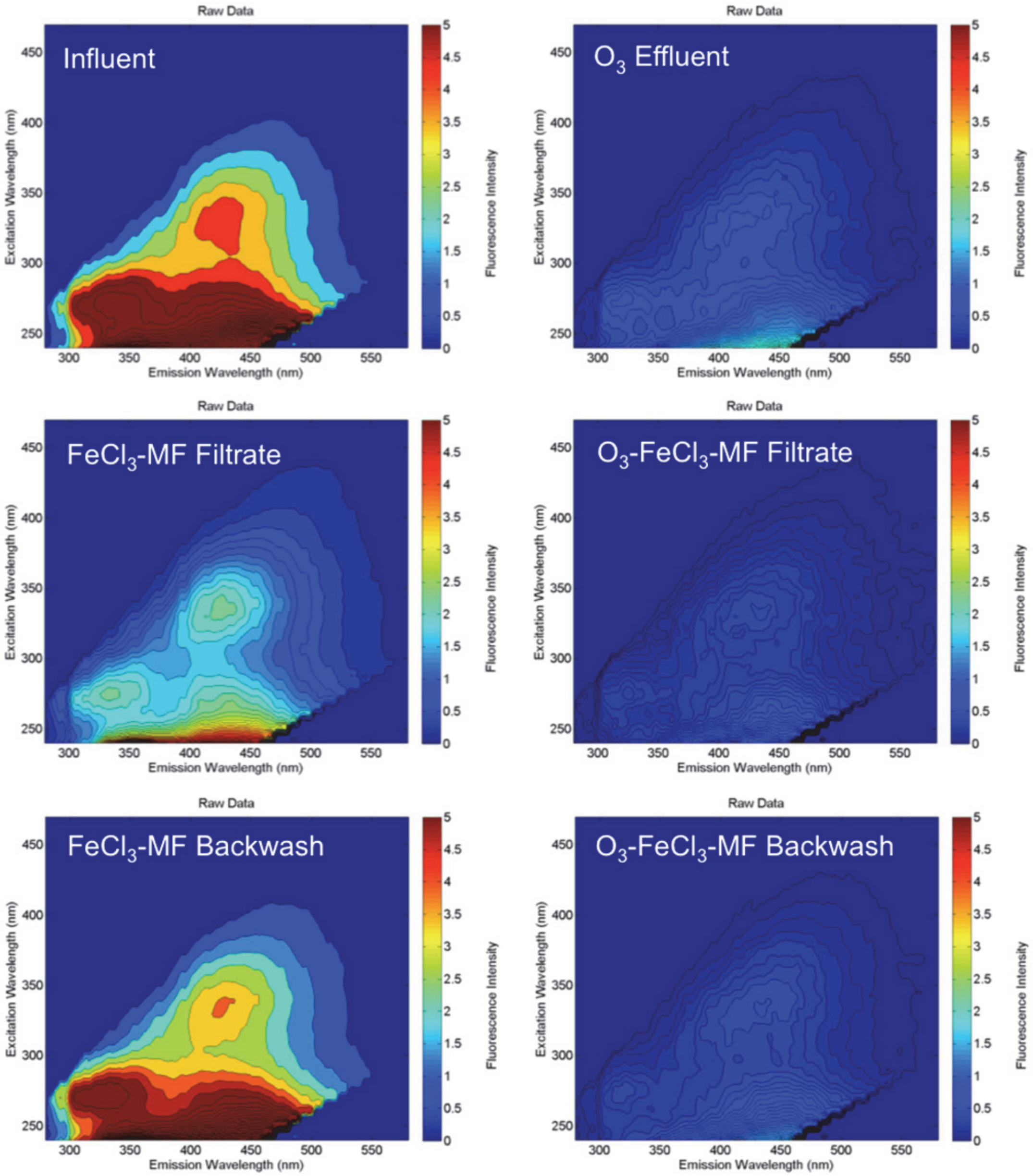

Figure 5.16. EEM images of water samples collected during Run 4 on 8/10/11.

Note: Samples were with a transferred ozone dose of 11 mg/L. The x-axis corresponds with the emission wavelength and the y-axis corresponds with the excitation wavelength. The fluorescence intensity scale is to the right of each image.

5.3.4.2 MF Performance

$FeCl_3$-MF performance data from Run 4 (Figure 5.17) showed a continuation of the stable TMP seen in the previous runs, easily surpassing the 21-day goal between CIPs. O_3-$FeCl_3$-MF had a similarly stable TMP during Run 4 (Figure 5.18), indicating $FeCl_3$ addition after ozonation coagulated Mn to prevent the fouling seen in Runs 1 to 3. This run demonstrated the viability of MF pretreatment of secondary effluent with ozone if Mn fouling can be avoided or controlled. Later runs investigated approaches to mitigate Mn fouling other than coagulation. Comparing the performance of $FeCl_3$-MF with O_3-$FeCl_3$-MF showed ozonation minimized the increase in TMP after the daily chlorine/caustic EFMs. Consequently, TMP recovery after the EFMs were minimal in the ozone train, suggesting organic fouling after ozonation was low and the daily chlorine/caustic EFMs were more frequent than necessary.

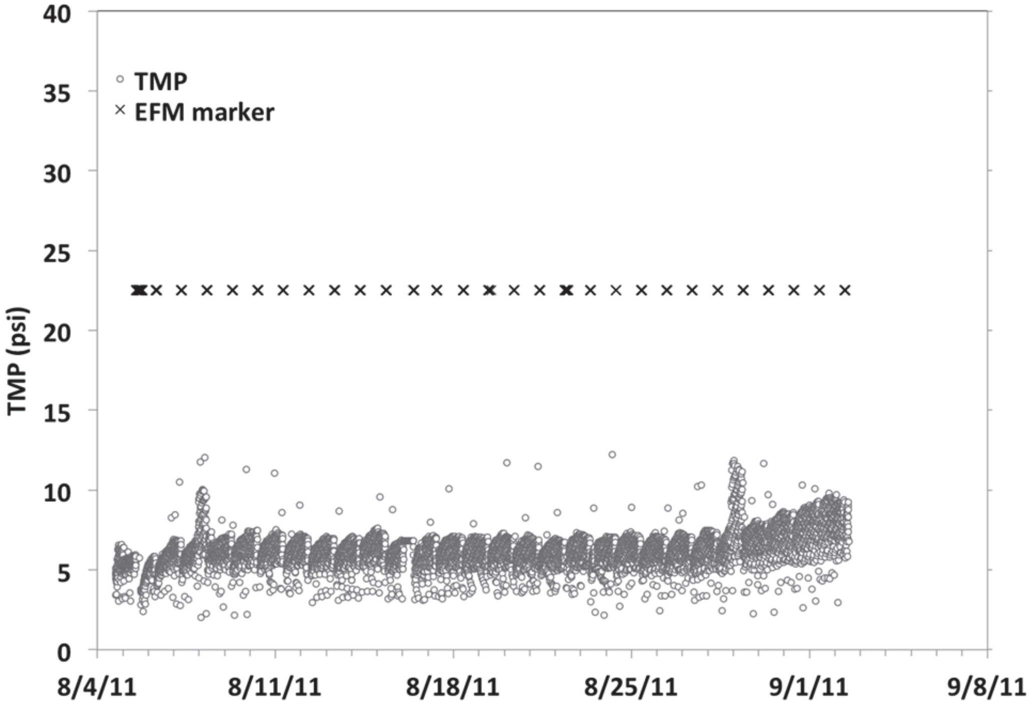

Figure 5.17. TMP data for Run 4 of $FeCl_3$-MF with X markers for daily chlorine/caustic EFMs.

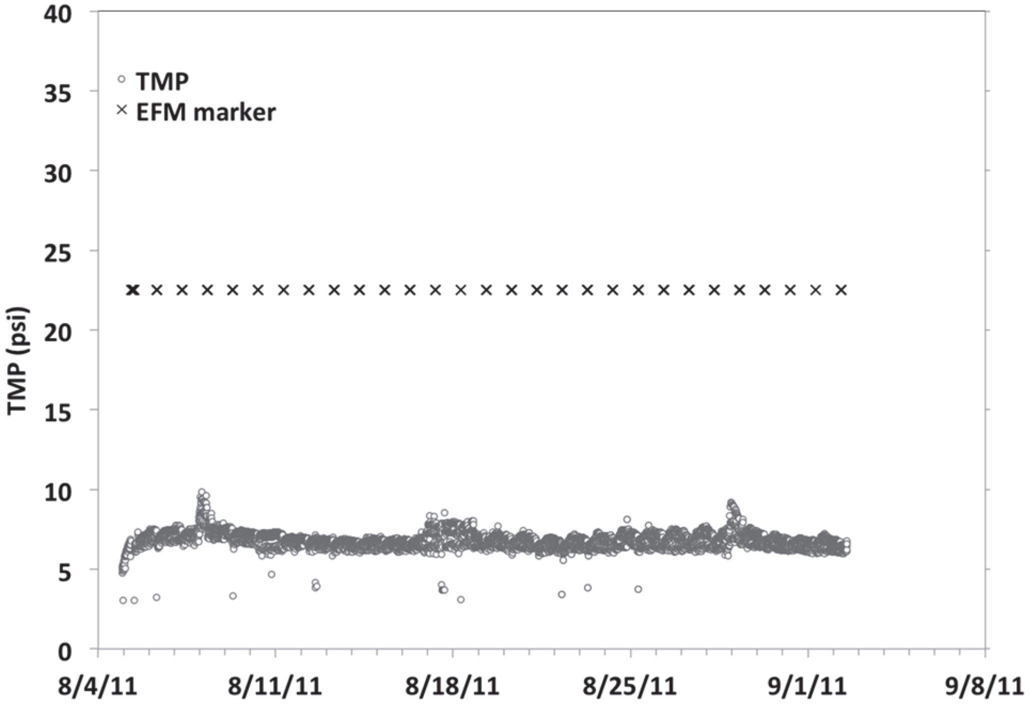

Figure 5.18. TMP data for Run 4 of O_3-$FeCl_3$-MF with X markers for daily chlorine/caustic EFMs.

5.3.5 Run 5 (9/8 to 10/19) – O_3-MF versus O_3-$FeCl_3$-MF

Run 5 focused on optimizing O_3-MF to minimizing the operating costs and complexity associated with a full-scale system that followed Run 4 operating conditions of daily chlorine/caustic EFM, 10 mg/L $FeCl_3$, and manual ozone dose control. Secondary effluent feeding both MF units was treated by ozonation with the dose set automatically based on the influent UVT as described in Chapter 4, Section 4.4.2.2). Only one treatment train (O_3-$FeCl_3$-MF) included $FeCl_3$ at a target dose of 3 mg/L. Another important difference was O_3-$FeCl_3$-MF used a 30-min backwash interval and O_3-MF used a 15-min backwash interval after preliminary testing with a 30-min backwash interval was unsuccessful. Both MF units were scheduled for a 3-day interval between chlorine/caustic EFMs (1700/700 mg/L, respectively) and a 9-day interval between citric acid EFMs (5000 mg/L). The citric acid EFMs included 5000 mg/L of Super Iron Out® to provide strong reductants ($S_2O_4^{2-}$ and $S_2O_5^{2-}$) to minimize Mn fouling by reducing insoluble Mn(IV) to soluble Mn(II).

5.3.5.1 Water Quality

Average TOC, turbidity, and UVA data from Run 5 (Table 5.17) showed the pilot plant influent water quality was similar to the average concentrations during Runs 3 and 4. The lower average transferred ozone dose for Run 5 (6 mg/L) reduce turbidity and UVA by approximately 20%, which was less than the removal from previous runs with average transferred ozone doses of 8 to 9 mg/L. Even with this lower ozone dose, ozonation still increased TOC by 1 mg/L.

There was little difference between the MF filtrate quality of both treatment trains, showing $FeCl_3$ addition to the MF feed did not improve filtrate quality beyond what can be achieved by ozone alone. Higher TOC, turbidity, and UVA in the backwash water of O_3-$FeCl_3$-MF could be attributed to $FeCl_3$ addition or the longer backwash interval for this MF unit. The longer backwash interval was likely the primary contributor to this effect, because more material would accumulate within the cake layer between backwashes. The water quality data indicated the primary benefit of $FeCl_3$ after ozonation was Mn fouling control.

As shown in Table 5.18, pilot plant influent total Fe and total Mn were within the same range as Runs 2 to 4. $FeCl_3$ addition increased total Fe and total Mn concentrations in O_3-$FeCl_3$-MF feed. The increase in $FeCl_3$ was lower than before because the $FeCl_3$ dose was much lower (3 mg/L) for most of Run 5. Removal of particulates, coagulated materials, and larger colloids by MF produced similar filtrate total Fe and total Mn concentrations in both treatment trains.

Water samples were collected on 9/13 and 10/7 for MW fractionation and EEM analysis. Both MW fractionation samples were analyzed for UVA, proteins, and carbohydrates, but only the second sample was tested for TOC. MW fractionation data from 9/13 and 10/7 are shown in Figures 5.19 and 5.20, respectively.

Table 5.17. Average TOC, Turbidity, and UVA Data During Run 5

Water Quality Parameter	Units	Pilot Plant Influent	Ozone Effluent	O_3-MF		O_3-$FeCl_3$-MF	
				Filtrate	Backwash	Filtrate	Backwash
TOC	mg/L	12 (0.4)	13 (0.5)	12 (0.8)	29 (12)	12 (0.6)	36 (13)
Turbidity	NTU	5.3 (1.4)	4.3 (1.4)	0.12 (0.03)	55 (30)	0.13 (0.14)	132 (38)
UVA	cm^{-1}	0.294 (0.037)	0.237 (0.042)	0.166 (0.019)	1.191 (0.413)	0.158 (0.016)	2.506 (0.743)

Note: Standard deviations are presented in parentheses below the averages.

Table 5.18. Average Fe (Total) and Mn (Total) Data During Run 5

Water Quality Parameter	Units	Pilot Plant Influent	O_3-MF		O_3-$FeCl_3$-MF	
			Feed	Filtrate	Feed	Filtrate
Fe (total)	mg/L	0.33 (0.12)	0.26 (0.10)	0.09 (0.02)	3.7 (1.2)	0.08 (0.02)
Mn (total)	mg/L	0.11 (0.01)	0.11 (0.02)	0.11 (0.03)	0.18 (0.06)	0.12 (0.05)

Note: Standard deviations are presented in parentheses below the averages.

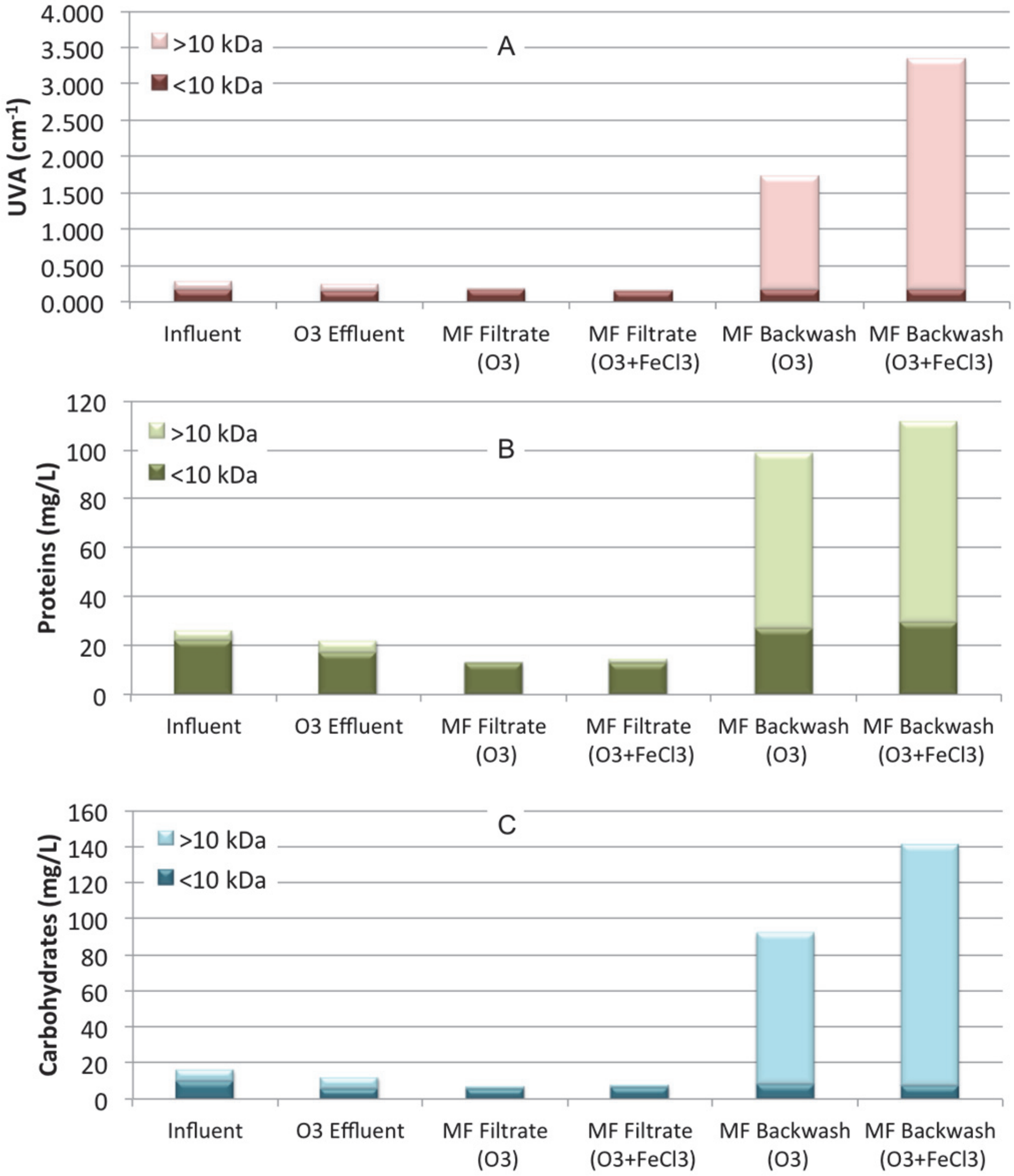

Figure 5.19. MW distribution of (A) UVA, (B) proteins, and (C) carbohydrates of samples collected during Run 5 on 9/13/11.

Note: This was with a transferred ozone dose of 6 mg/L.

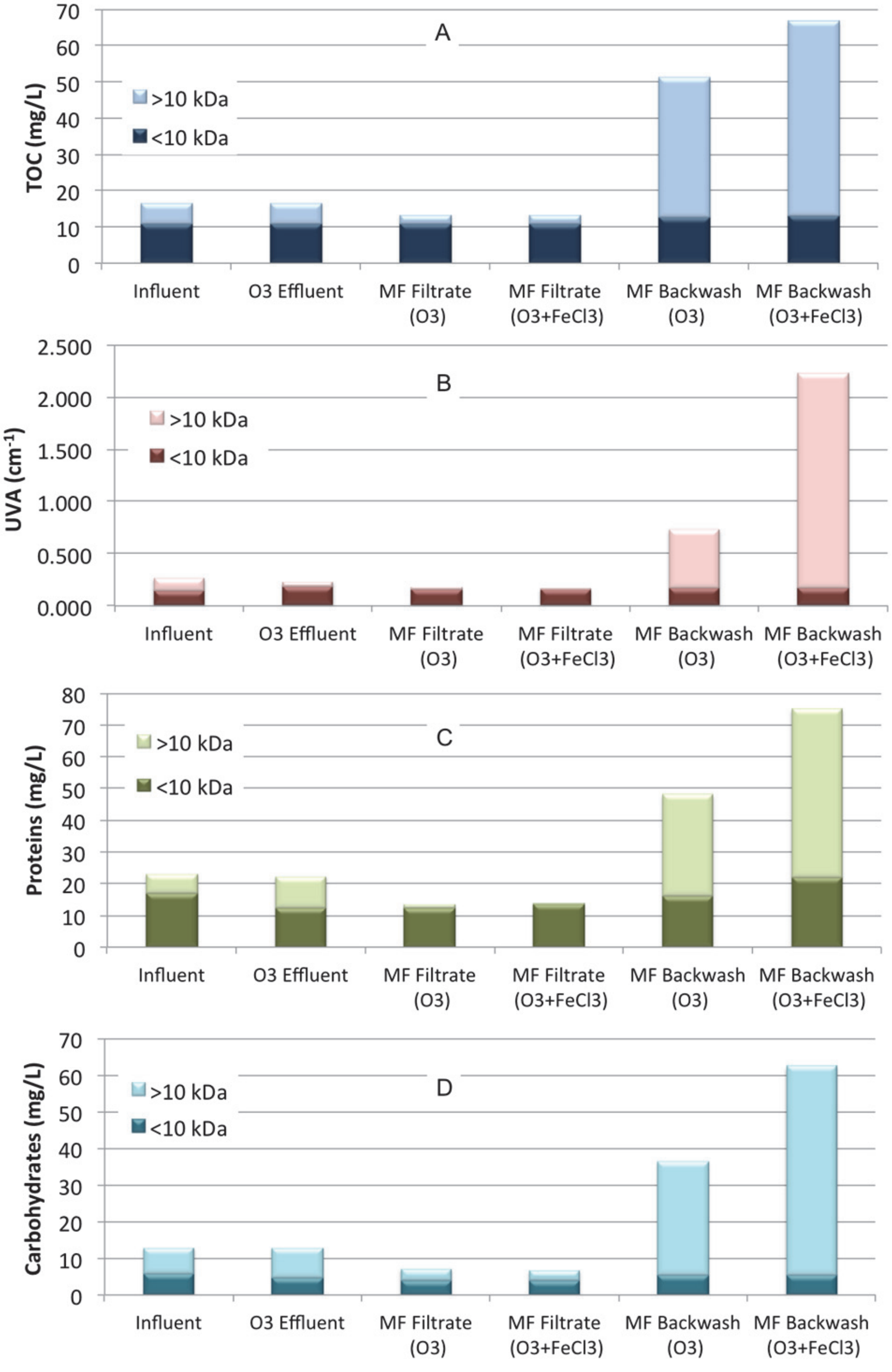

Figure 5.20. MW distribution of (A) TOC, (B) UVA, (C) proteins, and (D) carbohydrates of samples collected during Run 5 on 10/7/11.

Note: This was with a transferred ozone dose of 6 mg/L.

The overall trends for pilot plant influent, MF filtrate, and MF backwash data were similar to those of samples from the ozone train of previous runs. However, the magnitude of changes caused by ozonation was smaller because the transferred ozone dose was lower during Run 5. $FeCl_3$ addition did not appear to affect the concentrations or MW distributions of the organics in the MF filtrate of both treatment trains. The longer backwash interval for O_3-$FeCl_3$-MF contributed at least partially to the worse water quality compared to O_3-MF backwash.

Regional and total fluorescence data from EEM analysis of the samples collected on 9/13 and 10/7 are shown in Tables 5.19 and 5.20, respectively. EEM images of the same samples are shown in Figures 5.21 and 5.22, respectively. The lower influent fluorescence in those figures suggested water quality at the time of sample collection was better than it was for Runs 3 and 4. The regional and total fluorescence data showed ozone reduced fluorescence less in Run 5 (47 to 55%) compared to Run 3 (77 to 84%) and Run 4 (84 to 91%). The lower fluorescence reduction during ozonation was attributed to the lower ozone dose during sample collection for Run 5 (6 mg/L) compared to Runs 3 and 4 (8 and 11 mg/L, respectively).

Table 5.19. Integrated Regional and Total Fluorescence for Samples Collected on 9/13/11 and Normalized to the Pilot Influent Sample

	Pilot	Ozone	O_3-MF		O_3-$FeCl_3$-MF	
Region	**Influent**	**Effluent**	**Filtrate**	**Backwash**	**Filtrate**	**Backwash**
1	1.00	0.53	0.49	0.86	0.59	2.31
2	1.00	0.45	0.44	0.82	0.51	1.81
3	1.00	0.45	0.42	0.65	0.59	0.90
Total	1.00	0.48	0.46	0.81	0.56	1.88

Table 5.20. Integrated Regional and Total Fluorescence for Samples Collected on 10/7/11 and Normalized to the Pilot Influent Sample

	Pilot	Ozone	O_3-MF		O_3-$FeCl_3$-MF	
Region	**Influent**	**Effluent**	**Filtrate**	**Backwash**	**Filtrate**	**Backwash**
1	1.00	0.45	0.40	0.79	0.41	0.71
2	1.00	0.40	0.36	0.72	0.37	0.62
3	1.00	0.42	0.36	0.54	0.37	0.50
Total	1.00	0.42	0.38	0.73	0.39	0.64

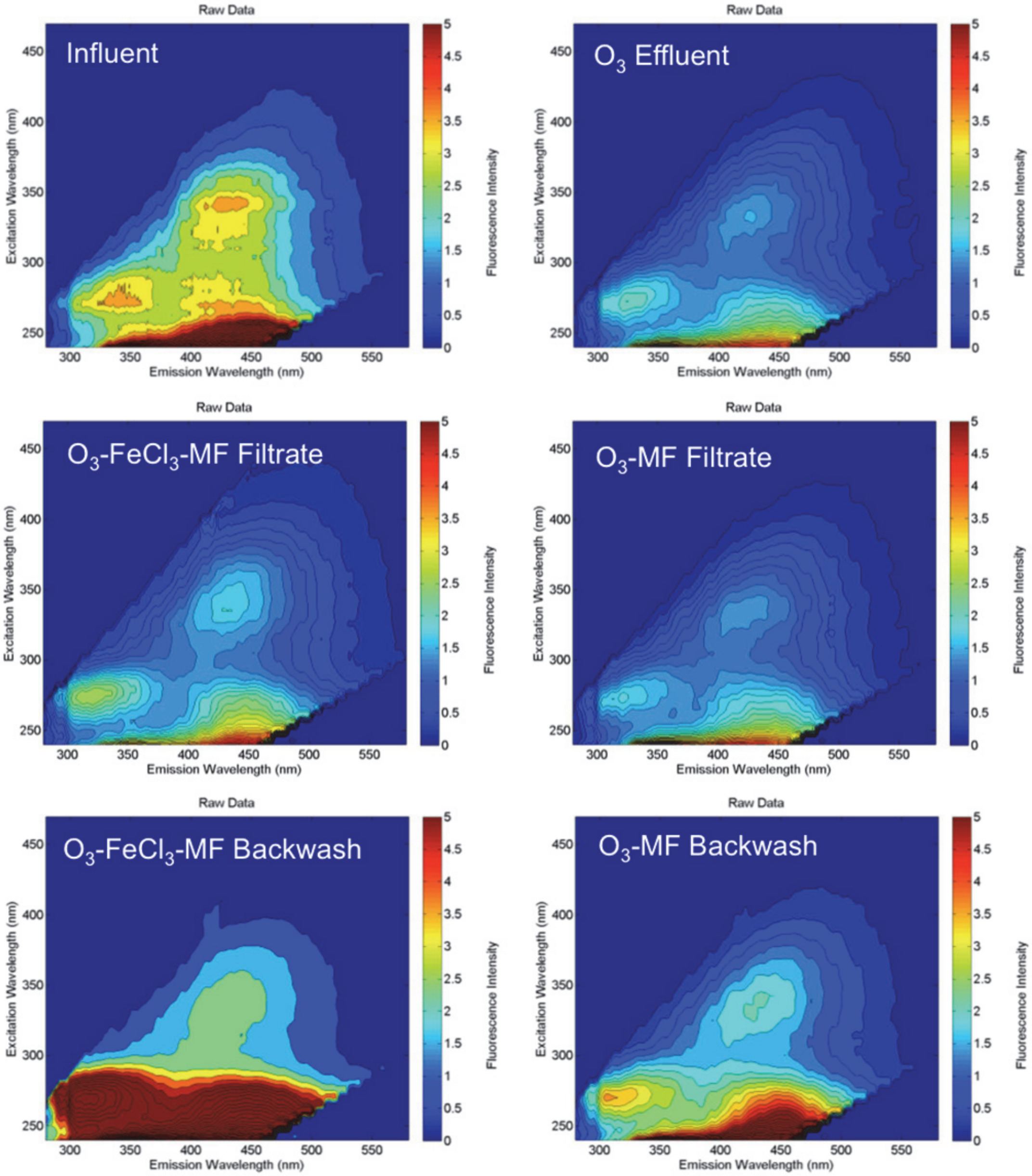

Figure 5.21. EEM images of water samples collected during Run 5 on 9/13/11.

Note: This was with a transferred ozone dose of 6 mg/L. The x- and y- axes correspond to the emission and excitation wavelengths, respectively. The fluorescence intensity scale is to the right of each image.

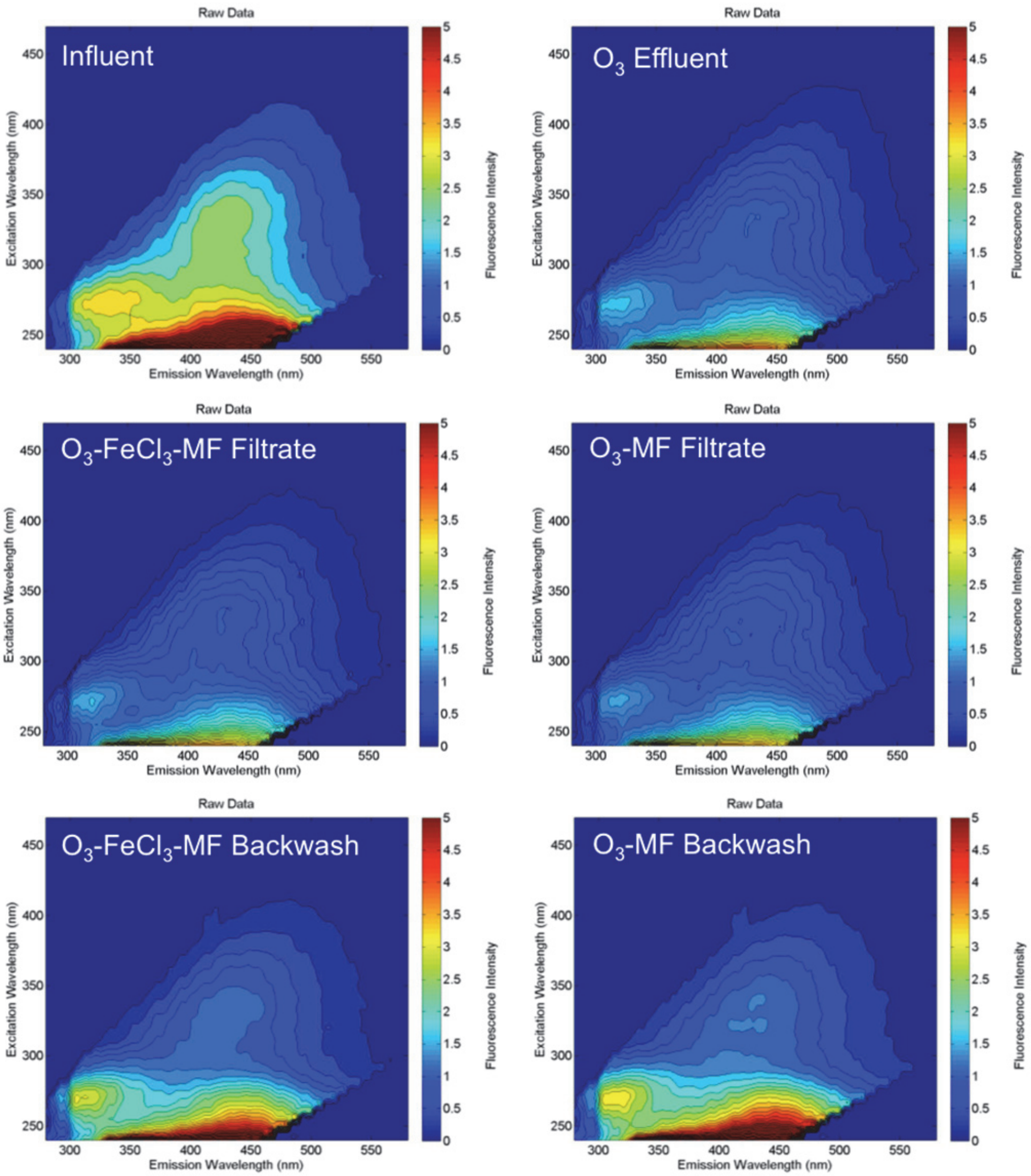

Figure 5.22. EEM images of water samples collected during Run 5 on 10/7/11.

Note: This was with a transferred ozone dose of 6 mg/L. The x-axis corresponds with the emission wavelength and the y-axis corresponds with the excitation wavelength. The fluorescence intensity scale is to the right of each image.

The effect of the lower ozone dose on fluorescence carried through the MF units to the filtrate and backwash samples, which had higher total and regional fluorescence than the same samples from the previous experiments. O_3-$FeCl_3$-MF filtrate fluorescence was higher than (9/13) or equal to (10/7) the fluorescence in O_3-MF filtrate. O_3-MF backwash had more consistency relative to the influent fluorescence, with the 10/7 sample having modestly lower regional and total fluorescence than the 9/13 sample. Meanwhile, O_3-$FeCl_3$-MF backwash had much higher fluorescence than O_3-MF backwash on 9/13 but modestly lower fluorescence than O_3-MF backwash on 10/7. Interestingly, the MF backwash EEM did not track the MW fractionation data as it did during Runs 3 and 4. The reason for this difference was undetermined.

5.3.5.2 MF Performance

Preliminary testing for O_3-MF began on 9/8 with the backwash interval set at 30 min and an ozone dose set manually at 6 mg/L. Figure 5.23 showed initial MF performance was acceptable, although TMP was less consistent than it was for O_3-MF during Runs 1 to 3. By 9/15, high TMP caused the MF unit to shut down automatically. Attempts to restore performance over the following days did not yield results, leading to a decision to return to the original 15-min backwash interval for the start of Run 5 on 9/23. At the same time, automated ozone dose control was implemented with adjustments being made based on influent UVT was implemented. These automatic adjustments varied the transferred ozone dose with water quality, resulting in a lower average ozone dose than during Runs 1 to 4.

The failure of the human-machine interface (HMI) computer prevented data recording from 9/23 until it was replaced on 9/29. During this time, the programmable logic controller was still operating the MF unit at the set points selected prior to HMI failure. Although no online MF data were available before the HMI was replaced, daily observation indicated the MF unit was operating normally during this time. After the HMI was replaced, TMP data showed stable performance for O_3-MF. Operating from 9/23 to 10/19, Run 5 was the first experiment of MF pretreatment with ozone to surpass the 21-day goal without $FeCl_3$ addition.

Two likely explanations for the success of O_3-MF during Run 5 compared with Runs 1 to 3 are (1) the implementation of ozone dose control that could limit overdosing that might have contributed to Mn fouling, and (2) the inclusion of Super Iron Out® in the citric acid EFMs removed Mn fouling and prevented pore blockage from causing a catastrophic rise in TMP. TOC, turbidity, and UVA data showed influent water quality during Run 5 was within the range of water quality seen during the previous runs. There also was nothing about total Fe and total Mn data that suggested changes in the concentrations of these constituents reduced MF fouling.

Similar EFM frequencies had been used during Run 2 (chlorine EFM every 2 days and citric acid EFM every 10 days) without success. Chlorine and citric acid concentrations in the EFM solutions were higher during Run 5 (1700 mg/L and 5000 mg/L, respectively) compared to Run 2 (640 mg/L and 2500 mg/L, respectively). However, chlorine EFMs are intended to remove organics that accumulate in spite of backwashes. The effect of ozonation on UVA, fluorescence, proteins, and carbohydrates would be expected to reduce fouling potential based on information from other research (Lozier et al., 2008; Trussell et al., 2009). The lower measurements of organics in O_3-MF backwash provided evidence to support this conclusion. Therefore, the higher EFM chlorine concentration during Run 5 should have no effect on Mn fouling. Although the higher citric acid concentration was intended to improve Mn removal, the addition of Super Iron Out® to the EFM solution was a more significant change, because it combined a low pH with strong reductants.

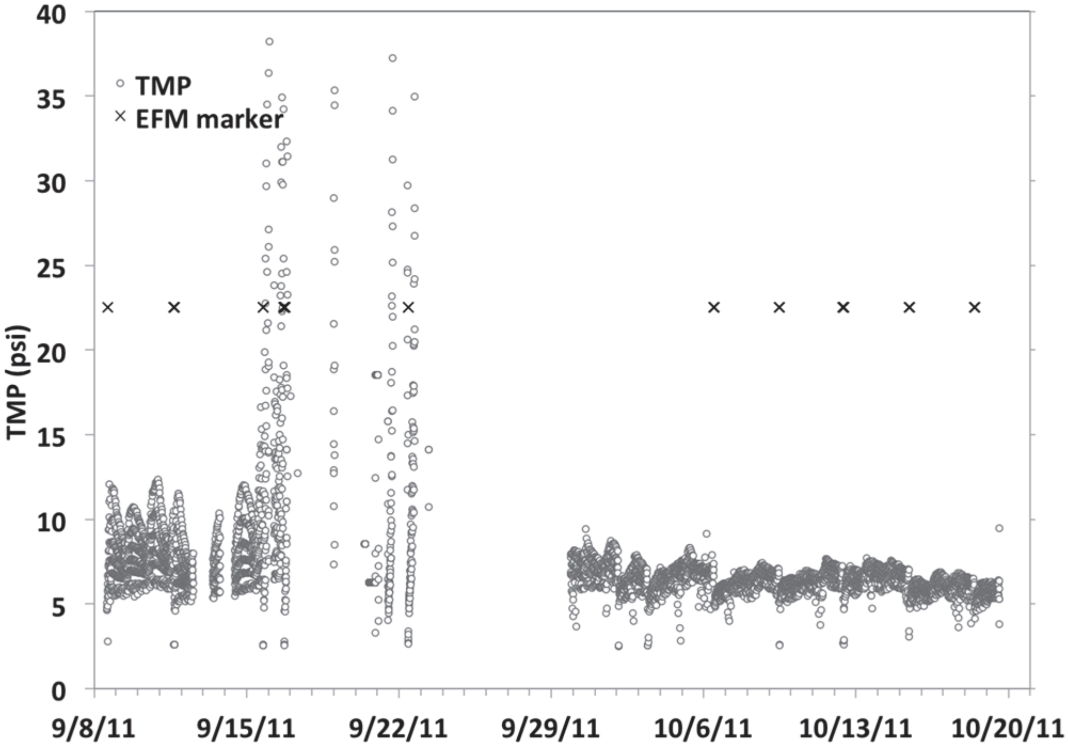

Figure 5.23. TMP data for preliminary testing and Run 5 of O_3-MF with X markers for chlorine/caustic EFMs.

O_3-$FeCl_3$-MF began Run 5 on 9/14 and used a 30-min backwash interval to determine if the combined benefits of ozonation and coagulation could improve water recovery. The initial $FeCl_3$ dose was 14 mg/L because the chemical feed pump could not operate low enough to compensate for the reduced flow treated by the MF unit. The flow to both MF units had to be lowered, because that flow was now being split between them. The original chemical feed pump could not operate low enough to deliver the target $FeCl_3$ dose of 3 mg/L. After the MF unit operated for one week with a $FeCl_3$ dose of 14 mg/L, the chemical feed pump was replaced with one that could deliver the target dose.

TMP data showed MF performance was stable for most of Run 5 with the only exception when there was a problem with the new $FeCl_3$ chemical feed pump (Figure 5.24). After the installation of the new pump, there were problems keeping it operational that resulted in no $FeCl_3$ being added for approximately 1 day. The 30-min backwash interval in the absence of $FeCl_3$ caused rising TMP to trigger automatic chlorine/caustic EFMs when it exceeded 21 psi. This performance was the same as preliminary testing of O_3-MF before Run 5 began (Figure 5.23). After $FeCl_3$ addition resumed, TMP stabilization demonstrated the necessity of $FeCl_3$ addition to maintain a 30-min backwash interval after ozonation.

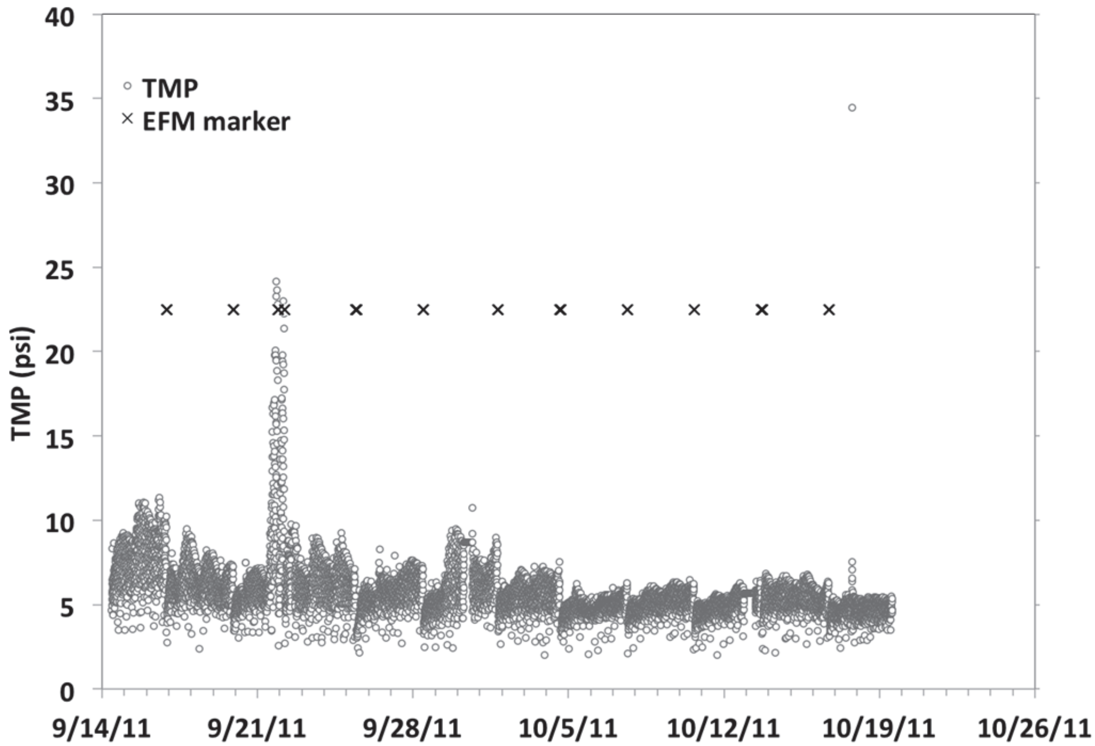

Figure 5.24. TMP data for Run 5 of O_3-$FeCl_3$-MF with X markers for chlorine/caustic EFMs.

5.3.6 Run 6 (10/20 to 11/16) – O_3-MF versus O_3-$FeCl_3$-MF

Minor operational changes were made to the MF units between Runs 5 and 6. The operating conditions for O_3-MF were identical, and the only changes for O_3-$FeCl_3$-MF were a lower $FeCl_3$ dose (2 mg/L versus 3 mg/L) and no Super Iron Out in the citric acid EFM. Backwash intervals were still 15 min for O_3-MF and 30 min for O_3-$FeCl_3$-MF. Ozone dose control was modified so the dose was automatically set based on influent UVT and trimmed based on ozone effluent UVT (Chapter 4, Section 4.4.2.2).

5.3.6.1 Water Quality

Run 6 water quality data (Table 5.21) approximately matched the low average turbidity and UVA from Run 4 and reported the lowest average TOC (11 mg/L) measured thus far. With an average transferred ozone dose of 10 mg/L, turbidity and UVA removals of 20% by ozonation were relatively low. MF filtrate water quality data were typical except for the unusually low TOC concentration after O_3-MF. Backwash data followed the trend from Run 5 where O_3-MF produced backwash with better water quality than backwash from O_3-$FeCl_3$-MF. Total Fe and total Mn data for Run 6 (Table 5.19) were undistinguished from the previous experiments.

Table 5.21. Average TOC, Turbidity, and UVA Data During Run 6

Water Quality Parameter	Units	Pilot Plant Influent	Ozone Effluent	O_3-MF		O_3-$FeCl_3$-MF	
				Filtrate	Backwash	Filtrate	Backwash
TOC	mg/L	11 (0.6)	12 (1.0)	9.0 (2.7)	20 (2.9)	12 (1.0)	22 (3.8)
Turbidity	NTU	4.8 (0.8)	3.9 (0.9)	0.12 (0.03)	33 (9)	0.10 (0.02)	70 (25)
UVA	cm^{-1}	0.282 (0.022)	0.222 (0.035)	0.159 (0.021)	0.766 (0.140)	0.162 (0.023)	1.317 (0.400)

Note: Standard deviations are presented in parentheses below the averages.

Table 5.22. Average Fe (Total) and Mn (Total) Data During Run 6

Water Quality Parameter	Units	Pilot Plant Influent	O_3-MF		O_3-$FeCl_3$-MF	
			Feed	Filtrate	Feed	Filtrate
Fe (total)	mg/L	0.26 (0.16)	0.19*	0.07*	1.7 (2.2)	0.09 (0.02)
Mn (total)	mg/L	0.12 (0.02)	0.10*	0.08*	0.14*	0.08*

* Standard deviation was not calculated because only two samples were analyzed.

Note: Standard deviations are presented in parentheses below the averages.

5.3.6.2 MF Performance

As shown by Figures 5.25 and 5.26, there was no significant difference between the overall MF performance for both trains during Runs 5 and 6. The MF units lost power on the evening of 10/22, causing a shutdown lasting approximately 36 h. The entire pilot plant also shut down from 10/30 to 11/3 when construction at ECLWRF interrupted the flow of secondary effluent for a few days. A malfunction of the chemical feed pump for $FeCl_3$ caused the TMP for O_3-$FeCl_3$-MF to rise from 10/24 to 10/25. Switching the backwash interval from 30 min to 15 min until the pump was fixed allowed TMP to recover.

The successful operation of O_3-MF during Run 6 was significant, because it repeated its performance from Run 5. TMP data for O_3-$FeCl_3$-MF demonstrated a lower $FeCl_3$ dose could be used to maintain a 30-min backwash interval. The unplanned cessation of $FeCl_3$ addition on 10/24 clearly demonstrated the requirement for $FeCl_3$ addition to operate with a backwash interval of 30 min because the TMP rose substantially without it. Run 6 also showed a lower $FeCl_3$ dose could be used to achieve this objective.

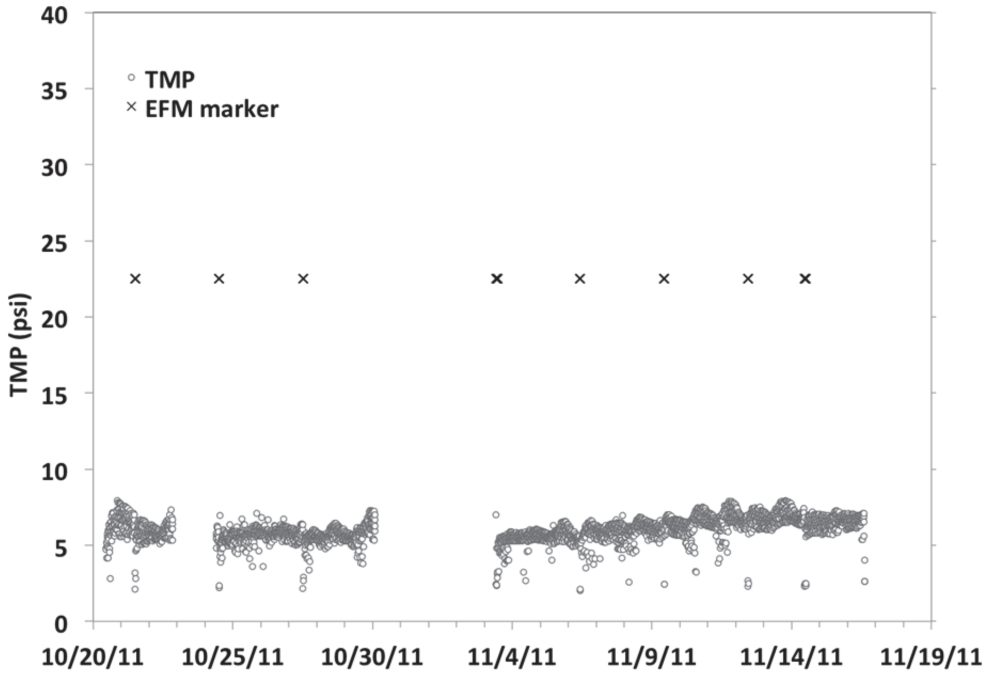

Figure 5.25. TMP data for Run 6 of O_3-MF with X markers for chlorine/caustic EFMs.

Note: Power loss and construction caused data gaps from 10/22 to 10/24 and 10/30 to 11/3.

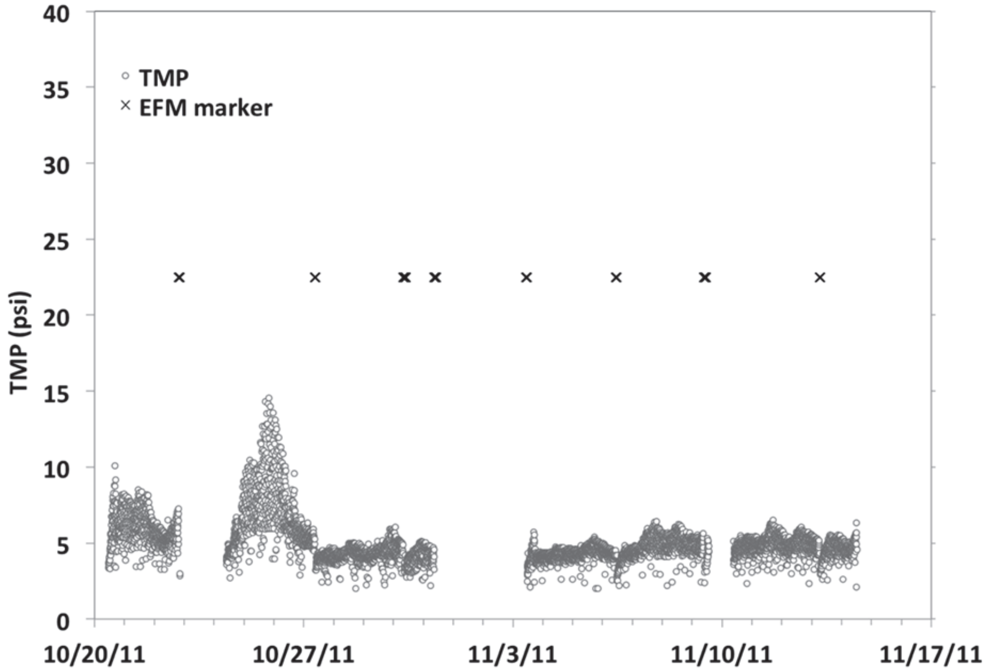

Figure 5.26. TMP data for Run 6 of O_3-$FeCl_3$-MF with X markers for chlorine/caustic EFMs.

Note: Power loss and construction caused data gaps from 10/22 to 10/24 and 10/30 to 11/3.

5.3.7 Run 7 (11/17 to 11/28) – $FeCl_3$-MF versus O_3-$FeCl_3$-MF

The operating conditions during Run 7 were modified to resemble those of Run 4, which tested $FeCl_3$-MF and O_3-$FeCl_3$-MF. Automated ozone dose control was based on ozone effluent UVT (Chapter 4, Section 4.4.2.2). $FeCl_3$ doses were 10 mg/L, backwash intervals were 15 min for both MF units, and chlorine/caustic EFMs were scheduled initially at 2-day intervals. No citric acid EFMs were planned because operation was expected to last approximately 10 days. The fluxes tested in Run 7 ranged from 35 to 50 gfd.

5.3.7.1 Water Quality

Average turbidity and UVA data were lower during Run 7 (Table 5.20) than any other run. UVA removal by ozonation with an average transferred ozone dose of 7 mg/L was approximately 20%, but turbidity removal was lower than any other experiment at 14%. O_3-$FeCl_3$-MF filtrate turbidity and UVA were nearly 20% lower than $FeCl_3$-MF filtrate quality. Differences between these water quality parameters for the MF backwash samples were only 13 and 6%, respectively, which was less than the difference when the same treatment trains were compared during Run 4. TOC, total Fe, and total Mn data were not available, because samples were not collected for analysis during this short test.

Table 5.23. Average TOC, Turbidity, and UVA Data During Run 7

Water Quality Parameter	Units	Pilot Plant Influent	Ozone Effluent	$FeCl_3$-MF		O_3-$FeCl_3$-MF	
				Filtrate	Backwash	Filtrate	Backwash
TOC	mg/L	N/S	N/S	N/S	N/S	N/S	N/S
Turbidity	NTU	4.3 (0.9)	3.7 (0.7)	0.14 (0.04)	80 (5)	0.12 (0.04)	90 (35)
UVA	cm^{-1}	0.266 (0.013)	0.216 (0.013)	0.186 (0.027)	2.274 (0.369)	0.159 (0.026)	2.405 (0.573)

5.3.7.2 MF Performance

During Run 7, both MF units were operating at high fluxes with 10 mg/L $FeCl_3$ added to the MF feed. $FeCl_3$-MF operated at 40 gfd for 2 days before the first chlorine/caustic EFM, which did little to reduce TMP (Figure 5.27). Rapidly decaying performance led to the initiation of another EFM that also caused no discernable improvement in performance. After the shutdown on 11/20, it was noticed the chemical feed pump for the chlorine/caustic solution was not working. After the pump was repaired, the MF unit was soaked in a chlorine solution overnight and restarted at 50 gfd after a couple chlorine/caustic EFMs. The MF unit shut down again on high TMP after a few hours of operation and was soaked again in a chlorine solution overnight. Another EFM was performed before resuming operation at 40 gfd, but the unit failed to shut down again. A final overnight soak and EFM was performed before another attempted restart, this time at 35 gfd. However, the MF unit was turned off after a few hours when the TMP continued to climb rapidly. It was determined the first few days of operation without an effective chlorine/caustic EFM overwhelmed the MF unit, which could not be returned to service without a CIP.

MF performance data for O_3-$FeCl_3$-MF, which began operation at 40 gfd, is shown in Figure 5.28. After 2 days of operation, TMP had risen from 5 to 9 psi. The first chlorine/caustic EFM dropped TMP down to 5 psi, restoring the MF unit to its starting TMP at the beginning of Run 7. However, the oxygen supply to the ozone generator ran out right after the EFM was performed. Consequently, that train operated without ozone for nearly 48 h. During this time, TMP increased from 5 to 16 psi, nearly doubling the increase of the first 2 days of operation. The peak TMP without ozone was even higher at 19 psi.

After the second chlorine/caustic EFM and the restoration of the oxygen supply to the ozone generator, the flux of the MF unit was increased to 50 gfd, and the chlorine/caustic EFM interval was reduced to 1 day. As shown by the data from 11/21 to 11/22, the TMP trended significantly higher at this flux. Therefore, the flux was decreased to 45 gfd shortly before the third chlorine/caustic EFM. The frequency of these EMFs was remained at once per day.

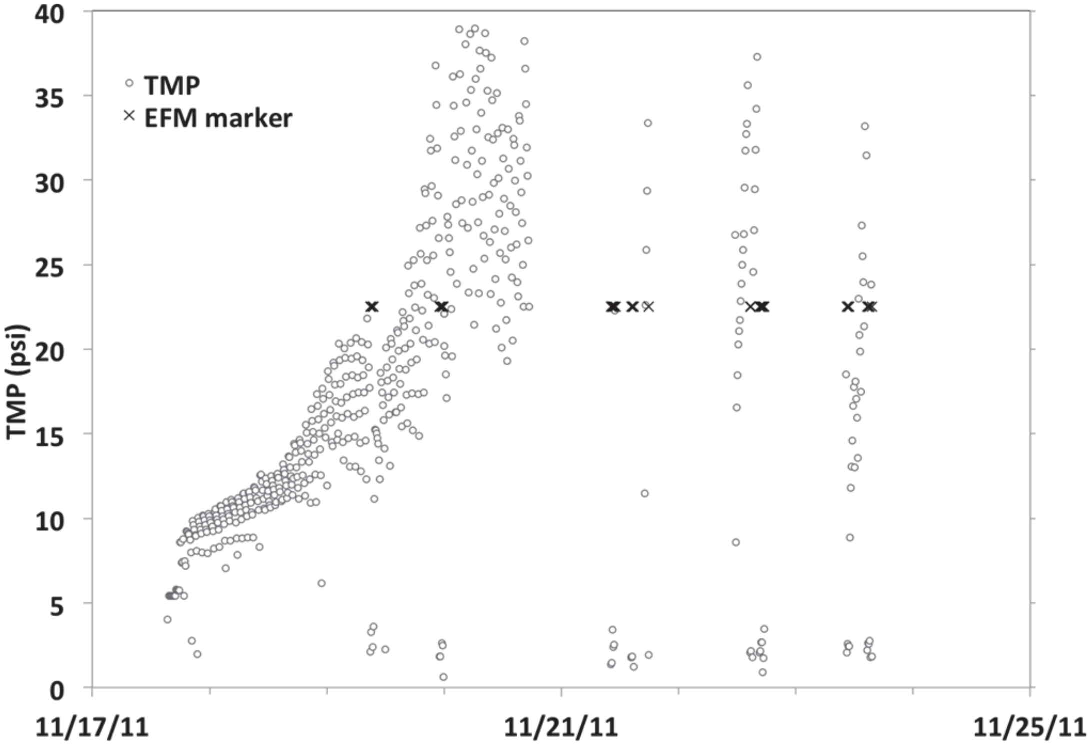

Figure 5.27. TMP data for Run 7 of $FeCl_3$-MF with X markers for chlorine/caustic EFMs.

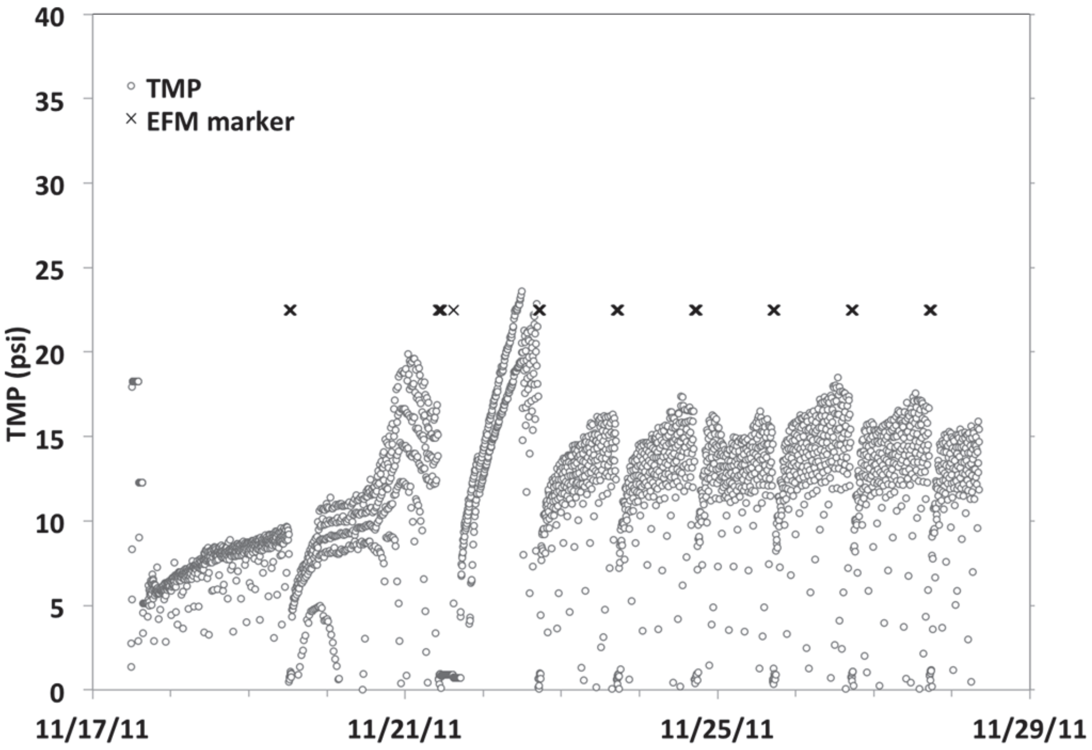

Figure 5.28. TMP data for Run 7 of O_3-$FeCl_3$-MF with X markers for chlorine/caustic EFMs.

Reducing the flux to 45 gfd resulted in stable operation for the remaining 6 days of operation. After each EFM, TMP rose from a low of approximately 10 psi to a peak of 16 to 18 psi. Although there was not enough time to continue Run 7 beyond the 11 days of data displayed in Figure 5.28, these data suggested ozonation provided the possibility of operating the MF unit with $FeCl_3$ addition at a higher flux than was possible by $FeCl_3$-MF. More pilot testing that investigated the maximum sustainable TMP when operating with ozone pretreatment would be required before the implementation of higher fluxes could be considered.

5.3.8 Run 8 (12/1 to 1/3) – O_3-MF versus O_3-$FeCl_3$-MF

Before starting Run 8, the fluxes of both MF units were increased to 30 gfd. The remaining operating conditions were the same as Run 6 with two notable exceptions. For O_3-$FeCl_3$-MF, the $FeCl_3$ dose for was reduced from 2 to 1 mg/L, and the backwash interval was 15 min instead of 30 min. For O_3-MF, Super Iron Out® was not used in the citric acid EFM to evaluate whether the improved performance for that treatment train was attributable to automated ozone dose control based on UVT or the inclusion of Super Iron Out® in the citric acid EFM. The transferred ozone dose continued to be adjusted automatically based on ozone effluent UVT, delivering an average dose of 8 mg/L over the course of this experiment.

5.3.8.1 Water Quality

During Run 8, average TOC, turbidity, and UVA data (Table 5.24) were similar to the data of the other runs. MF filtrate data for the treatment trains was nearly identical, showing $FeCl_3$ provided no water quality benefits for the measured parameters. Differences for backwash data followed the trend of better water quality for O_3-MF compared to O_3-$FeCl_3$-MF, although the differences were less than they were for Runs 5 and 6. The increased similarity could be a consequence of both MF units operating with a 15-min backwash interval. Total Fe and total Mn data (Table 5.25) also fell within the norm of what was measured during Runs 2 to 6 (no Fe or Mn measurements were made during Runs 1 and 7).

Water samples were collected for MW fractionation on 12/12 when the ozone dose was 7 mg/L. UVA, carbohydrate, and protein data for these samples are plotted in Figure 5.29. As with samples analyzed earlier in the project, ozonation and MF preferentially decreased the > 10 kDa fraction. Differences between the MF filtrate samples were minimal, demonstrating no discernable benefit from the low dose of $FeCl_3$ in O_3-$FeCl_3$-MF. In O_3-MF backwash, UVA and protein concentration was lower and carbohydrate concentration was higher compared to O_3-$FeCl_3$-MF backwash. The reason for this difference was not clear and was not seen in the two samples analyzed during Run 5, which compared the same treatment trains with some different operating parameters. The most relevant differences between these runs were the longer backwash interval (30 min versus 15 min) and higher ozone dose (10 mg/L versus 1 mg/L) during Run 5. However, neither of these differences should have caused cause diverging trends for the UVA, protein, and carbohydrate data.

Table 5.24. Average TOC, Turbidity, and UVA Data During Run 8

Water Quality Parameter	Units	Pilot Plant Influent	Ozone Effluent	O_3-MF		O_3-$FeCl_3$-MF	
				Filtrate	Backwash	Filtrate	Backwash
TOC	mg/L	12 (0.4)	14 (0.4)	13 (1.8)	22 (1.8)	13 (0.5)	23 (2.3)
Turbidity	NTU	5.5 (0.8)	4.2 (0.8)	0.12 (0.03)	36 (11)	0.12 (0.03)	47 (19)
UVA	cm^{-1}	0.305 (0.025)	0.240 (0.040)	0.166 (0.023)	0.857 (0.226)	0.163 (0.027)	1.107 (0.353)

Note: Standard deviations are presented in parentheses below the averages.

Table 5.25 Average Fe (Total) and Mn (Total) Data During Run 8

Water Quality Parameter	Units	Pilot Plant Influent	O_3-MF		O_3-$FeCl_3$-MF	
			Feed	Filtrate	Feed	Filtrate
Fe (total)	mg/L	0.34 (0.10)	0.29 (0.09)	0.10 (0.01)	0.77 (0.37)	0.09 (0.01)
Mn (total)	mg/L	0.13 (0.05)	0.13 (0.04)	0.10 (0.05)	0.15 (0.05)	0.11 (0.04)

Note: Standard deviations are presented in parentheses below the averages.

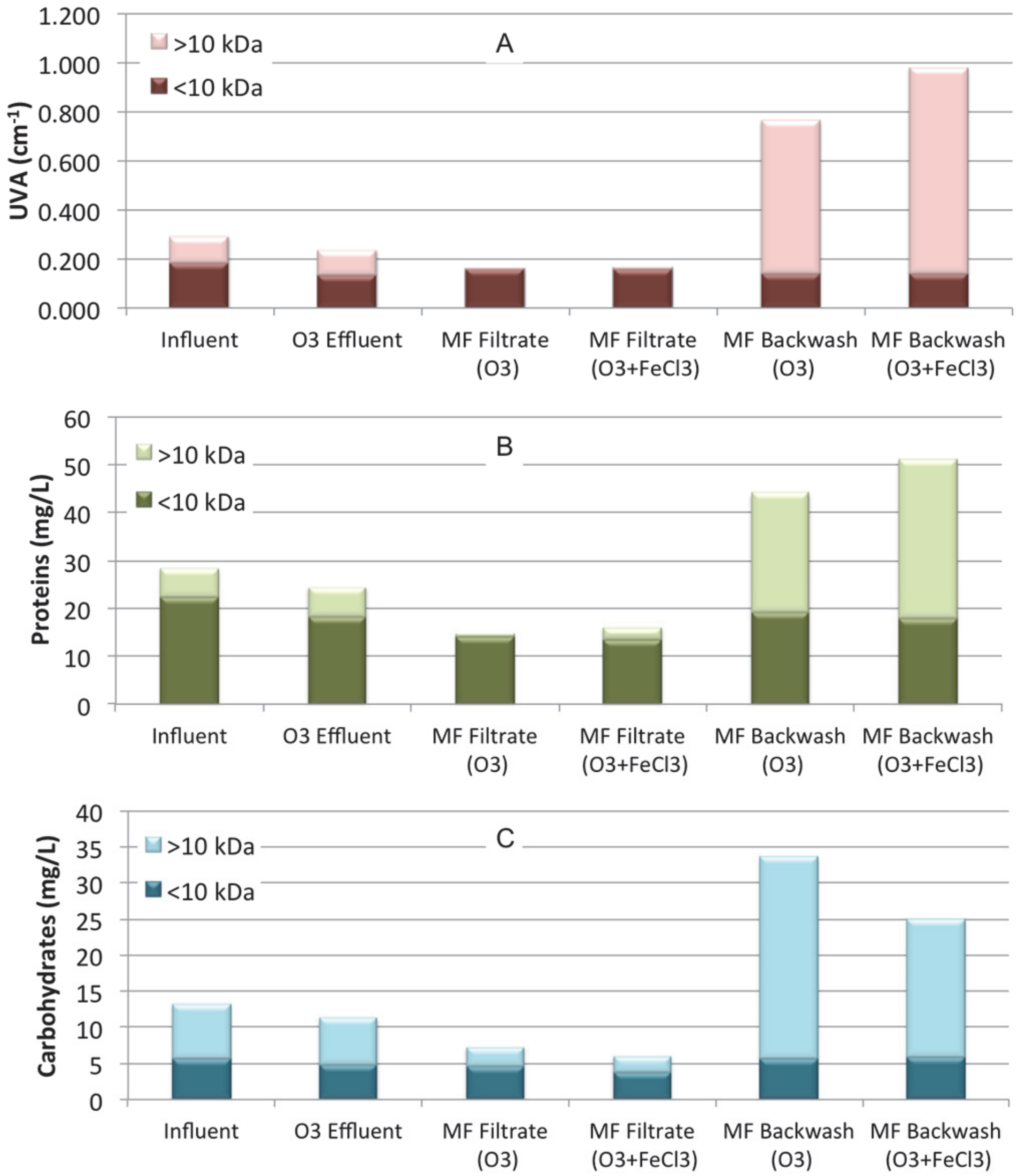

Figure 5.29. MW distribution of (A) UVA, (B) proteins and (C) carbohydrates of samples collected during Run 8 on 12/12/11.

5.3.8.2 MF Performance

Run 8 TMP data for O_3-MF (Figure 5.30) showed this experiment included the longest, continuous operation of O_3-MF during this project. The MF unit operated for 33 consecutive days without a shutdown, easily surpassing the 21-day goal while operating with at a flux of 30 gfd. O_3-MF was shut down because pilot testing was scheduled to end and not because the MF unit could not continue operation. The second EFM was delayed a few extra days without having a noticeable effect on MF performance. With few exceptions, TMP was below 10 psi for most of Run 8.

The first exception to the TMP trend occurred on 12/22 when the pilot plant received poor quality secondary effluent for approximately 12 h. At their worst, influent turbidity reached

60 NTU and influent UVT dropped to 11%. The transferred ozone dose was increased automatically to its maximum set point of 16 mg/L, but that barely improved the quality of the secondary effluent. For example, ozonation only increased UVT to 18%, indicating the poor quality secondary effluent overwhelmed the capability of the ozone system to treat it. The TMP of the MF unit increased rapidly and the poor water quality persisted for several hours, automatically triggering two EFMs. After the second EFM, the water quality improved enough that a third EFM was not initiated and the MF unit was able to resume normal operation.

After the episode of poor secondary effluent water quality, TMP data was elevated slightly, but the overall performance was still good. The maximum TMP before the scheduled chlorine/caustic EFM began showing an upward reaching of 10 psi or higher. These data provided evidence that foulants not removed by backwashing or EFMs were accumulating and beginning to impair performance. The loss of the oxygen supply to the ozone generator on 1/2/12 probably caused the peak TMP to be higher than it otherwise would have been right before Run 8 ended. These data indicated O_3-MF could have continued operating for several days after shutdown, although early signs of excessive fouling suggested the maximum runtime for O_3-MF was approaching.

Replacement of the air compressor for O_3-$FeCl_3$-MF delayed operation of that MF unit until 12/11. Once operation began, a stable TMP below 10 psi was achieved (Figure 5.31), although the spread between the maximum and minimum TMP was greater for O_3-$FeCl_3$-MF compared to O_3-MF. This trend could be a consequence of a thicker or higher density cake layer on O_3-$FeCl_3$-MF as the membrane accumulated organics coagulated by $FeCl_3$. The effect of poor quality secondary effluent on TMP resembled what happened to O_3-MF during that event. Automatic chlorine/caustic EFMs were triggered, but recovery was achieved once water quality began to improve. As with O_3-MF, performance was stable for the remainder of Run 8, with the TMP increase over the final 30 h of operation caused by the absence of ozonation when the tank supplying oxygen to the ozone generator was empty.

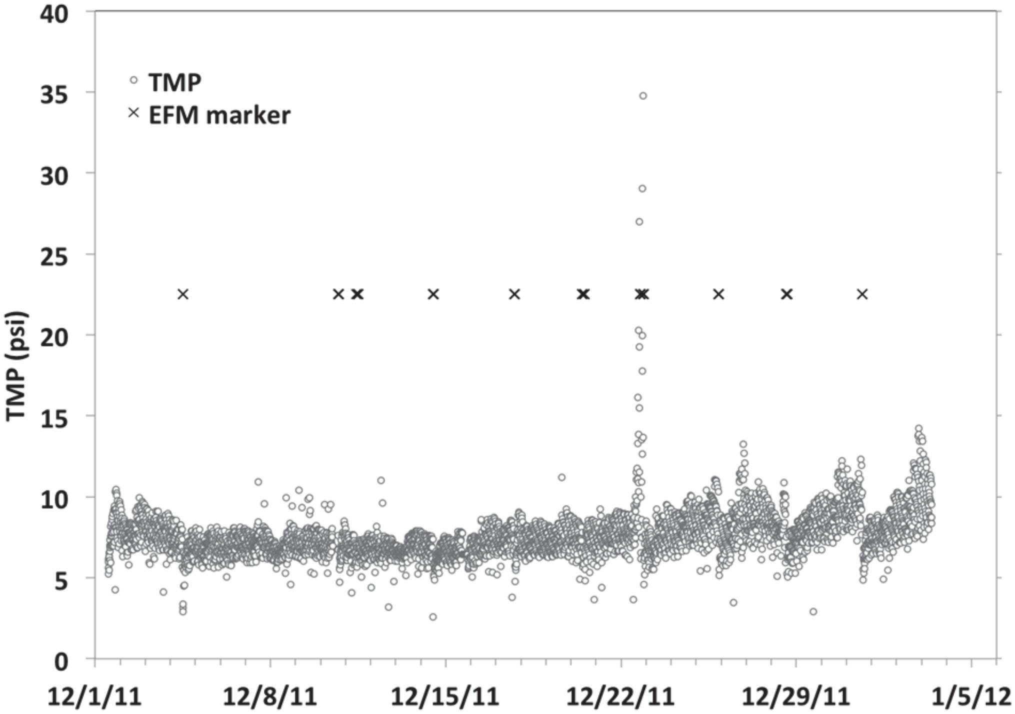

Figure 5.30. TMP data for Run 8 of O_3-MF with X markers for chlorine/caustic EFMs.

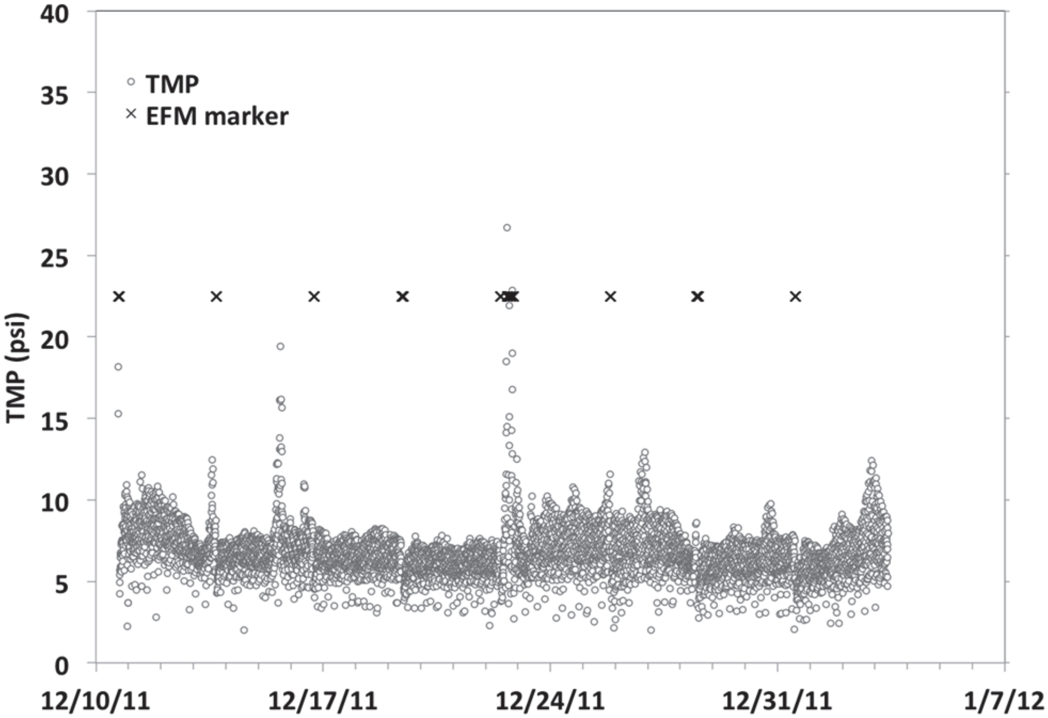

Figure 5.31. TMP data for Run 8 of O_3-$FeCl_3$-MF with X markers for chlorine/caustic EFMs.

5.4 Conclusions

The investigation of MF performance after pretreatment with ozone yielded useful information about the operation and optimization of this treatment process when treating non-nitrified secondary effluent. Ozonation was shown to improve water quality significantly, although this effect is highly dependent on the transferred ozone dose. Earlier runs with higher transferred ozone doses showed better improvements in average TOC, turbidity, and UVA than in later runs with lower doses. These data demonstrated the ability of ozone to tailor water quality to the particular needs of a project. Ozonation also was shown to improve MF backwash water quality compared to the MF unit with ferric chloride ($FeCl_3$) addition. These improvements would have the potential to reduce chemical usage in backwash recovery and solids handling facilities because dosages of coagulants are dependent on the organic content of the water. Further investigation is required to optimize water quality improvements with MF performance to determine the most cost-effective operating criteria.

Ozone pretreatment presented unexpected challenges in the form of Mn fouling that caused O_3-MF to shut down from high TMP before reaching the goal of 21 days between CIPs. Investigation of potential mitigation measures focused on $FeCl_3$ addition in the MF feed to coagulate Mn, the inclusion of strong reductants ($S_2O_4^{2-}$ and $S_2O_5^{2-}$) in the citric acid EFM to reduce Mn that has fouled the membrane from insoluble Mn(IV) to soluble Mn(II), and automated ozone dose control to prevent overdosing that could oxidize soluble Mn(II) to insoluble Mn(IV). The Run 4 comparison of $FeCl_3$-MF and O_3-$FeCl_3$-MF demonstrated $FeCl_3$ addition could solve this problem in the absence of ozone dose control or strong reductants in the citric acid EFM. Run 8 demonstrated ozone dose control allowed the MF unit to exceed the 21-day goal without using $FeCl_3$ or strong reductants in the citric acid EFM. Project constraints did not permit testing of citric acid EFMs with strong reductants in the absence of $FeCl_3$ addition or ozone dose control. Although the results with $FeCl_3$ and ozone dose control demonstrated this option was unnecessary in this instance, future research might show the inclusion of strong reductants in a citric acid EFM is a viable alternative for mitigating the effect of Mn fouling of MF membranes.

This study uncovered potential benefits of using both ozonation and coagulation before MF. Ozonation alone did not permit the MF unit to operate with a backwash interval of 30 min, but adding 2 mg/L $FeCl_3$ to the MF feed allowed it. In addition, ozonation followed by $FeCl_3$ addition permitted higher operating fluxes than $FeCl_3$ alone. Further investigation into operating MF at higher fluxes after ozonation could explore the maximum flux that could be achieved by ozone without $FeCl_3$ addition (30 gfd was successfully tested in Run 8) and the role coagulation might play in permitting operation with even higher fluxes.

Considering the research described in this chapter, there are several areas of potential cost savings that could offset the capital and operation and maintenance (O&M) costs of an ozone system. Avoiding $FeCl_3$ addition would eliminate costs associated with using that chemical. Improved MF backwash water quality could reduce the capital and O&M costs associated with solids handling facilities. Automated ozone dose control to prevent Mn fouling could lower power and liquid oxygen costs and improve process reliability by adjusting the dose based on water quality. If coagulation were to be used in combination with ozone, higher water recovery or higher fluxes could reduce MF capital costs or increase the production of an existing facility. Although additional testing would be necessary to realize the potential benefits of some of these options fully, cost savings such as these would help offset the cost of the ozone system.

Chapter 6

Reverse Osmosis Membrane Performance and Autopsy Data

6.1 Introduction

The goal of the research described in this chapter was to evaluate the impact of microfiltration (MF) pretreatment with ozone on downstream reverse osmosis (RO) performance. One consideration for ozonation in a water reuse treatment train was how other aspects of that treatment train might be affected. If ozonation reduced organic fouling of MF membranes while also improving RO performance, as has been seen in some research (Brown et al., 2008; Wang et al., 2010), then ozone pretreatment could be viewed more favorably. However, smaller organic molecules produced by ozone could pass through the MF membrane and potentially contribute to organic or biological fouling of downstream RO membranes. Ozonation is known to increase assimilable organic carbon (Ramseier et al., 2011) and biodegradable dissolved organic carbon (Siddiqui et al., 1997), which could increase the biofouling potential of the MF filtrate. If fouling is simply shifted from MF to RO, this strategy might not be cost effective. Therefore, the effect of ozone pretreatment on RO performance and fouling was evaluated.

6.2 Methods and Materials

Pilot testing at West Basin Municipal Water District's Edward C. Little Water Recycling Facility (ECLWRF) used two nearly identical RO units configured in a 2:2:1:1 array (Figure 6.1) with three 4-in elements per vessel (ESPA2-4040, Hydranautics, Oceanside, CA). This configuration resembled a full-scale RO process with a 2:1 array with six elements per vessel. One RO unit received MF filtrate from the ozone treatment train (Ozone RO) and the other unit received MF filtrate without preozonation (Control RO). The RO elements operated at 80% water recovery and a water flux of 12 gal/ft^2/day (gfd) for all but the last month of testing. Before the final month of testing, the RO units were upgraded to include four elements in Vessels 1a, 2a, and 3a. New ESPA2-4040 elements were added to the tail positions in Vessels 1b and 2b and the lead position in Vessel 3a, and the existing RO elements were moved forward or backward accordingly. This adjustment to the positions of the existing elements kept the first and last elements of each RO unit in their original positions in preparation for collecting RO specimens from these elements after testing ended. After the modification, the number of elements per RO unit increased from 18 to 21, permitting an increase of the water recovery from 80 to 85% while maintaining a flux of 12 gfd.

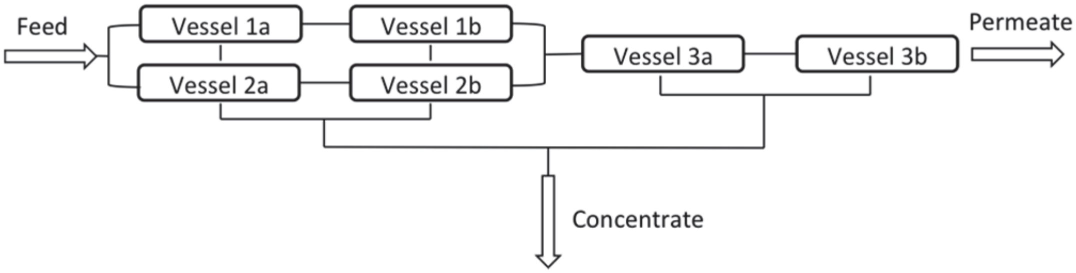

Figure 6.1. RO unit vessel configuration in 2:2:1:1 array with 3 elements per vessel that was the equivalent of a 2:1 array with 6 elements per vessel.

Note: After the RO units were modified, Vessels 1a, 2a, and 3a contained 4 elements each.

Figures 6.2 and 6.3 show different configurations of the upstream processes providing pretreatment for the RO units. Detailed descriptions and operating data for the ozone system and MF units can be found in Chapters 4 and 5, respectively. As described in those chapters, there were many changes to the upstream treatment processes during the operation of the RO units. However, the presence or absence of ozonation in the treatment train was the one constant during testing.

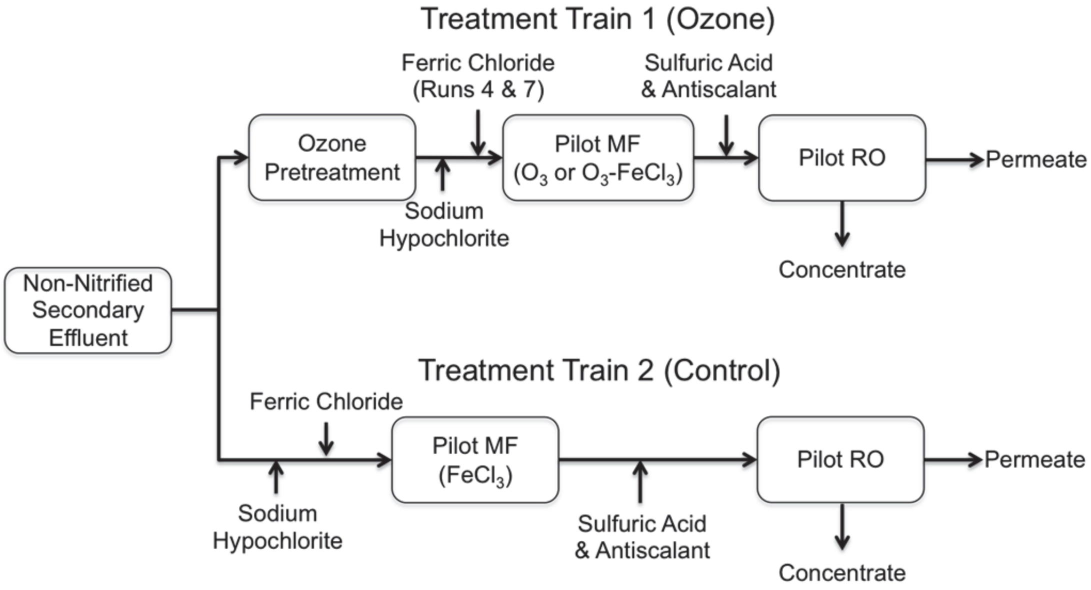

Figure 6.2. Process flow diagram during MF Runs 1 to 4 and 7.

Note: Neither RO unit operated during Run 7.

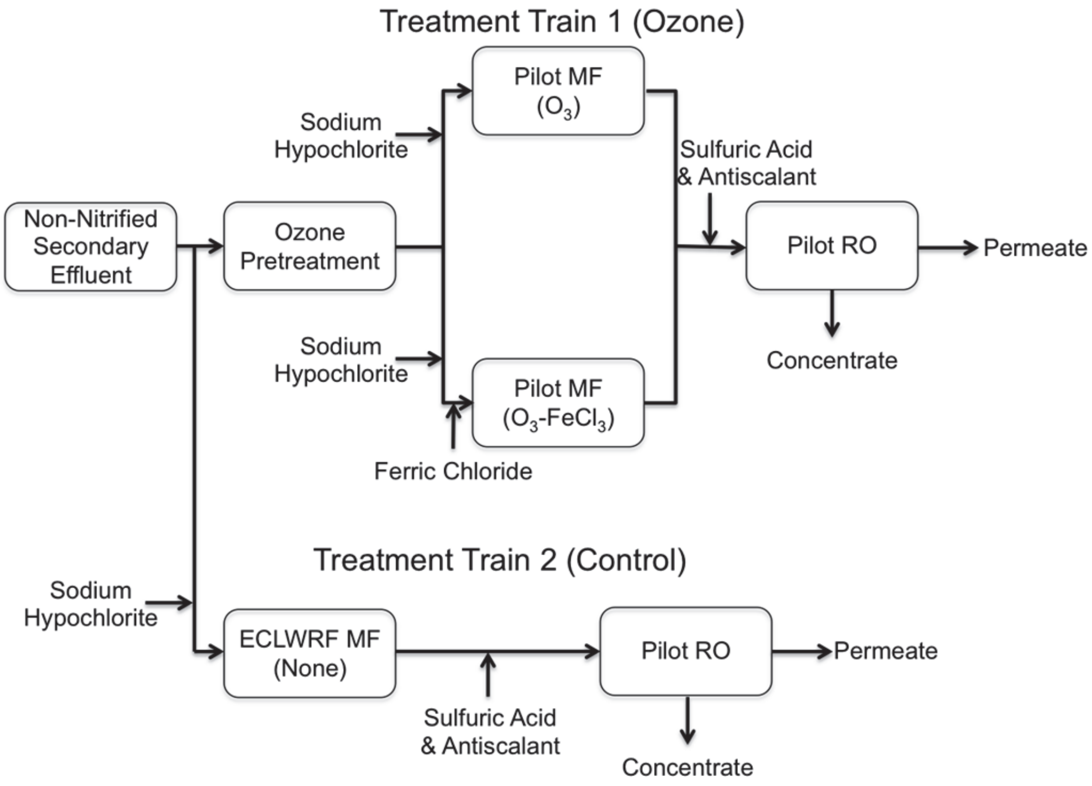

Figure 6.3. Process flow diagram for Runs 5, 6, and 8.

Note: During these runs, Control RO treated filtrate from the full-scale polypropylene MF units at ECLWRF.

To control scaling, RO feed water was dosed with 2 mg/L of a threshold inhibitor (Aquacare A102-FE, American Water Chemicals, Tampa, FL), and the pH was lowered to 6.3 using sulfuric acid. An equalization volume of 1600 gallons between the MF and RO units of each treatment train provided buffering capacity to sustain RO operation during MF backwashes and EFMs.

The CIP procedure for the RO units included first removing inorganic foulants from the second stage with a solution of 2% citric acid (pH = 2.0 to 2.5) that was heated to 104 °F. The second stage was flushed with the citric acid solution to remove the existing water. After flushing, the citric acid solution was circulated through the second stage for 30 min at 10 gpm before soaking for another 30 min. The second stage was then flushed with RO permeate.

This step was followed by removing organic foulants from both stages using a solution of 2% sodium triphosphate and 0.25% sodium dodecylbenzenesulfonate that was heated to 104 °F. Sulfuric acid or caustic were used as needed to adjust the solution pH to 10.0. The cleaning solution flushed the existing water out of the RO unit before being circulated through the first stage for 60 min at 20 gpm and allowed to soak for another 60 min. After cleaning the first stage, the cleaning solution was circulated through the second stage for 60 min at 10 gpm before 60 min of soaking. Finally, both stages were flushed separately with RO permeate before the unit was ready to be returned to service.

The RO units began operation in May 2011 and continued operating through early January 2012. During this time, the RO units were removed from service whenever the upstream MF units or ozone system shut down long enough to drain to RO feed tank, which had approximately 90 min of storage. Accounting for time spent in standby during shutdowns, the total operating times for Control RO and Ozone RO were 4162 h (173 days or 5.8 months) and 3644 h (152 days or 5.1 months), respectively. RO water quality samples were collected monthly, except for ultraviolet absorbance at 254 nm (UVA), which was collected daily (Table 6.1).

Table 6.1. Analytical Methods and Grab Sample Frequency from the Feed, Permeate, and Concentrate of Both RO Units

Water Quality Parameter	Analytical Method	RO Feed	RO Permeate	RO Concentrate
Alkalinity	SM2320B	Monthly	Monthly	Monthly
Ammonia	SM4500-NH_3 F	Monthly	Monthly	Monthly
Calcium	USEPA 200.8	Monthly	Monthly	Monthly
Chloride	USEPA 300.0	Monthly	Monthly	Monthly
Conductivity	SM2510B	Monthly	Monthly	Monthly
Magnesium	USEPA 200.8	Monthly	Monthly	Monthly
Nitrate	USEPA 300.0	Monthly	Monthly	Monthly
pH	SM4500-H+B	Monthly	Monthly	Monthly
Phosphate (ortho)	SM4500P-E	Monthly	Monthly	Monthly
Potassium	USEPA 200.8	Monthly	Monthly	Monthly
Silica	USEPA 200.8	Monthly	Monthly	Monthly
Sodium	USEPA 200.8	Monthly	Monthly	Monthly
Sulfate	USEPA 300.0	Monthly	Monthly	Monthly
TOC	SM5310C	Monthly	Monthly	---
UVA	SM5910B	---	Daily*	---

Notes: SM = Standard Method; USEPA = United States Environmental Protection Agency

*RO permeate from ECLWRF was also analyzed daily for UVA.

6.2.1 RO Autopsy Specimen Collection and Analysis

After the cessation of testing, an autopsy was performed on two elements from each RO unit so membrane specimens could be collected for analysis. Two specimens were collected from the leading edge of the first element of Vessel 1a and the trailing edge of the last element of Vessel 3a. Technology of Materials (Fullerton, CA) analyzed the RO membrane specimens for functional groups with Fourier transform infrared (FTIR) spectroscopy, morphology with scanning electron microscopy (SEM), and elemental composition with energy dispersive spectroscopy (EDS). SEM/EDS analysis was performed using an electron microscope with an energy dispersive X-ray spectrometer. This analysis was nondestructive and identified elements with an atomic weight greater than carbon with an accuracy of approximately 1%.

An RO membrane specimen from an ESPA2-4040 element that was wet-tested by the manufacturer also was analyzed to measure membrane characteristics. In addition, results from the wet-tested element provided baseline data for comparison with the membrane specimens collected from Control RO and Ozone RO. Technology of Materials analyzed this specimen with FTIR, SEM, EDS, and atomic force microscopy (AFM) to determine surface roughness. A wet-tested RO membrane specimen was also sent to the Advanced Water Technology Center at the Colorado School of Mines to measure contact angle and zeta potential. The contact angle was measured with a Ramé-hart Standard Goniometer Model 200-00 (Surface Science Instrument, Landing, NJ) using the sessile drop method. Zeta potential was measured using a 2 mM potassium chloride solution as the electrolyte with electrokinetic analysis (SurPASS, Anton-Paar). Both of these methods followed the approach described in Xu et al. (2010).

6.3 Results and Discussion

6.3.1 RO Performance

RO performance data did not reveal any negative effects associated with the preozonation of MF feed water. Data comparing feed pressure (Figure 6.4), specific flux (Figure 6.5), and salt rejection (Figure 6.6) showed initial performance by Ozone RO was better than Control RO. Feed pressure and specific flux were approximately 20% better for Ozone RO and salt rejection was similar during most of the first four months of testing. One exception was a time period spanning from late June through early July. Ozone RO experienced significant fouling caused by a failure of its antiscalant chemical feed pump that went unnoticed for a few weeks. The fouling became severe enough that a CIP was performed to restore performance. The CIP shown on Figures 6.4 to 6.6 restored feed pressure and specific flux but did not return salt rejection to previous levels. Lower salt rejection for Ozone RO persisted through the remainder of testing. It is unclear if the lower salt rejection is a residual effect of this fouling event or can be attributed to ozonation. Wang et al. (2010) found ozone pretreatment lowered RO fouling at the expense of reduced rejection of small organic compounds and higher salt rejection. Those findings were a possible explanation of the persistent difference in salt rejection between the RO units.

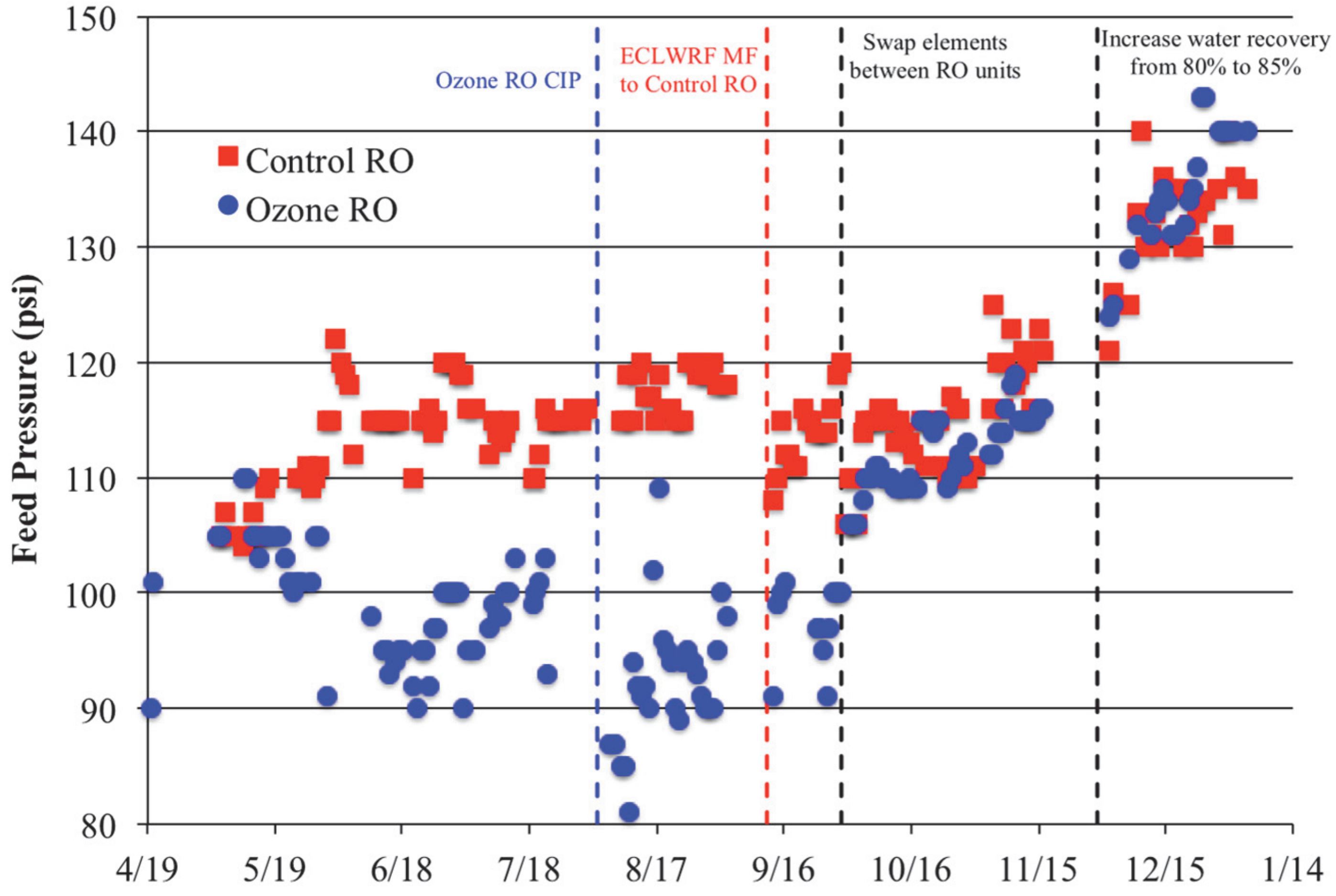

Figure 6.4. Daily feed pressure data for Control RO and Ozone RO.

Note: The RO units operated for a total of 152 days and 173 days, respectively.

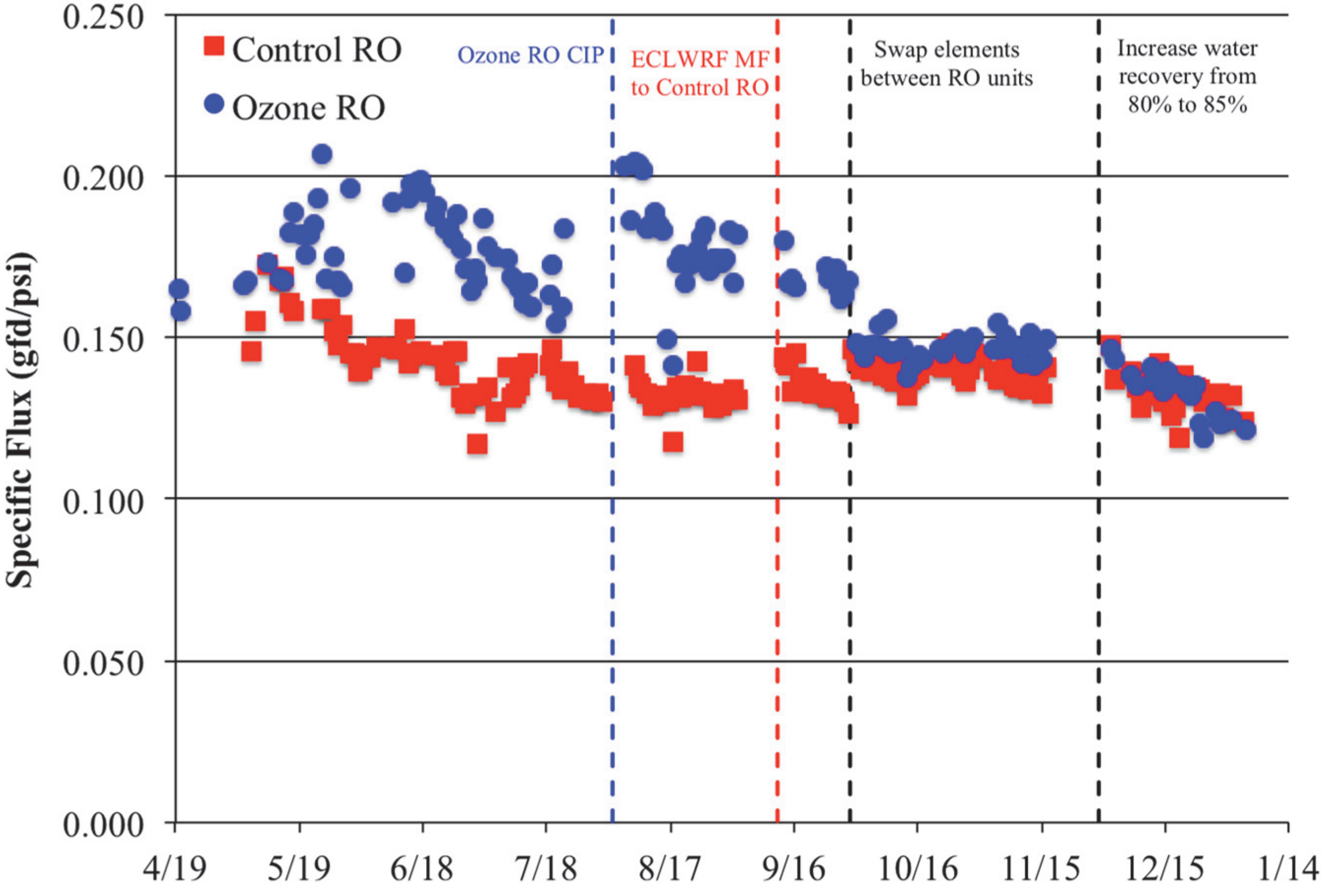

Figure 6.5. Daily specific flux data for Control RO and Ozone RO.

Note: The RO units operated for a total of 152 days and 173 days, respectively.

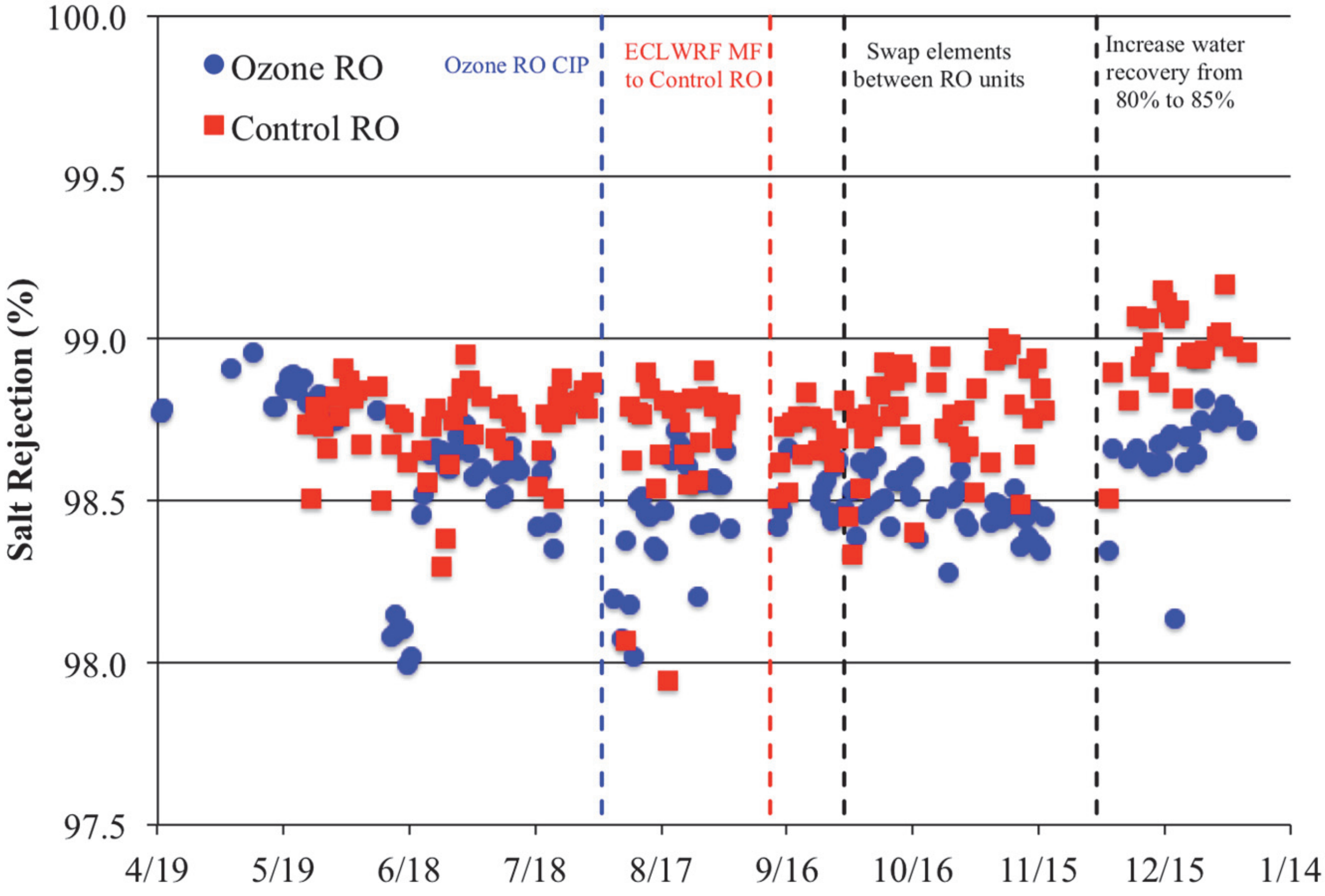

Figure 6.6. Daily temperature-corrected salt rejection data for Control RO and Ozone RO.

Note: The RO units operated for a total of 152 days and 173 days, respectively.

Starting with MF Run 5 in September, the Control RO feed was switched to filtrate of the full-scale MF membranes at ECLWRF. The feed source was changed, because both MF pilot units received ozone pretreatment during Runs 5, 6, and 8. Both RO units were in standby during Run 7. Compared to the MF pilot units, the full-scale MF membranes were made from a different material (polypropylene), had a larger nominal pore size (0.2 µm), operated at lower flux rates (approximately 15 gfd), did not have periodic enhanced flux maintenance cleans, and did not include ferric chloride addition. The secondary effluent supplying the pilot plant came from the same source as the feed to the ECLWRF MF units, so the initial water quality before treatment was the same. Comparing data from Figures 6.4 to 6.6 immediately before and after changing the feed water source to Control RO indicated any effect on RO performance was minimal.

During the operation of the RO pilot units through the end of September, pressure readings from Control RO were more stable than they were for Ozone RO. To improve the stability of the RO pressure measurements in the ozone train, the elements of each RO pilot unit were unloaded and the RO pilot equipment was switched between treatment trains. The RO elements were loaded into their new pilot units and resumed operation in the same treatment train as before the RO pilot equipment was switched. Care was taken to place the elements in the same order in their new RO units that they occupied in their original RO units. Before the switch, Ozone RO had lower feed pressure and higher specific flux than Control RO, which had higher salt rejection. After the switch, the performance of Control RO was unchanged but Ozone RO had a higher feed pressure and lower specific flux. From this point forward, the feed pressures and specific fluxes of both RO units tracked one another closely.

Around the same time as the elements were swapped between RO units, automated ozone dose control was implemented for the ozone system. It is possible the better RO performance during manual dose control was related to relatively high ozone doses compared to water quality. After implementation of dose control, the ozone dose was typically much lower when the water quality was best in the mornings (5 mg/L versus 8 to 10 mg/L). However, the dose from manual ozone dose control was probably too low when water quality tended to be worse in the evenings. Although the reasons for the initial better performance from Ozone RO and the eventual convergence in RO performance are unclear, the change in ozone dose control might be a significant contributor to this effect. Most important, these data showed no detrimental effect to RO performance caused by MF pretreatment with ozone.

The increase in feed pressure from October through the end of testing was attributed to two factors. First, water temperature peaked at 29 °C on 9/1 and declined to 23 °C on 1/3, the day testing ended. Decreasing water temperature increased the net driving pressure that had to be applied to maintain a water flux of 12 gfd. Specific flux data of both RO units (Figure 6.5), which was corrected for water temperature, were flat from late September through the middle of November. This performance was consistent with increasing feed pressure caused by decreasing water temperature.

The second explanation for the increasing specific flux was the increase in water recovery from 80 to 85% beginning on 12/1. The increase in feed pressure from this point corresponds with a gradual decline in specific flux for both RO units. Increasing the water recovery from 80 to 85% decreased the concentrate flow from 20 to 15% of the feed. That change increased the total dissolved solids (TDS) concentration of the concentrate by 33% while decreasing the crossflow velocity across the feed spacer within the RO element. Research has found lower crossflow velocities were associated with higher rates of deposition on the membrane surface and fouling (Chong et al., 2008; Subramani and Hoek, 2008). Therefore, the higher TDS concentration and lower crossflow velocity were the most likely explanation for the increasing feed pressure and decreasing specific flux during the last several weeks of testing.

6.3.2 Water Quality Data

Average water quality data for both RO units are shown in Table 6.2. With the exception of total alkalinity and sulfate, concentrations in the Control RO feed and the Ozone RO feed were similar. RO permeate concentrations for most measured water quality parameters were higher for Ozone RO than Control RO. This trend was consistent with salt rejection data (Figure 6.4) that could be attributed to a residual effect of the fouling event caused by the failure of the antiscalant chemical feed pump or a consequence of upstream ozonation (Wang et al., 2010).

6.3.3 Analysis of RO Specimens from Autopsied Elements

6.3.3.1 Characteristics of Wet-Tested ESPA2 Element

A membrane specimen collected from a factory wet-tested ESPA2-4040 was analyzed to provide reference data for comparison with pilot-tested RO elements. SEM images with magnifications of 124x, 496x, and 992x are shown in Figure 6.7. The EDS spectra in Figure 6.8 includes an embedded table with the percent by weight of all detected elements with an atomic weight greater than carbon. Excluding carbon, oxygen, and sulfur were the dominant elements (51.2 and 42.6%, respectively) with trace amounts of other elements (e.g., iron and chloride) also detected. The high percentage of sulfur was attributed to the porous polysulfone layer supporting the polyamide membrane. RO fouling would be expected to shift these percentages based on the nature of the foulant.

The FTIR spectra (Figure 6.9) showed functional groups characteristic of polyamide RO elements. Vibrational bands at 1586, 1488, and 1242 cm^{-1} are associated with the polysulfone support layer (Gabelich et al., 2006a). Features characteristic of polyamide membranes included the amide I band (C=O) at 1650 cm^{-1}, the amide II band (N−H) at 1540 cm^{-1}, and bands for the carbon double-bonded ring structure (C=C) at 1448, 1488, and 1607 cm^{-1} (Gabelich et al., 2006a). Potential effects of RO fouling on the FTIR spectra include changes to band intensity, shifting band locations, and the appearance of new bands.

AFM revealed the average root-mean square surface roughness of two different locations on the specimen was 55.5 nm. An example AFM image is shown in Figure 6.10. Zeta potential data (Figure 6.11) indicated the ESPA2 membrane was negatively charged (−36 mV) at the target pH of 6.5 in the RO feed during pilot testing. AFM and zeta potential analysis provided background information on the membrane properties and were not performed on the pilot-tested RO elements.

Table 6.2. Average RO Water Quality Data from the Feed, Permeate, and Concentrate of Both RO Units

Water Quality Parameter	Units	RO Feed		RO Permeate		RO Concentrate	
		Control	Ozone	Control	Ozone	Control	Ozone
Alkalinity	mg/L as $CaCO_3$	216	182	15	17	923	858
Ammonia	mg/L as N	39	39	2.0	2.4	183	189
Calcium	mg/L	44.0	45.3	0.03	0.13	221	225
Chloride	mg/L	177	172	2.9	5.0	878	872
Conductivity	µS/cm	1421	1428	51	64	5991	6115
Magnesium	mg/L	20.7	21.1	0.01	0.06	103	106
Nitrate	mg/L as N	2.9	3.1	0.5	0.5	12.6	15.4
pH	---	6.6	6.4	5.6	5.5	7.0	6.9
Phosphate (ortho)	mg/L	5.5	6.6	0.3	0.1	30	40
Potassium	mg/L	17.1	17.5	0.70	0.82	83.5	86.1
Silica	mg/L	22	22	0.27	0.55	105	110
Sodium	mg/L	148	150	6.2	7.4	712	731
Sulfate	mg/L	187	223	< 2	< 2	1025	1155
TOC	mg/L	11	13	0.2	0.4	NA	NA
UVA	cm^{-1}	NA	NA	0.018*	0.022*	NA	NA

Notes: NA = not applicable

* Average UVA of full-scale RO permeate was 0.016.

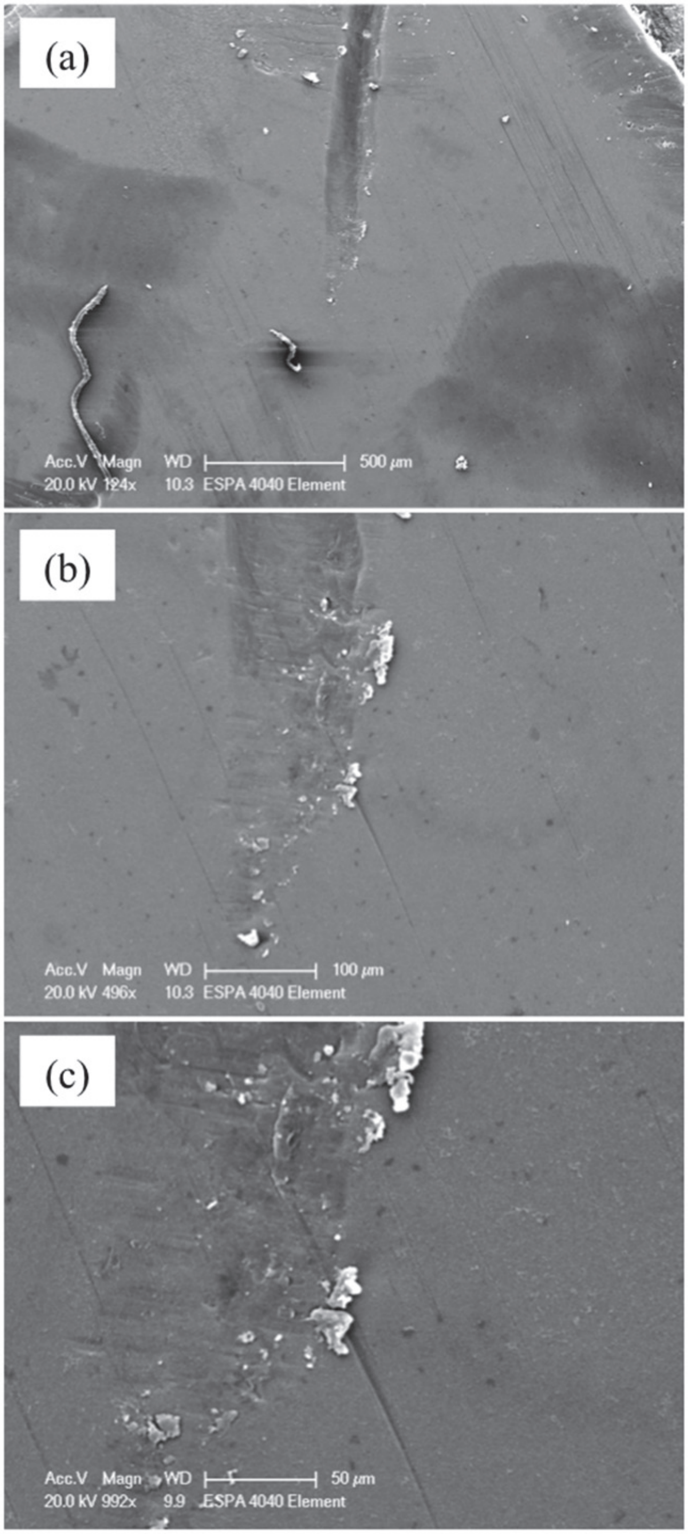

Figure 6.7. SEM image of wet-tested ESPA2 element with magnifications of (a) 124x, (b) 496x, and (c) 992x.

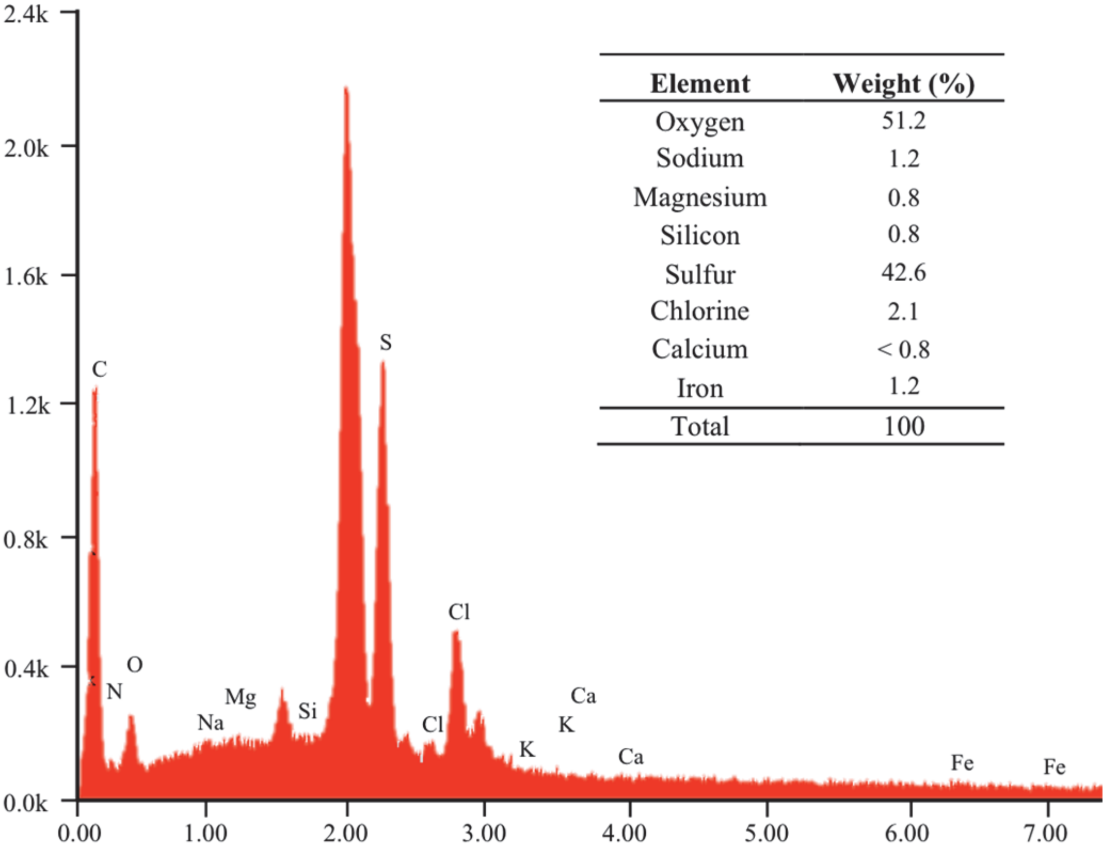

Element	Weight (%)
Oxygen	51.2
Sodium	1.2
Magnesium	0.8
Silicon	0.8
Sulfur	42.6
Chlorine	2.1
Calcium	< 0.8
Iron	1.2
Total	100

Figure 6.8. EDS spectra of wet-tested ESPA2 element..

Note: The embedded table displays the percent by weight of elements with atomic weights greater than carbon.

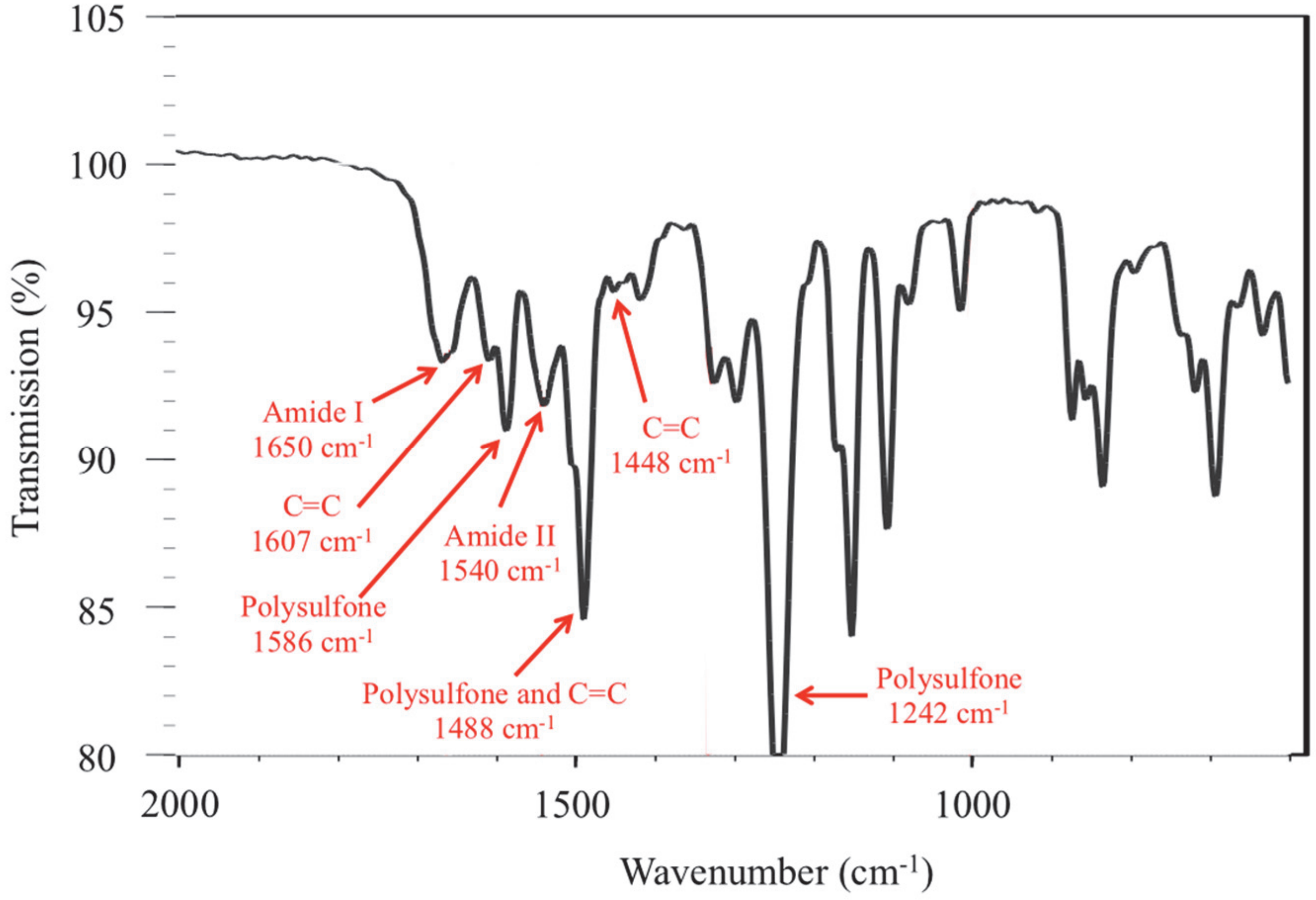

Figure 6.9. FTIR spectra for the wet-tested ESPA2 element.

Note: Vibrational bands characteristic of the polyamide membrane and its polysulfone support layer are identified.

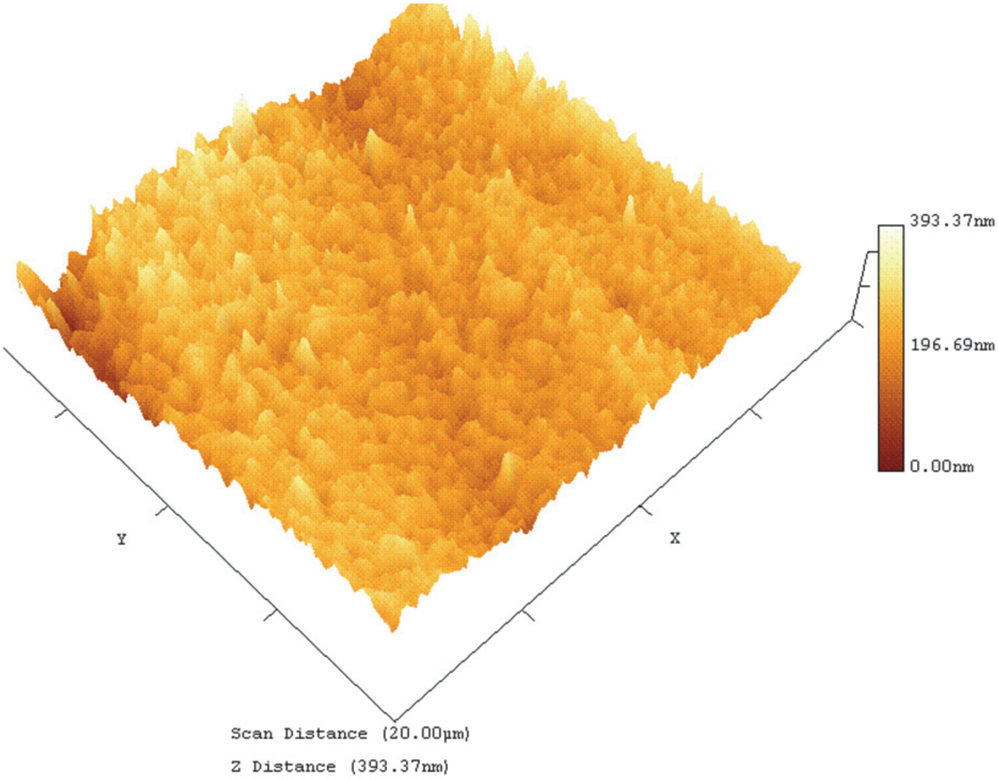

Figure 6.10. AFM image of wet-tested ESPA2 element.

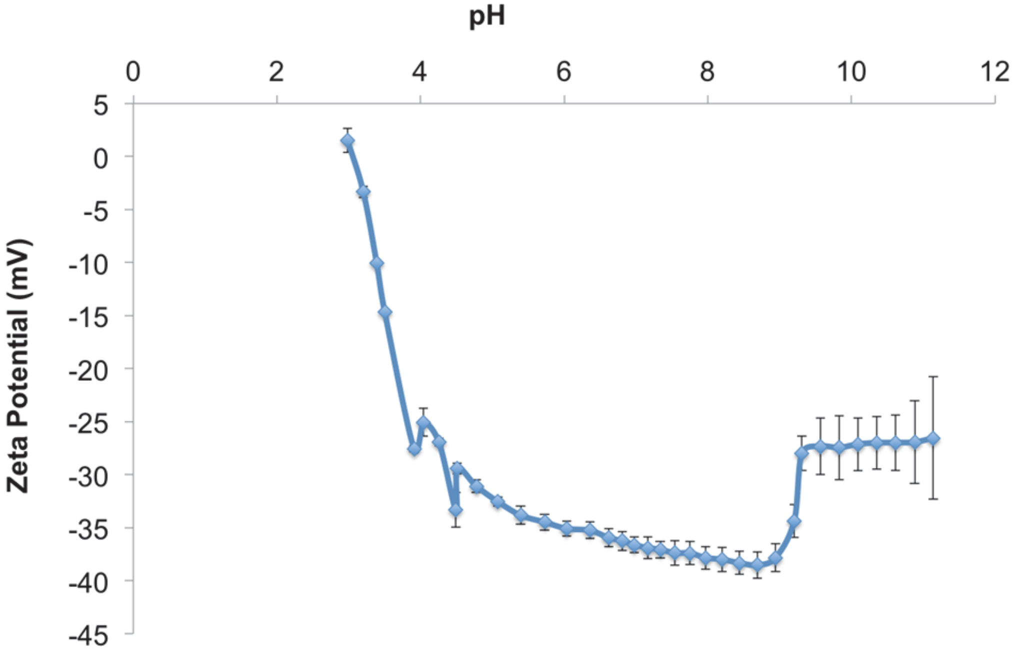

Figure 6.11. Zeta potential data for wet-tested ESPA2 element.

6.3.3.2 RO autopsy

After the completion of pilot testing, both RO units were shut down and flushed with RO permeate. The next day, two membrane specimens of the lead element of Vessel 1A and the tail element of Vessel 3b were collected from each RO unit. On the same day, one membrane specimen was collected from the factory wet-tested RO element that served as a reference for the pilot-tested elements. Pictures of the unrolled elements from pilot testing are shown in Figure 6.12, and a picture showing an example of where membrane specimens were removed from the elements are shown in Figure 6.13. Membrane specimens were stored in a refrigerator before shipment to Technology of Materials for SEM/EDS and FTIR and to Colorado School of Mines for AFM and zeta potential (wet-tested RO element only).

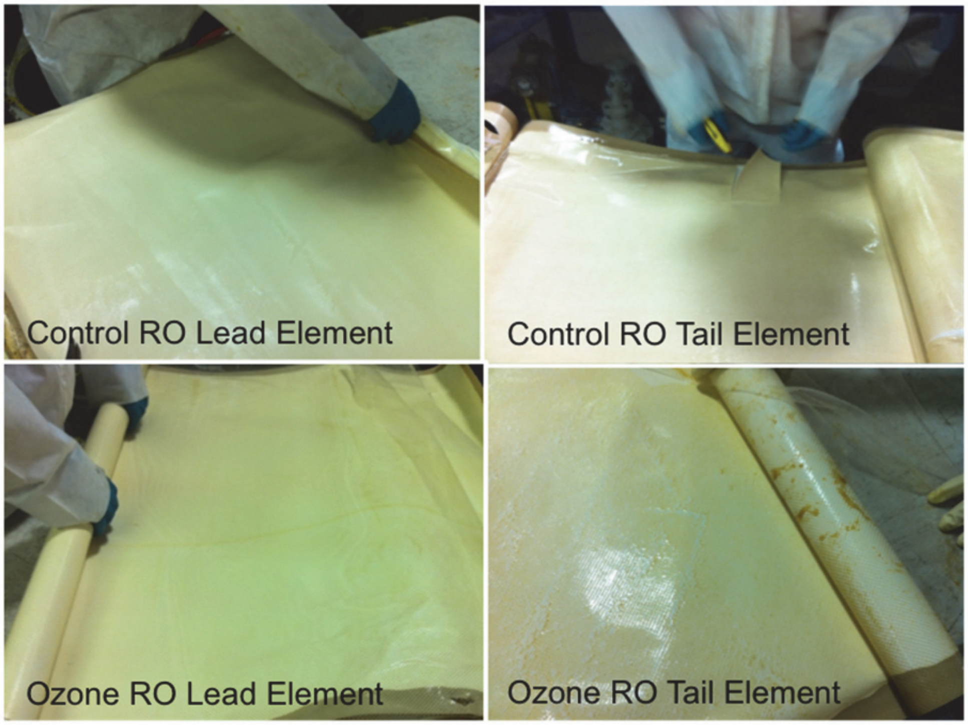

Figure 6.12. Membrane specimens (6-in x 6-in) were collected from these unrolled RO elements and analyzed for SEM/EDS and FTIR.

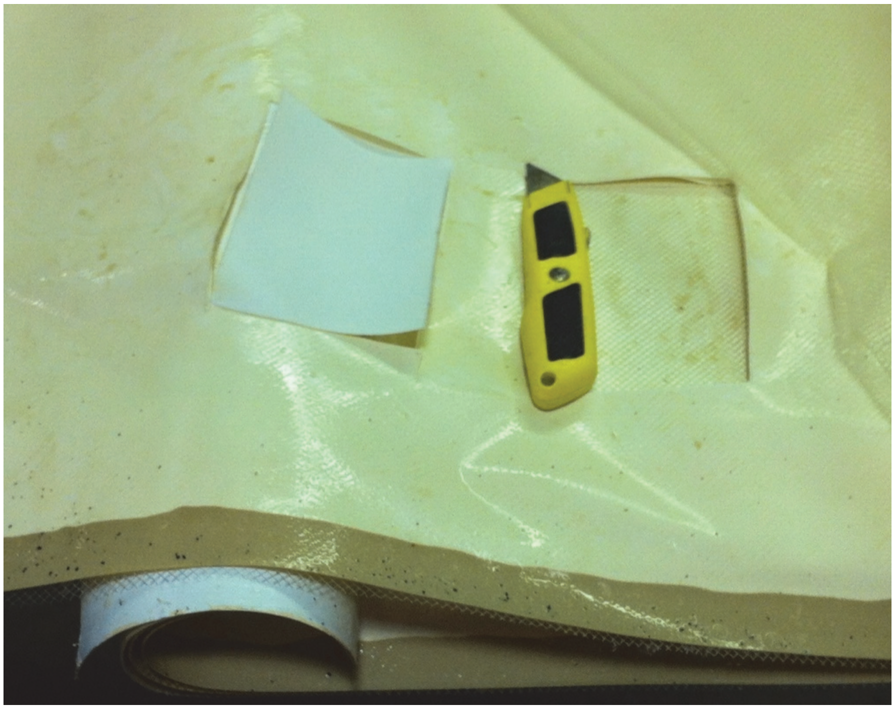

Figure 6.13. An example of the size of the membrane specimens and their location relative to the edge of the RO elements.

6.3.3.3 SEM Analysis

Two membrane specimens of each RO element (Control RO lead and tail and Ozone RO lead and tail) were analyzed using SEM but only one set of those images was reported, because the results were similar. SEM images showing the morphology of the fouling layer on the membrane specimens collected from the RO elements shown in Figures 6.14, 6.15, and 6.16. Magnifications in those images are 100x, 500x, and 1000x, respectively. The only exception is Figure 6.14(d), which had a magnification of 117x, which is slightly larger than the other images (100x) in that figure.

The SEM images in Figures 6.14 to 6.16 did not show distinctive evidence of foulants such as bacteria or crystalline structures associated with specific minerals. The absence of biofouling was attributed to the presence of a chloramine residual in the RO feed of both treatment trains for the duration of testing. The images were more indicative of an amorphous foulant that could be a mixture of particulate, inorganic, and organic materials. When comparing the lead and tail elements of Control RO and Ozone RO, there are some visual differences but nothing that clearly indicated the nature of the foulants in the RO units differed from one another.

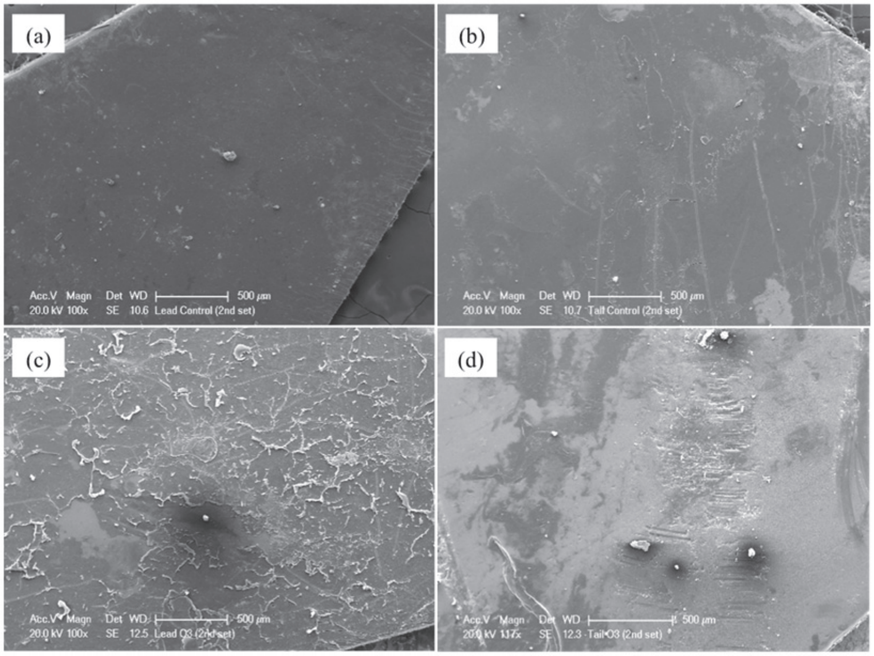

Figure 6.14. SEM images of Control RO lead (a) and tail (b) elements and Ozone RO lead (c) and tail (d) elements.

Note: Magnification is 100x for (a) to (c) and 117x for (d).

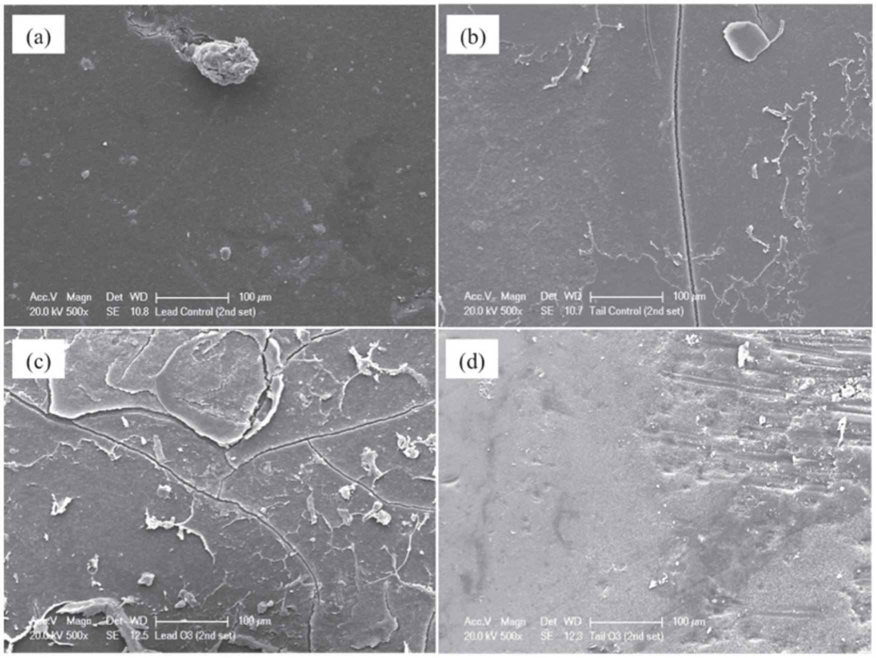

Figure 6.15. SEM images of Control RO lead (a) and tail (b) elements and Ozone RO lead (c) and tail (d) elements.

Note: Magnification is 500x for all images.

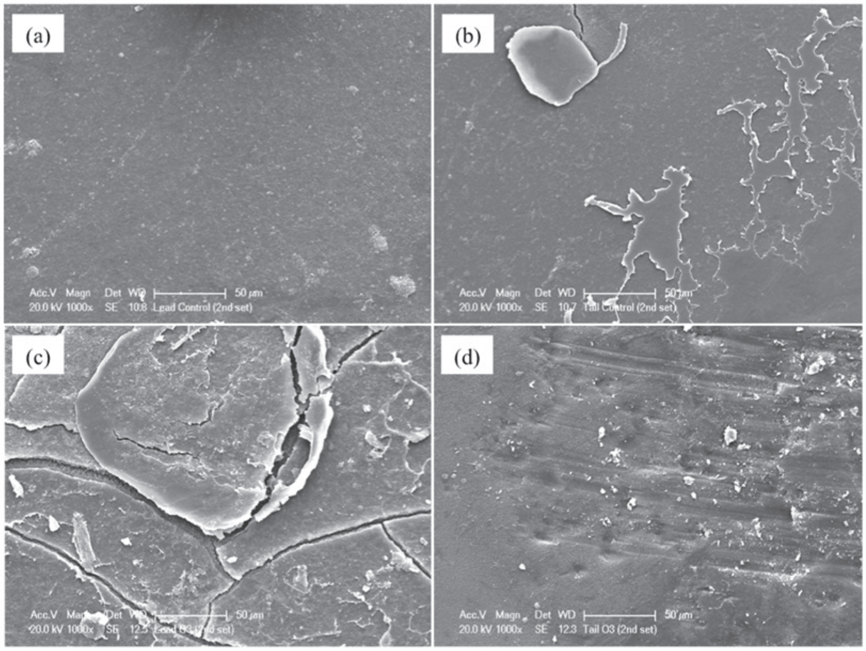

Figure 6.16. SEM images of Control RO lead (a) and tail (b) elements and Ozone RO lead (c) and tail (d) elements.

Note: Magnification is 1000x for all images.

6.3.3.4 EDS Analysis

EDS data for the reference wet-tested RO element and the Control RO and Ozone RO elements from pilot testing are included in Table 6.3. Results from the two membrane specimens collected from the pilot-tested RO elements were averaged together and reported for elements with atomic weights larger than carbon. One approach to comparing the degree of fouling is to compare the oxygen-to-sulfur (O/S) ratio between the RO elements. For the wet-tested RO element, the O/S ratio was 1.2, but it increased to 2.0 for the lead and tail Control RO elements and tail ozone RO element. The O/S ratio was even higher at 3.8 for the lead Ozone RO element, suggesting this RO element had more foulants on it than the others that were analyzed.

Each element showed increases in the proportion of oxygen detected by EDS compared to the wet-tested RO element. One possible explanation of this would be the presence of oxides such as carbonate and sulfate that are components of common RO foulants such as calcium carbonate ($CaCO_3$) and calcium sulfate. Minimal levels of calcium ($\leq 1.0\%$) were detected on the Control RO elements, but higher concentrations (3.0%) were found in the ozone train. More iron also was found on the Ozone RO elements compared to the Control RO elements. Possible explanations included higher deposition of iron- and calcium-based foulants on Ozone RO and a residual effect from inorganic fouling when the antiscalant feed pump for the Ozone RO was offline for several weeks. The CIP after that event might not have removed all of the foulants, leaving more iron and calcium for EDS to measure.

Table 6.3. Average EDS Data (% w/w) of Wet-Tested RO, Control RO, and Ozone RO Elements for Elements with Atomic Weights Larger than Carbon

	% w/w				
Element	**Wet-tested ESPA2**	**Avg. Lead Control**	**Avg. Lead Ozone**	**Avg. Tail Control**	**Avg. Tail Ozone**
Oxygen	51.2	61.2	64.2	57.4	58.1
Sodium	1.2	1.0	5.1	4.3	2.0
Magnesium	0.8	< 0.8	1.2	< 0.8	1.0
Silicon	0.8	< 0.8	0.8	< 0.8	1.4
Sulfur	42.6	31.9	17.0	28.5	26.8
Chlorine	2.1	2.2	5.0	5.6	2.5
Calcium	< 0.8	< 0.8	3.0	1.0	3.0
Iron	1.2	1.7	3.9	1.9	5.6
Total	100	100	100	100	100
O/S ratio	1.2	1.9	3.8	2.0	2.2

6.3.3.5 FTIR Spectroscopy

Results of FTIR spectroscopy for the membrane specimens collected from the lead and tail elements are shown in Figures 6.17 and 6.18, respectively. Vertical dashed lines in those figures denote vibrational bands associated with polyamide membranes and the underlying polysulfone support material. The FTIR spectra of the lead elements (Figure 6.17) showed the background spectrum (Figure 6.9) was distorted by fouling. The percentage transmission of the amide I band was greater than the amide II band in the background spectrum, but the lead elements showed the opposite. This change in the relative transmissions of these vibrational bands suggested proteins contributed to fouling. The lower percentage transmission of the amide I and II bands in the FTIR spectra from Ozone RO indicated more proteins were located on that element compared to Control RO. There was also a new vibrational band around 1040 cm^{-1}, which is associated with carbohydrates. As with the proteins, the spectra indicated more carbohydrates were present on the Ozone RO lead element. Other vibrational bands were no longer visible (e.g., 1607 cm^{-1}) or significantly altered from their original state (e.g., 1488 and 1242 cm^{-1}). The difference between the background spectrum and the spectra of the lead elements was greater for Ozone RO, indicating more foulants had accumulated on that element.

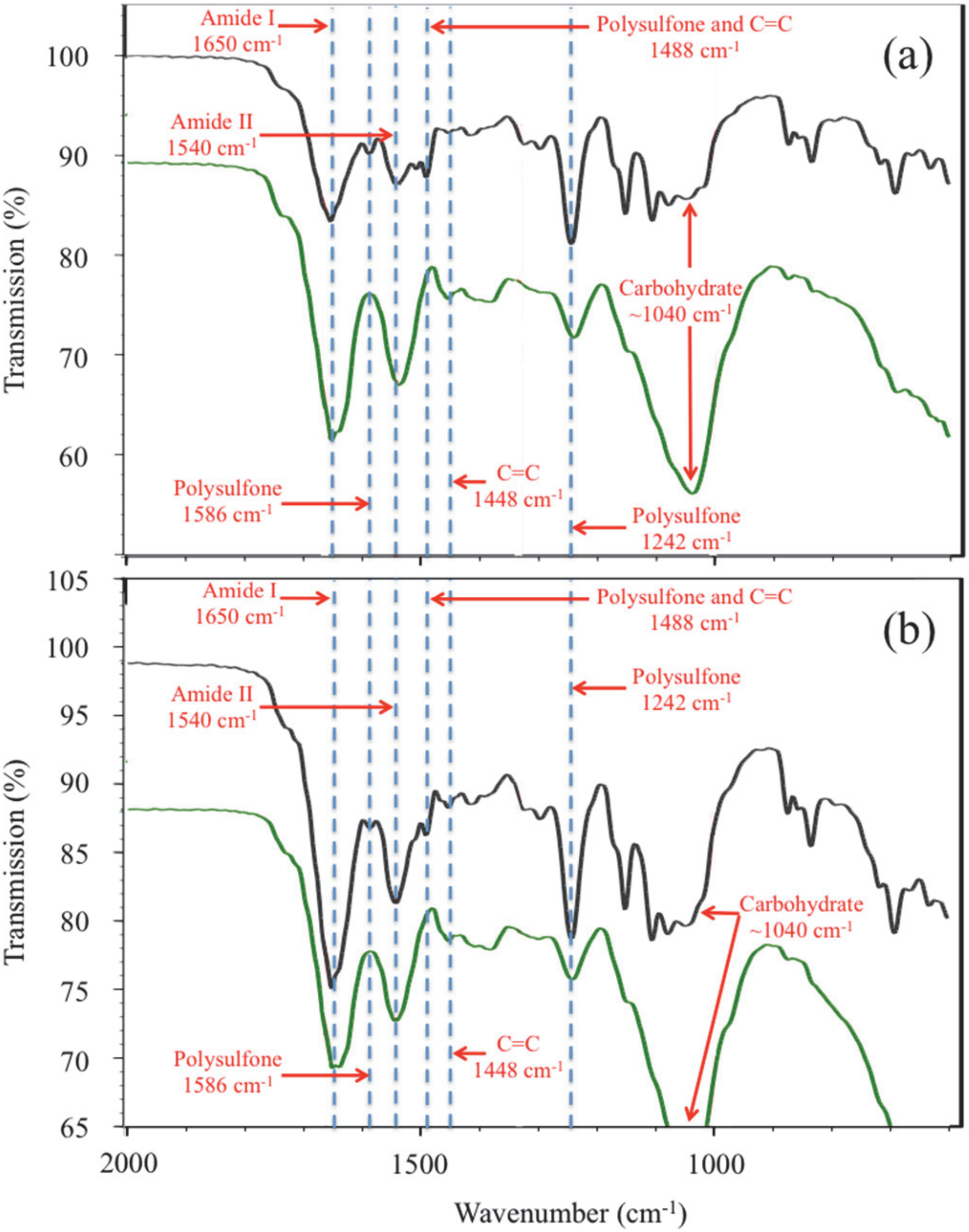

Figure 6.17. FTIR spectra of first (a) and second (b) lead element membrane specimens of Control RO (top black line in the figures) and Ozone RO (bottom green line in the figures).

Notes: Vibrational bands associated with the polyamide membrane and polysulfone support are identified using dashed lines. A new band indicative of carbohydrates (~1040 cm^{-1}) is shown on both figures. Note the scales of the y-axes are different.

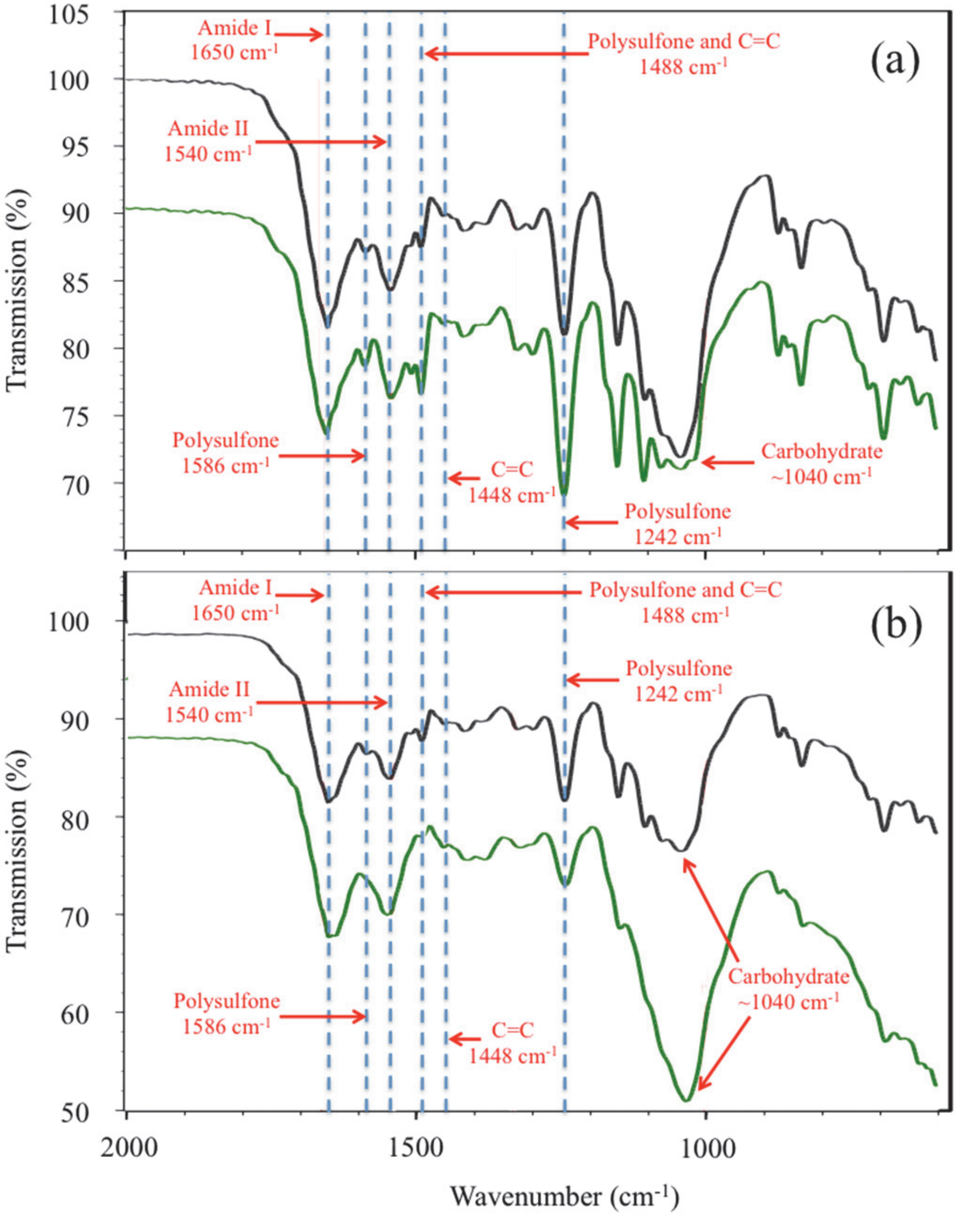

Figure 6.18. FTIR spectra of first (a) and second (b) tail element membrane specimens of Control RO (top black line in the figures) and Ozone RO (bottom green line in the figures).

Notes: Vibrational bands associated with the polyamide membrane and polysulfone support are identified using dashed lines. A band indicative of carbohydrates (~1040 cm^{-1}) is shown on both figures. Note the scales of the y-axes are different.

The same analysis performed on the tail elements (Figure 6.18) provided mixed results. The change in the relative transmissions of the amide I and amide II bands were similar, although the magnitude of the difference appeared to be less than it was for the lead elements. The vibrational band around 1040 cm^{-1} indicated carbohydrates were also present on the analyzed membrane specimens. However, the overall distortion of the spectra was greater for Control RO in Figure 6.18(a) and greater for Ozone RO in Figure 6.18(b). These results did not reflect the higher fouling detected on the Ozone RO lead element and suggested fouling of the tail elements of the RO trains was similar at the end of pilot testing.

6.4 Conclusions

RO performance data and results from analyzing membrane specimens collected from the lead and tail elements of Control RO and Ozone RO detected few differences between the treatment trains. Ozonation was initially associated with lower RO feed pressure and higher specific flux. These data were consistent with other research showing ozone pretreatment improved RO performance (Pisarenko et al., 2011; Stanford et al., 2011; Stanford et al., 2013). However, the benefits of ozone pretreatment dissipated after the RO units were switched between treatment trains while keeping the RO elements with their original treatment train.

Membrane autopsy data showed the accumulation of specific foulants were higher on Ozone RO compared to Control RO. Foulant morphology was similar, and neither membrane showed visual evidence of a dominant fouling mechanism. EDS detected more iron and calcium on the lead and tail elements of Ozone RO, although the levels were still low. These data suggested foulants, such as colloidal iron and $CaCO_3$, were more likely to be present on Ozone RO elements than Control RO elements. FTIR spectroscopy indicated there were more foulants—particularly proteins and carbohydrates—on the lead element of Ozone RO. The tail elements of both RO units had similar FTIR spectra, indicating the difference in organic fouling between the lead elements did not translated to the tail elements.

It is important to note the differences detected by the analysis of membrane specimens were not enough to lower Ozone RO performance relative to Control RO. Therefore, the higher amounts of organics, calcium, and iron on the Ozone RO elements were not enough to affect performance during the 5 months of cumulative operation logged by Ozone RO. In addition, more study of the initially superior performance of Ozone RO might prove beneficial, because the disappearance of this difference could not be explained satisfactorily. The potential to reduce feed pressure and to increase specific flux by as much as 20%, as was seen during the first several months of pilot testing, could lower power usage and decrease operating costs at water reuse facilities. Any savings could help offset the expense of implementing MF pretreatment with ozone, thereby improving process economics.

Chapter 7

NDMA and Bromate Formation and Emerging Contaminant Removal by Ozonation

7.1 Introduction

Adding ozonation to a water reuse treatment train to reduce microfiltration (MF) fouling had the potential to significantly affect other aspects of the treatment train. Effects on reverse osmosis (RO) performance were discussed in the previous chapter, but research also showed ozonation of wastewater effluent could form N-nitrosodimethylamine (NDMA) (Andrzejewski and Nawrocki, 2007; von Gunten et al., 2010; Zimmermann et al., 2010) and remove a significant amount of many contaminants of emerging concern (CECs) (Pisarenko et al., 2012; Snyder et al., 2007; Wert et al., 2009). Bromate, a potential human carcinogen with a maximum contaminant level of 10 µg/L as an annual average (USEPA, 2011), is a disinfection byproduct that can be formed by the ozonation of water containing bromide ions (Glaze et al., 1993). Therefore, bromate formation and fate after ozonation required investigation.

The goals of this portion of the pilot study were to investigate the effect of ozonation on NDMA formation, bromate formation, and CEC removal. NDMA, bromate and CEC concentrations in the RO permeate of treatment trains with and without ozone also were compared to determine the effect of ozonation on RO permeate quality. Bench-scale work included testing pH adjustment and prechlorination to minimize NDMA formation and determining if polymers used at the wastewater treatment plant supplying the pilot plant with non-nitrified secondary effluent were a source of NDMA precursors.

7.2 Methods and Materials

West Basin Municipal Water District's (West Basin's) Edward C. Little Water Recycling Plant (ECLWRF) in El Segundo, CA, was the location of the pilot plant. Process descriptions and experimental data for the control train (MF-RO) and the ozone train (O_3-MF-RO) were discussed in in Chapter 4 (ozone), Chapter 5 (MF), and Chapter 6 (RO). Additional descriptions of methods and materials relevant to the experiments and data described in this chapter follows.

7.2.1 Analyzing Samples for NDMA, CECs, and Bromate

7.2.1.1 Sample Collection Schedule

Table 7.1 shows the frequency and location of grab sample collection. Bromate and NDMA were part of the regularly schedule sample collection at the pilot plant. During the last 2 full months of testing, a total of six samples were collected from the pilot plant influent and ozone effluent for CEC analysis. Only four samples were collected from Control RO permeate and Ozone RO permeate for this purpose during the last full month of testing.

Table 7.1. Frequency of Grab Samples Collected from the Pilot Plant

	Sampling Frequency			
Water Quality Parameter	**Pilot Plant Influent**	**Ozone Effluent**	**Control RO Permeate**	**Ozone RO Permeate**
Bromate	---	Weekly	---	Weekly
CECs	~ Weekly (Nov & Dec)	~ Weekly (Nov & Dec)	Weekly (Dec)	Weekly (Dec)
NDMA	Weekly	Weekly	Weekly	Weekly

7.2.1.2 NDMA Sample Analysis

Nitrosamines were extracted from 500 ml of sample by passing a water sample through a solid phase extraction (SPE) cartridge (Enviro-Clean 521, UCT Inc., Bristol, PA) containing 2 g of 80-120 mesh coconut charcoal per U.S. Environmental Protection Agency (USEPA) Method 521. The cartridges were conditioned manually with dichloromethane (DCM), methanol and high-performance liquid chromatography (LC) water prior to extraction. The analyte compounds were eluted from the solid phase with methylene chloride. The eluent was then dried under gentle nitrogen stream for concentration followed by mass spectrometer (MS) analysis.

The Agilent gas chromatograph (GC) 7890 equipped with a 7000 MS (Agilent Technologies, Santa Clara, CA) and a 30 m × 0.25 mm × 0.25 µm DB-WAXetr column (Agilent Technologies, Santa Clara, CA) were employed for NDMA analysis of sample extracts (in DCM). Helium was used as carrier at a constant flow rate of 1.7 mL/min. A 5-µL sample was injected in unsplit mode at 200 °C. The injection temperature was 200 °C and the oven was set at 40 °C for 3 min, then an increase of 10 °C/min to 110 °C for 0 min, 15 °C/min to 200 °C for 0 min and then 40 °C/min to 240 °C for 0 . The MS/MS analysis was carried out in chemical ionization (CI) mode with ammonia using the multiple reaction monitoring (MRM) mode. The ion source was operated at 200 °C with electron energy of 70 eV and a filament current of 200 µA. The MRM transitions are provided in Table 7.2. NDMA-d6 and N-nitrosodi-n-propylamine-d14 (NDPA-d14) were employed as surrogate and internal standard for method and instrument correction. The instrument limits of detection and quantitation were 0.175 ppb and 0.250 ppb, respectively.

Table 7.2. MRM Transitions for GC-MS/MS Analysis of NDMA Following USEPA Method 521

Compound	Molecular Weight (g/mol)	Quantitative Mass (m/z)	Qualitative Mass (m/z)
NDMA	74.048	92	75
NDMA-d6	86.086	98	81
NPDA-d14	144.198	162	145

Note: Ammonia CI gas supplied $[NH_4]^+$, $[NH_4\text{-}NH_3]^{+,}$ and $[NH_4\text{-}(NH_3)_2]^+$ ions with mass over charge (m/z) values of 18, 35 and 52, respectively, for reaction with target analytes.

7.2.1.3 CEC Sample Analysis

CEC samples collected from the pilot plant influent, ozone effluent, Control RO permeate, and Ozone RO permeate were sent to MWH Labs (Monrovia, CA) for analysis using LC/MS/MS. Ozone doses at the time of sample collection were set by the automated dose control system and ranged from 11 to 17 mg/L (average = 14 mg/L). Because the pilot plant influent TOC was 11 to 12 mg/L, ozone to total organic carbon (O_3:TOC) ratio varied from 0.9 to 1.5 (average = 1.2). Most of the CECs with reportable results (Table 7.3) were analyzed using data from 6 samples for the influent and ozone effluent. However, data quality and results indicating a chemical was not detected in the pilot plant influent reduced the number of samples for several chemicals as noted in Table 7.3.

Table 7.3. The Detection Limit and Number of Samples with Usable Data for the CECs Measured in this Study

CEC	Class	Minimum Reporting Limit (ng/L)	No. of Samples
Acesulfame-K	Other[1]	20	6
Acetaminophen	PPCP	5	6
Amoxicillin	PPCP	20	6
Atenolol	PPCP	5	6
Caffeine	PPCP	5	4
Carbamazepine	PPCP	5	6
Cotinine	PPCP	10	6
DEET	Pesticide	6	3
Diuron	Pesticide	5	6
Gemfibrozil	PPCP	5	5
Iopromide	PPCP	5	4
Ketoprofen	PPCP	5	6
Lopressor	PPCP	20	6
Meprobamate	PPCP	5	6
Phenytoin	PPCP	20	6
Primidone	PPCP	5	6
Sucralose	Other[1]	100	4
Sulfamethoxazole	PPCP	5	6
TCEP	Other[2]	10	5
Triclosan	PPCP	10	6
Trimethoprim	PPCP	5	6

[1] Artificial sweetener

[2] Flame retardant

Results for other CECs were measured but not reported here because they were detected in fewer than three pilot plant influent samples or had concentrations too low to reliably measure removal. Low pilot plant influent concentrations can cause removal to be calculated incorrectly if the ozone effluent concentration is always below the detection limit. Examples of chemicals that were investigated but did not have usable results included bisphenol A, estradiol, fluoxetine, ibuprofen, naproxen, and progesterone.

RO permeate samples were only collected four times. For the purpose of calculating averages, CEC concentrations below the detection limit were assumed to be half of that limit. These assumed concentrations were averaged with measurements above the detection limit to calculate the average concentration for that CEC. The average results were reported as not detected (ND) if all samples were ND or if the average of the assumed ND concentrations and actual concentration were below the detection limit.

7.2.1.4 Bromate Sample Analysis

Because the secondary effluent feeding ECLWRF was known to contain bromide (average = 0.33 mg/L during testing), bromate samples were collected from ozone effluent and Ozone RO permeate. The bromate concentration was assumed to be 0 µg/L in the pilot plant influent and unchanged between the ozone effluent and Ozone RO feed. Samples were collected weekly when Ozone RO was operational and shipped to MWH Labs (Monrovia, CA) for analysis following USEPA Method 317.

7.2.2 Bench-Scale Sample Ozonation for NDMA Experiments

The different O_3 to dissolved organic carbon (O_3:DOC) ratio samples were prepared by filling up bottles to a predetermined volume calculated from the ozone stock solution concentration (50 mg O_3/L) and the desired O_3:DOC ratio (0.25, 0.50, 0.75, and 1.00). The volume of ozone stock solution was subtracted from the total bottle volume (1057 ml) to determine the required volume of sample. Changes to the final DOC concentration were considered when calculating the required volume of ozone stock solution. An example of a table based on these calculations for a sample with an initial DOC of 13.0 mg/L is shown in Table 7.4.

Table 7.4. Volumes of Ozone Stock Solution Added for Different O_3:DOC Ratios

O_3:DOC	Volume of Sample (mL)	Volume of Ozone Stock (mL)	Final DOC (mg/L)
0.00	1,057	0	13.0
0.25	992	65	12.2
0.50	935	122	11.5
0.75	885	172	10.9
1.00	839	218	10.3

An ozone generator (Modular 8HC, Wedeco, Germany) used pure oxygen to create ozone that was bubbled into distilled deionized (DDI) water at 1 °C using a fine-glass fritted diffuser. After reaching the desired ozone concentration in the stock solution, the room-temperature samples (approximately 24 °C) were ozonated by adding the stock solution to the top of the bottle. The samples were capped and stirred for 5 min using a magnetic stir plate. After stirring, the ozone residual was measured using the indigo method to confirm its decay. NDMA was extracted from the samples 24 to 48 h after ozone addition.

7.2.3 NDMA Formation Control Experiments

These experiments tested the effect of chloramination and pH suppression on NDMA formation. The bench-scale ozonation method described in Section 7.2.2 was used for these tests. Prior to ozonation, pilot plant influent samples of non-nitrified secondary effluent were treated with sodium hypochlorite (target total chlorine residual of 6 mg/L) and/or sulfuric acid (target pH of 6.5). Because the ammonia concentrations were approximately 40 mg/L, the added chlorine was rapidly converted to chloramines. The total chlorine residual was measured by titration. The target pH of 6.5 was 0.5 less than typical ambient pH of 7.0. This pH target was selected because it was representative of the pH adjustment in the feed of the full-scale RO trains at ECLWRF. Table 7.5 shows the combinations of pH adjustment and chloramination that were tested as part of these experiments. NDMA formation from these test conditions was compared to determine if chloramination or pH suppression reduced NDMA formation.

7.2.4 NDMA Formation from Wastewater Treatment Polymers

Two polymers used at the Hyperion Treatment Plant (HTP), which supplies ECLWRF with non-nitrified secondary effluent, were tested to determine if residuals of the polymers might contribute to NDMA formation during ozonation. The cationic polymer was used in the digested sludge centrifuge feed and the waste activated sludge thickening centrifuge feed. The anionic polymer was injected into the influent to the primary sedimentation tanks. The manufacturer and product information for the polymers was never provided. A dose of 10 mg/L of each polymer was added separately to DDI water and pilot plant influent. These samples, a sample of DDI water without polymer, and a sample of pilot plant influent without polymer were ozonated with 10 mg/L of ozone following the method described in Section 7.2.2. Test conditions for these experiments are shown in Table 7.6. The post-ozone NDMA concentration of each sample was compared to evaluate the effect of the polymers on NDMA formation during ozonation.

Table 7.5. Test Conditions for NDMA Formation Control Experiments

Experiment	Total Chlorine Residual	pH
1	0	7.0 (ambient)
2	0	6.5
3	6	7.0 (ambient)
4	6	6.5

Table 7.6. Test Conditions for Wastewater Treatment Polymer Sample

Experiment	Test Water	Polymer
1	DDI	none
2	DDI	10 mg/L cationic
3	DDI	10 mg/L anionic
4	Pilot plant influent	none
5	Pilot plant influent	10 mg/L cationic
6	Pilot plant influent	10 mg/L anionic

7.3 Results and Discussion

7.3.1 Pilot Plant Data

7.3.1.1 NDMA

Results for weekly NDMA samples collected from the control train (Figure 7.1) and the ozone train (Figure 7.2) showed a significant difference in NDMA concentrations of these treatment trains. Both treatment trains treated the same non-nitrified secondary effluent, so the influent NDMA concentrations were the same. In the control train, secondary effluent was treated with chloramination, ferric chloride addition, and polyvinylidene fluoride MF membranes prior to RO for the first 4 months of testing. On 9/12, the Control RO feed was switched to ECLWRF MF filtrate. Therefore, the influent was treated with chloramination followed by polypropylene MF membranes from that day forward. The chloramine doses of the pilot plant and full-scale control trains average 2 and 3 mg/L, respectively. Contact times between chloramination and Control RO were shorter for the full-scale MF (approximately 30 min) compared to the pilot-scale MF (approximately 60 to 90 min).

Average NDMA formation by chloramination, defined as the difference between the NDMA concentration of the pilot plant influent and Control RO feed, was 8 ng/L. Influent NDMA concentration increased during the last few months of the year, corresponding with lower water temperatures. This change was likely a consequence of reduced treatment efficiency at HTP as lower temperatures reduced the effectiveness of the secondary treatment process. NDMA rejection by Control RO ranged from 17 to 66% (average = 47%), which was in line with other research showing rejection from 24 to 56% (Plumlee et al., 2008) and approximately 40% for artificially fouled membranes (Steinle-Darling et al., 2007). NDMA concentrations in Control RO permeate ranged from 5 to 51 ng/L (average = 19 ng/L). The peak NDMA concentration measured would require 80.4% (0.84-log) reduction by an advanced oxidation process (AOP), such as ultraviolet light with hydrogen peroxide, (UV/H_2O_2) to satisfy the California Department of Public Health (CDPH) notification limit of 10 ng/L (CDPH, 2012).

In the ozone train, the ozone dose was set manually until 9/23, when automated dose control was implemented. Dose control initially was based on influent UVT, then influent and ozone effluent UVT, and finally ozone effluent UVT alone. These automated adjustments varied ozone doses based on water quality changes. NDMA samples were collected at ozone doses ranging from 4 to 17 mg/L (Figure 7.2).

NDMA formation by ozonation was 30 to 241 ng/L (average = 103 ng/L), greatly exceeding formation by chloramination in the control train. In addition, chloramination after ozonation increased the NDMA concentration another 0 to 130 ng/L (average = 30 ng/L). The highest NDMA concentrations and formation were measured during the last month of the year when the temperature was the lowest. As mentioned, this finding suggested less effective biological oxidation during secondary treatment at lower temperatures increased the concentration of NDMA and NDMA precursors in the pilot plant influent. Ozone RO rejection of NDMA was 10 to 46% (average = 28%), which was lower than NDMA rejection by Control RO. NDMA concentrations in Ozone RO permeate ranged from 45 to 260 ng/L (average = 117 ng/L). On the basis of the peak NDMA concentration, AOP would need to reduce NDMA by 96.2% (1.4-log removal) to satisfy the CDPH notification limit of 10 ng/L.

O_3:TOC ratio versus NDMA formation was graphed (Figure 7.3) to evaluate the relationship between ozone dose and NDMA formation by ozonation. Bench-scale testing of ozone dose to dimethylamine (DMA), a known NDMA precursor, showed a strong relationship between O_3:DMA ratio and NDMA formation (Andrzejewski et al., 2008). The data in Figure 7.3 showed no relationship between O_3:TOC ratio and NDMA formation, indicating TOC was a poor surrogate for measuring precursors in this source water. Research by Hollender et al. (2009) found NDMA formation from the ozonation of secondary effluent did not correlate with ozone dose. Those results suggested variable NDMA precursor concentrations in the ozone influent were more significant than changes to the ozone dose.

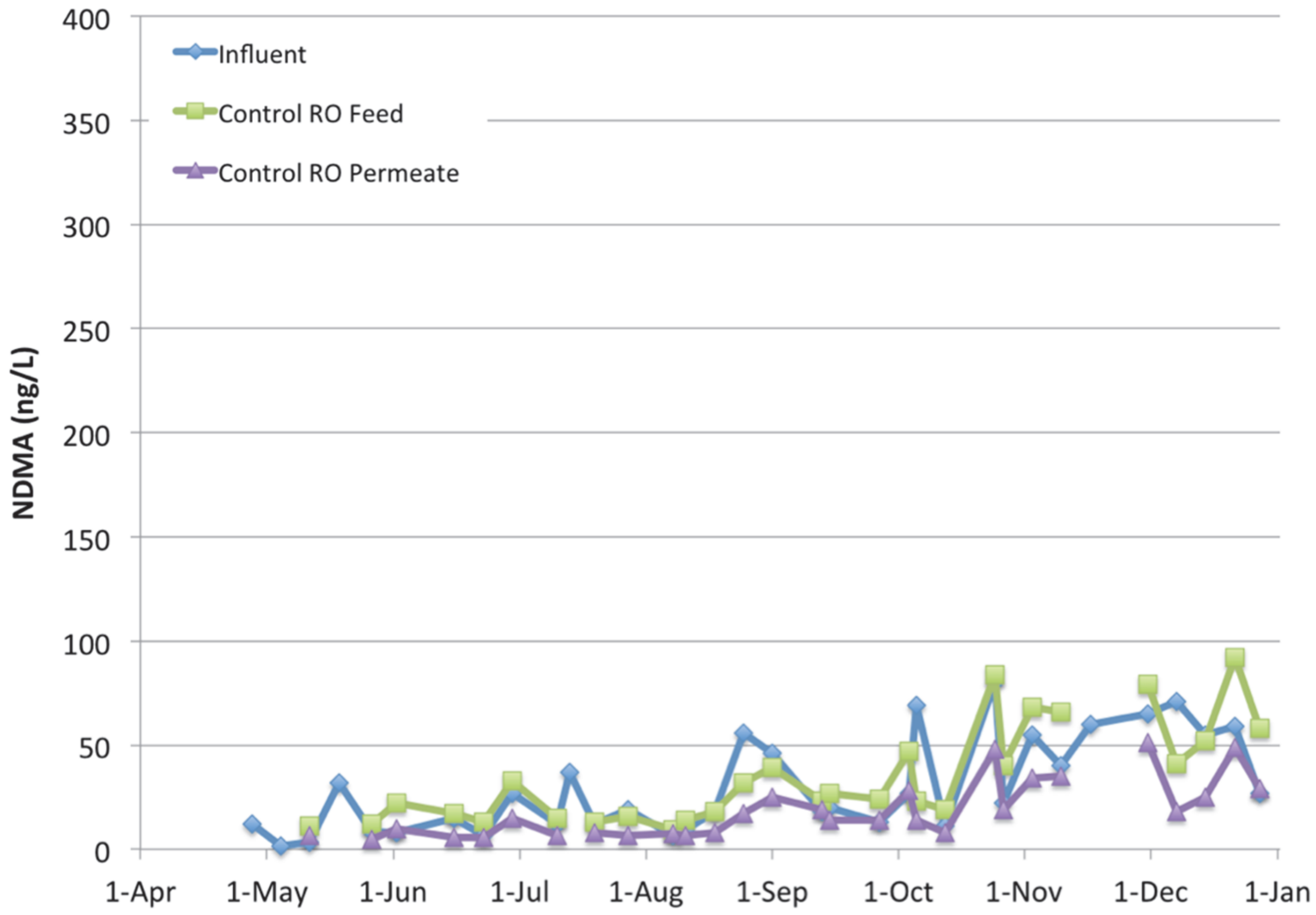

Figure 7.1. Weekly NDMA data for the control train. Control RO feed was switched from Control MF filtrate to ECLWRF MF filtrate on 9/12.

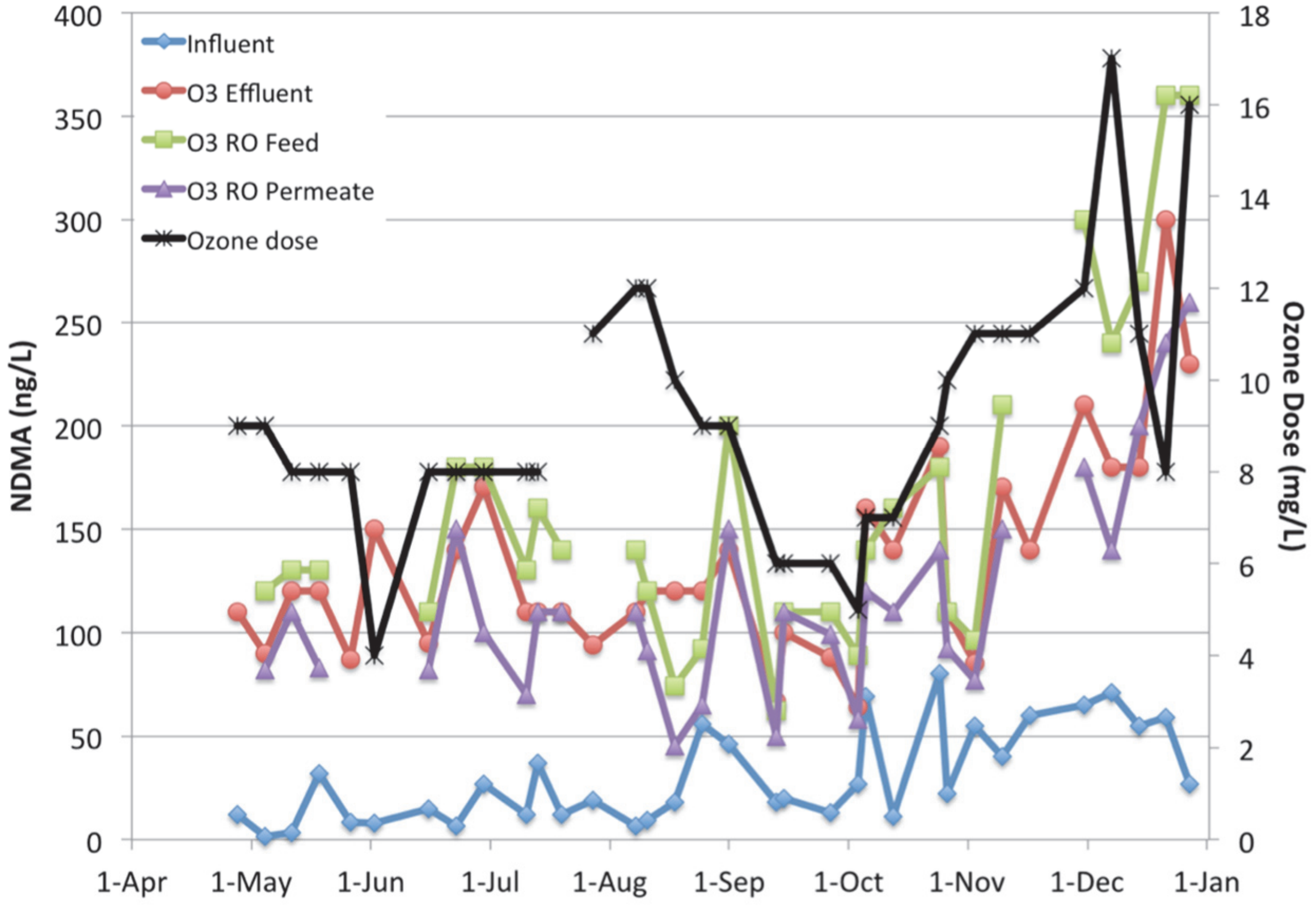

Figure 7.2. Weekly NDMA data and the transferred ozone dose at the time of sample collection for the ozone train.

Notes: Automated ozone dose control based on influent UVT was implemented on 9/23. Later adjustments to ozone dose control were based on influent and ozone effluent UVT and ozone effluent UVT alone.

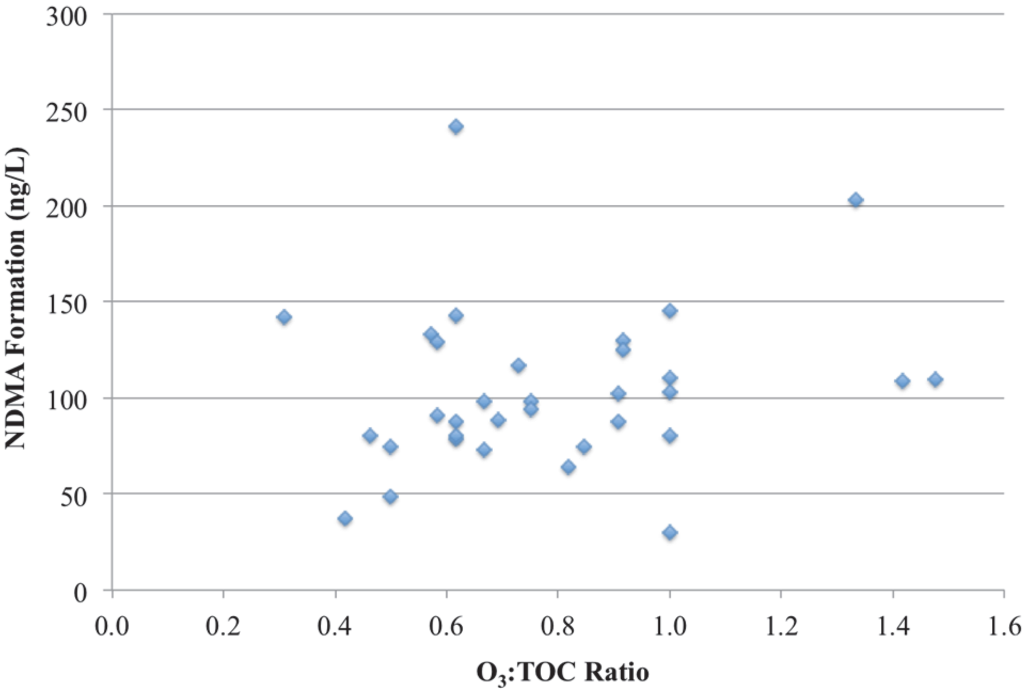

Figure 7.3. NDMA formation during pilot testing as a function of O_3:TOC ratio.

7.3.1.2 CECs

Significant amounts of many CECs were removed during ozonation. Average, standard deviation, and standard error data for CECs detected in pilot plant influent are shown in Table 7.7. Percentage removal of these CECs by ozonation varied significantly depending on the chemical (Figure 7.4). CECs, such as amoxicillin, carbamazepine, and trimethoprim, were reduced below their detection limits. Others, such as DEET, atrazine, and meprobamate, were more resistant to ozonation, but were still significantly removed by treatment. The most persistent chemicals were continine (38% reduction), sucralose (36% reduction), and TCEP (16% reduction). Although actual removals differed, these trends resembled other research with wastewater effluent (Pisarenko et al., 2012; Snyder et al., 2007; Wert et al., 2009). Excluding NDMA, which was discussed in Section 7.3.1.1, CECs were below the minimum reporting limit in the RO permeate of both treatment trains.

Table 7.7. Average Pilot Plant Influent Concentrations of CECs Used to Evaluate Their Removal by Ozonation

CEC	Minimum Reporting Limit (ng/L)	Average concentration (ng/L)	Standard Deviation	Relative Standard Deviation
Acesulfame-K	20	26,000	5,220	20%
Acetaminophen	5	54	19	35%
Amoxicillin	20	1,230	933	76%
Atenolol	5	243	102	42%
Caffeine	5	96	124	129%
Carbamazepine	5	180	21	12%
Cotinine	10	89	21	24%
DEET	6	343	191	56%
Diuron	5	138	117	17%
Gemfibrozil	5	2,880	502	52%
Iopromide	5	800	417	146%
Ketoprofen	5	377	552	65%
Lopressor	20	342	222	118%
Meprobamate	5	243	287	133%
Phenytoin	20	521	691	13%
Primidone	5	93	12	27%
Sucralose	100	23,700	6,380	44%
Sulfamethoxazole	5	340	150	52%
TCEP	10	208	108	50%
Triclosan	10	757	377	50%
Trimethoprim	5	373	186	20%

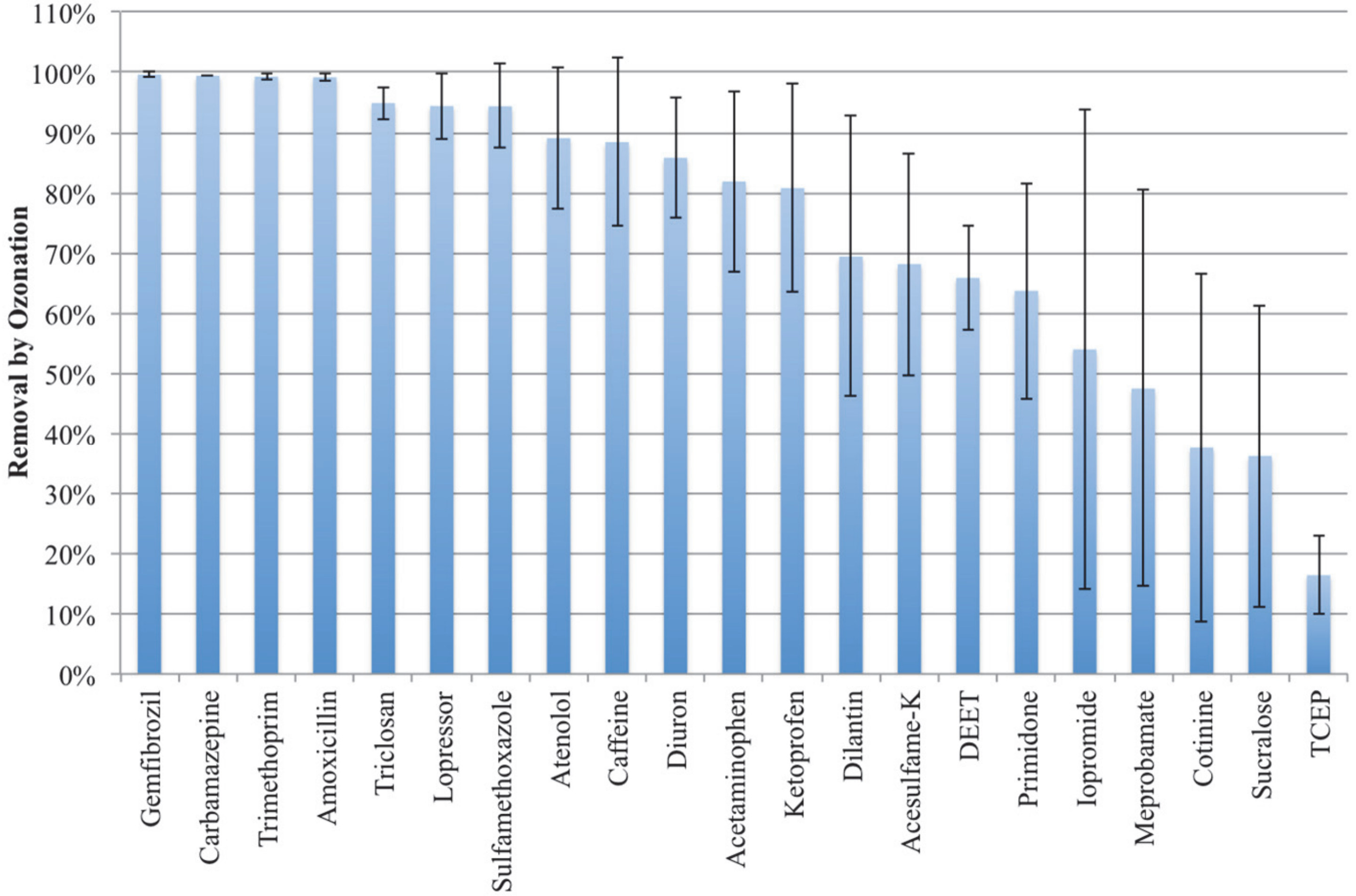

Figure 7.4. Removal of common CECs during ozonation of the pilot plant.

Notes: Ozone doses ranged from 11 to 17 mg/L, corresponding with O :TOC ratios of 0.9 to 1.5. Error bars represent the standard deviation.

7.3.1.3 Bromate Data

Ozone frequently produced enough bromate to exceed the 10-µg/L limit established by USEPA, but these concentrations were easily removed by RO. Ozonation at transferred ozone doses between 5 and 17 mg/L produced ozone effluent bromate concentrations ranging from below the method detection limit of 0.2 µg/L to a maximum of 48 µg/L (Figure 7.5). High bromate concentrations appeared to require high influent bromide concentrations and a higher than average ozone dose. However, some dates with elevated bromide and ozone dose did not lead to high bromate formation, suggesting there were other variable sources of ozone demand affecting bromate formation. Only once was bromate measured in Ozone RO permeate (0.5 µg/L), every other sample was below the detection limit. Maximum bromate rejection through the RO unit was > 99.6%. These data demonstrated bromate formation by ozonation should not cause problems for water reuse treatment trains including RO.

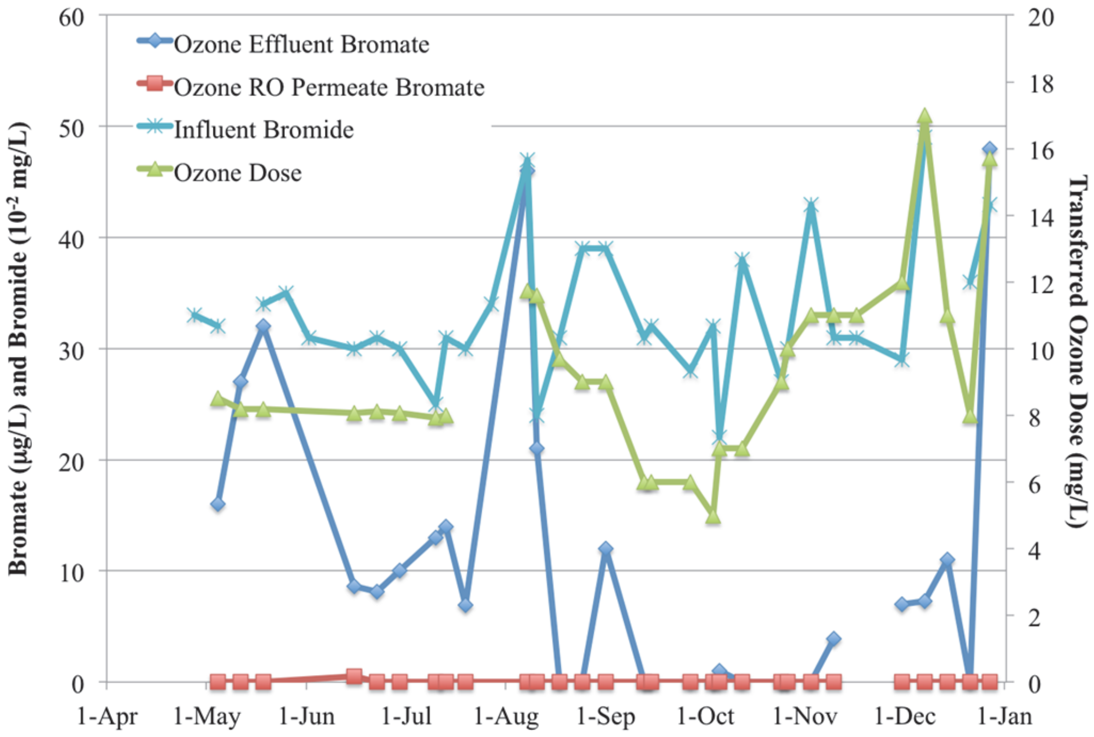

Figure 7.5. Influent bromide data, ozone effluent and Ozone RO permeate bromate data, and transferred ozone dose at the time of ozone effluent sample collection.

7.3.2 NDMA Formation Control Experiments

The bench-scale NDMA formation control experiments investigated the possibility of using pH adjustment or prechlorination to limit NDMA formation of pilot plant influent. Ambient pH was 7.0 and sulfuric acid was used to reduce it to 6.5 in pH-adjusted samples. Because the pilot plant influent was a non-nitrified secondary effluent, there were high levels of ammonia (~ 40 mg/L as N) available to convert sodium hypochlorite to chloramines. The total chlorine residual for the chloraminated samples was 6 mg/L. NDMA formation and changes in ultraviolet absorbance at 254 nm (UVA) were measured at O_3:DOC ratios of 0.00, 0.25, 0.50, 0.75, and 1.00.

As expected, UVA declined with increasing O_3:DOC ratio for all samples (Figure 7.6). Linear regression showed the correlations between O_3:DOC ratio and UVA was strong ($R^2 \leq 0.95$). The data trends were similar regardless of chemical addition before ozonation, although the reduction of UVA was greater for the pH 7 sample at O_3:DOC ratios ≥ 0.50. However, the significance of this difference was not clear because the samples were analyzed only once at each O_3:DOC ratio.

NDMA data after sample ozonation showed pH adjustment and prechlorination, either together or separately, caused no difference in NDMA formation (Figure 7.7). Earlier bench-scale studies found NDMA formation by ozonation declined with pH (Andrzejewski et al., 2008; Padhye et al., 2011). These previous studies suggested lowering pH to reduce NDMA formation was a potentially effective strategy. Considering the results of this experiment, a decrease in pH by only 0.5 units might not have been enough to produce a noticeable decline in NDMA formation. Chloramination and the combination of pH adjustment and chloramination were equally unsuccessful at reducing NDMA formation, but no other studies with similar test conditions were identified for comparison.

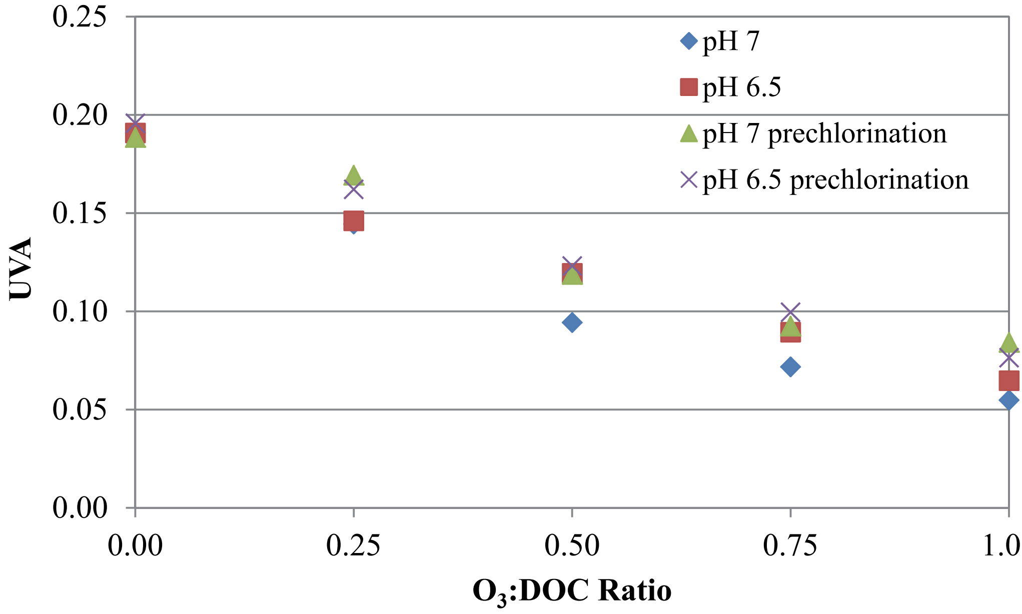

Figure 7.6. Change in UVA as a function of O_3:DOC ratio.

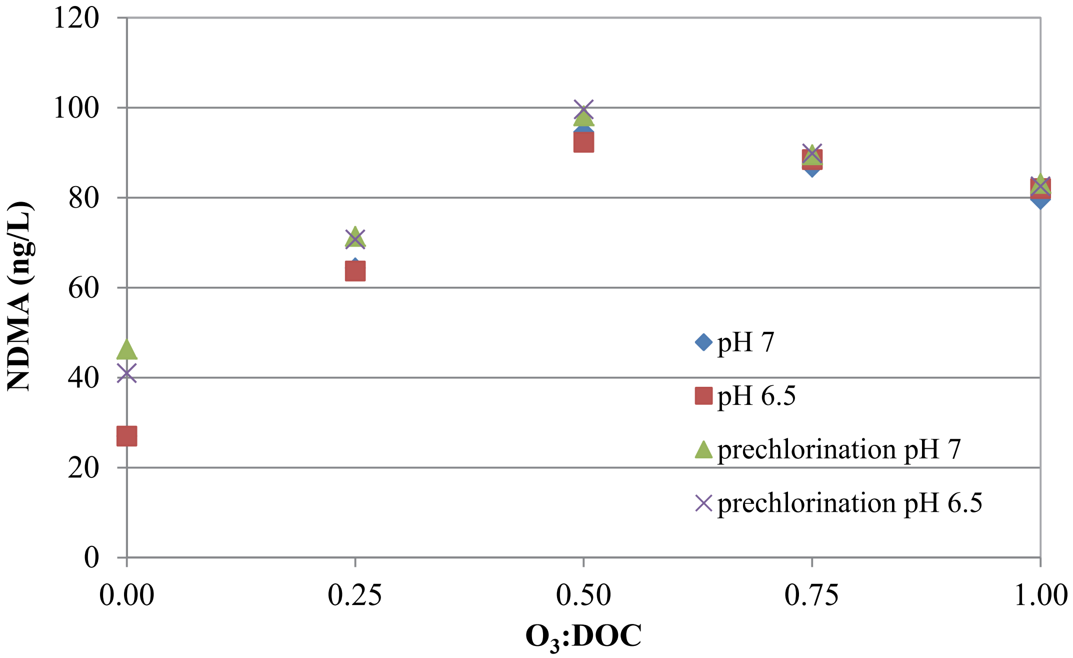

Figure 7.7. NDMA formation as a function of O_3:DOC ratio.

An increasing O_3:DOC ratio corresponded with an increasing NDMA concentration until reaching a O_3:DOC ratio of 0.50. At higher O_3:DOC ratios, NDMA concentration declined from its peak. In addition, NDMA formation peaked at a O_3:DOC ratio near 0.50, indicating the optimization of the ozone dose below that ratio could be an effective approach to reducing NDMA formation. Above an O_3:DOC ratio of 0.50, NDMA concentrations decreased, presumably because of to the destruction of NDMA or NDMA precursors at higher ozone doses. This finding was consistent with other research that detected a peak in NDMA production beyond which the NDMA yield was reduced as the ozone dose increased (Andrzejewski and Nawrocki, 2007).

7.3.3 NDMA Formation from Wastewater Treatment Polymers

The ozonation of pilot plant influent and DDI water with 10 mg/L of cationic or anionic polymer from HTP, the wastewater treatment plant supplying ECLWRF and the pilot plant with secondary effluent, did not increase NDMA formation (Table 7.8). NDMA in ozonated DDI water without polymer addition was 1 ng/L, and this concentration effectively was not changed by the addition of either polymer prior to ozonation. When adding the polymers to the pilot plant influent, NDMA formation actually was lower in the samples with either polymer. This result could have been caused by the polymer increasing the ozone demand and reducing the ozone available to form NDMA. Other research has demonstrated polymers such as poly(diallyldimethylammonium chloride), also known as polyDADMAC, can contribute to NDMA formation by ozonation and chloramination (Padhye et al., 2011; Park et al., 2009). This experiment demonstrated the polymers used at HTP did not contribute to NDMA formation by ozonation.

Table 7.8. NDMA Formation from Ozonation of Cationic and Anionic Polymer in West Basin Water

Sample	Test Water	Polymer	NDMA after Ozonation (ng/L)
1	DDI	none	1
2	DDI	10 mg/L cationic	1
3	DDI	10 mg/L anionic	3
4	Pilot plant influent	none	272
5	Pilot plant influent	10 mg/L cationic	235
6	Pilot plant influent	10 mg/L anionic	231

7.4 Conclusions

NDMA formation was the found to be a significant challenge for the implementation of ozonation for MF pretreatment in a water reuse treatment train. Concentrations in Ozone RO permeate averaged nine times higher than the concentrations in Control RO permeate. In the absence of other mitigation measures, these results indicated AOP treating Ozone RO permeate might need to be more robust than would otherwise be required. There were four causes of this disparity:

- High average NDMA formation by ozonation (104 ng/L)
- Higher average NDMA formation by chloramination in the ozone train (30 ng/L) compared to the control train (8 ng/L)
- Lower average NDMA rejection by Ozone RO (28%) compared to Control RO (47%)
- Although not measured, concentrations of NDMA precursors in the non-nitrified secondary effluent probably high

NDMA formation from ozonation of secondary wastewater effluent has been documented at 10 to 42 ng/L at O_3:DOC ratios near 1.0 (Hollender et al., 2009; Pisarenko et al., 2012; Zimmerman et al., 2011). Data presented in this chapter showed more NDMA formation than was measured in those other studies. For this project, NDMA formation was highest during the last month of testing (December), when formation peaked at 241 ng/L and Ozone RO permeate concentrations were 180 ng/L or higher for four out of five samples. These data demonstrated the need for additional testing during the winter months to determine if this trend was coincidental or related to seasonal changes, such as lower temperatures, that could reduce treatment efficiency at the upstream wastewater treatment plant. Other research (Hollender et al., 2009) suggested NDMA formation depended on variable precursor concentrations in the source water more than on ozone dose. NDMA precursor variability in the secondary effluent of this study could explain the absence of a relationship between NDMA formation and O_3:TOC ratio, Developing reliable NDMA precursor identification methods could allow researchers to link NDMA formation by ozonation to variations in ozone dose and the presence of specific precursors. In addition, NDMA precursor identification could be tracked along with wastewater treatment performance to evaluate the relationship between specific operating conditions and precursor concentrations.

Research investigating NDMA formation has revealed that higher dissolved oxygen concentrations are associated with more NDMA production by chloramination (Le Roux et al., 2011; Schreiber and Mitch, 2006). This finding could explain the higher NDMA formation by chloramination in the ozone train compared to the control train. Although dissolved oxygen concentrations were not monitored in either treatment train, ozonation should saturate the secondary effluent with oxygen, because the ozone feed gas was approximately 8% ozone, 92% oxygen, and 2% nitrogen. ORP after the dissipation of the any residual ozone was approximately 300 mV higher in the ozone effluent than in the pilot plant influent (see Chapter 4, Sections 4.3.2 and 4.4.2.1). One explanation for this change could have been a higher dissolved oxygen concentration.

Further study is required to explain the lower NDMA rejection by Ozone RO compared to Control RO. Wang et al. (2010) found ozone pretreatment lowered RO fouling at the expense of reduced rejection of small organic compounds and higher salt rejection. Because NDMA has a low molecular weight, perhaps ozonation somehow facilitated higher passage of NDMA through the RO membrane. However, additional research is needed to investigate this possibility and to explain the mechanism for how upstream ozonation could reduce NDMA rejection by RO.

Bromate formation and CEC destruction during ozonation followed past research on these subjects. Bromate concentrations after ozonation averaged 10 µg/L but ranged from ND to 48 µg/L. Because bromate was easily removed below the detection limit by RO, its formation should not be a concern for an O_3-MF-RO treatment train like the one that was pilot tested.

CEC removal by ozonation was significant for most chemicals and largely followed the results of other research using wastewater effluents (Pisarenko et al., 2012; Snyder et al., 2007; Wert et al., 2009). CEC data indicated the concentrations in the RO permeate of both treatment trains were similar. However, recent research has investigated CEC removal from the RO concentrate of water reuse treatment trains by ozonation and other oxidation processes (Benner et al., 2008; Dialynas et al., 2008; Joss et al., 2011; Westerhoff et al., 2009). RO concentrate treatment for CEC removal would reduce environmental loading of these chemicals by reducing their concentrations before concentrate disposal. The use of ozonation for MF pretreatment in the water reuse treatment train tested for this project would be equally protective of the environment by lowering CEC concentrations in RO concentrate. If future permit requirements for RO concentrate disposal included CECs, including ozonation in the treatment train could be used to help satisfy those requirements.

Chapter 8

Conclusions and Recommendations

Ozonation of a non-nitrified secondary wastewater effluent as pretreatment for a pilot-scale indirect potable reuse (IPR) treatment train with polyvinylidene fluoride (PVDF) microfiltration (MF) membranes followed by polyamide reverse osmosis (RO) membranes affected many aspects of water quality and process performance. Positive results of ozonation on MF-RO compared to the control treatment train of ferric chloride ($FeCl_3$) addition before MF-RO are listed here:

- Improved MF feed water quality
- Reduced or eliminated $FeCl_3$ addition before MF
- Longer intervals between chlorine/caustic enhanced flux maintenance (EFM) cleans for PVDF MF units
- Higher MF fluxes and longer backwash intervals when coupled with $FeCl_3$
- Improved MF backwash water quality
- No evidence of increased biological or organic fouling on RO membranes
- Removal of contaminants of emerging concern (CECs)

These positive effects have the potential to improve the cost-effectiveness of implementing preozonation in IPR treatment trains with MF-RO in several ways. Water quality changes by ozonation removed effluent organic matter associated with MF fouling. Lower organic fouling would not only benefit daily performance but could extend membrane life by slowing the rate of irreversible fouling that leads to membrane replacement. In addition, the usage of chemicals, such as $FeCl_3$ for coagulation and chlorine and caustic for EFMs, could be reduced. Higher fluxes could lower the membrane area needed to achieve the desired MF capacity and longer backwash intervals could increase water recovery. Ozonation could also increase the capacity of existing MF membranes by allowing them to operate at higher fluxes (Gerringer et al., 2011). Improved MF backwash water quality could reduce coagulant demand for backwash water recovery treatment. CEC removal would reduce the concentration of these chemicals in the RO concentrate flow, potentially reducing the environmental impact of concentrate disposal. The magnitude of these benefits would be project specific, depending on factors such as wastewater effluent quality, organic fouling potential in the MF feed, baseline MF process without ozonation, use of coagulants and handling of MF backwash water.

The effect of ozonation on RO performance was potentially beneficial but ultimately inconclusive. For more than half of pilot testing with RO, the feed pressure and specific flux of the RO unit in the ozone train were 20% better than they were for the RO unit in the control train. However, this difference was not detected after the RO units were swapped between treatment trains (the RO elements stayed with the same treatment process). While there are other potential explanations, such water quality effects caused by the switch to automated ozone dose control, it is likely this change was a consequence of the swap between the RO units, because it occurred concurrently with that event. Further research of ozonation before MF-RO is required to determine if the difference between RO feed pressure and specific flux during the first several months was a real benefit that could decrease energy usage or increase water production.

Pilot testing of preozonation with MF-RO uncovered some challenges associated with this application relative to the control train with $FeCl_3$ addition before the MF unit:

- Potential manganese fouling of PVDF MF membranes in the absence of mitigation measures
- Higher N-nitrosodimethylamine (NDMA) formation by ozonation leading to more NDMA in the RO permeate
- Bromate formation

Subcolloidal manganese was the suspected cause of inorganic fouling experienced by the PVDF MF membranes used in this research. A pilot study conducted a year earlier tested ozonation of the same source water before polypropylene MF membranes (Gerringer et al., 2011). The MF pilot unit in that study did not include $FeCl_3$ addition or have the flexibility of using citric acid EFMs to remove inorganic foulants between clean-in-places (CIPs). Gerringer et al. (2011) documented a significant improvement in MF performance from ozonation and found no evidence of inorganic fouling. The membrane materials used in Gerringer et al. (2011) and the current study (polypropylene and PVDF, respectively) were a suspected cause of these disparate results. Water quality and MF operational set points were two other factors that could have contributed to the differences in inorganic fouling between these studies.

The high NDMA formation by ozonation was likely caused by a significant amount of NDMA precursors in the secondary effluent feeding the pilot plant. Andrzejewski et al. (2008) demonstrated the strong relationship between ozone dose, the concentration of a known NDMA precursor (dimethylamine) and NDMA formation in bench-scale experiments. That study indicated lower ozone doses should reduce NDMA formation. However, as found in Hollender et al. (2009), the variability of NDMA precursor concentrations could be more important than the ozone dose. Applying Hollender et al. (2009) to the current research could explain why there was no relationship between the ozone-to-total organic carbon ratio and NDMA formation. If lower ozone doses or NDMA precursor identification and control were unable to reduce NDMA formation to acceptable levels, an advanced oxidation process of ultraviolet light and hydrogen peroxide could be sized to remove NDMA concentrations so they were below any regulatory limits.

As a result of this study, there are several areas of research that could improve the understanding of preozonation of a non-nitrified secondary effluent before a water reuse treatment train with MF-RO. Optimization of the automated ozone dose control system to minimize the ozone effluent ultraviolet transmittance dead band while maintaining acceptable MF performance could improve the cost efficiency of MF pretreatment with ozone. Another advantage of a lower ozone dose is the potential to decrease NDMA formation, which could reduce the size of the advanced oxidation step after RO in IPR treatment trains.

There are many approaches to MF optimization that could be explored. This research demonstrated MF membranes with preozonation followed by $FeCl_3$ were able to operate at a flux of 45 gfd for several days whereas MF with $FeCl_3$ alone experienced severe fouling at 40 gfd. Adding $FeCl_3$ after preozonation also was shown to extend the backwash interval from 15 min to 30 min when filtering secondary effluent at 27 gfd. Extending the CIP interval so there are more days of operation between cleanings would be another possibility. Further study would be required to establish an upper limit to those parameters under various water quality conditions and ozone doses.

Other possible areas of MF-related research included treatment of backwash water from the ozone train and confirmation of manganese as the source of fouling after ozonation. This study showed backwash water quality was better after ozonation, but jar testing of backwash water from MF units with and without preozonation would be required to confirm and quantify this expected benefit. Similar, available evidence suggested inorganic fouling of the MF membranes was caused by subcolloidal manganese, but this assumption was never confirmed by analyzing membrane fibers after a fouling event occurred. Although there was no other likely cause of this fouling, positively identifying the source of fouling could provide insight into the subcolloidal manganese fouling and increase the confidence in the tested mitigation measures.

Another area of potential study was the difference between RO performance in the control train (Control RO) and ozone train (Ozone RO) during the first half of study. There was a significant difference (~ 20%) in the RO feed pressure and specific flux data, indicating the possibility of lower power costs per unit of RO permeate. However, this difference vanished after the RO elements were switched between the pilot units. It was suspected the disappearance of this benefit was related to this switch, because there was no other identifiable reason for this sudden change. Because the RO units ended with similar feed pressures and specific fluxes over the remainder of testing, the worst-case scenario appeared to be no change in RO performance between treatment trains. If future research investigated this phenomenon and established it was real and lasting, lower power usage and/or lower capital costs to produce a given volume of water could make this ozone application more cost-effective. In additon, the capacity of existing RO systems could be increased without adding more membrane area. Because previous research indicated preozonation improved RO performance while increasing passage of small organics (Wang et al., 2010), close monitoring of RO permeate quality would help ensure product water quality goals were being met.

Potentially higher NDMA formation by ozone makes pilot testing of preozonation with source waters of other IPR applications critical, particularly if that water contains higher concentrations of NDMA precursors. Further research attempting to identify NDMA precursors in a given source water could suggest other strategies to limit formation. If precursors were linked to particular inputs into municipal wastewater, a program to control their addition to sewage upstream of the wastewater treatment plant could be attempted. Once precursors were known, the formation reactions could be defined and possibly controlled to reduce NDMA concentrations after ozonation. As suggested by other research (Andrzejewski et al., 2008; Padhye et al., 2011), lowering the pH beyond the 0.5 pH units attempted in this study could reduce NDMA formation. If successful, combining strategies, such as lower pH, precursor identification and optimized ozone dosing could be effective at mitigating NDMA formation during ozonation.

A potential advantage of including ozone in a water reuse treatment train was related to the draft recycled water regulations by the California Department of Public Health (CDPH) dated November 21, 2011 (CDPH, 2011). The draft regulations discussed requirements for the removal of enteric viruses, Giardia cysts and Cryptosporidium oocysts. The following discussion will focus on enteric viruses, which has a proposed removal requirement of 12-logs for groundwater replenishment reuse. Unit processes would be limited to a maximum removal of 6-logs, which is what would likely be achieved by UV/H_2O_2. Removal by RO would be limited to 2-logs or less if using a parameter, such as electroconductivity, to satisfy the proposed requirement for continuous monitoring to ensure membrane integrity. Given these assumptions, the typical IPR train of MF-RO-UV/H_2O_2 in California likely would receive ≤ 8-logs of removal credits for enteric viruses (0-logs for MF, ≤ 2-logs for RO, and 6-logs for UV/H_2O_2). Therefore, a minimum of 4-log removal would be required to reach the 12-log removal requirement without accounting for any safety factor. Although in situ treatment from surface spreading or well injection could satisfy the additional removals credits, not every utility will have enough hydraulic retention time (6 months with injection wells) in its groundwater basin for this option to be viable. In addition, any potential for direct potable reuse following these guidelines would require the 12-log requirement to be achieved within the treatment train.

Adding ozonation to MF-RO-UV/H_2O_2 could bridge the gap between this treatment train and CDPH's draft regulations. HiPOx, an ozone system from APTwater that has CDPH Title 22 approval for disinfection (CDPH, 2012), was shown to remove the equivalent of > 5.0-log removal of MS2 bacteriophage (Gerrity et al., 2011), a surrogate for human viruses. However, Gerrity et al. (2011) achieved that removal by ozonating after sand filtration or ultrafiltration. Another study demonstrated ozonation completely removed enteric viruses from poor quality secondary effluent (Xu et al., 2002). The concentration of enteric viruses in the secondary effluent limited the documented removal to 2.9-logs, but the actual removal possible under those conditions could have been higher. Additional pilot testing would be required to determine if ozonation before MF could earn enough disinfection credits to satisfy CDPH's draft regulations. Because HiPOx was able to achieve 5-log removal of MS2, it could be possible for a properly designed ozone system could improve MF performance while also providing enough disinfection credits to reduce the hydraulic retention time for subsurface treatment or to permit direct potable reuse.

References

Ahmad, A.; Mariadas, A.; Zulkali, M. Reduction of membrane fouling using a helical baffle for cross flow microfiltration. *Proceedings of the Membrane Science and Technology Symposium*, Johor Bahru, Johor, Malaysia, April 21–25, 2004.

Akmehmet, B.; Otker, M. Treatment of pharmaceutical wastewater containing antibiotics by O_3 and O_3/H_2O_2 processes. *Chemosphere*. **2003**, *50* (1), 85–95.

Al-Ahmad, A.; Daschner, F. D.; Kümmerer, K. Biodegradability of cefotiam, ciprofloxacin, meropenem, penicillin G, and sulfamethoxazole and inhibition of waste water bacteria, *Environ. Contam. Toxicol*. **1999**, *37* (2), 158–163.

Al-Ahmad, M.; Aleem, F. A. A.; Mutiri, A. Biofouling in RO membrane systems Part 1: Fundamentals and control. *Desalination.* **2000**, *132*, 173–179.

Al-Malack, M. H.; Anderson, G. K. Coagulation-crossflow microfiltration of domestic wastewater. *J. Membr. Sci.* **1996**, *121*, 59–70.

Amy, G. Fundamental understanding of organic matter fouling of membranes. *Desalination.* **2008**, *231* (1–3), 44–51.

Andrzejewski, P.; Kasprzyk-Hordern, B.; Nawrocki, J. N-nitrosodimethylamine (NDMA) formation during ozonation of dimethylamine-containing waters. *Water Res.* **2008**, *42*, 863–870.

Andrjewski, P.; Nawrocki, J. NDMA formation during treatment with strong oxidants of DMA containing water. *Water Sci. Technol*. **2007**, *56* (12), 125–131.

Asano, T.; Burton, F.; Leverenz, H.; Tsuchihashi, R.; Tchobanoglous, G. *Water Reuse: Issues, Technologies, and Applications*. McGraw-Hill Professional: New York, **2007**.

Bader, H.; Hoigne, J. Determination of ozone in water by the indigo method: A submitted standard method (Switzerland). *Ozone Sci. Eng*. **1982**, *4* (4), 169–176.

Bahr, C.; Schumacher, J.; Ernst, M.; Luck, F.; Heinzmann, B.; Jekel, M. SUVA as control parameter for the effective ozonation of organic pollutants in secondary effluent. *Water Sci. Technol*. **2007**, *55* (12), 267–274.

Baig, S.; Hansmann, G.; Paolini, B. Ozone oxidation of oestrogenic active substances in wastewater and drinking water. *Water Sci. Technol*. **2008**, *58* (2), 451–458.

Baker, A. Fluorescence excitation-emission matrix characterization of some sewage-impacted rivers. *Environ. Sci. Technol*. **2001**, *35*, 948–953.

Benner, J.; Salhi, E.; Ternes, T.; von Gunten, U. Ozonation of reverse osmosis concentrate: Kinetics and efficiency of beta blocker oxidation. *Water Res*. **2008**. *42*, 3003–3012.

Bertanza, G.; Pedrazzani, R.; Papa, M.; Mazzoleni, G.; Steimberg, N.; Caimi, L.; Montani, C.; Dilorenzo, D. Removal of BPA and NPnEOs from secondary effluents of municipal WWTPs by means of ozonation. *Ozone Sci. Eng*. **2010**, *32* (3), 204–208.

Brown, S.; Leonard, K.; Messimer, S. Evaluation of ozone pretreatment on flux parameters of reverse osmosis for surface water treatment. *Ozone Sci. Eng*. **2008**, *30* (2), 152–164.

Burkhardt-Holm, P. *Linking Water Quality to Human Health and Environment: The Fate of Micropollutants*. Institute of Water Policy (IWP): Singapore, 2011.

Buser, H. R.; Muller, M. D.; Theobald, N. Occurrence of the pharmaceutical drug clofibric acid and the herbicide mecoprop in various Swiss lakes and in the North Sea. *Environ. Sci. Technol*. **1998a**, *32* (1), 188–192.

Buser, H. R.; Poiger, T.; Muller, M. D. Occurrence and fate of the pharmaceutical drug diclofenac in surface waters: Rapid photodegradation in a lake. *Environ. Sci. Technol.* **1998b**, *32* (22), 3449–3456.

Buser, H. R.; Poiger, T.; Muller, M. D. Occurrence and environmental behavior of the chiral pharmaceutical drug ibuprofen in surface waters and in wastewater. *Environ. Sci. Technol.* **1999**, *33* (15), 2529–2535.

Buxton, H. *A national reconnaissance of pharmaceuticals and other wastewater products in U.S. waters*. Endocrine Disruptors and Pharmaceutically Active Chemicals in Drinking Water Workshop, Chicago, IL, April 19–21, 2000.

Calderón-Preciado, D.; Jimenez-Cartagena, C.; Matamoros, V.; Bayona, J. M. Screening of 47 organic microcontaminants in agricultural irrigation waters and their soil loading. *Water Res*. **2011**, *45* (1), 221–231.

Camel, V.; Bermond, A. The use of ozone and associated oxidation processes in drinking water treatment. *Water Res.* **1998**, *32*, 3208–3222.

Cancilla, D. A.; Baird, J.; Geis, S.; Corsi, S. Studies of the environmental fate and effect of aircraft deicing fluids: detection of 5-methyl-1H-benzotriazole in the fathead minnow (*Pimephales promelas*). *Environ. Toxicol. Chem*. **2003**, *22* (1), 134–140.

CDPH. Alternative treatment technology report for recycled water. 2012. http://www.cdph.ca.gov/certlic/drinkingwater/Documents/DWdocuments/AlternativeTreatmentTechnologyReportfor RecycledWater-October2012.pdf (accessed November 1, 2012).

CDPH. Groundwater replenishment reuse DRAFT regulation. 2011. http://www.cdph.ca.gov/certlic/drinkingwater/Documents/Recharge/DraftRechargeReg-2011-11-21.pdf (accessed August 23, 2012).

CDPH. NDMA and other nitrosamines – Drinking water issues. 2012. http://www.cdph.ca.gov/certlic/drinkingwater/Pages/NDMA.aspx (accessed April 20, 2012).

Chae, S.-R.; Yamamura, H.; Ikeda, K.; Watanabe, Y. Comparison of fouling characteristic of two different poly-vinylidene fluoride microfiltration membranes in a pilot-scale drinking water treatment system using pre-coagulation/sedimentation, sand filtration, and chlorination. *Water Res*. **2008**, *42*, 2029–2042.

Chakravarti, D.; Venugopal, D.; Mailander, P.; Meza, J.; Higginboham, S.; Cavalieri, E.; Rogan, E. The role of polycyclic hydrocarbon-DNA adducts in inducing mutations in mouse skin. *Mutation Res. / Genetic Toxicol. Environ. Mutagenesis*. **2008**, *649* (1–2), 161–178.

Chen, W.; Westerhoff, P.; Leenheer, J. A.; Booksh, K. Fluorescence excitation-emission matrix regional integration to quantify spectra for dissolved organic matter. *Environ. Sci. Technol*. **2003**, *37*, 5701–5710.

Choi, J.; Valentine, R. Formation of N-nitrosodimethylamine (NDMA) from reaction of monochloramine: A new disinfection by-product. *Water Res*. **2002**, *36* (4), 817–824.

Choi, J.; Valentine, R. N-nitrosodimethylamine formation by free-chlorine-enhanced nitrosation of dimethylamine. *Environ. Sci. Technol.* **2003**, *37* (21), 4871–4876.

Chon, K.; Lee, S.; Chon, K.; Hussain, A.; Cho, J. Developing organic fouling indices of microfiltration and nanofiltration membranes for wastewater reclamation. *Desalin. Water Treat.* **2010**, *18* (1–3), 61–70.

Chong, T. H.; Wong, F. S.; Fane, A. G. Implications of critical flux and cake enhanced osmotic pressure (CEOP) on colloidal fouling in reverse osmosis: experimental observations. *J. Membr. Sci.* **2008**, *314* (1–2), 101–111.

Cox, C. Diazinon: Toxicology. *J. Pesticide Reform*. **2000**, *20* (2–3), 15–21.

Croué, J.; Grasset, L.; Bacle, S.; Jacquemet, V. Nanofiltration membrane autopsy of a full scale unit: Characterization of the organic and inorganic constituents of the foulants. *Proceedings of the American Water Works Association Membrane Technology Conference*, Atlanta, GA, March 2003.

Croué, J.; Koudjonou, B.; Legube, B. Parameters affecting the formation of bromate ion during ozonation. *Ozone Sci. Eng*. **1996**, *18* (1), 1–18.

Desbrow, C.; Routledge, E.; Brightly, G.; Sumpter J.; Waldock, M. Identification of estrogenic chemicals in STW Effluent: 1. Chemical fractionation and in vitro biological screening. *Environ. Sci. Technol*. **1998**, *32* (11), 1549–1558.

Dialynas, E.; Mantzavinos, D.; Diamadopoulos, E. Advanced treatment of the reverse osmosis concentrate produced during reclamation of municipal wastewater. *Water Res*. **2008**, *42*, 4603–4608.

Drewes, J.; Reinhard, M.; Fox, P. Comparing microfiltration-reverse osmosis and soil-aquifer treatment for indirect potable reuse of water. *Water Res*. **2002**, *37* (15), 3612–3621.

Dubois, M.; Gilles, K. A.; Hamilton, J. K.; Rebers, P. A.; Smith, F. Colorimetric Method for Determination of Sugars and Related Substances. *Anal. Chem*. **1956**, *28*, 350–356.

Esplugas, S.; Bila, D.; Krause L.; Dezotti, M. Ozonation and advanced oxidation technologies to remove endocrine disrupting chemicals (EDCs) and pharmaceuticals and personal care products (PPCPs) in water effluents. *J. Hazard Mater*. **2007**, *149* (3), 31–42.

Fair, P.; Hing-Biu, L.; Adams, J.; Darling, C.; Pacepavicus, G.; Alaee, M.; Bossart, G.; Henry, N.; Muir, D. Occurrence of triclosan in plasma of wild Atlantic bottlenose dolphins (*Tursiops truncates*) and in their environment. *Environ. Pollut*. **2009**, *57*, 2248–2254.

Farahbakhsh, K.; Smith, D. Removal of coliphages in secondary effluent by microfiltration-mechanisms of removal and impact of operating parameters. *Water Res*. **2004**, *38*, 585–592.

Furukawa, D. *A Global Perspective of Low Pressure Membranes*. National Water Research Institute: Fountain Valley, CA, 2008.

Gabelich, C. J.; Franklin, J.; Gerringer, F. W.; Ishida, K.; Suffet, I. H. Enhanced oxidation of polyamide membranes using monochloramine and ferrous iron. *J. Membr. Sci*. **2005**, *258* (1–2), 64–70.

Gabelich, C. J.; Ishida, K.; Gerringer, F. W.; Evangelista, R.; Kalyan, M.; Suffet, I. H. Control of residual aluminum from conventional treatment to improve reverse osmosis performance. *Desalination.* **2006a**, *190*, 147–160.

Gabelich, C. J.; Gerringer, F. W.; Lee, C. C.; Knocke, W. R. Sequential manganese desorption and sequestration in anthracite coal and silica sand filter media. *J. Am. Water Works Assn.* **2006b**, *98* (5), 116–127.

Genz, C.; Miehe, U.; Gnirss, R.; Jekel, M. The effect of pre-ozonation and subsequent coagulation on the filtration of WWTP effluent with low-pressure membranes. *Water Sci. Technol.* **2011**, *64* (6), 1270–1276.

Gerringer, F. W.; Budhia, R.; Serna, M.; Trussell, R. S. Ozone pretreatment of a non-nitrified secondary effluent before microfiltration. *Proceedings of the American Water Works Association Membrane Technology Conference*, Long Beach, CA, March 2011.

Gerringer, F. W.; Rosario-Ortiz, F. L.; Suffet, I. H. Characterization of the changes in polarity and size of natural organic matter during water treatment. *J. Environ. Eng. Manage*. **2009**, *19* (1), 11–20.

Gerrity, D.; Gamage, S.; Holady, J. C.; Mawhinney, D. B.; Quinones, O.; Trenholm, R. A.; Snyder, S. A. Pilot-scale evaluation of ozone and biological activated carbon for trace organic contaminant mitigation and disinfection. *Water Res*. **2011**, *45*, 2155–2165.

Gesto, M.; Soengas, J.; Miguez, J. Acute and prolonged stress responses of brain monoaminergic activity and plasma cortisol levels in rainbow trout are modified by PAHs (naphthalene, B-naphthoflavone and benzo(a)pyrene) treatment. *Aquatic Toxicol*. **2008**, *86* (3), 341–351.

Gesto, M.; Tintos, A.; Soengas, J.; Miguez, J. Effects of acute and prolonged naphthalene exposure on brain monoaminergic neurotransmitters in rainbow trout. *Comp. Biochem. Physiol. Part C: Toxicol. Pharmacol*. **2006**, *144* (2), 173–183.

Gibson, A.; Morgan, R.; Nikitin, A. The effect of caffeine on the bacterial populations in a freshwater aquarium system. Student Summer Scholars. 2009, paper 31.

Glater, J.; Zachariah, M.; McCray, S.; McCutchan, J. Reverse osmosis membrane sensitivity to ozone and halogen disinfectants. *Desalination.* **1983**, *48*, 1–16.

Glaze, W. Drinking-water treatment with ozone. *Environ. Sci. Technol*. **1987**, *21* (3), 224–230.

Glaze, W. Reaction products of ozone: a review. *Environ Health Persp*. **1986**, *69*, 151–157.

Glaze, W.; Weinberg, H.; Cavanagh, J. Evaluating the formation of brominated DBP's during ozonation. *J. Am. Water Works Assn*. **1993**, *85* (1), 96–103.

Guo, Y.; Krasner, S. Occurrence of primidone, carbamazepine, caffeine, and precursors for N-nitrosodimethylamine in drinking water sources impacted by wastewater. *J. Am. Water Resour.* **2009**, *45* (1), 58–67.

Gyparakis, S.; Diamadopoulos, E. Formation and reverse osmosis removal of bromate ions during ozonation of groundwater in coastal areas. *Sep. Sci. Tech*. **2007**, *42*, 1465–1476.

Hasegawa, E.; Yamada, H.; Tsuno, H. Effective Ozonation of Secondary Effluents with Initial Ozone Demand. *Ozone Sci. Eng.* **2008**, *30*, 376–386.

Hashino, M.; Mori, Y.; Fujii, Y.; Nakatani, K.; Hori, H.; Takahashi, K.; Motoyama, N.; Mizuno, K.; Minegishi, T. Advanced water treatment system using ozone and ozone resistant microfiltration module. *Water Sci. Technol. Water Supply*. **2001**, *1* (5–6), 169–175.

Hayes, T.; Collins, A.; Lee, M.; Mendoza, M.; Noriega, N.; Stuart, A.; Vonk, A. Hermaphroditic, demasculinized frogs after exposure to the herbicide atrazine at low ecologically relevant doses. *PNAS*. **2002**, *99* (8), 5476–5480.

Heberer, T. H.; Stan, H. J. Determination of clofibric acid and N-(phenylsulfonyl)-sarcosine in sewage, river and drinking water. *Int. J. Environ. Anal. Chem*. **1997**, *67*, 113–124.

Her, N.; Amy ,G.; Yoon, J.; Song, M. Novel methods for characterizing algogenic organic matter and associated nanofiltration membrane fouling. *Water Sci. Technol. Water Supply*. **2003**, *3* (5–6), 165–174.

Hilal, N.; Ogunbiyi, O.; Miles, N.; Nigmatullin, R. Methods employed for control of fouling in MF and UF membranes: a comprehensive review. *Sep. Sci. Technol*. **2005**, *40* (10), 1957–2005.

Hoek, E. V.; Elimelech, M. Cake-enhanced concentration polarization: A new fouling mechanism for salt-rejecting membranes. *Environ. Sci. Technol*. **2003**, *37* (24), 5581–5588.

Hollender, J.; Zimmermann, S. G.; Koepke, S.; Krauss, M.; McArdell, C. S.; Ort, C.; Singer, H.; von Gunten, U.; Siegrist, H. Elimination of organic micropollutants in a municipal wastewater treatment plant upgraded with a full-scale post-ozonation followed by sand filtration. *Environ. Sci. Tech*. **2009**, *43* (20), 7862–7869.

Hong, S.; Elimelech, M. Chemical and physical aspects of natural organic matter (NOM) fouling of nanofiltration membranes. *J. Membr. Sci*. **1997**, *132* (2), 159–181.

Horacek, J.; Simko, J.; Waberzinek, G. *Carbamazepine and risk of hypothyroidism: A prospective study.* European Congress of Endocrinology, Budapest, Hungary, April 28–May 2, 2007.

Hotchkiss, A.; Nelson, R. An environmental androgen, 17beta-trenbolone, affects delayed-type hypersensitivity and reproductive tissues in male mice*. J. Toxicol. Environ. Health Part A*. **2007**, *70* (2), 138–140.

Huang, H.; Lee, N.; Young, T.; Amy, G.; James, C.; Jacangelo, J. Natural organic matter fouling of low pressure, hollow fiber membranes: Effects of NOM source and hydrodynamic conditions. *Water Res*. **2007**, *41* (17), 3823–3832.

Huang, H.; Schwab, K.; Jacangelo J. Pretreatment for low pressure membranes in water treatment: a review. *Environ. Sci. Technol*. **2009**, *43* (9), 3011–3019.

Huber, M.; Gobel, A.; Joss, A.; Hermann, N.; Loffler, D.; McArdell, C.; Ried, A.; Siegrist, H.; Ternes, T.; von Gunten, U. Oxidation of pharmaceuticals during ozonation of municipal wastewater effluents: a pilot study. *Environ. Sci. Technol*. **2005**, *39* (11), 4290–4299.

Huber, M.; Ternes, T.; von Gunten, U. Removal of estrogenic activity and formation of oxidation products during ozonation of 17α-ethinylestradiol. *Environ. Sci. Technol*. **2004**, *38* (19), 5177–5186.

Ikehata, K.; El-Din, M.; Snyder, S. A. Ozonation and advanced oxidation treatment of emerging organic pollutants in water and wastewater. *Ozone Sci. Eng*. **2003**, *30* (1), 21–26.

Janssen, S. Health effects of halogenated fire retardants. *Proceedings of Flame Retardant Dilemma*, Berkeley, CA, April, 19, 2007.

Jarusutthirak, C.; Amy, G.; Croué, J. Fouling characteristics of wastewater effluent organic matter isolates on NF and UF membranes. *Desalination* **2002**, *145* (1–3), 247–255.

Jorsarei, S.; Shibahara, H.; Ayustawati, M.; Hirano, Y.; Shiraishi, Y.; Khalatbari, A.; Pasha, Y.; Suzuki, M. The in-vitro effects of nicotine, cotinine and leptin on sperm parameters analyzed by CASA system. *Iranian J. Reproductive Med*. **2008**, *6* (3), 157–165.

Joss, A.; Baenninger, C.; Foa, P.; Koepke, S.; Krauss, M.; McArdell, C. S.; Rottermann, K.; Wei, Y.; Zapata, A.; Siegrist, H. Water reuse: > 90% water yield in MBR/RO through concentrate recycling and CO2 addition as scaling control. *Water Res*. **2011,** *45*, 6141–6151.

Kimura, K.; Hane, Y.; Watanabe, Y.; Amy, G.; Ohkuma, N. Irreversible membrane fouling during ultrafiltration of surface water. *Water Res*. **2004**, *38* (14–15), 3431–3441.

Kimura, K.; Yamamura, H.; Watanabe, Y. Irreversible fouling in MF/UF membranes caused by natural organic matters (NOMs) isolated from different origins. *Sep. Sci. Technol.* **2006**, *41* (7), 1331–1344.

Kolodziej, E.; Gray, J.; Sedlak, D. Quantification of steroid hormones with pheromonal properties in Municipal wastewater effluent. *Environ. Toxicol. Chem*. **2003**, *22* (11), 2622–2629.

Kummer, V.; Maskova, J.; Zraly, Z.; Neca, J.; Simeckova, P.; Vondracek, J.; Machala, M. Estrogenic activity of environmental polycyclic aromatic hydrocarbons in uterus of immature Wistar rats. *Toxicol. Lett*. **2008**, *180* (3), 212–221.

Laabs, C.; Amy, G.; Jekel, M. Organic colloids and their influence on low-pressure membrane filtration. *Water Sci. Technol*. **2004**, *50* (12), 311–316.

Lange, R.; Dietrich, D. Environmental risk assessment of pharmaceutical drug substances – Conceptual considerations. *Toxicol. Lett*. **2002**, *131* (1–2), 97–104.

Langlais, B.; Reckhow, D.; Brink, D. *Ozone in Water Treatment – Application and Engineering*. Lewis Publishers: Chelsea, MI, 1991.

Le Roux, J; Gallard, H.; Croué, J.-P. Chloramination of nitrogenous contaminants (pharmaceuticals and pesticides): NDMA and halogenated DBPs formation. *Water Res*. **2011**, *45,* 3164–3174.

Lee, N.; Amy, G.; Croué, J.; Buisson, H. Identification and understanding of fouling in low-pressure membrane (MF/UF) filtration by natural organic matter (NOM). *Water Res.* **2004**, *38* (20), 4511–4523.

Lee, N.; Amy, G.; Lozier, J. Understanding natural organic matter fouling in low-pressure membrane filtration. *Desalination*. **2005a**, *178* (1–3 Spec. Iss.), 85–93.

Lee, S.; Cho, J.; Elimelech, M. Combined influence of natural organic matter (NOM) and colloidal particles on nanofiltration membrane fouling. *J. Membr. Sci*. **2005b**, *262*, 27–41.

Lee, S.; Lee, C. Effect of operating conditions on CaSO4 scale formation mechanism in nanofiltration for water softening. *Water Res*. **2000**, *34* (15), 3854–3866.

Lee, S.; Lee, K.; Wan, W.; Choi, Y. Comparison of membrane permeability and a fouling mechanism by pre-O_3 followed by membrane filtration and residual O_3 in membrane cells. *Desalination*. **2005c**, *178* (1–3), 287–294.

Lehman, S.; Liu, L. Application of ceramic membranes with pre-ozonation for treatment of secondary wastewater effluent. *Water Res*. **2009**, *43* (7), 2020–2028.

Li, A.; Chen, Z.; Yang, L. Formation, detection and removal of NDMA in water treatment process. *Advanced Mater. Res. Harbin* **2010**, *113* (116), 1402–1406.

Liberti, L., Notarnicola, M.; Lopez, A. Advanced treatment for municipal wastewater reuse in agriculture. III–Ozone disinfection. *Ozone Sci. Eng*. **2000**, *22* (2), 151–166.

Lim, A.; Bai, R. Membrane fouling and cleaning in microfiltration of activated sludge wastewater. *J. Membr. Sci*. **2003**, *216* (1–2), 279–290.

Lishman, L.; Smyth, S.; Sarafin, K.; Kleywegt, S.; Toito, J.; Peart, T.; Lee, B.; Servos, M.; Beland, M.; Seto, P. Occurrence and reductions of pharmaceuticals and Personal care products and estrogens by municipal wastewater treatment plants in Ontario, Canada. *Sci. Total Environ*. **2006**, *367* (2–3), 544–558.

Lowry, O. H.; Rosebrough, N. J.; Farr, A. L.; Randall, R. J. Protein Measurement with the Folin Phenol Reagent. *J. Biol. Chem*., **1951**, *193*, 265–275.

Lozier, J.; Cappucci, L.; Amy, G.; Lee, N.; Jacangelo, J.; Huang, H.; Young, T.; Croué, J.; Mysore, C.; Cemeraux, C.; Clouet, J.; Heijmann, B. *Natural Organic Matter Fouling of Low-pressure Membrane Systems*. AWWARF: Denver, CO, 2008.

Lucas, M. S.; Peres, J. A.; Lan, B. Y.; Puma, G. L. Ozonation kinetics of winery wastewater in a pilot-scale bubble column reactor. *Water Res*. **2009**, *43*, 1523–1532.

MacDonald, B. C.; Lvin, S. J.; Patterson, H. Correction of fluorescence inner filter effects and the partitioning of pyrene to dissolved organic carbon. *Anal. Chim. Acta*. **1997**, *338*, 155–162.

Marhaba, T.; Medlar, S. Treatment of drinking water containing bromate and bromide ions, critical issues in water and wastewater treatment. *Proceedings of the National Conference of Environmental Engineering*, Boulder, CO, July 11–13, 1994.

McGlynn, K. A., Quraishi, S.; Graubard, B.; Weber, J.; Rubertone, M.; Erickson, R. Persistent organochlorine pesticides and risk of testicular germ cell tumors. *J. Natl. Cancer Inst*. **2008**, *100* (9), 663–671.

Meng , F.; Zhou, Z.; Ni, B.-J.; Zhang, X.; Huang, G.; Jia, X.; Li, S.; Xiong, Y.; Kraume, M. Characterization of the size-fractionated biomacromolecules: Tracking their role and fate in a membrane bioreactor. *Water Res*. **2011**, *45*, 4661–4671.

Mettayil, J.; Quinton, R.; Ball, S. Anticonvulsant induced central hypothyroidism. *Proceedings of the Society for Endocrinology BES 2009*, Harrogate, U.K., March 16–19, 2009.

Minnesota Department of Health. *Drinking Water Contaminant of Emerging Concern Program.* Biennium, Interim Report, Saint Paul, MN, 2010.

Mitch, W.; Sedlak, D. Formation of N-nitrosodimethylamine (NDMA) from dimethylamine during chlorination. *Environ. Sci. Technol*. **2002a**, *36* (4), 588–595.

Mitch, W.; Sedlak, D. Factors controlling nitrosamine formation during wastewater chlorination. *Water Sci. Technol. Water Supply*. **2002b**, *2* (3), 191–198.

MWH. *Water Treatment: Principles and Design*, 2nd ed.; Wiley & Sons: Hoboken, NJ, 2005.

Najm, I.; Trussell, R. R. NDMA formation in water and wastewater. *J. Am. Water Works Assn*. **2001**, *93* (2), 92–99.

Nakada, H.; Kiri, K.; Shinohara, H.; Harada, A.; Kuroda, K.; Takizawa, S.; Takada, H.; Evaluation of pharmaceuticals and personal care products as water-soluble molecular markers of sewage. *Environ. Sci. Technol*. **2008**, *42* (17), 6347–6353.

National Pesticide Information Center. Diazinon General Fact Sheet. Oregon State University and USEPA: Washington, DC, 2009. http://npic.orst.edu/factsheets/Diazgen.pdf (accessed April 26, 2012).

National Toxicology Program, U.S. Department of Health and Human Services. Bisphenol A (BPA). 2010. http://www.niehs.nih.gov/health/assets/docs_a_e/bisphenol-a-factsheet.pdf (accessed April 20, 2012).

Nguyen, S.; Roddick, F. Effects of ozonation and biological activated carbon filtration on membrane fouling in ultrafiltration of an activated sludge effluent. *J. Membr. Sci*. **2010**, *363* (1–2), 271–277.

Nguyen, T.; Fan, L.; Roddick, F.; Harris, J. A comparative study of microfiltration and ultrafiltration of activated sludge-lagoon effluent. *Desalination*. **2009**, *236* (1–3), 208–215.

O'Melia C. R.: Becker, W. C.: Au, K-K. Removal of humic substances by coagulation. *Water Sci. Technol.*, **1999**, *40* (9), 47–54.

OzoneLab^{TM} Ozone Exposure Services. 2011. http://www.ozoneservices.com/ services/o3exposure. htm (accessed April 23, 2012).

Padhye, L.; Luzinova, Y.; Cho, M.; Mizaikoff, B.; Kim, J.-H.; Huang, C-H. PolyDADMAC and dimethylamine as precursors of N-nitrosodimethylamine during ozonation: Reaction kinetics and mechanisms. *Environ. Sci. Tech*. **2011**, *45* (10), 4353–4359.

Pal, A.; Gin, K.; Lin, A.; Reinhard, M. Impacts of emerging organic contaminants on freshwater resources: Review of recent occurrences, sources, fate and effects. *Sci. Total Environ*. **2010**, *408* (24), 6062–6069.

Park, C.; Hong, S.; Chung, T.; Choi, Y. Performance evaluation of pretreatment processes in integrated membrane system for wastewater reuse. *Desalination*. **2010**, *250* (2), 673–676.

Park, S.-H.; Piyachaturawat, P.; Taylor, A.; Huang, C.-H. Potential N-nitrosodimethylamine (NDMA) formation from amine-based water treatment polymers in the reactions with chlorine-based oxidants and nitrosifying agents. *Water Sci. Technol*. **2009**, *9* (3), 279−288.

Perera, F.; Li, Z.; Whyatt, R.; Hoepner, L.; Wang, S.; Camann, D.; Rauh, V. Prenatal airborne polycyclic aromatic hydrocarbon exposure and child IQ at age 5 years. *Pediatrics*. **2009**, *124* (2), 195–202.

Pisarenko, A. N.; Stanford, B. D.; Yan, D.; Gerrity, D.; Snyder, S. A. Effects of ozone and ozone/peroxide on trace organic contaminants and NDMA in drinking water and water reuse applications. *Water Res*. **2012**, *46*, 316–326.

Pisarenko, A. N.; Yan, D.; Snyder, S. A.; Stanford, B. D. Comparing oxidative organic fouling control in RO membrane applications. *IDA J. Desal. Water Reuse* **2011**, *3* (2), 45–49.

Plumlee M. H.; López-Mesas, M.; Heidlberger, A.; Ishida, K. P.; Reinhard, M. N-nitrosodimethylamine (NDMA) removal by reverse osmosis and UV treatment and analysis via LC-MS/MS. *Water Res*. **2008**, *42*, 347–355.

Pomati, F.; Netting, A.; Calamari, D.; Neilan, B. Effects of erythromycin and ibuprofen on the growth of Synechocystis sp. and Lemna minor. *Aquatic Toxicol*. **2004**, *67* (4), 387–396.

Rakness, K. *Ozone in Drinking Water Treatment: Process Design, Operation, and Optimization*. AWWA: Denver, CO, 2005.

Rakness, K. L.; Najm, I.; Elovitz, M.; Rexing, D.; Via, S. Cryptosporidium log-inactivation with ozone using effluent CT_{10}, geometric mean CT_{10}, extended integrated CT_{10} and extended CSTR calculations. *Ozone Sci. Eng*. **2005**, *27* (5), 335–350.

Ramseier, M. K.; Peter A.; Traber, J.; von Gunten, U. Formation of assimilable organic carbon during oxidation of natural waters with ozone, chlorine dioxide, chlorine, permanganate, and ferrate. *Water Res*. **2011**, *45* (5), 2002–2010.

Reddy, A. V. R.; Mohan, D. J.; Bhattacharya, A.; Shah, V. J.; Ghosh, P. K. Surface modification of ultrafiltration membranes by preadsorption of a negatively charged polymer 1. Permeation of water-soluble polymers and inorganic salt solutions and fouling resistance properties. *J. Membr. Sci*. **2003**, *214* (2), 211–221.

Rosenberger, S.; Laabs, C.; Lesjean, B.; Gnriss, R.; Amy, G.; Jekel, M.; Schrotter, J.-C. Impact of colloidal and soluble organic material on membrane performance in membrane bioreactors for municipal wastewater treatment. *Water Res*. **2006**, *40*, 710–720.

Sarp, S.; Stanford, B.; Snyder, S. A.; Cho, J. Ozone oxidation of desalinated seawater with respect to optimized control of boron and bromate. *Desal. Water Treat*. **2011**, *27* (1–3), 308–312.

Schäfer, A. I.; Pihlajamäki, A; Fane, A. G.; Waite, T. D.; Nyström, M. Natural organic matter removal by nanofiltration: Effects of solution chemistry on retention of low molar mass acids versus bulk organic matter. *J. Membr. Sci*. **2004**, *242* (1–2), 73–85.

Schlecht, C.; Klammer, H.; Jarry, H.; Wuttke, W. Effects of estradiol, benzophenone-2 and benzophenone-3 on the expression pattern of the estrogen receptors (ER) alpha and beta, the estrogen receptor-related receptor 1 (ERR1) and the aryl hydrocarbon receptor (AhR) in adult ovariectomized rats. *Toxicology* **2004**, *205* (1–2), 123–130.

Schlichter, B.; Mavrov, V.; Chmiel, H. Study of a hybrid process combining O_3 and membrane filtration — Filtration model solutions. *Desalination*. **2003**, *156* (1–3), 257–265.

Schlompf, M.; Cotton, B.; Conscience, M.; Haller, V.; Steinmann, B.; Lichtensteiger, W. In vitro and in vivo estrogenicity of UV screens. *Environ. Health Perspect*. **2001**, *109* (3), 239–244.

Schneider, R. P.; Ferreira, L. M.; Binder, P.; Bejarano, E. M.; Góes, K. P.; Slongo, R.; Machado, C. R.; Rosa, G. M. Z. Dynamics of organic carbon and of bacterial populations in a conventional pretreatment train of a reverse osmosis unit experiencing severe biofouling. *J. Membr. Sci*. **2005**, *266* (1–2), 18–29.

Scholz, S.; Gutzeit, H. O. 17-alpha-ethinylestradiol affects reproduction, sexual differentiation and aromatase gene expression of the medaka (*Oryzias latipes*). *Aquatic Toxicol*. **2000**, *50* (4), 363–373.

Schreiber, I. M.; Mitch, W. A. Nitrosamine formation pathway revisited: The importance of chloramine speciation and dissolved oxygen. *Env. Sci. Tech*. **2006**, *40* (19), 6007–6014.

Shih, W-Y.; Rahardianto, A.; Lee, R-W.; Cohen, Y. Morphometric characterization of calcium sulfate dehydrate (gypsum) scale on reverse osmosis membranes. *J. Membr. Sci.* **2005**, *252* (1–2), 253–263.

Siddiqui, M. S.; Amy, G. L.; Murphy, B. D. Ozone enhanced removal of natural organic matter from drinking water sources. *Water Res*. **1997**, *31* (12), 3098–3106.

Snyder, S. A.; Wert, E. C.; Lei, H.; Westerhoff, P.; Yoon, Y. *Removal of EDCs and Pharmaceuticals in Drinking and Reuse Treatment Processes*. AWWA Research Foundation: Denver, CO, **2007a**.

Snyder, S. A.; Wert, E. C.; Zegers, R.; Drury, D. Oxidation of EDCs and pharmaceuticals in reuse water. *Proceedings of the Water Environment Federation Disinfection*, Pittsburgh, PA, February 4–7, 2007b.

Song, Y.; Dong, B.; Gao, N.; Xia, S. Huangpu River water treatment by microfiltration with ozone pretreatment. *Desalination*. **2010**, *250* (1), 71–75.

Stanford, B. D.; Pisarenko, A. N.; Holbrook, D. R.; Snyder, S. A. *Pilot-scale oxidative technologies for reducing fouling potential in water reuse and drinking water treatment membranes*. WRRF 08-08 Final Report. WateReuse Research Foundation: Alexandria, VA, 2013.

Stanford, B. D.; Pisarenko, A. N.; Holbrook, D. R.; Snyder, S. A. Preozonation effects on the reduction of reverse osmosis membrane fouling in water reuse. *Ozone Sci. Eng*. **2011**, *33*, 379–388.

Steinle-Darling, E.; Zedda, M.; Plumlee, M. H.; Ridgway, H. F.; Reinhard, M. Evaluating the impacts of membrane type, coating, fouling, chemical properties and water chemistry on reverse osmosis rejection of seven nitrosoalkylamines, including NDMA. *Water Res*. **2007**, *41*, 3959−3967.

Suarez, S.; Dodd, M.C.; Omil, F.; von Gunten, U. Kinetics of triclosan oxidation by aqueous ozone and consequent loss of antibacterial activity: relevance to municipal wastewater ozonation. *Water Res*. **2007**, *41* (12), 2481–2490.

Subramani, A.; Hoek, E. M. V. Direct observation of initial microbial deposition onto reverse osmosis and nanofiltration membranes. *J. Membr. Sci*. **2008**, *319* (1−2), 111−125.

Sui, Q.; Huang, J.; Deng, S.; Yu, G.; Fan, Q. Occurrence and removal of pharmaceuticals, caffeine and DEET in wastewater treatment plants of Beijing. *China Water Res*. **2010**, *44* (2), 417–426.

Summit Brands. Super Iron Out® Material Safety Data Sheet. 2011. http://www.summitbrands.com/summit/downloads/msds/usa/MSDS%20Super%20Iron%20Out.pdf. (accessed September 19, 2012).

Suslow, T. Oxidation-reduction potential (ORP) for water disinfection monitoring. University of California Agriculture and Natural Resources: Davis, CA, 2004. http://anrcatalog.ucdavis.edu/Postharvest/8149.aspx (accessed April 23, 2012)

Świetlik, J.; Dąbrowska, A.; Raczyk-Stanisławiak, U.; Nawrocki, J. Reactivity of natural organic matter fractions with chlorine dioxide and ozone. *Water Res*. **2004**, *38* (3), 547–558.

Takizawa, S.; Fu, L.; Pradhan, N.; Ike, T.; Ohtaki, M.; Ohgaki, S. Pretreatment processes for membrane filtration of raw water containing manganese. *Water Sci. Technol. Water Supply*. **2001**, *1* (5–6), 341–348.

Tam, L. S.; Tang, T. W.; Lau, G. N.; Sharma, K. R.; Chen, G. H. A pilot study for wastewater reclamation and reuse with MBR/RO and MF/RO systems. *Desalination*. **2003**, *202* (1–3), 106–113.

Taniguchi, M.; Kilduff, J. E.; Belfort, G. Low fouling synthetic membranes by UV-assisted graft polymerization: monomer selection to mitigate fouling by natural organic matter. *J. Membr. Sci*. **2003**, *222* (1–2), 59–70.

Ternes, T. A.; Stüber, J.; Herrmann, N.; McDowell, D.; Ried, A.; Kampmann, M.; and Teiser, B. Ozonation: A tool for removal of pharmaceuticals, contrast media and musk fragrances from wastewater? *Water Res*. **2003**, *3* (8), 1976–1982.

Thorpe, K.; Hetheridge, M.; Hutchinson, T. H.; Scholze, M.; Sumpter, J. P.; Tyler, C. R. Assessing the interactive effects of binary mixtures of environmental oestrogens in rainbow trout (oncorhynchus mykiss) using vitellogenin induction. *Env. Sci. Tech*. **2001**, *35* (12), 2476–2481.

Trussell, R. S.; Jang, N. J.; Merlo, R. P.; Kim, I. S.; Hermanowicz S. W.; Jenkins D. Changes in mixed liquor and organic foulant properties affect membrane fouling for non-nitrifying and nitrifying biological conditions. *Water Env. Res*. **2009**, *81* (3), 255–264.

United States Bureau of Reclamation (USBR). DBP: Bromate Fact Sheet. 2009a. http://www.usbr.gov/pmts/water/publications/ primer.html (accessed April 20, 2012)

USBR. Secondary/Emerging Constituents Report, Southern California Regional Brine-Concentrate Management Study – Phase I. U.S. Department of the Interior. 2009b.

United States Environmental Protection Agency (USEPA). Basic information about disinfection byproducts in drinking water: Total trihalomethanes, haloacetic acids, bromate, and chlorite. http://water.epa.gov/drink/ contaminants/basicinformation/ disinfectionbyproducts.cfm (accessed November 23, 2011).

USEPA. Integrated risk information system (IRIS) on isophorone. USEPA: Washington, DC, 1999.

USEPA. Integrated risk information system (IRIS). 2005. http://cfpub.epa.gov/iris/quickview. cfm?substance_nmbr=0035 (accessed April 20, 2012).

USEPA. Integrated risk information system (IRIS), N-nitrosodimethylamine (CASRN 62-75-9). 2009. http://www.epa.gov/iris/subst/0045.htm (accessed April 20, 2012).

USEPA. *Primer for municipal wastewater treatment systems. Office of Water and Office of Wastewater Management*, EPA-832-R-04-00. Washington, DC, 2004.

USEPA. Treating contaminants of emerging concern: A literature review database. Office of Water, EPA-820-R-10-002. Washington, DC, 2010.

van der Hoek, J. P.; Rijnbende, D. O.; Lokin, C. J. A.; Bonné, P. A. C.; Loonen, M. T.; Hofman. J. A. M. H. Electrodialysis as an alternative for reverse osmosis in an integrated membrane system. *Desalination*. **1998**, *117* (1–3), 159–172.

Veldhoen, N.; Skirrow, R. C.; Osachoff, H.; Wigmore, H.; Clapson, D. J.; Gunderson, M. P.; Van Aggelen, G.; Helbing, C. C. The bactericidal agent triclosan modulates thyroid hormone-associated gene expression and disrupts postembryonic anunran development. *Aquat*ic *Toxicol*. **2006**, *80* (3), 217–227.

von Gunten, U.; Pinkrnell, U. Ozonation of bromide-containing drinking waters: A delicate balance between disinfection and bromate formation. *Water Sci. Tech*. **2000**, *41* (7), 53–59.

von Gunten, U. Ozonation of drinking water: Part II. Disinfection and by-product formation in presence of bromide, iodide or chlorine. *Water Res*. **2003a**, *37* (7), 1469–1487.

von Gunten, U. Ozonation of drinking water: Part I. Oxidation kinetics and product formation. *Water Res*. **2003b**, *37* (7), 1443–1467.

von Gunten, U.; Salhi, E.; Schmidt, C. K.; Arnold, W. A. Kinetics and mechanisms of NDMA formation upon O_3 of N,N-dimethylsulfamide containing waters – Bromide catalysis. *Environ. Sci. Tech*. **2010**, *44* (15), 5762–5768.

Wakeman, R. J.; Williams, C. J. Additional techniques to improve microfiltration. *Sep. Purif. Technol*. **2002**, *26* (1), 3–18.

Wang, D. L.; Li, K.; Teo, W. K. Preparation and characterization of polyvinylidene fluoride (PVDF) hollow fiber membranes. *J. Membr. Sci*. **1999**, *163* (2), 211–220.

Wang, H. Y.; Guan, Y. T.; Mizuno, T.; Tsuno, H. RO filtration of biologically treated textile and dyeing effluents using ozonation as a pre-treatment. *Water Sci. Tech*. **2010**, *62* (4), 751–758.

Wang, X.; Wang, L.; Liu, Y.; Duan, W. Ozonation pretreatment for ultrafiltration of the secondary effluent. *J. Memb. Sci*. **2007**, *287* (2), 187–191.

Wert, E. C.; Rosario-Ortiz, F. L.; Drury, D. D.; Snyder, S. A. Formation of oxidation byproducts from ozonation of wastewater. *Water Res*. **2007**, *41* (7), 1481–1490.

Wert, E. C.; Rosario-Ortiz, F. L.; Snyder, S. A. Using ultraviolet absorbance and color to assess pharmaceutical oxidation during ozonation of wastewater. *Env. Sci. Tech*. **2009**, *43* (13), 4858–4863.

Westerhoff, P.; Aiken, G.; Debroux, J.; Amy, G. Relationships between the structure of natural organic matter and its reactivity towards molecular ozone and hydroxyl radicals. *Water Res*. **1999**, *33* (10), 2265–2276.

Westerhoff, P.; Moon, H.; Minakata, D.; Crittenden, J. Oxidation of organics in retentates from reverse osmosis wastewater reuse facilities. *Water Res*. **2009**. *43*, 3992–3998.

World Health Organization. *Some Traditional Herbal Medicines, Some Mycotoxins, Naphthalene and Styrene / IARC Working Group on the Evaluation of Carcinogenic Risks to Humans.* IARC Press: Lyon, France, 2002.

Xu, S. *Environmental Fate of Carbaryl*. Environmental Monitoring Branch, Department of Pesticide Regulation, California Environmental Protection Agency: Sacramento, CA, 2000.

Xu, P.; Bellona, C.; Drewes, J. E. Fouling of nanofiltration and reverse osmosis membranes in municipal wastewater reclamation: membrane autopsy results from pilot-scale investigations. *J. Membr. Sci*, **2010**, *353* (1–2), 111–121.

Xu, P.; Janex, M.-L.; Savoye, P.; Cockx, A.; Lazarova, V. Wastewater disinfection by ozone: Main parameters for process design. *Water Res*. **2002**, *36,* 1043–1055.

Yamashita, N.; Yasojima, M.; Nakada, N.; Miyajima, K.; Komori, K.; Suzuki, Y.; Tanaka, H. Effects of antibacterial agents, levofloxacin and clarithromycin, on aquatic organisms. *Water Sci. Tech*. **2006**, *53* (11), 65–72.

Yang, L.; Chen, Z.; Shen, J.; Xu, Z.; Liang, H.; Tian, J.; Ben, Y.; Zhai, X.; Shi, W.; Li, G. Reinvestigation of the nitrosamine-formation mechanism during ozonation. *Env. Sci. Tech*. **2009**, *43* (14), 5481–5487.

Yang, M.; Zhang, Y.; Qi, R.; Uesugi, K.; Myoga, H. Improved O_3/H_2O_2 oxidation process for wastewater reclamation. *Water Sci. Tech*. **2001**, *43* (10), 311–318.

You, S-H; Tseng, D-H; Hsu, W-C. Effect and mechanism of ultrafiltration membrane fouling removal by ozonation. *Desalination*. **2007**, *202* (1–3), 224–230.

Yu, C.-P.; Yu, Y.-H. Identifying useful real-time control parameters in ozonation process. *Water Sci. Tech*. **2000,** *42* (3–4), 435–440.

Zhu, H. T.; Wen, X. H.; Huang, X. Pre-ozonation for dead-end microfiltration of the secondary effluent: suspended particles and membrane fouling. *Desalination*. **2008**, *231* (1–3), 166–174.

Zhu, H. T.; Wen, X. H.; Huang, X. Membrane organic fouling and the effect of pre-ozonation in microfiltration of secondary effluent organic matter. *J. Membr. Sci*. **2010**, *352* (1–2), 213–221.

Zimmermann, S. G.; Wittenwiler, M.; Hollender, J.; Krauss, M.; Ort, C.; Siegrist, H.; von Gunten, U. Kinetic assessment and modeling of an ozonation step for full-scale municipal wastewater treatment: Micropollutant oxidation, by-product formation and disinfection. *Water Res*. **2010**, *45* (2), 605–617.

Zurita, J. L.; Repetto, G.; Los, A.; Salguero, M.; Lopez-Artiguez, M.; Camean, A. M. Toxicological effects of the lipid regulator gemfibrozil in four aquatic systems. *Aquatic Toxicol*. **2007**, *81* (1), 106–115.

Practical Solutions for Water Scarcity

WATEREUSE RESEARCH

1199 North Fairfax Street, Suite 410
Alexandria, VA 22314 USA
(703) 548-0880
Fax (703) 548-5085
E-mail: Foundation@WateReuse.org
www.WateReuse.org/Foundation